THE MINOR PLANET BULLETIN

BULLETIN OF THE MINOR PLANETS SECTION OF THE ASSOCIATION OF LUNAR AND PLANETARY OBSERVERS

VOLUME 48, NUMBER 3, A.D. 2021 JULY-SEPTEMBER 201.

IN MEMORIAM: DERALD D. NYE (1935-2021)

In this space we note the March 26 passing of Derald D. Nye, retired Distributor for the *Minor Planet Bulletin*, having served in that role for 37 years from 1983 through 2019; spanning *MPB* volumes 10-46. Derald wrote of this experience on these pages (*MPB 40*, 53). Derald was a native of Kansas and graduate of Kansas State University, beginning a 30-year career with IBM that included programming work for the Saturn 1B and Saturn V rockets in the Apollo program. Derald and wife Denise were avid eclipse chasers, together making 28 expeditions until Denise's passing in 2006. They are together honored with their names merged for asteroid 3685 Derdenye. Derald's lifetime sum of eclipse expeditions reached 42, the last of which was at sea in Indonesia in 2016. I had the honor of being a shipboard expedition leader, but truth-be-told, I relied on Derald for every bit of insight. Watching that eclipse at Derald's side was the personal highlight for me. Derald's faithful quiet service and dry wit are just two of many attributes that will be missed by his friends.

Richard Binzel, Editor

LIGHTCURVE ANALYSIS OF ASTEROIDS (21242) 1995 WZ41 AND (44896) 1999 VB12

Caroline E. Odden, Claire Cahill, Victoria Darling, Ethan Ellsweig, Troy Mao, Katherine Wang, Yuxin Xie, Jeremy Zhou
Phillips Academy Observatory (MPC I12)
180 Main Street
Andover, MA 01810 USA
ceodden@andover.edu

(Received: 2021 Apr 15)

Photometric observations of asteroids (21242) 1995 WZ4 and (144896) 1999 VB12 and were made from the Phillips Academy Observatory (PAO) from 2020 December 23 to 2021 February 25. The respective rotational periods and amplitudes were determined to be: (21242) 1995 WZ41, P = 5.452 ± 0.001 h, A = 0.58 ± 0.07 mag; (44896) 1999 VB12, P = 8.054 ± 0.001 h, A = 0.69 ± 0.07 mag.

CCD photometric observations of the asteroids were made from the Phillips Academy Observatory. The asteroids were chosen from the CALL (2020) website. All observations were made with a 0.50-m *f*/6.8 Ritchey-Chrétien (RC) Astrograph telescope manufactured by PlaneWave Instruments and Andor Tech iKon DW436 CCD camera with a 2048×2048 array of 13.5-micron pixels. The resulting image scale was 0.81 arcseconds per pixel. All images were corrected using dark frames, flat-fields, and bias frames using *AstroImageJ* software (Collins et. al., 2017; Collins, 2018). All exposures were taken through a luminance filter at -50°C and were unbinned. Exposures were 300 s in length and unguided.

MPO Canopus (Warner, 2018) was used to make photometric measurements of the images using differential photometry as well as to generate the final lightcurves. Comparison stars were chosen to have near solar-color, a B-V value close to 0.8, and a V-R value close to 0.45 (Warner, 2012). In addition, brighter comparison stars were favored. Data merging and period analysis were done with *MPO Canopus* using the Fourier Analysis for Lightcurves (FALC) algorithm developed by Alan Harris (Harris et al., 1989) and modified by Petr Pravec (Warner, 2012). The research was conducted for the Astronomy Research course at Phillips Academy, a high school in Andover, Massachusetts.

Number	Name	20yy/mm/dd	Phase	L_{PAB}	B_{PAB}	Period(h)	P.E.	Amp	A.E.	Grp
21242	1995 WZ41	20/12/23-21/01/25	21.7,29.5	65	-12	5.452	0.001	0.57	0.03	MB-M
44896	1999 VB12	21/01/08-02/05	4.4,14.0	108	8	8.056	0.001	0.65	0.03	MB-M

Table I. Observing circumstances and results. The phase angle is given for the first and last date. If preceded by an asterisk, the phase angle reached an extremum during the period. L_{PAB} and B_{PAB} are the approximate phase angle bisector longitude/latitude at mid-date range (see Harris et al., 1984). Grp is the asteroid family/group (Warner et al., 2009).

(21242) 1995 WZ41. This main-belt asteroid was discovered in 1995 at Kushiro Observatory (JPL) and did not have any previous rotational period results in the Asteroid Lightcurve Database (LCDB) (Warner et al., 2009). Images were taken over four nights from 2020 December 23 to 2021 February 25.

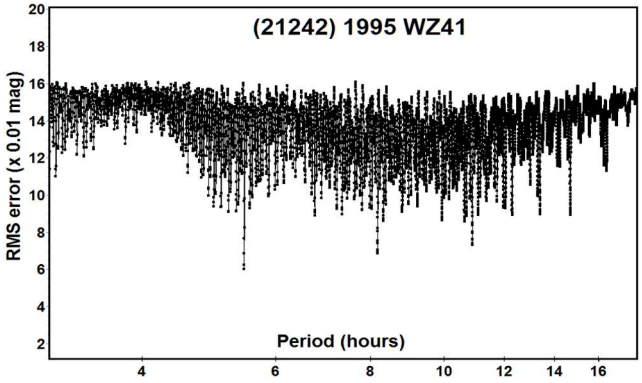

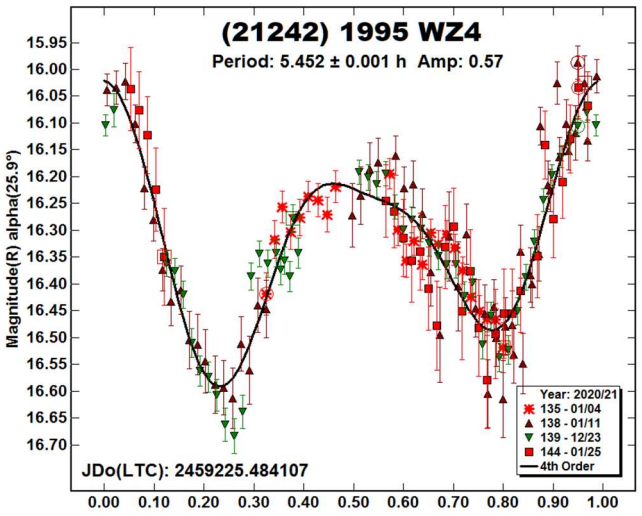

Analysis of 169 data points indicated a rotational period of 5.452 ± 0.001 h with amplitude 0.57 ± 0.03 mag. The composite lightcurve is well covered, and a bimodal solution is expected given the amplitude (Harris et. al, 2014). The period spectrum favors strongly the reported period.

(44896) 1999 VB12. Discovered at Fountain Hills in 1999 by C. W. Juels (JPL, 2019), this main-belt asteroid did not have any rotational period recorded in the Asteroid Lightcurve Database (LCDB) (Warner et al., 2009).

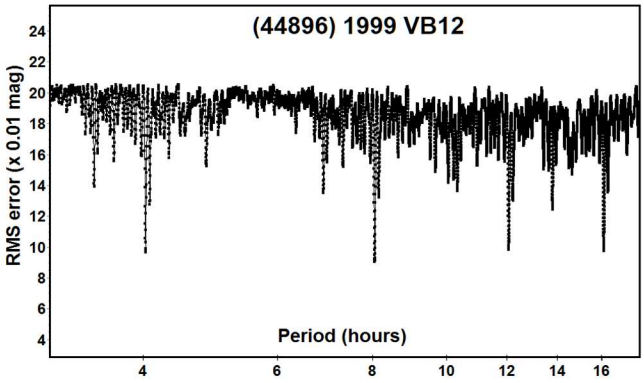

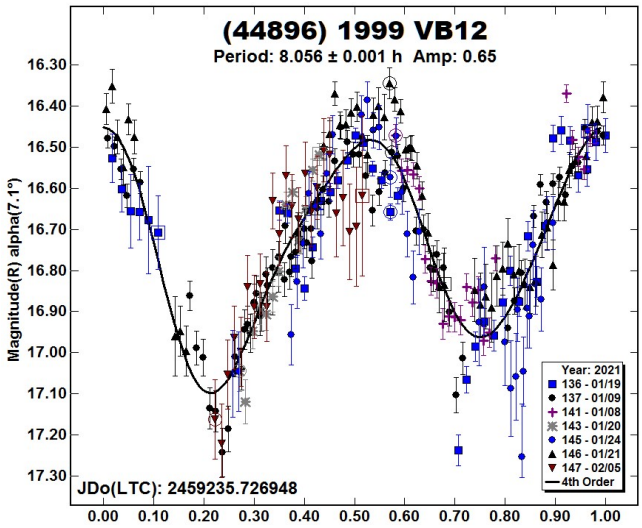

Images were taken over six nights from 2021 January 8 to February 5. Analysis of 268 data points yielded a rotational period of 8.056 ± 0.001 h with amplitude 0.57 ± 0.03 mag. Some data were removed due to background star contamination. This resulted in small gaps between 0.05 and 0.20 phase. However, sessions 136 and 137 extend before and after these gaps, and the bimodal solution is expected given the amplitude (Harris et. al, 2014).

Acknowledgements

Research at the Phillips Academy Observatory is supported by the Israel Family Foundation. Funding for the Andor Tech camera and PlaneWave telescope at Phillips Academy was provided by the Abbot Academy Association, the Donald T. Ganem Fund, and the Taylor Family.

References

CALL (2020): Potential Lightcurve Targets (with LCDB data) Query web site.
http://www.minorplanet.info/PHP/call_OppLCDBQuery.php

Collins, K.A. (2018) *AstroImageJ* software v. 3.2.21.
http://www.astro.louisville.edu/software/astroimagej/

Collins, K.A.; Kielkopf, J.F.; Stassun, K.G.; Hessman, F.V. (2017). "AstroImageJ: Image processing and photometric for ultra-precise astronomical light curves." *Astron. J.* **153**, 77.

Harris, A.W.; Young, J.W.; Scaltriti, F.; Zappala, V. (1984). "Lightcurves and phase relations of the asteroids 82 Alkmene and 444 Gyptis." *Icarus* **57**, 251-258.

Harris, A.W.; Young, J.W.; Bowell, E.; Martin, L.J.; Millis, R.L.; Poutanen, M.; Scaltriti, F.; Zappala, V.; Schober, H.J.; Debehogne, H.; Zeigler, K. (1989). "Photoelectric Observations of Asteroids 3, 24, 60, 261, and 863." *Icarus* **77**, 171-186.

Harris, A.W.; Pravec, P.; Galad, A.; Skiff, B.A.; Warner, B.D.; Vilagi, J.; Gajdos, S.; Carbognani, A.; Hornoch, K.; Kusnirak, P.; Cooney, W.R.; Gross, J.; Terrell, D.; Higgins, D.; Bowell, E.; Koehn, B.W. (2014). "On the maximum amplitude of harmonics on an asteroid lightcurve." *Icarus* **235**, 55-59.

JPL (2019). Small Body Database Browser.
http://ssd.jpl.nasa.gov/sbdb.cgi

Warner, B.D. (2012). *The MPO Users Guide: A Companion Guide to the MPO Canopus/PhotoRed Reference Manuals*. BDW Publishing, Colorado Springs, CO.

Warner, B.D. (2018). MPO Software, *MPO Canopus* v10.7.12.2. Bdw Publishing. *http://bdwpublishing.com*

Warner, B.D.; Harris, A.W.; Pravec, P. (2009). "The Asteroid Lightcurve Database." *Icarus* **202**, 134-146. Updated 2020 Oct 22.
http://www.minorplanet.info/lightcurvedatabase.html

LIGHTCURVE BASED ROTATIONAL PERIOD FOR ASTEROIDS 1995 WZ41 AND 99942 APOPHIS

Pablo Loera-González, Lorenzo Olguín & Julio Saucedo-Morales
Departamento de Investigación en Física
Universidad de Sonora
Hermosillo, Sonora, México
pablo.loera@unison.mx

Ramona Núñez-López
Departamento de Física, Matemáticas e Ingeniería
Universidad de Sonora, Unidad Regional Norte
Caborca, Sonora, México

Rafael Domínguez-González
Hermosillo, Sonora, México

(Received: 2021 April 14, Revised: 2021 May 2)

Asteroids (21242) 1995 WZ41 and 99942 Apophis were studied during the late 2020 and early 2021 at the Observatorio Estelar Carl Sagan at Universidad de Sonora. We obtained for the former a period P = 5.4534 ± 0.0002 h and A = 0.56 mag, and for the later P = 30.4966 ± 0.0033 h and A = 0.63 mag.

Results from observations taken from October 2020 to April 2021 are presented. All observations were taken with EOCS 16-inch SCT telescope and a SBIG ST9 CCD. Images are unfiltered and had exposure time adjusted between 120 s and 240 s according to the object's brightness at the observing date. During the observation season we chose two asteroids: main belt 1995 WZ41 and NEA 99942 Apophis, the later as part of our collaboration with the 99942 Apophis 2021 observing campaign from the International Asteroid Warning Network. Images were reduced in a typical bias-dark-flat manner and photometric measurements conducted on *MPO Canopus* version 10.7.3.0 (Warner, 2017).

(21242) 1995 WZ41 is a main-belt asteroid discovered on 25 November 1995 by Ueda and Kaneda at Kushiro (Park and Chamberlain, 2021). This asteroid was observed during six nights between 23 October 2020 and 7 January 2021. A 4th order fit was used to obtain a result of P = 5.4534 ± 0.0002 h and A = 0.56 mag. The resulting lightcurve shows a two maxima and two minima structure typical of an ellipsoidal body. While the two maximum points are fairly equal (the second one looks somewhat lower but the scatter of data points blurs the distinction), the minima show difference having the second less pronounced than the first. Two "shoulders" can be seen at the 0.3 and 0.9 mark of the period but it is unclear if they are a feature of the lightcurve or just an effect of noise. We encourage further observations at better observing conditions to improve the quality of the lightcurve and reduce data dispersion. This result is similar to the one obtained by Zeigler (2021) of P = 5.456 ± 0.01 h and A = 0.47 mag which was the only period we found published.

Number	Name	20yy mm/dd	Phase	L_{PAB}	B_{PAB}	Period(h)	P.E.	Amp	A.E.	Grp
21242	1995 WZ41	20-21 10/23-01/07	*19.8,26.6	57.7	-4.3	5.4534	0.0002	0.56	0.10	MB
99942	Apophis	21 02/18-03/20	*25.8,45.3	154.4	-11.1	30.4966	0.0033	0.63	0.10	ATEN

Table I. Observing circumstances and results. The phase angle is given for the first and last date. If preceded by an asterisk, the phase angle reached an extrema during the period. L_{PAB} and B_{PAB} are the approximate phase angle bisector longitude/latitude at mid-date range (see Harris et al., 1984). Grp is the asteroid family/group (Warner et al., 2009).

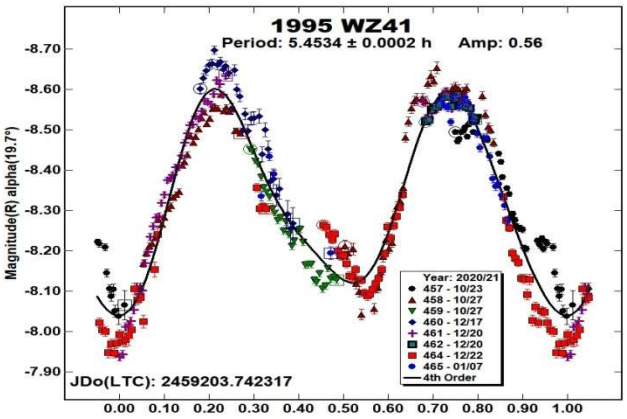

99942 Apophis. This Aten near-Earth asteroid (NEA) was observed in 2021 March 18 to April 20. A total of 70 h was used to obtain a lightcurve with P = 30.4966 ± 0.0033 h in a 2nd order fit. It must be noted that the light curve is not complete as it lacks coverage around the 0.60 mark of the period, regardless, all other data points fall within the expected tendency of the lightcurve. The lightcurve shows a typical two maxima and two minima for an ellipsoidal body. The difference between the second maximum and minimum is larger (0.6 mag) than between the first pair (0.5 mag). Our result is similar to others published by Beherend (2005) with 30.57 ± 0.01 h, Oey (2014) had 30.53 ± 0.05 h, Pravec et al. (2014) at 30.56 h and Warner (2021) 30.67 ± 0.06 h.

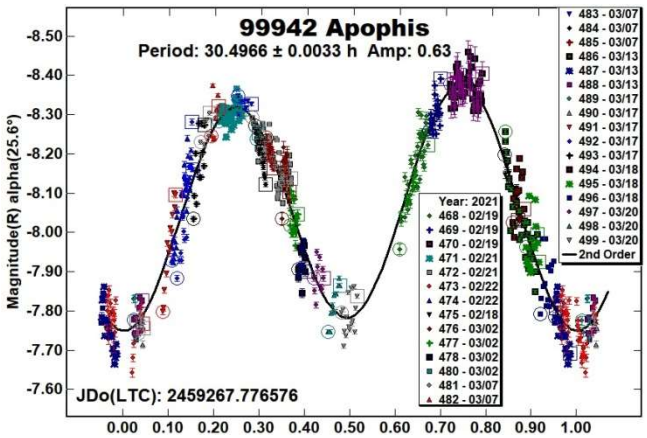

References

Beherend, R. (2005). Observatoire de Geneve web site. *https://obswww.unige.ch/~behrend/r099942a.png*

Harris, A.W.; Young, J.W.; Scaltriti, F.; Zappala, V. (1984). "Lightcurves and phase relations of the asteroids 82 Alkmene and 444 Gyptis." *Icarus* **57**, 251-258.

Oey, J. (2014). "Lightcurve Analysis of Asteroids from Blue Mountains Observatory in 2013." *Minor Planet Bulletin* **41-4**, 276-281.

Park, R.S.; Chamberlain, A.B. (2021) JPL Small-body database browser. *https://ssd.jpl.nasa.gov/sbdb.cgi?sstr=1995%20WZ41;orb=0;cov=0;log=0;cad=0#discovery*

Pravec, P.; Scheirich, P.; Ďurech, J.; Pollock, J.; Kušnirák, P.; Hornoch, K.; Galád, A.; Vokrouhlický, D.; Harris, A.W.; Jehin, E.; Manfroid, J.; Opitom, C.; Gillon, M.; Colas, F.; Oey, J.; Vraštil, J.; Reichart, D.; Ivarsen, K.; Haislip, J.; LaCluyze, A. (2014). "The tumbling spin state of (99942) Apophis." *Icarus* **233**, 48-60.

Warner, B.D.; Harris, A.W.; Pravec, P. (2009). "The Asteroid Lightcurve Database." *Icarus* **202**, 134-146. Updated 2020 Oct. 22. *http://www.minorplanet.info/lightcurvedatabase.html*

Warner, B.D. (2017). MPO Canopus software. *http://bdwpublishing.com*

Warner, E.; Wells, G.; Bamberger, D. (2021). IAWN 99942 Apophis 2021 Observing Campaing website. *https://iawn.net/obscamp/Apophis/apophis_gallery.shtml*

Ziegler, K. (2021). "CCD Photometric Observations of Asteroids 4493 Naitomitsu, (21242) 1995 WZ41, (68130) 2001 AO17, and (183230) 2002 TC58." *Minor Planet Bulletin* **48-2**, 123-124.

ROTATIONAL PERIOD AND LIGHTCURVE DETERMINATION OF 3390 DEMANET AND (18640) 1998 EF9

Alfonso Noschese
AstroCampania Associazione, Naples, Italy
Osservatorio Salvatore Di Giacomo (L07)
Via Salvatore Di Giacomo 7b, 80051
Agerola (Na) ITALY
and
Osservatorio Elianto (K68)
via V. Emanuele III, 95, 84098
Pontecagnano (SA) Italy
a.noschese@astrocampania.it

Antonio Vecchione
AstroCampania ETS, Naples, ITALY
Osservatorio Salvatore Di Giacomo (L07)
Via Salvatore Di Giacomo 7b, 80051
Agerola (Na) ITALY

(Received: 2021 Apr 13)

Photometric observations of two asteroids were performed in order to acquire lightcurves and to determine the rotational periods. The synodic period and lightcurve amplitude were found for 3390 Demanet and (18640) 1998 EF9

This asteroid photometry campaign was carried on by Amateur Astronomers belonging to AstroCampania Association. The targets were selected mainly in order to acquire lightcurves to determine rotational periods not reported before. All the images reported here were unbinned with no filter and had master flats and darks applied. The exposure time depended upon various experimental conditions such as magnitude of the target, sky motion, and Moon illumination. Image processing, measurement, and period analysis were done using *MPO Canopus* (Warner, 2019), which incorporates the Fourier analysis algorithm (FALC) developed by Harris (Harris et al., 1989). The Comp Star Selector feature in *MPO Canopus* was used to limit the comparison stars to near solar color. Night-to-night calibration was done using field stars from the ATLAS catalog (Tonry et al., 2018).

Observations of 3390 Demanet and (18640) 1998 EF9 were performed at Elianto Observatory (K68) located in the south of Italy (Pontecagnano) using a 0.3-m Newton telescope operating at *f*/4 equipped with a Moravian KAF1603 ME CCD camera (1536×1024 array of 9-micron pixels) with a clear filter.

(3390) Demanet was discovered on 1984 March 2 by H. Debehogne at La Silla. It is a main-belt asteroid with a semi-major axis of 2.25 AU, orbital period of 3.4 years, eccentricity of 0.115, and inclination of 3.389 deg. This asteroid has an estimated diameter of 5.1 kilometers and an absolute magnitude of 13.3 (JPL, 2021). There were no previous lightcurve entries in the LCDB for this this asteroid. CCD photometric observations were performed between 2021 February 15 and March 4. Thirteen observation sessions produced 638 data points for lightcurve analysis. Exposure times ranged from 360 s to 420 s. Our observations led to a well-defined period of 2.5946 ± 0.0002 h with an amplitude of 0.17 mag.

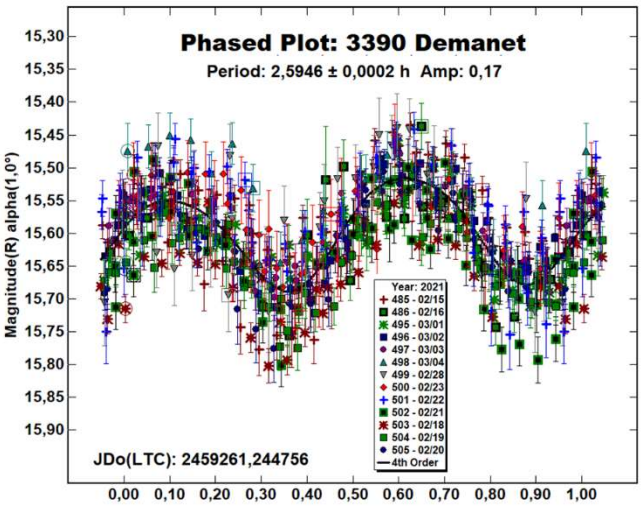

(18640) 1998 EF9 is a main belt asteroid, discovered by Beijing Schmidt CCD Asteroid Program at Xinglong on 1998 March 7. It has a semi-major axis of 2.429 AU, orbital period of 3.79 years, eccentricity of 0.296, and inclination of 20.375 deg. This about 6.7 kilometers body has an absolute magnitude of 13.23 and a geometric albedo of 0.271. No rotational period and lightcurve were reported for this object at the best of our knowledge (JPL, 2021). A total of 124 lightcurve data points were collected in three observing sessions between 2021 January 16-26, with 360 s exposure times. Our observations led to period of 3.6301 ± 0.0003 h with an amplitude of 0.63 mag.

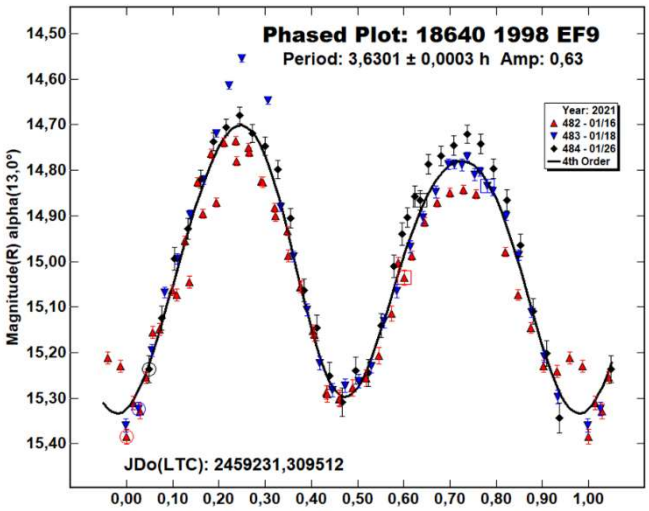

Number	Name	20yy mm/dd	Pts	Phase	L_{PAB}	B_{PAB}	Period(h)	P.E.	Amp	A.E.	Grp
3390	Demanet	21/02/15-21/03/04	638	1.03,8.69	149	1	2.5946	0.0002	0.17	0.02	MB
18640	1998 EF9	21/01/16-21/01/26	124	13.00,18.11	107	16	3.6301	0.0003	0.63	0.02	MB

Table I. Observing circumstances and results. The phase angle is given for the first and last date. L_{PAB} and B_{PAB} are the approximate phase angle bisector longitude and latitude at mid-date range (Harris *et al.*, 1984). Grp is the asteroid family/group (Warner et al., 2009).

References

Harris, A.W.; Young, J.W.; Scaltriti, F.; Zappala, V. (1984). "Lightcurves and phase relations of the asteroids 82 Alkmene and 444 Gyptis." *Icarus* **57**, 251-258.

Harris, A.W.; Young, J.W.; Bowell, E.; Martin, L.J.; Millis, R.L.; Poutanen, M.; Scaltriti, F.; Zappala, V.; Schober, H.J.; Debehogne, H.; Zeigler, K.W. (1989). "Photoelectric Observations of Asteroids 3, 24, 60, 261, and 863." Icarus **77**, 171-186.

JPL (2021). Small-Body Database Browser. *https://ssd.jpl.nasa.gov/sbdb.cgi*

Tonry, J.L.; Denneau, L.; Flewelling, H.; Heinze, A.N.; Onken, C.A.; Smartt, S.J.; Stalder, B.; Weiland, H.J.; Wolf, C. (2018). "The ATLAS All-Sky Stellar Reference Catalog." *Astrophys. J.* **867,** A105, 1-16.

Warner, B.D.; Harris, A.W.; Pravec, P. (2009). "The Asteroid Lightcurve Database." Icarus **202**, 134-146. Updated 2020 Ocotber. *http://www.minorplanet.info/lightcurvedatabase.html*

Warner, B.D. (2019). MPO Software. MPO Canopus version 10.8.1.1. Bdw Publishing. *http://minorplanetobserver.com*

ROTATION PERIOD DETERMINATION FOR ASTEROIDS 2243 LONNROT, (10859) 1995 GJ7, (18640) 1998 EF9 AND (49483) 1999 BP13

Alessandro Marchini, Leonardo Cavaglioni,
Chiara Angelica Privitera
Astronomical Observatory, DSFTA - University of Siena (K54)
Via Roma 56, 53100 - Siena, ITALY
marchini@unisi.it

Riccardo Papini, Fabio Salvaggio
Wild Boar Remote Observatory (K49)
San Casciano in Val di Pesa (FI), ITALY

(Received: 2021 April 6)

Photometric observations of four main-belt asteroids were conducted in order to determine their synodic rotation periods. For 2243 Lonnrot we found P = 3.813 ± 0.004 h, A = 0.14 ± 0.05 mag; for (10859) 1995 GJ7 we found P = 2.956 ± 0.001 h, A = 0.17 ± 0.05 mag; for (18640) 1998 EF9 we found P = 3.630 ± 0.001 h, A = 0.63 ± 0.02 mag; for (49483) 1999 BP13 we found P = 6.365 ± 0.005 h, A = 0.24 ± 0.03 mag.

CCD photometric observations of four main-belt asteroids were carried out in 2021 January - March at two Italian observatories. At the Astronomical Observatory of the University of Siena (K54), a facility inside the Department of Physical Sciences, Earth and Environment (DSFTA, 2021), we used a 0.30-m *f*/5.6 Maksutov-Cassegrain telescope, SBIG STL-6303E NABG CCD camera, and clear filter; the pixel scale was 2.30 arcsec when binned at 2×2 pixels and all exposures were 300 seconds. At the Wild Boar Remote Observatory (K49) data were obtained with a 0.235-m f/10 (SCT) telescope, a SBIG ST8-XME NABG CCD camera unfiltered; the pixel scale was 1.60 arcsec in binning 2×2 and all exposures were 300 seconds.

Data processing and analysis were done with *MPO Canopus* (Warner, 2018). All images were calibrated with dark and flat-field frames and the instrumental magnitudes converted to R magnitudes using solar-colored field stars from a version of the CMC-15 catalogue distributed with *MPO Canopus*. Table I shows the observing circumstances and results.

A search through the asteroid lightcurve database (LCDB; Warner et al., 2009) indicates that our results may be the first reported lightcurve observations and results for these asteroids.

2243 Lonnrot (1941 SA1) was discovered on 1941 September 25 by Y. Vaisala at Turku and named after Elias Lonnrot (1802-1884), a physician in Kajaani and later professor of the Finnish language in Helsinki. [Ref: Minor Planet Circ. 7944] It is a main-belt asteroid with a semi-major axis of 2.248 AU, eccentricity 0.197, inclination 6.843°, and an orbital period of 3.37 years. Its absolute magnitude is H = 12.5 (JPL, 2021). The WISE/NEOWISE satellite infrared radiometry survey (Masiero et al., 2014) found a diameter D = 8.628 ± 0.113 km using an absolute magnitude H = 12.8.

Observations were conducted over two nights and collected 106 data points. The period analysis shows a possible solution for the rotational period of P = 3.813 ± 0.004 h with an amplitude A = 0.14 ± 0.05 mag as the most likely bimodal solution for this asteroid. The asteroid crossed by serendipity the same field of

(10859) 1995 GJ7 on March 21 and 23, therefore exposure was not optimized for its magnitude. Despite this and the few data points collected, the model fit is quite good. Further observations are strongly encouraged to nail down the actual period.

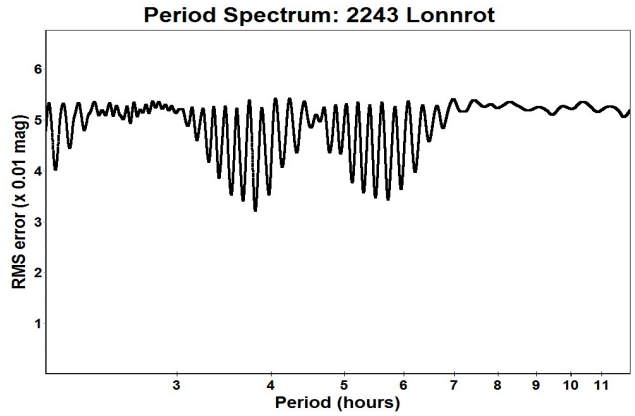

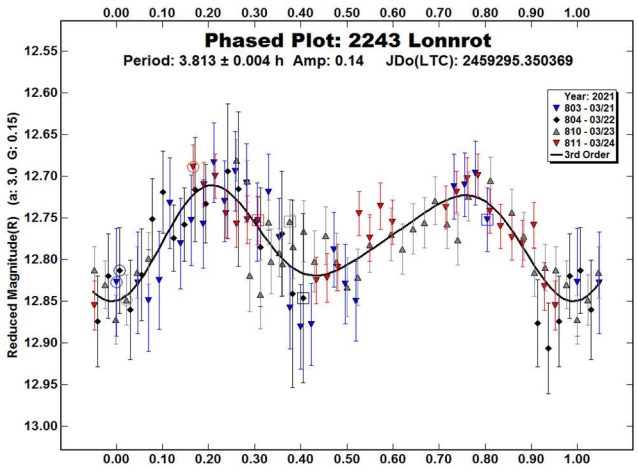

(10859) 1995 GJ7 was discovered on 1995 April 1 by S. Otomo at Kiyosato. It is a main-belt asteroid with a semi-major axis of 2.658 AU, eccentricity 0.158, inclination 9.221°, and an orbital period of 4.33 years. Its absolute magnitude is H = 12.87 (JPL, 2021). The WISE/NEOWISE satellite infrared radiometry survey (Masiero et al., 2012) found a diameter D = 7.758 ± 1.109 km using an absolute magnitude H = 12.80.

Observations over five nights collected 224 data points. The period analysis shows a bimodal solution for the rotational period of P = 2.956 ± 0.001 h with an amplitude A = 0.17 ± 0.05 mag.

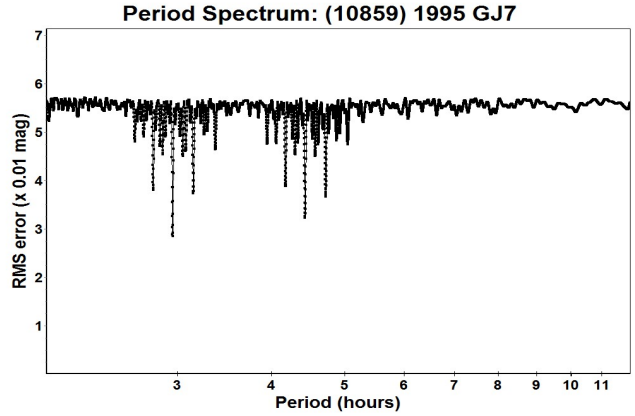

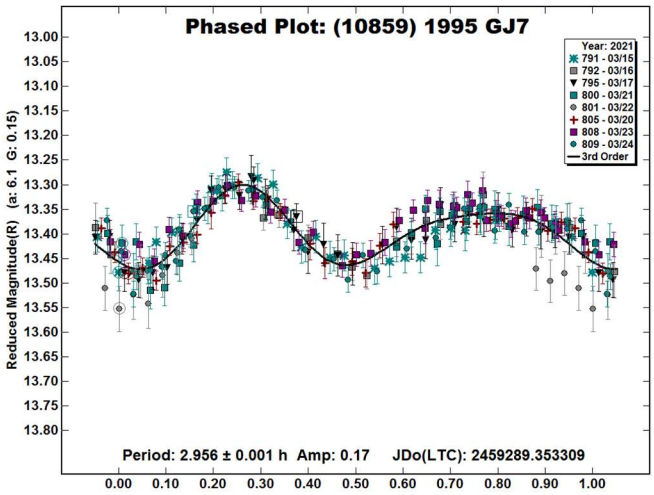

(18640) 1998 EF9 was discovered on 1998 March 7 by Beijing Schmidt CCD Asteroid Program at Xinglong. It is a main-belt asteroid with a semi-major axis of 2.429 AU, eccentricity 0.296, inclination 20.375°, and an orbital period of 3.79 years. Its absolute magnitude is H = 13.23 (JPL, 2021). The WISE/NEOWISE satellite infrared radiometry survey (Masiero et al., 2011) found a diameter D = 6.727 ± 0.060 km using an absolute magnitude H = 12.9.

Observations were conducted over four nights and collected 87 data points. The period analysis shows a result for the rotational period of P = 3.630 ± 0.001 h with an amplitude A = 0.63 ± 0.02 mag.

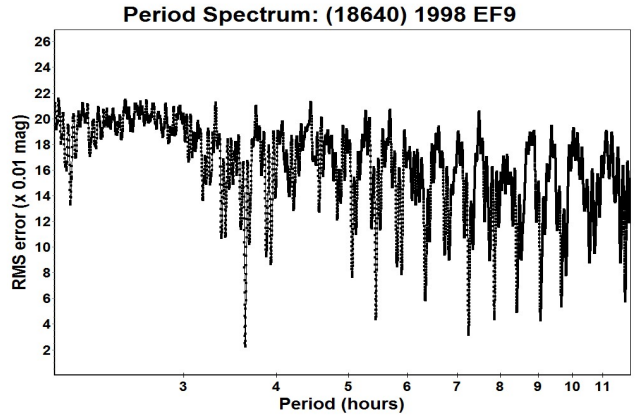

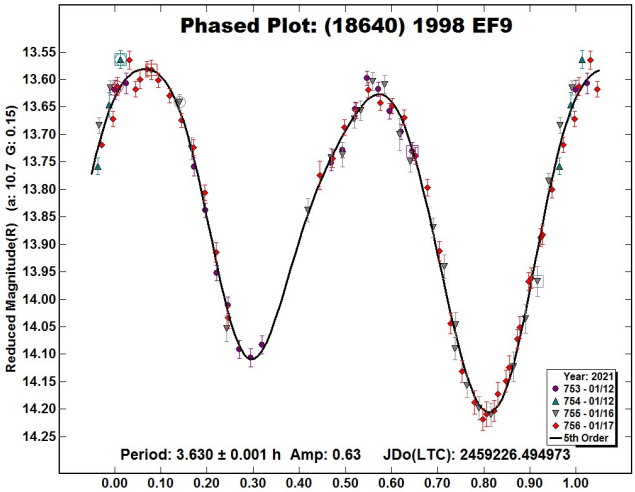

(49483) 1999 BP13 was discovered on 1999 January 25 by K. Korlevic at Visnjan. It is a main-belt asteroid with a semi-major axis of 2.691 AU, eccentricity 0.233, inclination 6.634°, and an orbital period of 4.42 years. Its absolute magnitude is H = 13.15 (JPL, 2021). The WISE/NEOWISE satellite infrared radiometry survey (Masiero et al., 2011) found a diameter D = 13.046 ± 0.841 km using an absolute magnitude H = 13.1.

Observations over two nights collected 144 data points. The period analysis shows a solution for the rotational period of P = 6.365 ± 0.005 h with an amplitude A = 0.24 ± 0.03 mag.

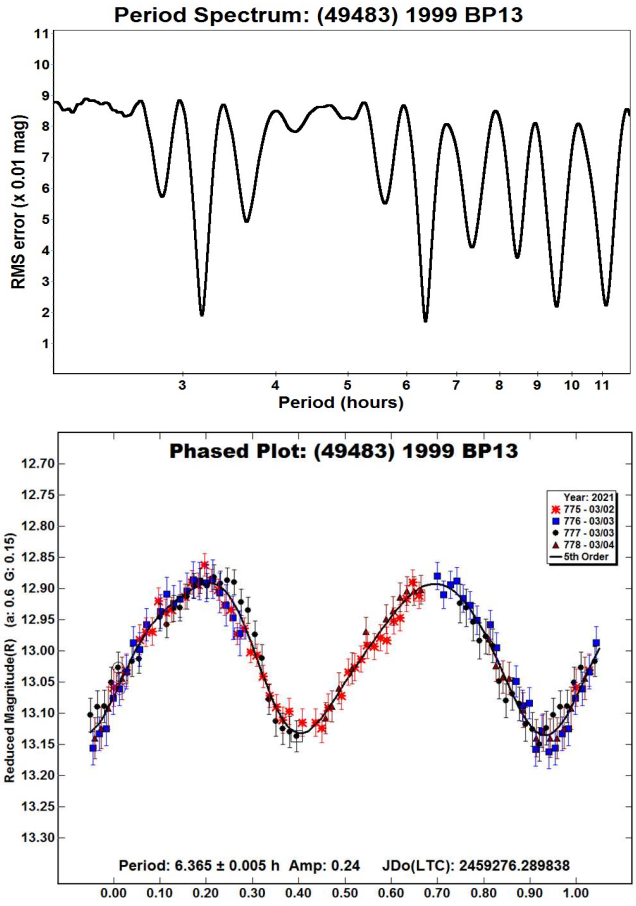

Acknowledgements

Leonardo Cavaglioni and Chiara Angelica Privitera, students of the course in Physics and Advanced Technologies at the Department of Physical Sciences, Earth and Environment, actively participated to the observations and data analysis of some asteroids presented in this article during their internship activities at the Astronomical Observatory of the University of Siena, and appear deservedly as authors. Minor Planet Circulars (MPCs) are published by the International Astronomical Union's Minor Planet Center. *https://www.minorplanetcenter.net/iau/ECS/MPCArchive/MPCArchive_TBL.html*

References

DSFTA (2021). Dipartimento di Scienze Fisiche, della Terra e dell'Ambiente - Astronomical Observatory. *https://www.dsfta.unisi.it/en/research/labs/astronomical-observatory*

Harris, A.W.; Young, J.W.; Scaltriti, F.; Zappala, V. (1984). "Lightcurves and phase relations of the asteroids 82 Alkmene and 444 Gyptis." *Icarus* **57**, 251-258.

JPL (2021). Small-Body Database Browser. *http://ssd.jpl.nasa.gov/sbdb.cgi#top*

Masiero, J.R.; Mainzer, A.K.; Grav, T.; Bauer, J.M.; Cutri, R.M.; Dailey, J.; Eisenhardt, P.R.M.; McMillan, R.S.; Spahr, T.B.; Skrutskie, M.F.; Tholen, D.; Walker, R.G.; Wright, E.L.; DeBaun, E.; Elsbury, D.; Gautier IV, T; Gomillion, S.; Wilkins, A. (2011). "Main Belt Asteroids with WISE/NEOWISE. I. Preliminary Albedos and Diameters." *Astrophys. J.* **741**, A68.

Masiero, J.R.; Mainzer, A.K.; Grav, T.; Bauer, J.M.; Cutri, R.M.; Nugent, C.; Cabrera, M.S. (2012). "Preliminary Analysis of WISE/NEOWISE 3-Band Cryogenic and Post-cryogenic Observations of Main Belt Asteroids." *Astrophys. J. Letters* **759**.

Masiero, J.R.; Grav, T.; Mainzer, A.K.; Nugent, C.R.; Bauer, J.M.; Stevenson, R.; Sonnett, S. (2014). "Main-belt Asteroids with WISE/NEOWISE: Near-infrared Albedos." *Astrophys. J.* **791**, 121.

Warner, B.D.; Harris, A.W.; Pravec, P. (2009). "The Asteroid Lightcurve Database." *Icarus* **202**, 134-146. Updated 2020 Oct. *http://www.minorplanet.info/lightcurvedatabase.html*

Warner, B.D. (2018). MPO Software, *MPO Canopus* v10.7.7.0. Bdw Publishing. *http://minorplanetobserver.com*

Number	Name	2021/mm/dd	Phase	L_{PAB}	B_{PAB}	Period(h)	P.E.	Amp	A.E.	Grp
2243	Lonnrot	03/21-03/24	3.0,2.1	187	3	3.813	0.004	0.14	0.05	MB
10859	1995 GJ7	03/15-03/24	6.2,2.1	186	3	2.956	0.001	0.17	0.05	MB
18640	1998 EF9	01/11-01/18	10.7,13.5	105	-14	3.630	0.001	0.63	0.02	MB
49483	1999 BP13	03/02-03/04	0.5,1.2	161	-1	6.365	0.005	0.24	0.03	MB

Table I. Observing circumstances and results. The first line gives the results for the primary of a binary system. The second line gives the orbital period of the satellite and the maximum attenuation. The phase angle is given for the first and last date. If preceded by an asterisk, the phase angle reached an extrema during the period. L_{PAB} and B_{PAB} are the approximate phase angle bisector longitude/latitude at mid-date range (see Harris *et al*., 1984). Grp is the asteroid family/group (Warner *et al*., 2009).

LIGHTCURVE AND ROTATION PERIOD OF THE TUMBLING ASTEROID 1513 MATRA

Frederick Pilcher
Organ Mesa Observatory
4438 Organ Mesa Loop
Las Cruces, NM 88011 USA
fpilcher35@gmail.com

Vladimir Benishek
Belgrade Astronomical Observatory
Volgina 7, 11060 Belgrade 38, SERBIA

(Received: 2021 Mar 30)

Minor planet 1513 Matra is tumbling with a main period of 117.6 ± 0.1 h, maximum amplitude 0.67 ± 0.02 mag, and second period near 92.3 h.

To obtain the data for this investigation, Pilcher at the Organ Mesa Observatory used a Meade 35-cm LX200 GPS Schmidt-Cassegrain, SBIG STL-1001E CCD, clear filter, 120 second exposure times, unguided. Benishek used a Meade 35-cm LX 200 Schmidt-Cassegrain telescope with SBIG ST-8XME and SBIG ST-10XME CCDs, exposure times from 120 to 240 seconds, clear filter, unguided. Image photometric measurement and lightcurve construction were done by *MPO Canopus* software. Calibration stars of near solar colors were selected from the CMC15 catalog. Because the internal consistency of magnitudes in the GAIA 2 catalog is better than in the CMC15, the magnitudes of all calibration stars were converted to the G magnitude system in the GAIA 2 catalog as presented on the VizieR web site.

Previously published periods of 1513 Matra are by Binzel and Mulholland (1983, >24 h) and by Rowe (2019, 34.8 h). After the first several sessions by Pilcher, it became clear that the lightcurve did not repeat with any one period and, therefore, that 1513 Matra was tumbling. At this time Benishek kindly accepted Pilcher's invitation to collaborate. A total of 32 sessions 2021 Jan. 18 - March 20 were obtained by the two observers. Petr Pravec kindly analyzed the data with simultaneous dual-period software that includes the ability to find both the axial rotation period and the precession period for tumbling asteroids. His analysis is the conclusion of this report:

It is definitely a tumbler. The main period of 117.6 h is well determined (uncertainty about 0.1 h), but the second period is less secure. It is likely 92.3 h, but not entirely certain. So, I rate this NPA rotation solution as PAR -2 tending to -3 (see the scale in Pravec et al, 2005). Note that there remain systematics in the residuals, which is because only the Fourier order 2 could be fitted to the data. Higher orders would be needed to explain some small features of the lightcurves, but there are not enough data for a robust fit of higher order 2-period Fourier series.

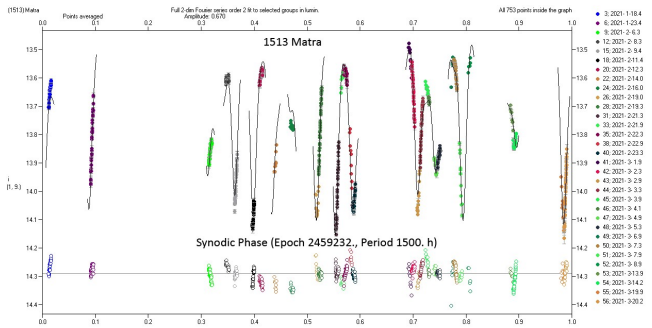

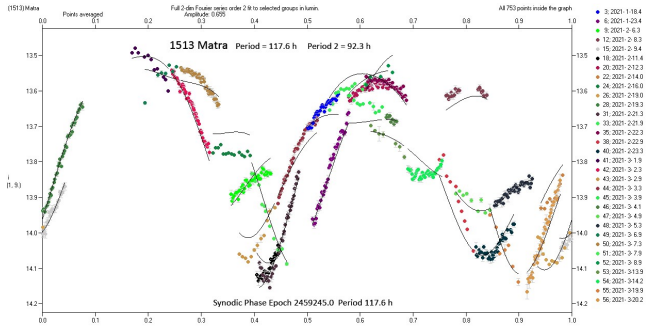

Acknowledgements

The authors thank P. Pravec for permission to publish his unphased and phased lightcurves in this paper.

References

Binzel, R.P.; Mulholland, J.D. (1983). "A photometric lightcurve survey of small main belt asteroids." *Icarus* **56**, 519-533.

Harris, A.W.; Young, J.W.; Scaltriti, F.; Zappala, V. (1984). "Lightcurves and phase relations of the asteroids 82 Alkmene and 444 Gyptis." *Icarus* **57**, 251-258.

Pravec, P.; Harris, A.W.; Scheirich, P.; Kusnirak, P.; Sarounova, L.; Hergenrother, C.W.; Mottola, S.; Hicks, M.D.; Masi, G.; Krugly, Yu.N.; Shevchenko, V.G.; Nolan, M.C.; Howell, E.S.; Kaasalainen, M.; Galad, A.; Brown, P.; Degraff, D.R.; Lambert, J.V.; Cooney, W.R.; Foglia, S. (2005). "Tumbling Asteroids." *Icarus* **173**, 108-131.

Rowe, B. (2019). "Lightcurve analysis of 8 asteroids from RMS Observatory." *Minor Planet Bull.* **46**, 92-94.

VizieR web site. *vizier-u.strasbg.fr/viz-bin/VizieR*

Number	Name	yyyy/mm/dd	Phase	L_{PAB}	B_{PAB}	Period(h)	P.E.	Amp	A.E.
1513	Matra	2021/01/18-2021/03/20	*16.9,17.9	148	1	117.6 92.3	0.1	0.67	0.02

Table I. Observing circumstances and results. The phase angle is given for the first and last date. An asterisk before the phase values indicates that a maximum or minimum was reached during the period. L_{PAB} and B_{PAB} are the approximate phase angle bisector longitude and latitude at mid-date range (see Harris *et al.*, 1984).

DETERMINING THE ROTATIONAL PERIOD OF MAIN-BELT ASTEROID 282 CLORINDE

Roberto Bonamico
BSA Osservatorio (K76)
Strada Collarelle 53
12038 Savigliano, Cuneo, ITALY
info@osservatorioastronomicobsa.it
http://www.osservatorioastronomicobsa.it

Gerard van Belle
Lowell Observatory Anderson Mesa (688)
1400 W Mars Hill Rd, Flagstaff, AZ
gerard@lowell.edu
https://lowell.edu

(Received: 2021 April 15, Revised: 2021 April 25)

Based on CCD photometric observations of the main-belt asteroid 282 Clorinde, we report the results of the lightcurve analysis: P = 49.353 ± 0.004 h, A = 0.26 mag.

In the framework of the asteroid scientific project that is called "Investigating the most ancient asteroids" (*http://users.uoa.gr/~kgaze/research_asteroids_en.html*), we obtained time resolved photometry of the asteroid 282 Clorinde.

Thanks to the integration of the data obtained from the measurements obtained at two astronomical observatories: Astronomical Observatory BSA and Lowell Observatory Anderson Mesa, it was possible to observe Clorinde for a long interval, namely from 26 November 2020 to 06 March 2021. From all of these data sessions, we obtained almost complete coverage of the phase angle range between 9.6 and 27.3 degrees. The equipment and the respective sessions by each author are reported in Table I. The calibration stars were: For Astronomical Observatory BSA; catalog CMC15; for Lowell Observatory Anderson Mesa; from the Panstarrs_transformed catalog.

Sessions from the several individual observers were adjusted vertically for best fit. The resulting period becomes P = 49.352 h and the lightcurve amplitude A = 0.26. These results differ substantially from previous published ones: Behrend (*http://obswww.unige.ch/~behrend/page_cou.html*) P = 12.142 h, and Binzel and Mulholland (1983) P = 6.42 h.

Observer Observatory (MPC code)	Telescope	CCD	F	Sessions
Roberto Bonamico Osservatorio Astronomico BSA (K76)	0.30-m NRT f/5	ATIK 314L+	C	302, 313
Gerard van Belle Lowell Observatory Anderson Mesa (688)	PW1000 1-m CDK	FLI ML16803	C	274, 299

Table I. Observing equipment and sessions. NRT: Newtonian Reflector, CDK: Corrected Dall Kirkham.

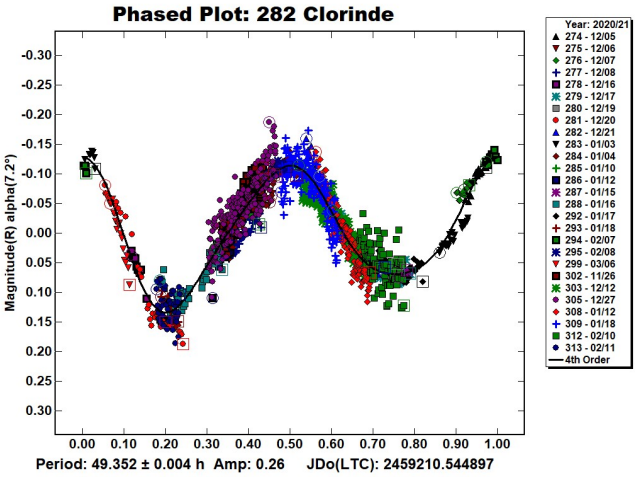

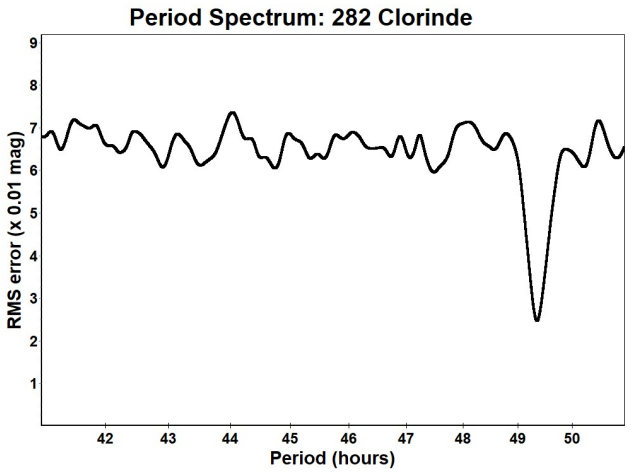

References

Binzel, R.P.; Mulholland, J.D. (1983). "A photoelectric lightcurve survey of small main belt asteroids." *Icarus*, **56**, 519-533. *https://doi.org/10.1016/0019-1035(83)90170-7*

Harris, A.W.; Young, J.W.; Scaltriti, F.; Zappala, V. (1984). "Lightcurves and phase relations of the asteroids 82 Alkmene and 444 Gyptis." *Icarus* **57**, 251-258.

Warner, B.D.; Harris, A.W.; Pravec, P. (2009). "The Asteroid Lightcurve Database." *Icarus* **202**, 134-146. Updated 2021 04 13. *http://www.minorplanet.info/lightcurvedatabase.html*

Number	Name	yyyy mm/dd	Phase	L_{PAB}	B_{PAB}	Period(h)	P.E.	Amp	A.E.	Grp
282	Clorinde	2020/11/26-2021/03/06	9.6,27.3	81.1	-9.0	49.352	0.004	0.26	0.01	

Table II. Observing circumstances and results. The phase angle is given for the first and last date. If preceded by an asterisk, the phase angle reached an extrema during the period. L_{PAB} and B_{PAB} are the approximate phase angle bisector longitude/latitude at mid-date range (see Harris et al., 1984). Grp is the asteroid family/group (Warner et al., 2009).

ROTATION PERIOD OF KORONIS FAMILY MEMBER (1442) CORVINA

Stephen M. Slivan
Massachusetts Institute of Technology,
Dept. of Earth, Atmospheric, and Planetary Sciences
77 Mass. Ave. Rm. 54-410, Cambridge, MA 02139
slivan@mit.edu

Francis P. Wilkin
Union College Dept. of Physics and Astronomy
Schenectady, NY

(Received: 2021 April 5)

We report lightcurve observations of (1442) Corvina made during 2021 March. Analysis of our data, together with constraints from survey "sparse" data recorded during the 2019 and the 2020-21 apparitions, yields an unambiguous rotation period of 77.92 ± 0.03 h.

We observed Koronis family member (1442) Corvina as part of an ongoing program to study rotation properties of the family's brighter objects (Slivan et al., 2008). In the literature we find no rotation period information for Corvina, making it the largest Koronis member lacking any period determination. Four nights of inconclusive unpublished relative photometry from near sea level in New England in 2012 did not show a clear brightness variation, suggesting a long period or a small amplitude.

To test for a long-period lightcurve of detectable amplitude we observed Corvina near its western stationary point in 2021 March, specifically to permit using the same on-chip field comparison stars over a series of nights, although it also limited the length of single-night spans of observability to about 5 h. Our observations were made on 9 nights over an 11-night interval (Table I) remotely using two telescopes operated by Telescope Live: SPA-2 in Oria, Spain, and CHI-1 in the Rio Hurtado Valley, Chile; details about both systems are summarized in Table II. A Sloan *r'* filter was used for all images, and image processing and measurement were as described by Slivan et al. (2008). To reduce systematic differences in the zero-points of our relative photometry from the two different detectors, we specifically chose comparison stars having similar color to Corvina's B-V = 0.87 ± 0.03 (Tedesco, 1989) based on the stars' photometry in the APASS DR10 catalog. Inter-comparison of the stars' brightnesses on our images confirmed no significant variation during our observing program.

UT date 2021	Tel. ID	Num. vis.	Obs. span (h)	SPA (°)	SPA corr. (mag)
Mar 11	SPA-2	1	0.36	15.3	0.000
Mar 12	SPA-2	1	0.36	15.5	-0.007
Mar 13	SPA-2	1	0.36	15.7	-0.014
Mar 14	SPA-2	1	0.36	15.9	-0.020
Mar 15	SPA-2	2	5.11	16.1	-0.025
Mar 17	SPA-2	1	0.36	16.5	-0.038
Mar 18	SPA-2	3	4.50	16.6	-0.043
Mar 19	CHI-1	1	0.16	16.8	-0.049
Mar 21	SPA-2	1	0.36	17.1	-0.058

Table I: Nightly circumstances. Columns are: UT date, telescope ID, number of observation visits made by the telescope, elapsed time spanned by the night's observations, solar phase angle, and brightness correction applied to correct for the change in solar phase angle since Mar 11.

Tel. ID	Dia. (m)	CCD camera	FOV (′)	Bin	Scale (″/pix)	Int. (s)
SPA-2	0.7	FLI-PL16803	29×29	2×2	0.86	120
CHI-1	0.6	FLI-PL9000	32×32	1×1	0.62	240

Table II: Telescopes and cameras information. Columns are: telescope ID, telescope diameter, CCD camera, detector field of view, image binning used, image scale, and image integration time used.

We reduced our Corvina observations for light-time and to unit distances, and for changing solar phase angle using the MPC adopted value of G = 0.15 for the slope parameter. The reduced photometry shows an overall brightness variation of about 0.2 mag which we conclude is due to the amplitude of Corvina's rotation lightcurve.

To identify candidate rotation periods, we used a "noise spectrum" approach, fitting a Fourier series model including through the 2nd harmonic to the observations to test a range of trial rotation periods. The search low bound is 18 h, which we estimate as the shortest period for a doubly-periodic lightcurve consistent with the 4.5-h span of (very slowly) increasing brightness that we detected on Mar 18. The search high bound is 300 h which is 2.5× the longest-period local minimum that we found at about 120 h. The resulting graph (Fig. 1, upper graph) shows four local minima candidate periods corresponding to roughly 0.4, 0.6, 1.4, and 1.6 half-rotations per day, all of which we individually confirmed are consistent with doubly-periodic lightcurves by inspection of the folded composites.

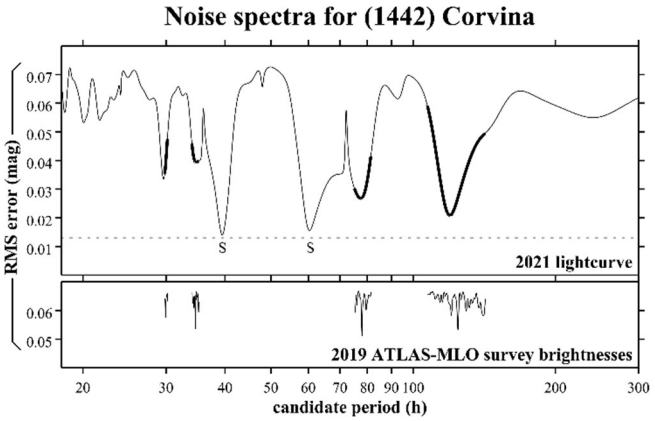

Figure 1. "Noise spectrum" graphs from fitting Fourier series models including through the 2nd harmonic, separately to two independent sets of photometry of (1442) Corvina. The upper graph shows the result from fitting to our 2021 lightcurve data, where the horizontal dashed line at 0.013 mag marks the mean of the nightly error bars on the photometry. The four ranges of periods that correspond to self-consistent doubly-periodic composites are highlighted in bold on the graph; the two remaining local minima marked "S" correspond to singly-periodic composites and were not further considered. The lower graph shows the result from fitting to ATLAS-MLO survey *o*-band brightnesses recorded during Corvina's 2019 apparition for the ranges identified by the upper graph, which refines the candidate periods.

Our data favor the two longer candidate periods over the two shorter ones, but in hopes of conclusively distinguishing which of the four is the true period we checked the asteroid brightness data that are publicly available online from the MPC astrometry Web site for additional observations. There we found suitable observations of Corvina from the ATLAS astrometric survey (Tonry et al., 2018), sparse in time but calibrated to a common brightness zero-point and available from both the 2019 and the 2020-21 apparitions. It is the

2019 ATLAS-MLO *o*-band data that have the most observations and cover the longest time span. We reduced those data for light-time and to unit distances, and for changing solar phase angle using a slope parameter value $G_o = 0.146$ which we obtained by fitting the Lumme-Bowell model to the reduced magnitudes. Fitting a 2nd-order Fourier series model to the reduced data for the period ranges determined from the 2021 lightcurves refines the candidate periods (Fig. 1, lower graph), but does not resolve the true period from the aliases because the photometry errors of about 0.04-0.05 mag limit the detectable level of self-inconsistency in the composite lightcurves.

Although ATLAS-MLO made fewer observations of Corvina during the following apparition in 2020-21 than it did during 2019, the later data still are sufficient for trial folded composite lightcurves. We reduced these data for light-time and to unit distances, reduced for changing solar phase angle using the slope parameter value determined from the 2019 data, and finally shifted the *c*-band data in brightness to composite with the *o*-band data.

We found that these 2020-21 data are less noisy than the 2019 data, enough that self-inconsistency of trial composites rules out the two shortest candidate periods, leaving only one alias still to distinguish from the true period.

There is additional information available from these data – because the longitude of the survey telescope at 156°W is very different from the 2°W longitude of the SPA-2 telescope that we mainly used for our own observations during the same apparition, the two data sets record different points on the rotation phase of Corvina's lightcurve. Thus, even though folding either data set individually at either remaining candidate period gives a self-consistent composite lightcurve, a mismatch in rotation phase of the composites folded at the same period would indicate an alias period. Comparison of the folded rotation phase for the two remaining candidate periods (Fig. 2) rules out 124.44 h, leaving only 77.96 h as being consistent with all of the observations from the 2020-21 apparition.

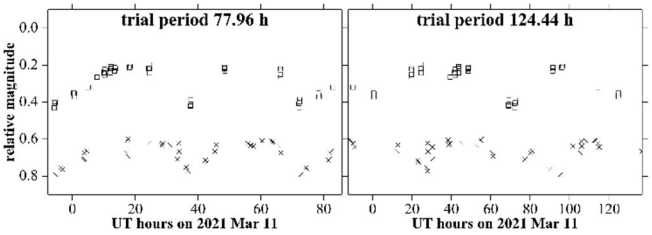

Figure 2. Lightcurves of (1442) Corvina during its 2020–21 apparition, composited to the same date and folded at two trial periods, for two independent sets of photometry: our lightcurve data (□), and ATLAS-MLO *o*-band and *c*-band survey brightnesses (×) combined for presentation. In the left graph folded at 77.96 h both composites share the same rotation phase, while in the right graph folded at 124.44 h the two composites are markedly out of phase, distinguishing that 77.96 h is consistent with the data but 124.44 h is not.

Having resolved the ambiguity in the period, we obtained our final result of 77.92 ± 0.03 h (Fig. 3) by fitting a 4th-order Fourier series model for the period to the combined data from the 2020-21 apparition, and estimated the error by adjusting the trial folding period to check self-consistency of the resulting composites.

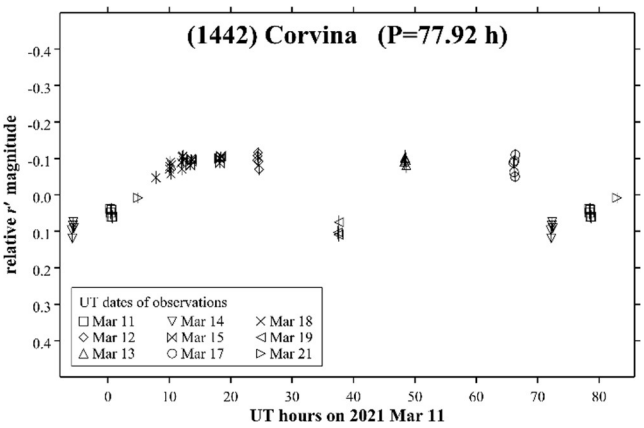

Figure 3. Folded composite lightcurve of (1442) Corvina during its 2020–21 apparition, light-time corrected, showing one rotation period plus the earliest and latest 10% repeated. The relative photometry was measured using the same comparison star on all nine nights; the asteroid brightnesses have been corrected for distance changes, and the solar phase corrections applied are given in Table I. Measurements from the 120-s images have been averaged so that each point on the graph represents an effective integration time of 240 s; the nightly error bars range from 0.008 to 0.018 mag.

Acknowledgments

We thank Marco Rocchetto for assistance with the remote observing. F. Wilkin received funding from the Faculty Research Grant at Union College. This work has made use of the AAVSO Photometric All-Sky Survey (APASS), funded by the Robert Martin Ayers Sciences Fund and NSF AST-1412587. This work also has made use of data and services provided by the International Astronomical Union's Minor Planet Center; specifically, the brightnesses accompanying astrometry from the Asteroid Terrestrial-impact Last Alert System (ATLAS) survey observing program.

References

Slivan, S.M.; Binzel, R.P.; Boroumand, S.C.; Pan, M.W.; Simpson, C.M.; Tanabe, J.T.; Villastrigo, R.M.; Yen, L.L.; Ditteon, R.P.; Pray, D.P.; Stephens, R.D. (2008). "Rotation Rates in the Koronis Family, Complete to $H \approx 11.2$." *Icarus* **195**, 226–276.

Tedesco, E.F. (1989). "Asteroid Magnitudes, UBV Colors, and IRAS Albedos and Diameters." In *Asteroids II* (R.P. Binzel, T. Gehrels, M.S. Matthews, eds.) pp 1090–1138. Univ. Arizona Press, Tucson.

Tonry, J.L.; Denneau, L.; Heinze, A.N.; Stalder, B.; Smith, K.W.; Smartt, S.J.; Stubbs, C.W.; Weiland, H.J.; Rest, A. (2018). "ATLAS: A High-cadence All-sky Survey System." *PASP* **130**, 064505.

Number	Name	yyyy mm/dd	Phase	L_{PAB}	B_{PAB}	Period(h)	P.E.	Amp	A.E.
1442	Corvina	2021 03/11-03/21	15.3,17.1	124	-1	77.92	0.03	0.19	0.02

Table III. Observing circumstances and results. Solar phase angle is given for the first and last dates. L_{PAB} and B_{PAB} are the phase angle bisector longitude and latitude at mid-date range.

ASTEROID PHOTOMETRY FROM THE PRESTON GOTT OBSERVATORY

Dr. Maurice Clark
Department of Physics and Chemistry
Troy University, Troy AL 36801
maclark@troy.edu

(Received: 2021 April 15, Revised: 2021 April 26)

Asteroid period and amplitude results obtained at the Preston Gott Observatory during December 2020 and January 2021 are presented.

During the last week of December 2020 and the first week of January 2021, I was able to spend several nights using the Preston Gott Observatory of the Texas Tech University. Several 12" Schmidt-cassegrain telescopes, with SBIG ST9XE CCDs were used. All images were unfiltered and were reduced with dark frames and twilight sky flats. Image analysis was accomplished using differential aperture photometry with *MPO Canopus*. Period analysis was also done in *MPO Canopus*. Differential magnitudes were calculated using reference stars from the UCAC4 catalog.

Considerable cloudiness severely interfered with the observations; however, some useful results were obtained. These results are summarized in Table I, and the lightcurve plots are presented below. The data and curves are presented without additional comment except were circumstances warrant.

4612 Greenstein. A search of the Asteroid Lightcurve Database did not reveal any previously reported period for asteroid 4612 Greenstein.

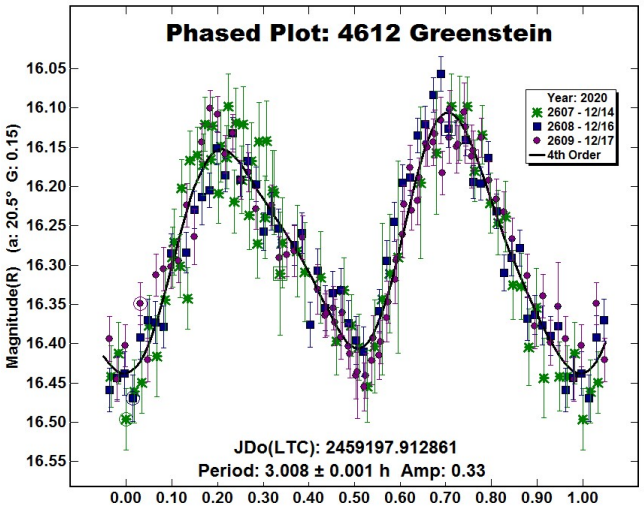

4724 Brocken. Considering that a full lightcurve was not obtained, the period presented in this paper is in reasonable agreement with that found by Klinglesmith, et al. (2013).

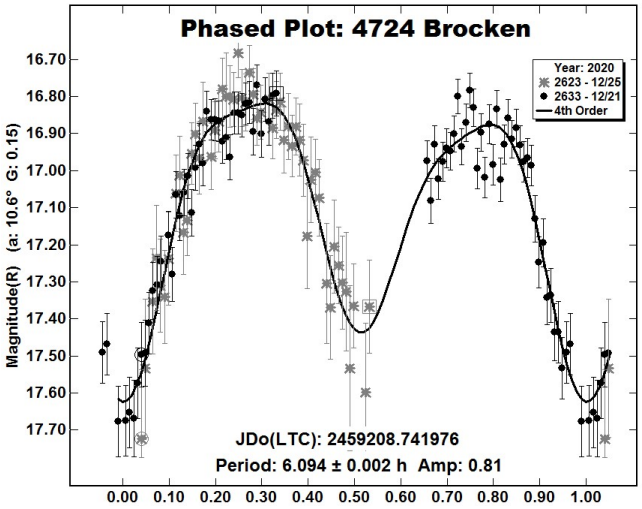

11927 Mount Kent. The lightcurve appeared distinctly asymmetric with one maximum being slightly higher than the other and the rise to that maximum being slightly longer. A search of the Asteroid Lightcurve Database did not reveal any previously reported period for asteroid 11927 Mount Kent.

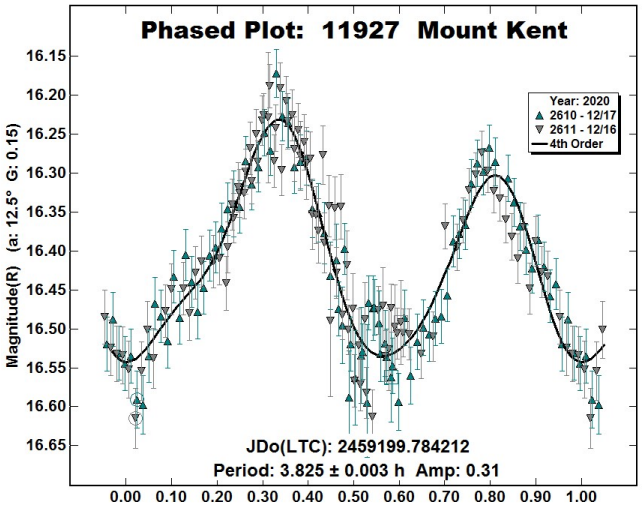

Number	Name	2020 mm/dd	Phase	L_{PAB}	B_{PAB}	Period(h)	P.E.	Amp	A.E.	Grp
4612	Greenstein	12/14-12/17	18.1	126.1	2.5	3.008	0.001	0.33	0.02	MBA
4724	Brocken	12/21-12/25	11.8	117.9	3.2	6.094	0.002	0.81	0.02	MBA
11927	Mount Kent	12/16-12/17	13.8	59.6	-13.7	3.825	0.003	0.31	0.05	MBA
12844	1997 JE10	12/21-12/25	10.5	62	-1.8	6.539	0.003	0.56	0.05	MBA
13614	1994 VF2	12/16-12/20	16.2	114.3	14.5	15.85?	0.04	0.19	0.1	MBA
16435	Fandly	12/16-12/17	20.4	57	-8.8	7.552	0.007	0.37	0.02	MBA
20384	1998 KW51	12/21-12/27	2.9	82	-2.8	6.30	0.01	0.24	0.05	MBA

Table I. Observing circumstances and results. The phase angle is given for the first and last date. L_{PAB} and B_{PAB} are the approximate phase angle bisector longitude and latitude at mid-date range (see Harris *et al.*, 1984). Grp is the asteroid family/group (Warner *et al.*, 2009).

(12844) 1997 JE10. A search of the Asteroid Lightcurve Database did not reveal any previously reported period for asteroid (12844) 1997 JE10.

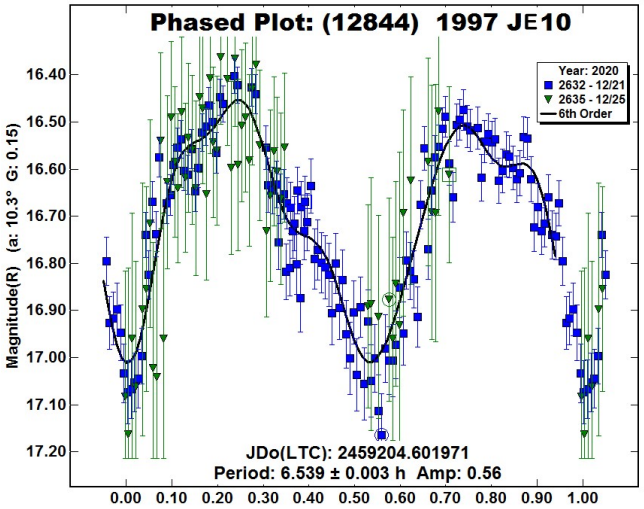

(13614) 1994 VF2. The period presented here is the best that could be derived from the data obtained. However, it is extremely uncertain and probably not correct. A search of the Asteroid Lightcurve Database did not reveal any previously reported period for asteroid (13614) 1994 VF2.

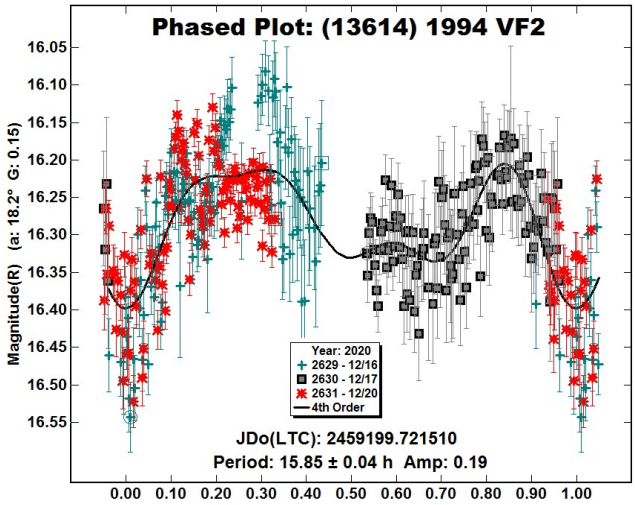

16435 Fandly. A search of the Asteroid Lightcurve Database did not reveal any previously reported period for asteroid 16435 1997 Fandly.

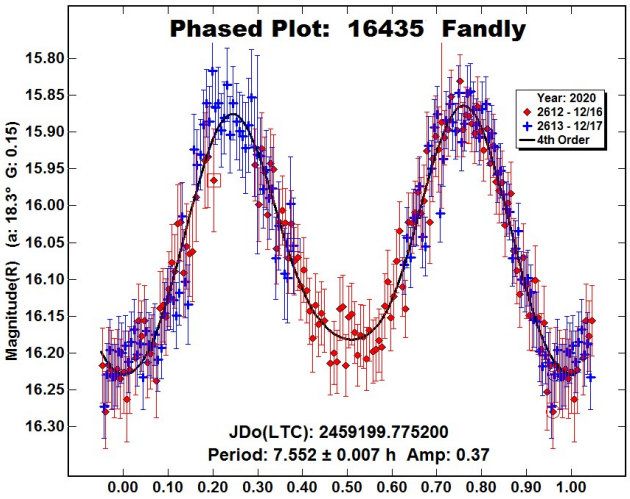

(20384) 1998 KW51. A simple bimodal lightcurve could not be fitted to the data obtained. The result presented here is the best that could be derived and is extremely uncertain. A search of the Asteroid Lightcurve Database did not reveal any previously reported period for asteroid (20384) 1998 KW51.

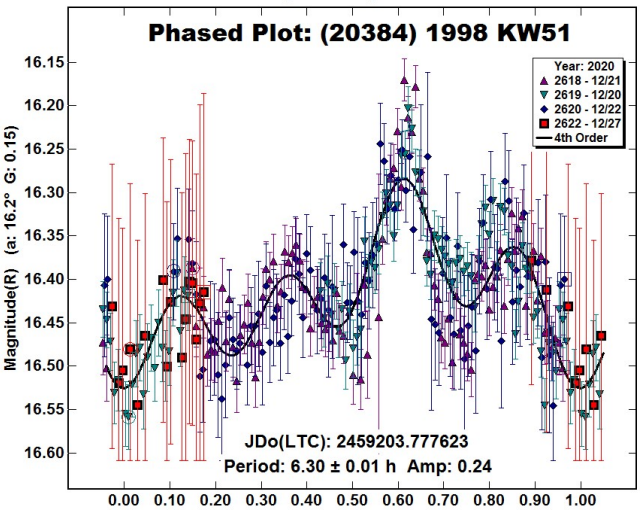

Acknowledgments

I would like to thank Dr Vallia Antoniou for allowing the use of the Preston Gott Observatory for this work, and Brian Warner for all of his work with the program *MPO Canopus* and for his efforts in maintaining the "CALL" website.

References

Harris, A.W.; Young, J.W.; Scaltriti, F.; Zappala, V. (1984). "Lightcurves and phase relations of the asteroids 82 Alkmene and 444 Gyptis." *Icarus* **57**, 251-258.

Klinglesmith, et al. (2013) "Lightcurves for 1394 Algoa, 3078 Horrocks, 4724 Brocken, and 6329 Hikonejyo from Etscorn Campus Observatory." *Minor Planet Bull.* **40**, 16-17.

Warner, B.D.; Harris, A.W.; Pravec, P. (2009). "The Asteroid Lightcurve Database." *Icarus* **202**, 134-146. Updated 2021 04 13. *http://www.minorplanet.info/lightcurvedatabase.html*

LIGHTCURVES OF FOUR ASTEROIDS

Andrea Ferrero
Bigmuskie Observatory (B88)
via Italo Aresca 12
14047 Mombercelli, Asti, ITALY
bigmuskie@outlook.com

(Received: 2021 April 13)

In this paper we present the lightcurves of four main-belt asteroids: 2712 Keaton, P = 3.360 ± 0.001 h, A = 0.18 mag; 4422 Jarre, P = 7.013 ± 0.001 h, A = 0.11 mag; (5343) 1999 RA44, P =590.48 ± 0.46 h, A = 0.57 mag; (49548) 1999 CP83, P = 2.758 ± 0.001 h, A = 0.11 mag.

During the first four months of 2021, the Bigmuskie Observatory focused on finding the rotational period of four main-belt asteroids. All targets were found on the CALL website ephemeris generator (Warner, 2021) and choosen because of am uncertain or no reported period.

Because of the very low brightness of all the targets, well beyond 16 mag and even near 18 mag, observations for (25343) 1999 RA44, were made without a filter in order to achive as good as possible signal-to-noise ratio. The telescope was a Marcon 0.30-m *f*/8 Ritchey-Chretién telescope coupled with a Moravian G3 01000 camera with a KAF-1001E CCD. The pixel array 1024×1024×24 microns provided a scale of exactly 2 arcsec/pixel and a field of view of 36×36 arcmin. Telescope and camera were controlled by *Maxim DL* (Diffraction Limited, 2020) and *The Sky 6 Pro* (Bisque, 2020). *Voyager* (Starkeeper, 2020) controlled the entire observatory. Photometric reductions were done with *MPO Canopus* v 10.7.12.9.(Warner, 2018), which permits obtaining fast results and precise night-to-night zero-point calibration using the Comparison Star Selector utility.

2712 Keaton. A previous period of 5.87 ± 0.04 h measured by Chang et al. (2019) is reported in the LCDB Database. Four observations over a period of about a month starting from February 25 to March 22 led now to a different period of $P = 3.360 \pm 0.001$ h with an amplitude of $A = 0.11$ mag. An attempt to fit the sessions to the previously reported period produced no result.

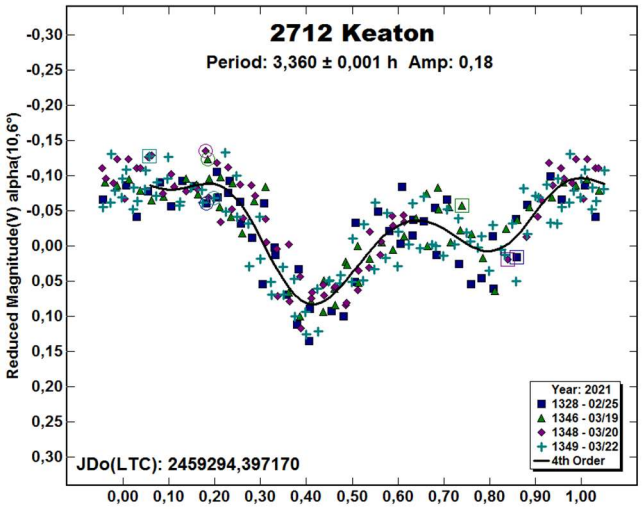

4422 Jarre. Two periods were reported for this target, a shorter one of 5.428 ± 0.004 h measured by Behrend (2002) and a longer one of 7.002 ± 0.011 h by Polakis (2020). After eight sessions, this target leads to a period very close to the one reported by Polakis: $P = 7.013 \pm 0.001$ h, $A = 0.11$ mag.

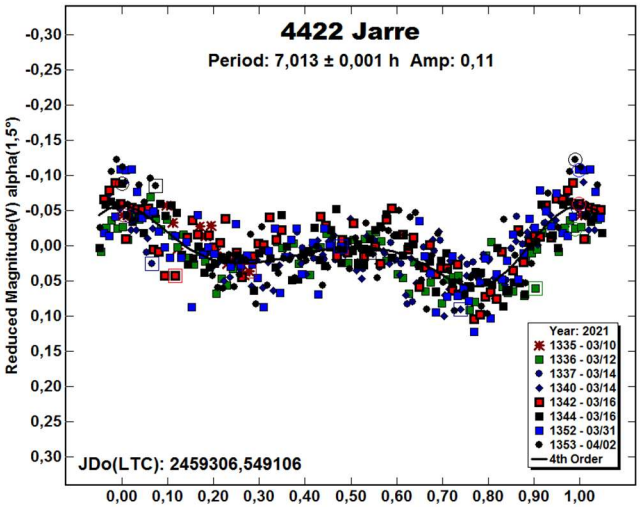

(25343) 1999 RA44. No previous period for this target is reported on the LCDB. It required about three months of work to reach a result. As more sessions were added, many periods appeared, and only in the end *MPO Canopus* pointed in the direction of the period reported in this paper. The final period is $P = 590{,}48 \pm 0.46$ h, $A = 0.57$ mag. Unfortunately, bad weather together with a full moon made it almost impossible to measure the target during rotation phase 0.40 - 0.70. After the last session of March 20, it was too faint, close to 19 mag. Any new measurements showed an uncertainty larger than the amplitude of the curve and so they were useless.

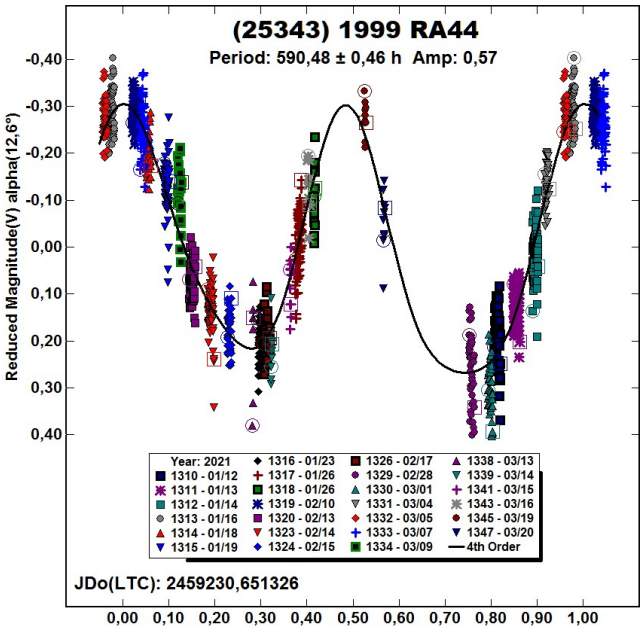

Number	Name	yyyy mm/dd	Phase	L_{PAB}	B_{PAB}	Period(h)	P.E.	Amp	A.E.	Grp
2712	Keaton	2021 02/25-03/22	10.6,4.0	174	0	3.360	0.001	0.18	0.05	MB-I
4422	Jarre	2021 03/10-04/02	1.2,11.1	167	2	7.013	0.001	0.11	0.05	FLOR
25343	1999 RA44	2021 01/12-03/20	12.6,24	131	10	590.48	0.46	0.57	0.05	FLOR
49548	1999 CP83	2021 02/24-04/08	4.4,20.1	161	6	2.758	0.001	0.11	0.05	MB-I

Table I. Observing circumstances and results. The phase angle is given for the first and last date. If preceded by an asterisk, the phase angle reached an extrema during the period. L_{PAB} and B_{PAB} are the approximate phase angle bisector longitude/latitude at mid-date range (see Harris et al., 1984). Grp is the asteroid family/group (Warner et al., 2009).

(49548) 1999 CP83. No previous period was reported for this target in the LCDB. The author found a very short period, evident since the first session, of P = 12.981 ± 0.002 h and A = 0.10 mag.

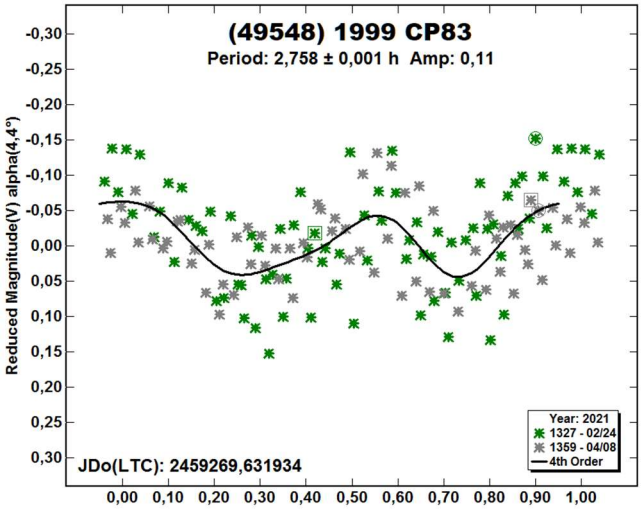

References

Behrend, R. (2020). Observatoire de Geneve web site. *http://obswww.unige.ch/~behrend/page_cou.html*

Bisque (2020). Software Bisque. *The Sky Pro 6*. *http://www.bisque.com*

Chang, C.-K; Lin, H.-W.; Ip, W.-H.; Chen, W.-P.; Yeh, T.-S.; Chambers, K.C.; Magnier, E.A.; Huber, M.E.; Flewelling, H.A.; Waters, C.Z.; Wainscoat, R.J.; Schultz, A.S.B. (2019). "Searching for Super-fast Rotators Using the Pan-STARRS 1." *Ap. J. Supl. Ser.* **241**:6.

Diffraction Limited (2020). *Maxim DL* software. *http://diffractionlimited.com/product/maxim-dl/*

Harris, A.W.; Young, J.W.; Scaltriti, F.; Zappala, V. (1984). "Lightcurves and phase relations of the asteroids 82 Alkmene and 444 Gyptis." *Icarus* **57**, 251-258.

Polakis, T. (2020). "Photometric Observations of Twenty-Three Minor Planets" *Minor Planet Bulletin* **47**, 94-101.

Starkeeper (2020). Voyager Observatory control software. *http://software.starkeeper.it*

Warner, B.D.; Harris, A.W.; Pravec, P. (2009). "The Asteroid Lightcurve Database." *Icarus* **202**, 134-146. Updated 2021 04 13. *http://www.minorplanet.info/lightcurvedatabase.html*

Warner, B.D. (2018). *MPO Canopus* software. *http://bdwpublishing.com*

Warner, B.D. (2021). CALL website ephemeris generator. *http://www.minorplanet.info/PHP/call_OppLCDBQuery.php*

LIGHTCURVES AND ROTATION PERIODS OF 47 AGLAJA, 504 CORA, 527 EURYANTHE, 593 TITANIA, AND 594 MIREILLE

Frederick Pilcher
Organ Mesa Observatory (G50)
4438 Organ Mesa Loop
Las Cruces, NM 88011 USA
fpilcher35@gmail.com

(Received: 2021 April 13)

Synodic rotation periods and amplitudes are found for 47 Aglaja: 13.175 ± 0.002 h, 0.02 mag; 504 Cora: 7.5872 ± 0.0002 h, 0.18 ± 0.01 mag; 527 Euryanthe: 42.75 ± 0.01 hours, 0.14 ± 0.01 mag; 593 Titania: 9.899 ± 0.001 h, 0.26 ± 0.02 mag; 594 Mireille: 4.9685 ± 0.0002 hours, 0.32 ± 0.02 mag.

Observations to produce the results reported in this paper were made at the Organ Mesa Observatory with a Meade 35 cm LX200 GPS Schmidt-Cassegrain, SBIG STL-1001E CCD, unguided. Exposure times were 60 seconds with R filter for 593 Titania and clear filter for all other targets. Image photometric measurement and lightcurve construction were done by *MPO Canopus* software. To reduce the number of data points on the lightcurves and make them easier to read, data points have been binned in sets of 3 with maximum time difference 5 minutes.

47 Aglaja. The Lightcurve Data Base (Warner et al. 2009, updated 2020 October) lists 11 previously published rotation periods for 47 Aglaja, nine of which are close to the preferred value of 13.178 hours, and with amplitudes ranging from 0.02 to 0.21 magnitudes. Pal et al. (2020) report a period twice as great, 26.4112 hours. New observations on 8 nights 2021 Jan. 6 - Feb. 7 can be fit to an asymmetric lightcurve with period 13.175 ± 0.002 h, amplitude 0.02 magnitudes. The period is consistent with many previously published periods except for Pal et al. (2020). The very small amplitude compared with the largest found shows that its rotational pole is close, probably within 10 degrees, to its location in the sky on the dates of observation near celestial longitude 142º, latitude 4º.

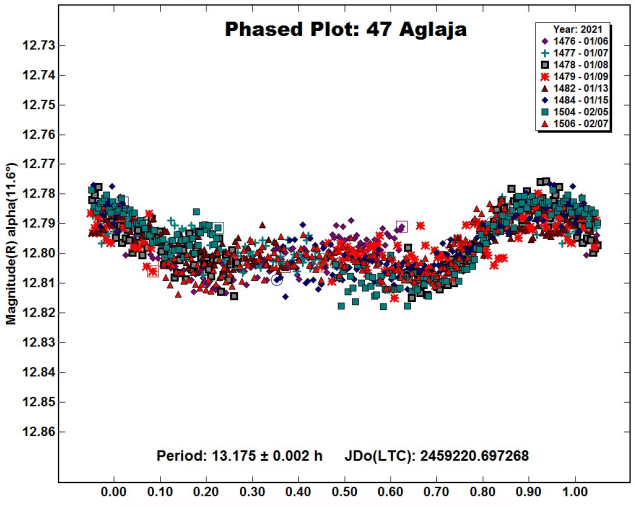

504 Cora. The Lightcurve Data Base (Warner et al. 2009, updated 2020 October) lists 9 previously published rotation periods for 504 Cora, eight of which are within 0.01 hours of the preferred period of 7.587 hours. New observations on 4 nights 2021 Jan. 12 - Feb. 4 provide an excellent fit to a lightcurve with period 7.5872 ± 0.0002 hours, amplitude 0.18 ± 0.01 magnitudes. This period is in excellent agreement with previously published periods.

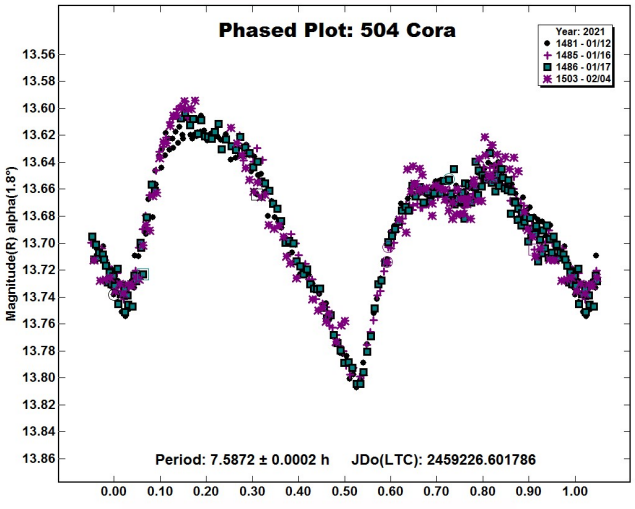

527 Euryanthe. Previously published rotation periods are by Brinsfield (2010), 26.06 h; Polakis and Skiff (2019), 42.986 h; Polakis (2020), 43.40 h; this author (Pilcher, 2020), 42.93 h.

This author thanks Brian Warner (private communication) for independently analyzing the data from Pilcher (2020). Following Warner's suggestion, this author made several small adjustments to the zero points of individual session lightcurves and found that 42.885 ± 0.003 hours, amplitude 0.14 ± 0.01 magnitudes is a better fit with lower rms deviation from the order ten Fourier series best representing the data. The 42.93-hour period is retracted and the lightcurve phased to 42.885 hours is presented in this paper.

Sixteen new sessions obtained 2021 Feb. 24 - Apr. 10 provide an excellent fit to a lightcurve with period 42.75 ± 0.01 hours, amplitude 0.14 ± 0.01 magnitudes. This period is within 0.3% of this author's revised year 2020 period of 42.885 hours and farther removed from all other period determinations.

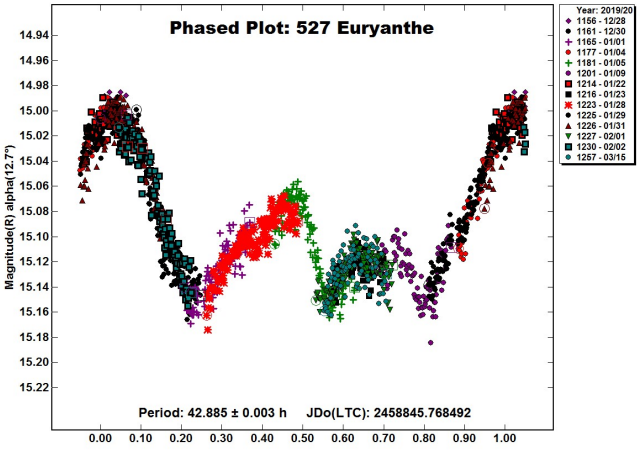

Number	Name	yyyy/mm/dd	Phase	LPAB	BPAB	Period(h)	P.E	Amp	A.E.
47	Aglaja	2021/01/06-2021/02/07	11.6 1.8	142	4	13.175	0.002	0.02	0.01
504	Cora	2021/01/12-2021/02/04	* 1.8, 8.0	115	3	7.5872	0.0002	0.18	0.01
527	Euryanthe	2019/12/28-2020/03/15	*12.7, 15.6	133	3	42.885	0.003	0.14	0.01
527	Euryanthe	2021/02/24-2021/04/10	17.5 6.6	210	12	42.75	0.01	0.14	0.01
593	Titania	2020/12/31-2021/01/27	14.4, 10.8	122	16	9.899	0.001	0.26	0.02
594	Mireille	2021/03/29-2021/04/13	18.6, 25.8	165	17	4.9685	0.0002	0.32	0.02

Table I. Observing circumstances and results. Pts is the number of data points. The phase angle is given for the first and last date, unless a minimum (second value) was reached. LPAB and BPAB are the approximate phase angle bisector longitude and latitude at mid-date range (see Harris *et al.*, 1984).

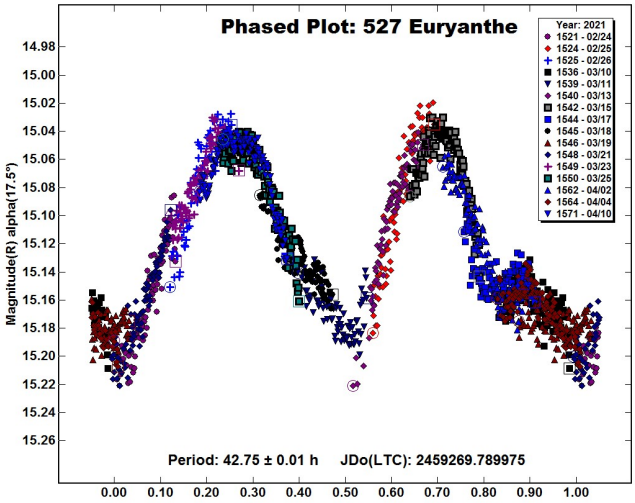

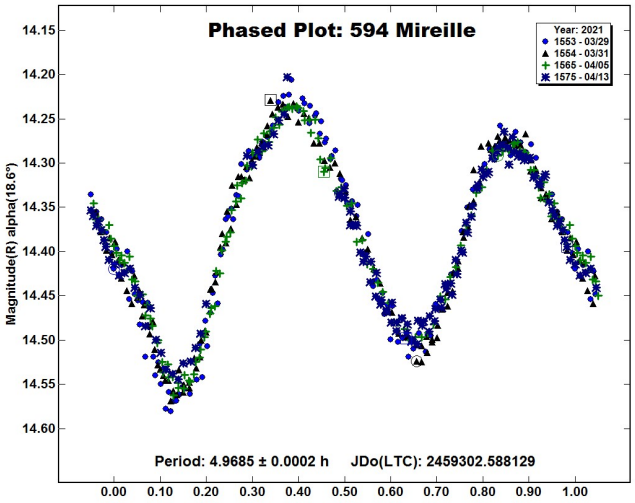

593 Titania. The Lightcurve Data Base (Warner et al. 2009, updated 2020 October) lists 4 previously published rotation periods for 593 Titania, all within 0.04 hours of the preferred value of 9.8968 hours. New observations on 4 nights 2020 Dec. 31 - 2021 Jan. 27 provide an excellent fit to a lightcurve with period 9.899 ± 0.001 hours, amplitude 0.26 ± 0.02 magnitudes. This period is in excellent agreement with previously published periods.

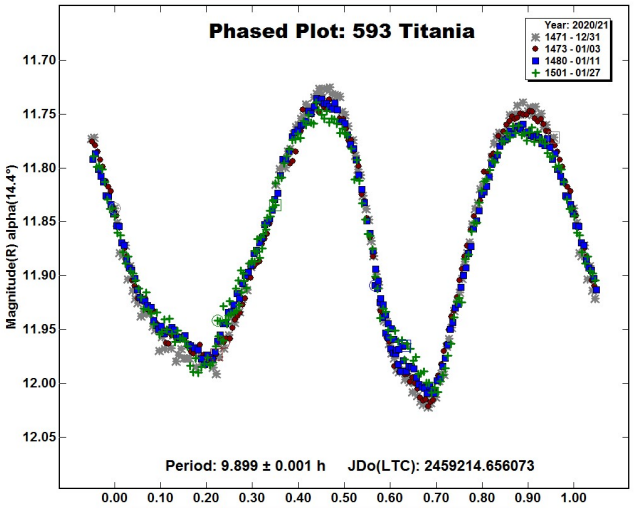

594 Mireille. Previously published rotation periods are by Wisniewski (1991), 4.966 h; Polakis and Skiff (2017), 4.9671 h; and Benishek (2018), 4.9688 h. New observations on 4 nights 2021 Mar. 29 - Apr. 13 provide an excellent fit to a lightcurve with period 4.9685 ± 0.0002 hours, amplitude 0.32 ± 0.02 magnitudes. This period is in excellent agreement with previously published periods.

References

Benishek, V. (2018). "Lightcurve and rotation period determinations for 29 asteroids." *Minor Planet Bull.* **45**, 82-91.

Brinsfield, J.W. (2010). "Asteroid lightcurve analysis at the Via Capote Observatory: 4th quarter." *Minor Planet Bull.* **37**, 50-53.

Harris, A.W.; Young, J.W.; Scaltriti, F.; Zappala, V. (1984). "Lightcurves and phase relations of the asteroids 82 Alkmene and 444 Gyptis." *Icarus* **57**, 251-258.

Pal, A.; Szakáts, R.; Kiss, C.; Bódi, A.; Bognár, Z.; Kalup, C.; Kiss, L.L.; Marton, G.; Molnár, L.; Plachy, E.; Sárneczky, K.; Szabó, G.M.; Szabó, R. (2020). "Solar System Objects Observed with TESS - First Data Release: Bright Main-belt and Trojan Asteroids from the Southern Survey." *Ap. J. Supl. Ser.* **247**, 26-34.

Pilcher, F. (2020). "Lightcurves and rotation periods of 83 Beatrix, 86 Semele, 118 Peitho, 153 Hilda, 527 Euryanthe, and 549 Jessonda." *Minor Planet Bull.* **47**, 192-195.

Polakis, T.; Skiff, B. (2017). "Lightcurve analysis for 341 California, 594 Mireille, 1115 Sabauda, 1504 Lappeenranta, and 1926 Demiddelaer." *Minor Planet Bull.* **44**, 299-302.

Polakis, T.; Skiff, B. (2019). "Lightcurves of eleven main-belt minor planets." *Minor Planet Bull*. **46**, 152-157.

Polakis, T. (2020). "Photometric observations of thirty minor planets." *Minor Planet Bull.* **47**, 177-186.

Warner, B.D.; Harris, A.W.; Pravec, P. (2009). "The Asteroid Lightcurve Database." *Icarus* **202**, 134-146. Updated 2020 October. *http://www.minorplanet.info/lightcurvedatabase.html*

Wisniewski, W.Z. (1991). "Physical studies of small asteroids I. Lightcurves and taxonomy of ten asteroids." *Icarus* **90**, 117-122.

COLLABORATIVE ASTEROID PHOTOMETRY FROM UAI: 2021 JANUARY-MARCH

Lorenzo Franco
Balzaretto Observatory (A81), Rome, ITALY
lor_franco@libero.it

Alessandro Marchini, Leonardo Cavaglioni,
Riccardo Papini, Chiara Angelica Privitera
Astronomical Observatory, DSFTA - University of Siena (K54)
Via Roma 56, 53100 - Siena, ITALY

Giorgio Baj
M57 Observatory (K38), Saltrio, ITALY

Gianni Galli
GiaGa Observatory (203), Pogliano Milanese, ITALY

Giulio Scarfi
Iota Scorpii Observatory (K78), La Spezia, ITALY

Pietro Aceti, Massimo Banfi
Seveso Observatory (C24), Seveso, ITALY

Paolo Bacci, Martina Maestripieri
GAMP - San Marcello Pistoiese (104), Pistoia, ITALY

Massimiliano Mannucci, Nico Montigiani
Osservatorio Astronomico Margherita Hack (A57)
Florence, ITALY

Luciano Tinelli
GAV (Gruppo Astrofili Villasanta), Villasanta, ITALY

Fabio Mortari
Hypatia Observatory (L62), Rimini, ITALY

(Received: 2021 Apr 10)

Photometric observations of six asteroids were made in order to acquire lightcurves for shape/spin axis modeling. The synodic period and lightcurve amplitude were found for 374 Burgundia, 472 Roma, 593 Titania, 1106 Cydonia, 1152 Pawona, and 3332 Raksha. We also found color index (V-R) for 472 Roma and 1152 Pawona along with H-G parameters for: 472 Roma and 3332 Raksha.

Collaborative asteroid photometry was done inside the Italian Amateur Astronomers Union (UAI; 2021) group. The targets were selected mainly in order to acquire lightcurves for shape/spin axis modeling. Table I shows the observing circumstances and results.

The CCD observations were made in 2021 January-March using the instrumentation described in the Table II. Lightcurve analysis was performed at the Balzaretto Observatory with *MPO Canopus* (Warner, 2019). All the images were calibrated with dark and flat frames and converted to R magnitudes using solar colored field stars from a version of the CMC15 catalogue distributed with *MPO Canopus*. For brevity, the following citations to the asteroid lightcurve database (LCDB; Warner et al., 2009) will be summarized only as "LCDB".

374 Burgundia is an S-type (Bus and Binzel, 2002) middle main-belt asteroid discovered on 1893 September 18 by A. Charlois at Nice. Collaborative observations were made over five nights. The period analysis shows a synodic period of $P = 6.966 \pm 0.001$ h with an amplitude $A = 0.11 \pm 0.02$ mag. The period is close to the previously published results in the LCDB.

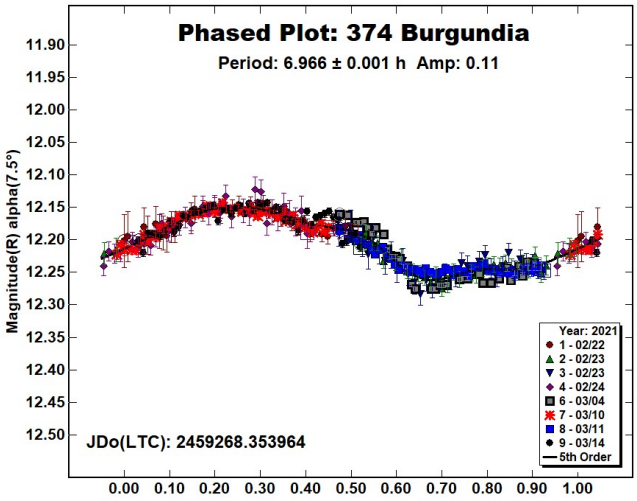

472 Roma is an S-type (Tholen, 1984) middle main-belt asteroid discovered on 1901 July 1 by L. Carnera at Heidelberg. Collaborative observations were made over eight nights. The period analysis shows a synodic period of $P = 9.796 \pm 0.001$ h with an amplitude $A = 0.35 \pm 0.04$ mag. The period is close to the previously published results in the LCDB.

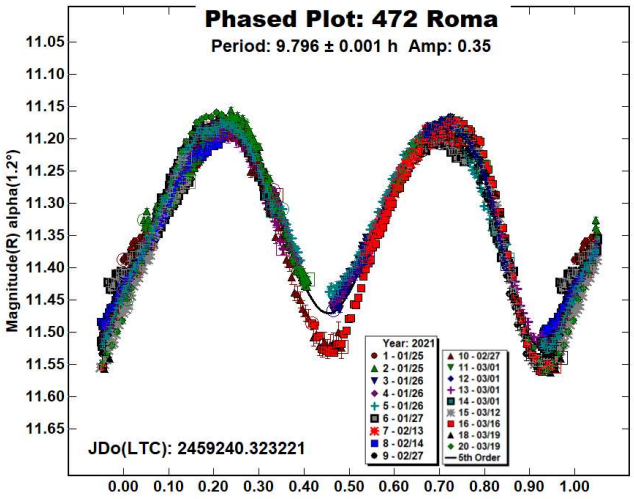

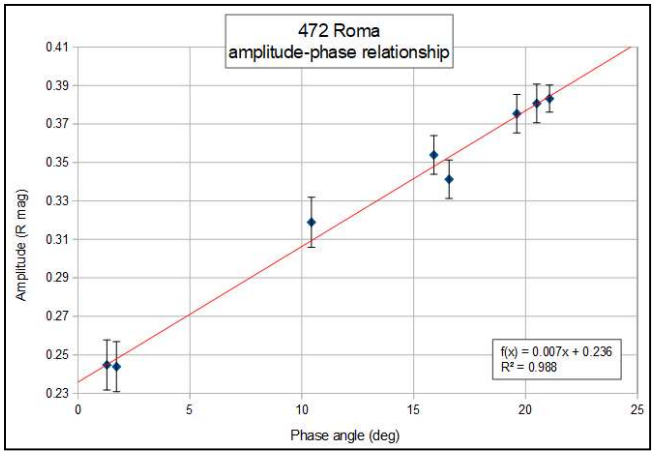

The measured amplitudes were related to the phase angle as shown by the amplitude-phase plot. By linear fit we obtained a slope $s = 0.007 \pm 0.001$ mag deg^{-1} and intercept $A(0°) = 0.236 \pm 0.021$ mag. This gives $m = s/A(0°) = 0.030 \pm 0.008$ deg^{-1}. This result agrees with the empirical formula by Zappala et al. (1990): $A(\alpha) = A(0°)m\alpha+A(0°)$, where α is the solar phase angle and m is a parameter (deg^{-1}) that varies according to the taxonomic type. Typical values are 0.030, 0.015, 0.013 respectively for S-type, C-type and M-type.

The nearly concurrent and independent sessions acquired by G. Scarfi and G. Baj on 2021 March 19 in the V and R bands allowed us to determine the color index (V-R) = 0.49 ± 0.01 mag. This value is consistent with a medium albedo S-type taxonomic class (Shevchenko and Lupishko, 1998).

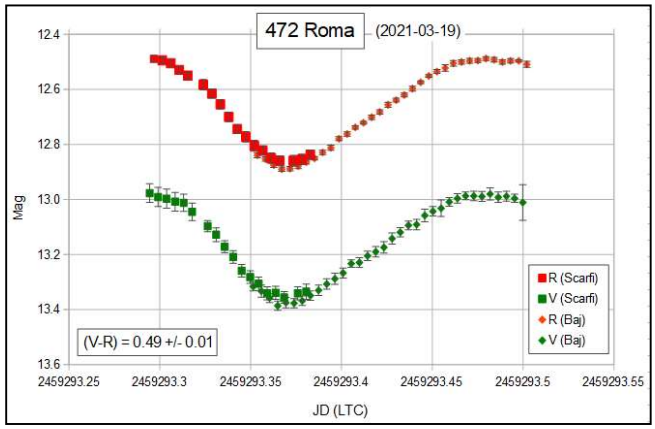

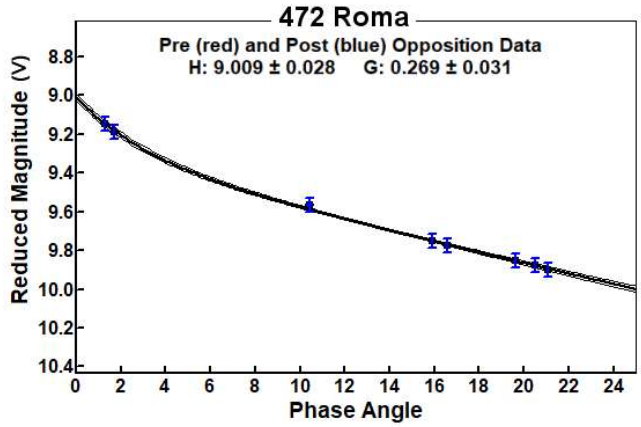

The H-G parameters were determined using the H-G calculator function implemented in *MPO Canopus*. For each lightcurve, the R mag were measured as half peak-to-peak and converted in V mag by adding the color index (V-R) previously determined. We derived $H = 9.01 \pm 0.03$ mag and $G = 0.27 \pm 0.03$. The H value is close to result found in the LCDB and the G value is consistent with a medium albedo S-type taxonomic class (Shevchenko and Lupishko, 1998).

593 Titania is a C-type (Tholen, 1984) middle main-belt asteroid discovered on 1906 March 20 by A. Kopff at Heidelberg. Collaborative observations were made over five nights. We found a synodic period of $P = 9.898 \pm 0.001$ h with an amplitude $A = 0.26 \pm 0.03$ mag. The period is close to the previously published results in the LCDB.

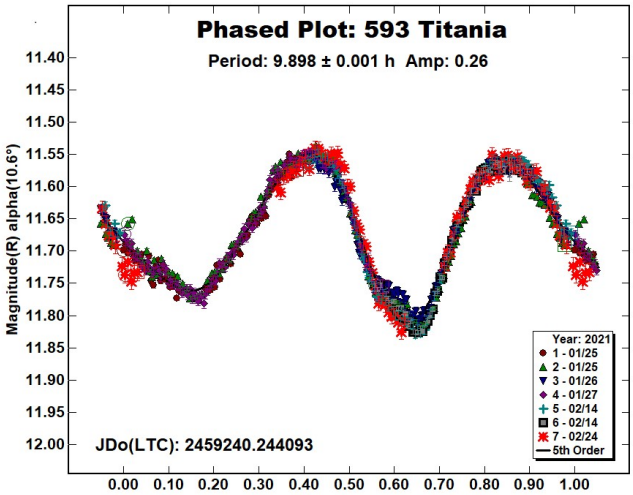

1106 Cydonia is an S-type (Bus and Binzel, 2002) middle main-belt asteroid discovered on 1929 February 5 by K. Reinmuth at Heidelberg. Collaborative observations were made over three nights. We found a synodic period of $P = 2.679 \pm 0.001$ h with an amplitude $A = 0.05 \pm 0.02$ mag. The period is close to the previously published results in the LCDB.

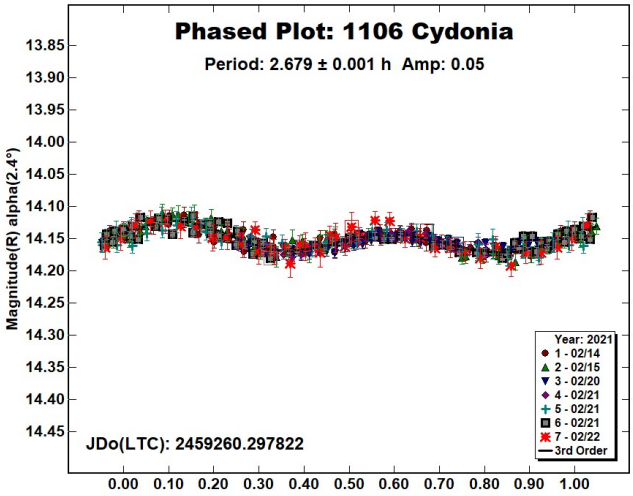

1152 Pawona is an Sl-type (Bus and Binzel, 2002) inner main-belt asteroid discovered on 1930 January 8 by K. Reinmuth at Heidelberg. Collaborative observations were made over eight nights. We found a synodic period of $P = 3.4152 \pm 0.0002$ h with an amplitude $A = 0.19 \pm 0.03$ mag. The period is close to the previously published results in the LCDB.

The sessions acquired by G. Baj on 2021 February 28 and March 1 in the V and R bands allowed us to determine the color index (V-R) = 0.52 ± 0.04 mag. This value is consistent with a medium albedo S-type taxonomic class (Shevchenko and Lupishko, 1998).

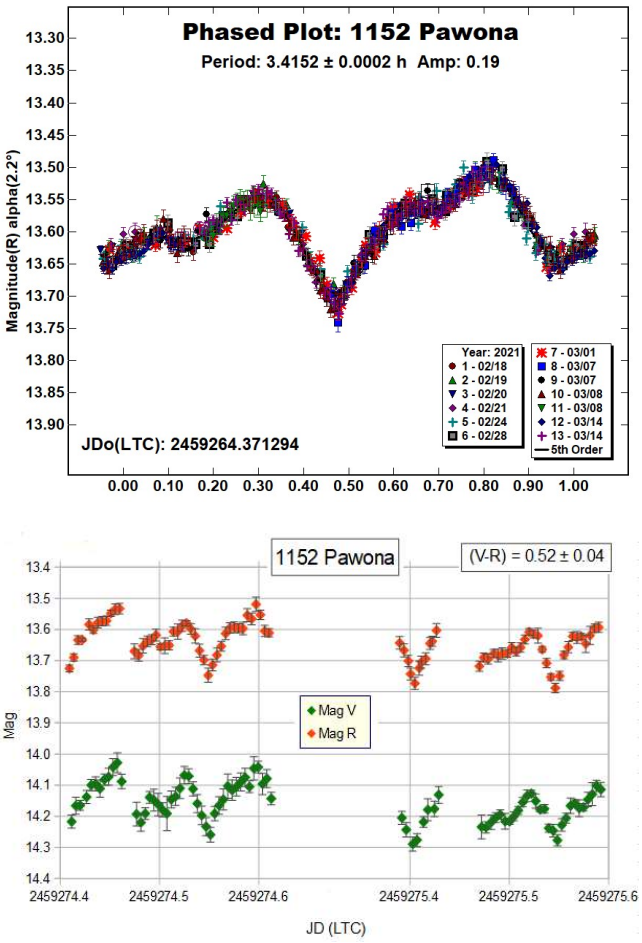

3332 Raksha is a medium-albedo inner main-belt asteroid discovered on 1978 July 4 by L. Chernykh at Nauchnyj. Collaborative observations were made over six nights. We found a synodic period of P = 4.8052 ± 0.0003 h with an amplitude A = 0.40 ± 0.03 mag. The period is close to the previously published results in the LCDB.

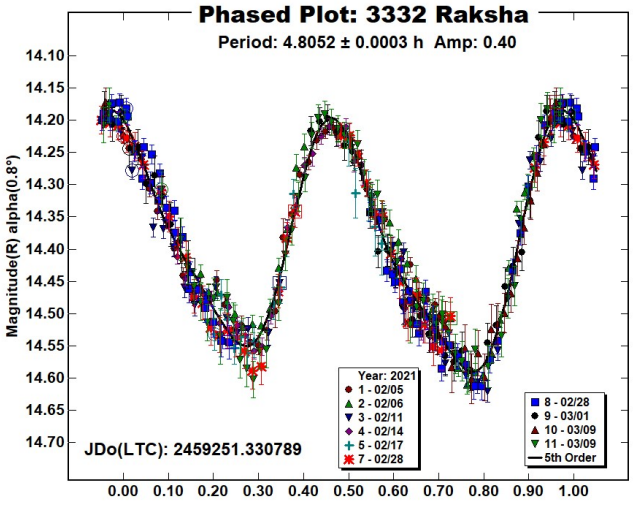

For each lightcurve were measured the half peak-to-peak R band magnitude, deriving H_R = 11.46 ± 0.05 mag and G = 0.25 ± 0.08. The G value is close to medium albedo S-type taxonomic class (Shevchenko and Lupishko, 1998).

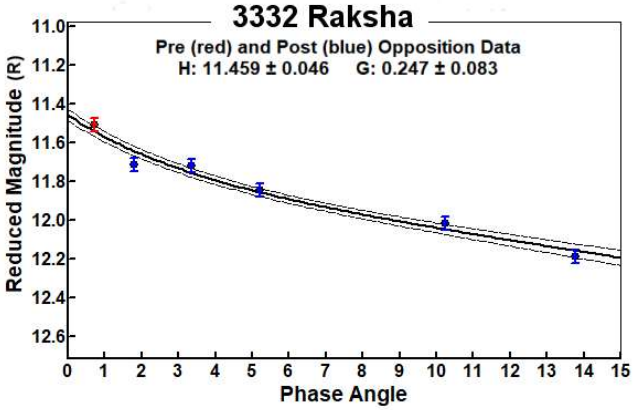

Acknowledgements

The authors want to thank a group of high school students involved in an interesting vocational guidance project about astronomy at the Astronomical Observatory of the University of Siena. Despite the health emergency for Covid-19, they attended some online observing sessions and participated remotely in data analysis. From Liceo "G. Galilei" in Erba (Como): C. Bonaccorsi; A. Farina; A. Gandolfi; S. Luceri; S. Maggi; A. Malossi; A. Micicché; V. Valnegri; L. Vassena from Liceo "G. Galilei" in Siena: L. Baldi; M. Barbati; F. Behari; M. Benvenuti; F. Berni; T. Bicchi; D. Bracciali; G. Brunelli; L. Calomino; F. Capannoli; A. Ciubotaru; G. Di Sanzo; L. Elia; C. Faraoni; Y. Fokam; M.S. Forconi; F. Forte; V. Galello; F. Galli; T. Giani; B. Granai; L. Granieri; T. Iorio; A. Lika; L. Marchetti; I. Mazic; A. Nannetti; A. Oros; C. Panerati; A. Persico; G. Pieri; P. Pilenga; A. Podda; R. Prosperi; A. Prugnoli; D. Rabissi; F. Ricci; E. Rosini; G. Salomone; N. Sammicheli; A. Sansoni; B. Sansoni; L. Sennati; M. Sinatra; M. Torzoli; A. Ulaj; E. Versace; A. Zyko from Liceo "T. Sarrocchi" in Siena: M. Ambrogio; N. Bandini; E. Batelli; M. Becatti; E. Bechi; M. Bernini; B. Boscagli; M. Brotto; F. Carapelli; L. Cinesi; S. Cortonesi; G. Cresti; F. Croccolino; D. Cuccunato Polato; A. Dami; M.V. D'Angelo; S. Di Cairano; B. Fabbri; A. Fantauzzo; F. Fantozzi; L. Fedolfi; A. Galvagni; F. Gazzei; D. Grazzini; D. Guidolotti; E. Iannucci; M. La Rocca; T. Lari; L. Lorenzini; J. Maggiorelli; A. Marino; L. Massari;I. Mazzieri; A. Migliorini; L. Mucciarelli; F. Nannetti; M. Nannini; A. Nardini; N. Osti; T. Paciotti; S. Pecciarelli; R. Piattelli; M. Pistella; L. Profeti; A. Quarato; F. Radi; S. Rappuoli; F. Rossetti; A.P. Santoro; A. Scarselli; J. Serafin; G. Stocchi; G. Trombetti; N.B.C. Vasconetto; M. Viani.

Number	Name	2021 mm/dd	Phase	L_{PAB}	B_{PAB}	Period(h)	P.E.	Amp	A.E.	Grp
374	Burgundia	02/22-03/14	*7.4,4.5	169	-9	6.966	0.001	0.11	0.02	MB-M
472	Roma	01/25-03/19	1.2,21.0	124	1	9.796	0.001	0.35	0.04	MB-M
593	Titania	01/25-02/24	10.5,19.1	123	19	9.898	0.001	0.26	0.03	MB-M
1106	Cydonia	02/14-02/22	*2.3,1.9	151	-1	2.679	0.001	0.05	0.02	MB-M
1152	Pawona	02/18-03/14	*2.2,10.1	155	-1	3.4152	0.0002	0.19	0.03	MB-I
3332	Raksha	02/05-03/09	*0.7,13.7	139	1	4.8052	0.0003	0.40	0.03	MB-I

Table I. Observing circumstances and results. The first line gives the results for the primary of a binary system. The second line gives the orbital period of the satellite and the maximum attenuation. The phase angle is given for the first and last date. If preceded by an asterisk, the phase angle reached an extremum during the period. L_{PAB} and B_{PAB} are the approximate phase angle bisector longitude/latitude at mid-date range (see Harris et al., 1984). Grp is the asteroid family/group (Warner et al., 2009).

Observatory (MPC code)	Telescope	CCD	Filter	Observed Asteroids (#Sessions)
Astronomical Observatory of the University of Siena(K54)	0.30-m MCT f/5.6	SBIG STL-6303e (bin 2x2)	C,Rc	374(3),472(3),593(1),1106(2),1152(2),3332(3)
M57 (K38)	0.30-m RCT f/5.5	SBIG STT-1603	Rc,V	472(5),593(3),1152(3),3332(2)
GiaGa Observatory (203)	0.36-m SCT f/5.8	Moravian G2-3200	Rc	472(3),1152(2)
Iota Scorpii(K78)	0.40-m RCT f/8.0	SBIG STXL-6303e (bin 2x2)	Rc,V	472(2),592(1),3332(1)
Seveso Observatory (C24)	0.30-m SCT f/6.3	SBIG ST9	Rc	374(1),3332(1)
GAMP (104)	0.60-m NRT f/4.0	Apogee Alta	C	1106(2)
Osservatorio Astronomico Margherita Hack (A57)	0.35-m SCT f/8.3	SBIG ST10XME (bin 2x2)	Rc	1152(1)
GAV	0.20-m SCT f/6.3	SXV-H9	Rc	593(1)
Hypatia Observatory (L62)	0.25-m RCT f/5.4	SBIG ST8-XE	Rc	374(1)

Table II. Observing Instrumentations. MCT: Maksutov-Cassegrain, NRT: Newtonian Reflector, RCT: Ritchey-Chretien, SCT: Schmidt-Cassegrain

References

Bus, S.J.; Binzel, R.P. (2002). "Phase II of the Small Main-Belt Asteroid Spectroscopic Survey - A Feature-Based Taxonomy." *Icarus* **158**, 146-177.

Harris, A.W.; Young, J.W.; Scaltriti, F.; Zappala, V. (1984). "Lightcurves and phase relations of the asteroids 82 Alkmene and 444 Gyptis." *Icarus* **57**, 251-258.

Shevchenko, V.G.; Lupishko, D.F. (1998). "Optical properties of Asteroids from Photometric Data." *Solar System Research*, **32**, 220-232.

Tholen, D.J. (1984). "Asteroid taxonomy from cluster analysis of Photometry." Doctoral Thesis. University Arizona, Tucson.

UAI (2021). "Unione Astrofili Italiani" web site. *https://www.uai.it*

Warner, B.D.; Harris, A.W.; Pravec, P. (2009). "The asteroid lightcurve database." *Icarus* **202**, 134-146. Updated 2020 Oct 22. *http://www.minorplanet.info/lightcurvedatabase.html*

Warner, B.D. (2019). MPO Software. *MPO Canopus* v10.8.1.1. Bdw Publishing. *http://minorplanetobserver.com*

Zappalà, V.; Cellino, A.; Barucci, A.M.; Fulchignoni, M.; Lupishko, D.F. (1990). "An analysis of the amplitude-phase relationship among asteroids." *Astron. Astrophys*. **231**, 548-560.

PHOTOMETRIC OBERSVATIONS OF (68347) 2001 KB67, (494999) 2010 JU39, AND (455432) 2003 RP8

Steven D. Newcomb
Dept. of Space Studies
University of North Dakota
Grand Forks, ND 58202
steven.newcomb@und.edu

Sherry K. Fieber-Beyer
Dept. of Space Studies
University of North Dakota
Grand Forks, ND 58202

(Received: 2021 April 2)

CCD Photometric observations were obtained of (68347) 2001 KB67, (494999) 2010 JU39, and (455432) 2003 RP8 between June 2018 and August 2019. The rotation rates determined for (68347) 2001 KB67 and (455432) 2003 RP8 were similar to those found in previous research, but the period for (494999) 2010 JU39 differs from previously published results.

Observations

Observations of three near-Earth asteroids were obtained using the University of North Dakota's Space Studies Observatory, located near Emerado, ND. This facility features three telescopes, which are remotely accessible to offsite users. Onsite telescope operators are present to handle hardware and software needs as they arise, and to take flat field images for all remote observers.

The photometric data were obtained using a 16-inch Meade LX200R telescope that is coupled with an Apogee U9000 CCD camera. The observations were conducted over the summers of 2018 and 2019. The data for asteroid 68347 (2001 KB67) were collected on 3, 4 & 6 June 2018. The data for asteroid (494999) 2010 JU39 were obtained on 25 & 26 June 2019. The data for asteroid (455432) 2003 RP8 were obtained 29 & 30 July and 2 August 2019.

The exposure times varied for each asteroid due to their apparent magnitudes. For example, the integration times for (68347) 2001 KB67 were at 120 seconds with a 180 second pause in between each exposure. The integration times for (494999) 2010 JU39 were 100 seconds with a 180 second pause, and the integration times for (455432) 2003 RP8 were 60 seconds with a 180 second pause. All of the images were obtained using a broadband R-filter.

On each night, dark and flat frame calibration images were obtained. The dark frames were taken at the same exposure length and CCD temperature as the science images for each asteroid. The flat frames were obtained by the onsite telescope operators and were taken at either dusk or dawn depending on the sky circumstances.

The data were calibrated (dark- and flat-frame corrected) using *AstroImage J* version 3.2.0. Data that were of poor quality were excluded from further analysis (weather deterioration, saturation, poor counts, etc.). Differential photometry and asteroid period determination utilized *MPO Canopus* version 10.7.11.1. The calibrated data were imported into *Canopus* for analysis. Because each of the asteroids moved rapidly, the background stars shifted throughout each night of observation. Therefore, during analysis we grouped images that shared comparison stars into individual sessions resulting in the use of multiple sessions for each when determining each period solution.

We utilized the standard circular aperture in *Canopus* for photon and background counts. In particular, we used an 11/11/2/11 aperture size to analyze (68347) 2001 KB67. For (494999) 2010 JU39 and (455432) 2003 RP8, we used the default aperture settings of 13/13/2/11.

Results

MPO Canopus corrected for the time it takes the light to travel from each of the asteroids to the Earth for their respective nights of observation. We plotted lightcurves for each night's usable data. A single lightcurve for each of the asteroids was produced, and then least squares fit with a Fourier series.

(68347) 2001 KB67 is a near-Earth Aten-class object, which is also designated as a potentially hazardous asteroid (PHA). It was observed on 3, 4 & 6 June 2018. Its period was determined using a 3rd order harmonic: 6.3500 ± 0.0446 hours with an amplitude of 0.24 ± 0.02 mag. See Figure 1. This was similar to the period of 6.354 ± 0.004 hours reported by Warner (2018), and the period of 6.357 ± 0.0012 hours found by Loera-Gonzalez et al. (2019).

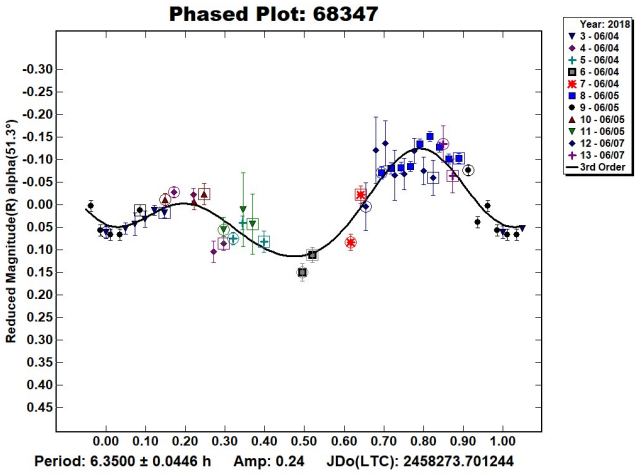

Figure 1. Lightcurve for (68347) 2001 KB67 showing a period of 6.3500 ± 0.0446 hours with an amplitude of 0.24 ± 0.02 mag.

Number	Name	yyyy mm/dd	Phase	L_{PAB}	B_{PAB}	Period(h)	P.E.	Amp	A.E.
68347	2001 KB67	2018 06/03-06/07	54.9,46.0	255	27	6.350	0.045	0.24	0.02
494999	2010 JU39	2019 06/25-06/26	41.6,41.0	294	26	2.278	0.016	0.13	0.01
455432	2003 RP8	2019 07/29-08/02	19.7,36.4	299	15	4.200	0.015	0.30	0.02

Table I. Observing circumstances and results. The phase angle is given for the first and last date. If preceded by an asterisk, the phase angle reached an extrema during the period. L_{PAB} and B_{PAB} are the approximate phase angle bisector longitude/latitude at mid-date range (see Harris et al., 1984).

(494999) 2010 JU39 is an Aten class near-Earth Asteroid that is also designated as a PHA. It was observed on 25 & 26 June 2019. Its period was derived using a 3rd order harmonic: 2.2782 ± 0.0161 hours with an amplitude of 0.13 ± 0.01. See Figure 2. This value differs from 30.2 ± 0.1 hours reported by Warner & Stephens (2019), which itself was based on a half-period of 15.11 ± 0.04 hours.

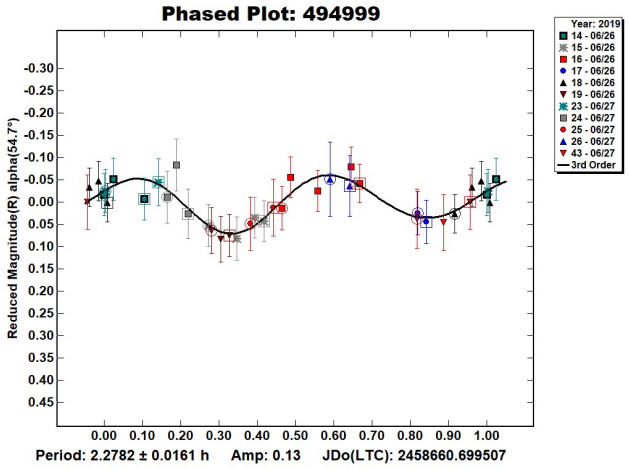

Figure 2. Lightcurve for (494999) 2010 JU39 showing a period of 2.2782 ± 0.0161 hours with an amplitude of 0.13 ± 0.01 mag.

(455432) 2003 RP8 is a near-Earth Amor asteroid that was observed on 29 & 30 July 2019, and 2 August 2019. Its period was derived using a 3rd order harmonic: 4.2000 ± 0.0149 hours with an amplitude of 0.30 ± .02 mag. See Figure 3. This value is similar to the 4.2736 ± 0.0007-hour period reported by Warner & Stephens (2020).

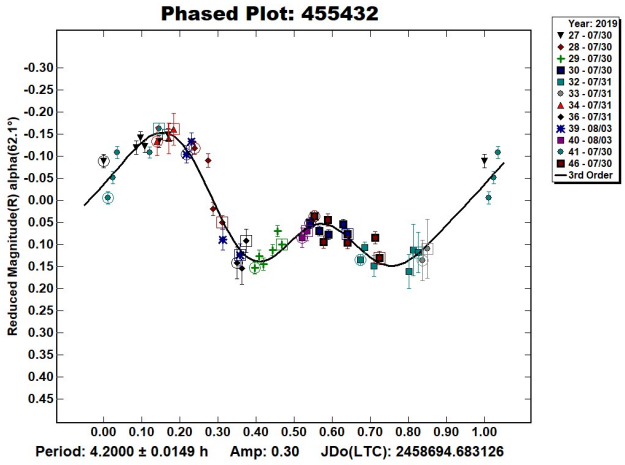

Figure 3. Lightcurve for (455432) 2003 KP8 showing a period of 4.2000 ± 0.0149 hours with an amplitude of 0.30 ± .02 mag.

Acknowledgements

The authors wish to thank the University of North Dakota Space Studies Observatory and its staff for the use of the observatory facilities, and for assistance in collecting the data for this study. We would also like to acknowledge Brian Warner for his unwavering assistance.

References

Harris, A.W.; Young, J.W.; Scaltriti, F.; Zappala, V. (1984). "Lightcurves and phase relations of the asteroids 82 Alkmene and 444 Gyptis." *Icarus* **57**, 251-258.

Loera-Gonzalez, P.; Olguin, L.; Contreras, M.E.; Morales, J.S.; Schuster, W.; Sada, P.V. (2019). "Results of the first semester of the 2018 Mexican asteroid photometry campaign." *Minor Planet Bulletin* **46**, 283-285.

Warner, B.D. (2018). "Near-Earth Asteroid lightcurve analysis at CS3-Palmer divide station: 2018 April-June." *The Minor Planet Bulletin* **45**, 366-379.

Warner, B.D.; Stephens, R.D. (2019). "Near-Earth asteroid lightcurve analysis at the center for Solar System Studies: 2019 March-July." *Minor Planet Bulletin* **46**, 423-438.

Warner B.D.; Stephens, R.D. (2020). "Near-Earth asteroid lightcurve analysis at the center for solar system studies: 2019 July-September." *Minor Planet Bulletin* **47**, 23-34.

LIGHTCURVE ANALYSIS OF ASTEROIDS 1939 LORETTA, 2099 OPIK, 2699 KALININ, 2779 MARY, 3108 LYUBOV, 5182 BRAY, AND 9098 TOSHIHIKO

Michael Fauerbach
Florida Gulf Coast University
and SARA Observatories
10501 FGCU Blvd.
Ft. Myers, FL33965-6565
mfauerba@fgcu.edu

(Received: 2021 February 13)

Photometric observations of seven main-belt asteroids were obtained on five nights between 2019 November 22 and 2019 December 28. The following rotational periods were determined: 1939 Loretta, 23.92 ± 0.02 h; 2099 Opik, 6.44 ± 0.01 h; 2699 Kalinin, 2.928 ± 0.001 h; 2779 Mary, 3.62 ± 0.01 h; 3108 Lyubov, 4.83 ± 0.01 h; 5182 Bray, 2.88 ± 0.01 h; 9098 Toshihiko, 3.46 ± 0.01 h.

Photometric observations obtained with the Southeastern Association for Research in Astronomy (SARA) consortium 1-m Jacobus Kapteyn Telescope at the Observatorio del Roque de los Muchachos on the Spanish island of La Palma are presented. The telescope is coupled with an Andor iKon-L series CCD. A detailed description of the instrumentation and setup can be found in Keel et al. (2017). The data was calibrated using *MaximDL* and photometric analysis was performed using *MPO Canopus* (Warner, 2017).

1939 Loretta. This asteroid is a member of the Themis family of asteroids. The asteroid was observed on three nights for approximately 6 h each night. The rotational period of 1939 Loretta is close to 24 h and therefore only part of the lightcurve could be observed. However, the period is well-defined as the data contains a steep and sharp minimum. As no maximum was observed we cannot determine the amplitude for the lightcurve. The current data yields a rotational period of 23.92 ± 0.02 h. This is in excellent agreement with the two previous measurements by Ďurech and Hanuš (2018, 23.931 ± 0.002 h) and Fauerbach (2019, 23.88 ± 0.02 h).

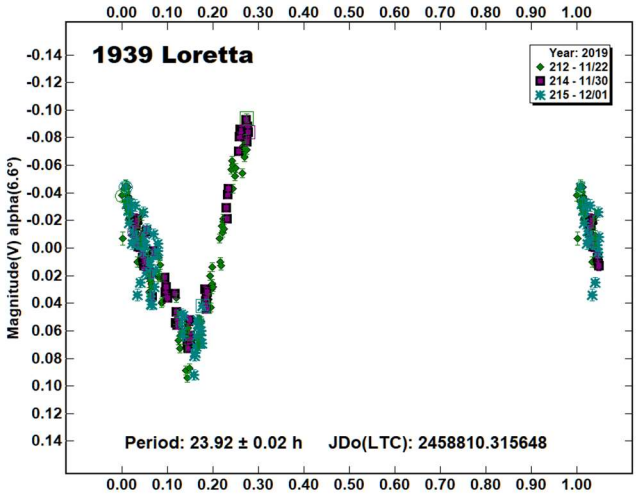

2099 Opik is a Mars-crossing asteroid. Goretti (2000) derived a period of 9.3 ± 0.1 h with an amplitude of 0.7 mag based on sparse data. Behrend (2005) reports a period of 6.4430 ± 0.0002 h with an amplitude of 0.21 mag. The present data yields a period of 6.44 ± 0.01 h with an amplitude of 0.19 mag. This is in excellent agreement with the result by Behrend. As their results indicate a more intricate lightcurve, the current data is presented with both a bimodal, and a 4th-order fit.

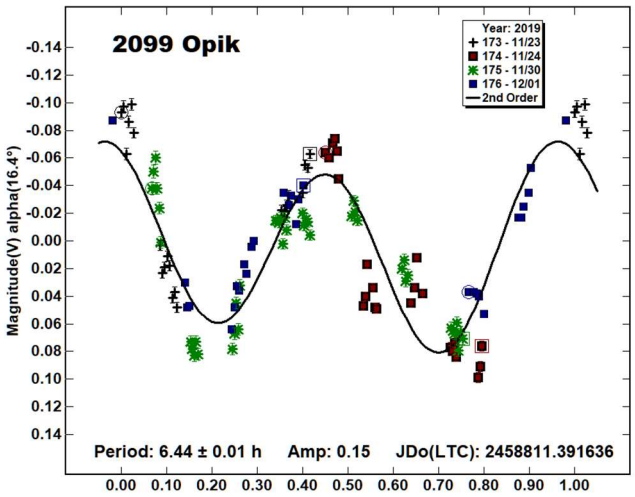

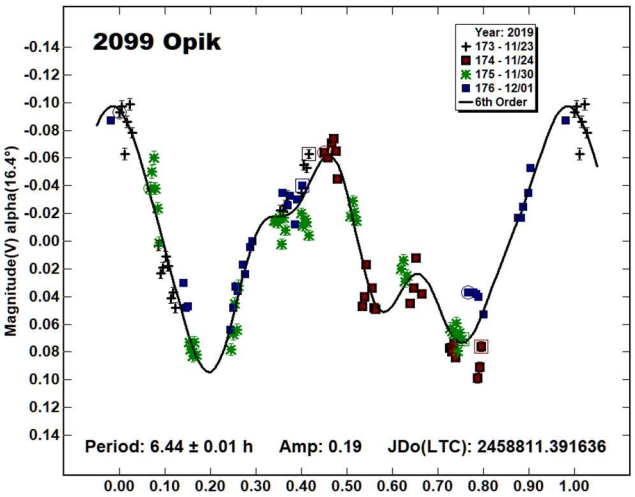

2699 Kalinin. We observed 2699 Kalinin on four nights over a four-week period. A rotational period of 2.928 ± 0.001 h with an amplitude of 0.19 mag was obtained. This is in excellent agreement with the result by Ambrosioni (2011, 2.9279 h) and by our own group (Fauerbach and Zabala, 2019, 2.928 h).

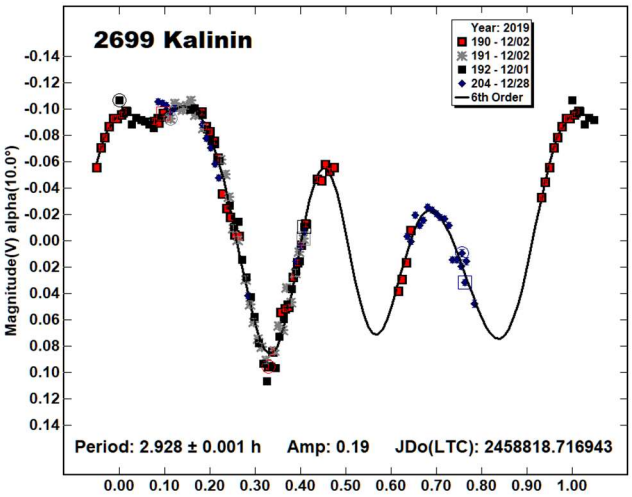

2779 Mary is a member of the Flora group of asteroids. A rotational period of 3.62 ± 0.01 h with an amplitude of 0.11 mag was obtained. The only prior period determination is from Behrend (2006) with a derived period of 3.36 ± 0.05 h. This is in fair agreement with the current measurement.

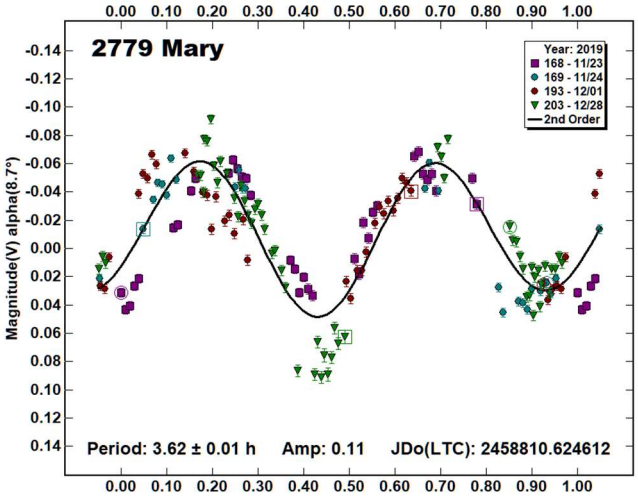

3108 Lyubov is a member of the Flora group/family. The only prior period determination is by Waszczak et al. (2015). They derived a period of 2.658 ± 0.0004 h with an amplitude of 0.18 mag. Our best fit for a bimodal model results in a period of 2.66 ± 0.01 h with an amplitude of 0.15 mag. This seems to be in very good agreement with the period determined by Waszczak, however a closer look at the data shows a rather large scatter of our data. If one takes higher order solutions into consideration a much better fit with a period of 4.83 ± 0.01 h and a magnitude of 0.21 mag appears. For the current publication, the later result is the preferred one.

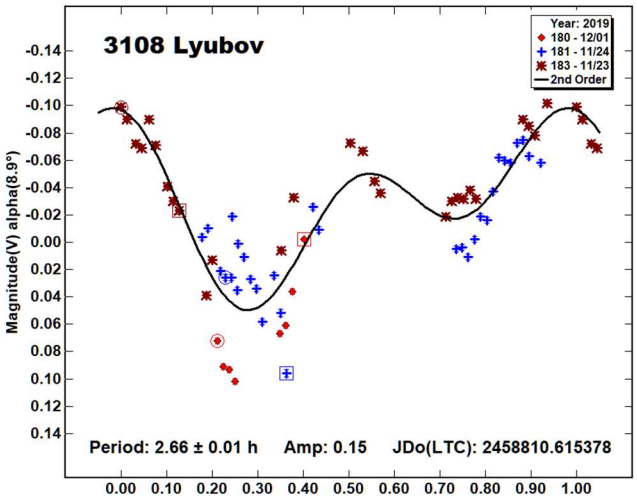

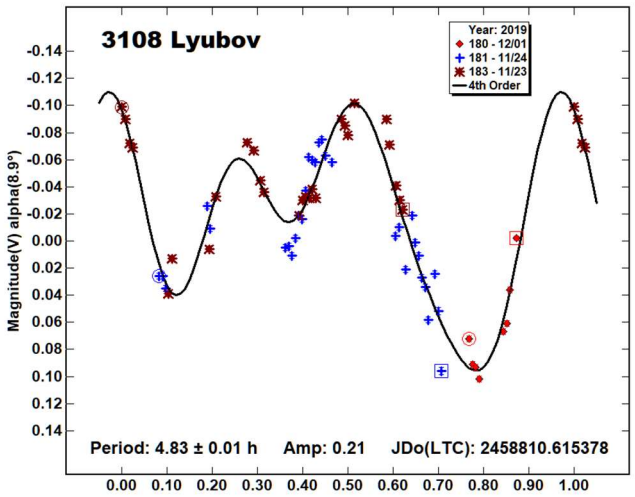

5182 Bray. This is a member of the Eunomia family. We observed 5182 Bray on two successive nights and measured a rotational period of 2.88 ± 0.01 h with an amplitude of 0.28 mag. This is in excellent agreement with previous publications by Klinglesmith (2014, 2.883 h) and Behrend (2018, 2.884 h), as well as our previous result (Fauerbach, 2019, 2.86 h).

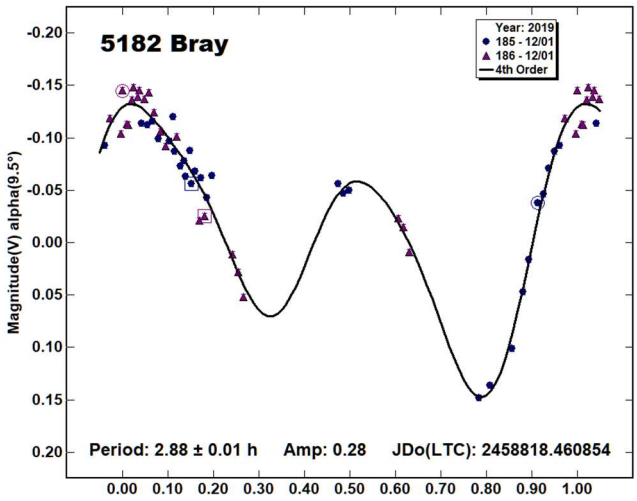

9098 Toshihiko. We observed 9098 Toshihiko on three nights for more than 6 h every night. Unfortunately, the data is very noisy and of lower-than-expected quality. The only prior period determination is by Chang et al. (2016). They derived a period of 6.19 ± 0.12 h with an amplitude of 0.13 mag. Our best fit for a bimodal model results in a period of 6.93 ± 0.01 h with an amplitude of 0.09 mag. Due to the noisy nature of the data, the solution is not unique. Many other solutions, including the half-period provide a similar good fit. Looking at the individual nights the half-period of 3.46 ± 0.01 h with an amplitude of 0.11 mag appears to be the preferred solution and will be reported here.

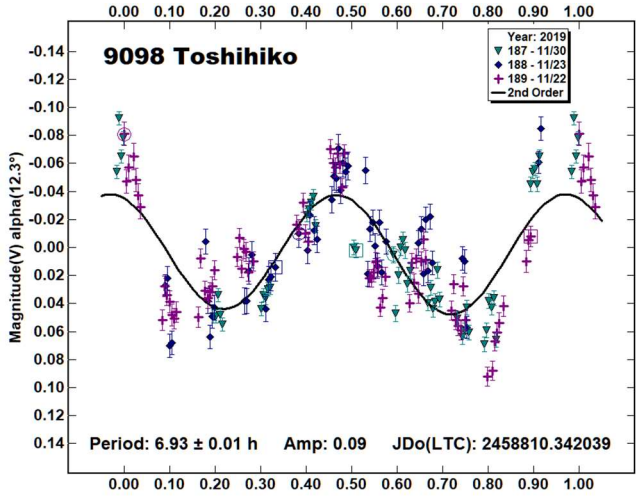

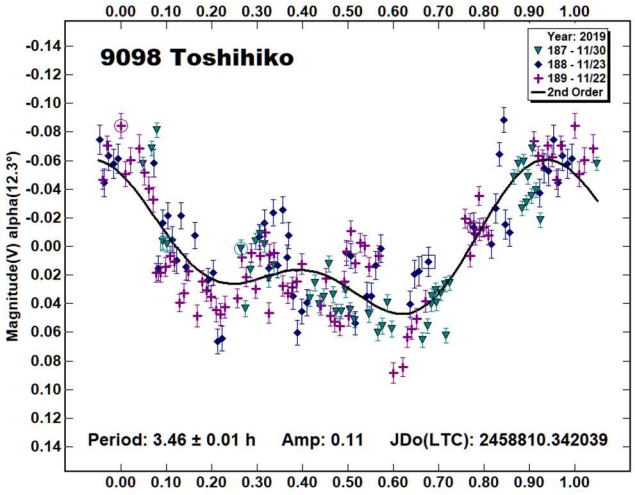

References

Ambrosioni, C., Colazo, C., Mazzone, F. (2011). "Period Determination for 1996 Adams and 2699 Kalinn by AOACM." *Minor Planet Bulletin* **38**, 102.

Behrend, R. (2005, 2006, 2018). Observatoire de Geneve web site. *http://obswww.unige.ch/~behrend/page_cou.html*

Chang, C.-K.; Lin, H.-W.; Ip, W.-H.; Prince, T.A.; Kulkarni, S.R.; Levitan, D.; Laher, R.; Surace, J. (2016). "Large Super-fast Rotator Hunting Using the Intermediate Palomar Transient Factory." *Astrophys. J. Suppl. Series* **227**, article id. 20.

Ďurech, J., Hanuš, J. (2018) "Reconstruction of asteroid spin states from Gaia DR2 photometry." *Astronomy & Astrophysics* **620**, A91.

Fauerbach, M. (2019). "Photometric Observations for 8 Main-belt Asteroids: 2017 April - May." *Minor Planet Bulletin* **46**, 1.

Fauerbach, M., Zabala, F. (2019). "Photometric Observations of Asteroids 570 Kythera, 1334 Lundmarka, 2699 Kalinin, and 5182 Bray." *Minor Planet Bulletin* **46**, 3.

Goretti, V. (2000). "CCD Photometry of the Mars-crosser Asteroid 2099 Opik." *Minor Planet Bulletin* **27**, 46.

Harris, A.W.; Young, J.W.; Scaltriti, F.; Zappala, V. (1984). "Lightcurves and phase relations of the asteroids 82 Alkmene and 444 Gyptis." *Icarus* **57**, 251-258.

Keel, W.C.; Oswalt, T.; Mack, P.; Henson, G.; Hillwig, T.; Batcheldor, D.; Berrington, R.; De Pree, C.; Hartmann, D.; Leake, M.; Licandro, J.; Murphy, B.; Webb, J.; Wood, M.A. (2017). "The Remote Observatories of the Southeastern Association for Research in Astronomy (SARA)." *PASP* **129**:015002 (12pp). *http://iopscience.iop.org/article/10.1088/1538-3873/129/971/015002/pdf*

Klinglesmith III, D.A. (2014). Posting on CALL web site. *http://www.MinorPlanet.info/call.html*

Warner, B.D.; Harris, A.W.; Pravec, P. (2009). "The Asteroid Lightcurve Database." *Icarus* **202**, 134-146. Updated 2020 Oct. *http://www.minorplanet.info/lightcurvedatabase.html*

Warner, B.D. (2017). *MPO Canopus* software version 10.7.10.0. *http://www.bdwpublishing.com*

Waszczak, A., Chang, C.-K., Ofek, E.O., Laher, R., Masci, F., and 8 coauthors. (2015). "Asteroid Light Curves from the Palomar Transient Factory Survey: Rotation Periods and Phase Functions from Sparse Photometry." *Astron. J.* **150**, A75, 35 pp.

Number	Name	yyyy mm/dd	Phase	L_{PAB}	B_{PAB}	Period(h)	P.E.	Amp	A.E.	Grp
1939	Loretta	2019 11/22-12/01	6.5,9.1	38	0	23.92	0.02			THM
2099	Opik	2019 11/23-12/01	16.4,21.3	48	-14	6.44	0.01	0.19	0.01	MC
2699	Kalinin	2019 12/01-12/28	10.0,5.5	89	8	2.928	0.001	0.19	0.01	MB-M
2779	Mary	2019 11/23-12/28	*8.7,10.1	77	0	3.62	0.01	0.11	0.02	FLOR
3108	Lyubov	2019 11/23-12/01	13.5,8.9	80	-5	1.83	0.01	0.21	0.01	FLOR
5182	Bray	2019 11/30-12/01	9.3,9.5	55	-20	2.88	0.01	0.28	0.03	EUN
9098	Toshihiko	2019 11/22-11/30	8.9,12.2	40	0	3.46	0.01	0.11	0.02	MB-O

Table I. Observing circumstances and results. The phase angle is given for the first and last date. If preceded by an asterisk, the phase angle reached an extrema during the period. L_{PAB} and B_{PAB} are the approximate phase angle bisector longitude/latitude at mid-date range (see Harris et al., 1984). Grp is the asteroid family/group (Warner et al., 2009).

LIGHTCURVES OF FOURTEEN ASTEROIDS

Eric V. Dose
3167 San Mateo Blvd NE #329
Albuquerque, NM 87110
mp@ericdose.com

(Received: 2021 Apr 14)

By applying dozens of comparison stars from the ATLAS refcat2 catalog to each working image, we have obtained lightcurves and synodic rotation periods for fourteen asteroids.

We present asteroid lightcurve photometry results achieved by following the workflow process described by Dose (2020a), with later improvements (Dose, 2020b). This workflow applies to each image an ensemble of typically 30-150 ATLAS refcat2 catalog (Tonry et al, 2018) comparison ("comp") stars as a basis for asteroid photometry. Diagnostic plots and numerous comp stars allow for effective identification and removal of outlier, variable, and poorly measured comp stars.

The present workflow produces a time series of asteroid magnitude estimates on Sloan r' (SR) catalog basis, unreduced and without H-G adjustment. These magnitudes are imported directly into *MPO Canopus* software (Warner, 2018) where they are adjusted for distances and phase-angle dependence, fit by Fourier analysis including identifying and ruling out of aliases, and plotted. Phase-angle dependence is corrected with a H-G model, using $G = 0.15$ for each asteroid unless otherwise specified.

No nightly zero-point adjustments (DeltaComps in *MPO Canopus* terminology) were made to any session herein, other than by adjusting the G value (H-G). All lightcurve data herein have been submitted to ALCDEF.

Lightcurve Results

Fourteen asteroids were observed from Deep Sky West observatory (IAU V28) at 2210 meters elevation in northern New Mexico. Images were acquired with a 0.35-meter SCT reduced to f/7.7; a SBIG STXL-6303E camera cooled to -35C and fitted with a Clear filter (Astrodon); and a PlaneWave L-500 direct-drive mount. The equipment was operated remotely via ACP software version 8.3 (DC-3 Dreams), running plan text files generated for each night by the author's python scripts (Dose, 2020a). Observations often cycled between 2-4 asteroids. Exposure times targeted 5-8 millimagnitudes uncertainty in asteroid instrumental magnitude, subject to a maximum of 900 seconds and a minimum of 90 seconds to ensure suitable comp-star photometry. All exposures were autoguided.

FITS images were plate-solved by *PinPoint* (DC-3 Dreams) or *TheSkyX* (Software Bisque) and were calibrated using temperature-matched, median-averaged dark images and recent flat images of a flux-adjustable flat panel. Every photometric image was visually inspected; all images with poor tracking, obvious interference by cloud or moon, or having stars or other light sources within 10 arcseconds of the target asteroid were excluded. Photometry-ready images that pass these screens were submitted to the workflow, which applies separately measured second-order transforms from Clear filter to deliver asteroid magnitudes in Sloan r' passband.

In this work, "period" refers to an asteroid's synodic rotation period, "SR" denotes the Sloan r' passband, and errors are given in parentheses after the value and are in units of the last decimal place.

414 Liriope. This bright outer main-belt asteroid was found to have period 11.007(2) hours, differing from one early lightcurve report of 7.353 h (Alvarez, 2012) and two survey reports of 7.38 h (Chang, 2015) and 7.34 h (Waszczak, 2015), but in close agreement with two very recent reports of 11.005 h (Colazo, 2020) and 11.0065 h (Pál, 2020). The candidate periods near 7.36 h are close to 2/3 of 11.007 h, corresponding to bimodal interpretation of this apparently trimodal lightcurve. At the present viewing aspect, we observed a single deep minimum, which reduced aliasing and modal ambiguity.

Our trimodal lightcurve is generally similar in shape to that of (Colazo, 2020), except for being roughly mirrored in time about our phase of 0.62. Fourier fit to the present data has RMS error of 8 millimagnitudes and indicates a G value close to 0.10.

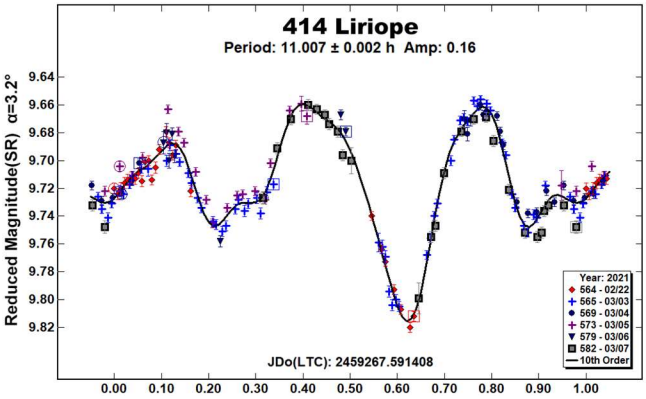

576 Emanuela. This asteroid of undetermined type was found to have period 20.370(3) h, differing from reports of >26 h (Wetterer, 1999), 14 h (Behrend, 2003web), and 14.04 h (Behrend, 2019web), but agreeing reasonably with reports of 20.406 h (as monomodal; Pilcher, 2017), 20.404 h (Pilcher, 2018), and more closely with a very recent report of 20.372 h (Pilcher, 2020). Reports of about 14 h represent an alias of ½ period per 24 hours from ours.

Small but systematic error trends are likely due to the lightcurve amplitude's depending on viewing phase angle (range 1.5-14.5º) (Zappalá, 1990), though a small tumbling effect is possible. Fourier fit to the present data has RMS error of 14 millimagnitudes and indicates a G value close to 0.08.

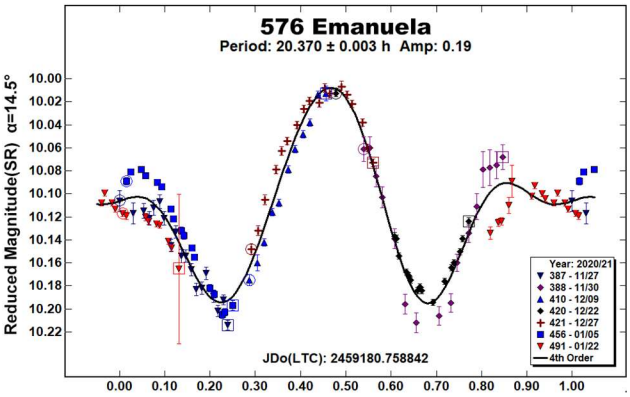

Number	Name	yyyy mm/dd	Phase	L_{PAB}	B_{PAB}	Period(h)	P.E.	Amp	A.E.	Grp
414	Liriope	2021 02/22-03/07	3.2,6.9	147	7	11.007	0.002	0.16	0.01	MB-O
576	Emanuela	2020-21 11/27-01/22	*14.5,1.5	118	1	20.370	0.003	0.19	0.03	UKN
594	Mireille	2021 02/24-03/05	*6.8,5.6	164	7	4.968	0.001	0.38	0.02	UKN
768	Struveana	2021 02/11-02/20	8.4,6.9	157	18	10.753	0.001	0.35	0.02	UKN
783	Nora	2020-21 12/01-02/05	*19.0,1.5	134	-3	53.820	0.040	0.13	0.03	MB-I
786	Bredichina	2021 02/22-03/16	*8.2,8.5	164	18	10.753	0.001	0.35	0.02	UKN
983	Gunila	2020-21 12/08-01/22	*13.3,4.9	119	-13	33.385	0.012	0.07	0.01	MB-O
1041	Asta	2021 02/03-03/02	6.4,12.0	131	16	7.978	0.001	0.16	0.02	MB-O
1591	Baize	2021 03/07-04/01	*19,3,18.4	187	34	7.808	0.002	0.04	0.01	PHO
2180	Marjaleena	2021 01/24-03/20	*3.9,15.5	126	-11	7.702	0.001	0.34	0.03	EOS
2288	Karolinum	2021 02/11-03/16	*12.9,10.8	164	19	43.151	0.008	0.27	0.02	UKN
3061	Cook	2020-21 10/22-01/16	*5.8,19.7	42	-3	135.250	0.080	0.44	0.08	UKN
9563	Kitty	2020-21 11/18-01/18	*15.3,15.6	85	-2	5.382	0.001	1.06	0.12	MB-I
16452	Goldfinger	2021 02/08-04/11	*15.0,16.1	169	-2	3.884	0.001	0.19	0.05	V

Table I. Observing circumstances and results. The phase angle is given for the first and last date. If preceded by an asterisk, the phase angle reached an extrema during the period. L_{PAB} and B_{PAB} are the approximate phase angle bisector longitude/latitude at mid-date range (see Harris et al., 1984). Grp is the asteroid family/group (Warner et al., 2009).

594 Mireille. This high-albedo asteroid of undetermined type was found to have period 4.9685(5) h, in close agreement with previous reports of 4.966 h (Wisniewski, 1991), 4.9671 h (Polakis and Skiff, 2017), and 4.9688 h (Benishek, 2018).

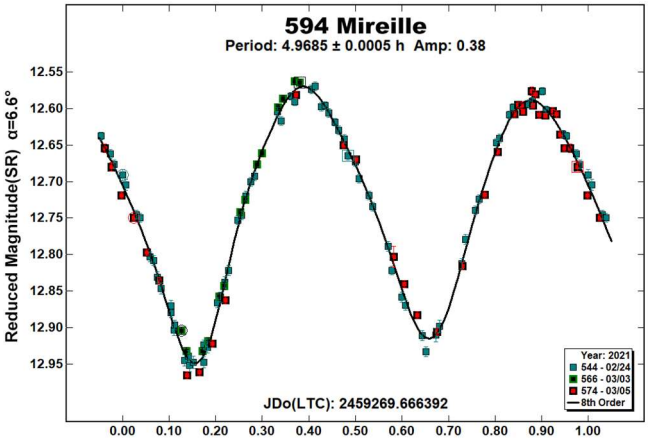

The present lightcurve represents a new viewing angle (phase angle bisector) for this asteroid, in which the two halves of the bimodal lightcurve are more nearly equal than seen before. Best Fourier fit has RMS error of 10 millimagnitudes and indicates G of 0.80.

768 Struveana. The present period of 10.753(1) h for this asteroid of undetermined type matches the author's determination of 10.744(6) h (Dose, 2020a), made during its previous apparition. The best present Fourier fit has RMS error of 11 millimagnitudes.

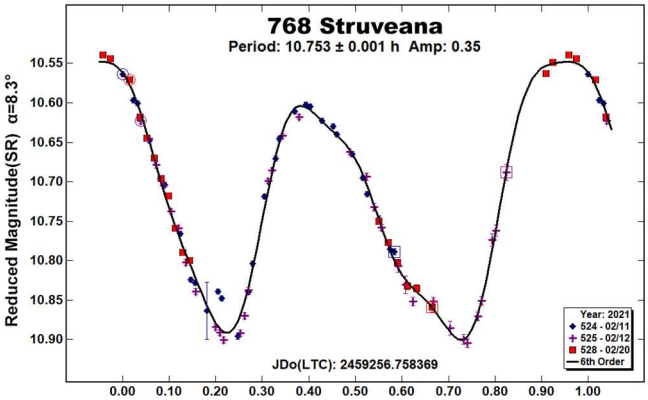

783 Nora. This inner main-belt asteroid is found to have period 53.82(4) h, in reasonable agreement with the previously reported 55.53 h (Polakis, 2018) and 54.22 h (Polakis, 2020), and is consistent with a report of >24 h (Lagerkvist, 1992), but differs from earlier reports of 34.4 h (Florcazk, 1997), and 9.6 h (Behrend, 2007web). The current best Fourier fit has RMS error of 8 millimagnitudes and indicates a *G* value of 0.80.

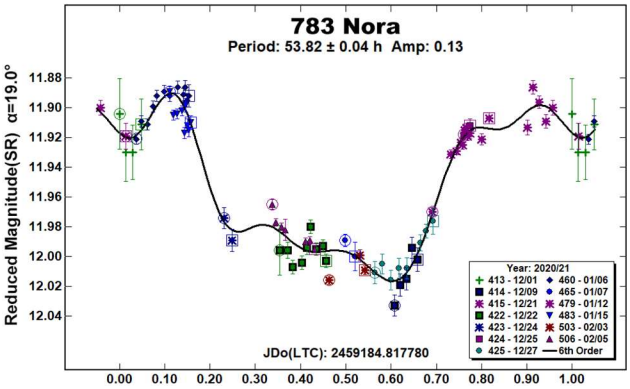

786 Bredichina. This low-albedo asteroid of undetermined type was found to have period 29.747(7) h, in fair agreement with recent reports of 29.434 h (Garcerán, 2015) and 29.8094 h (Pál, 2020), but differing from earlier reports of 18.61 h (Gil-Hutton and Cañada, 2003) and 27.88 h (Behrend, 2010web).

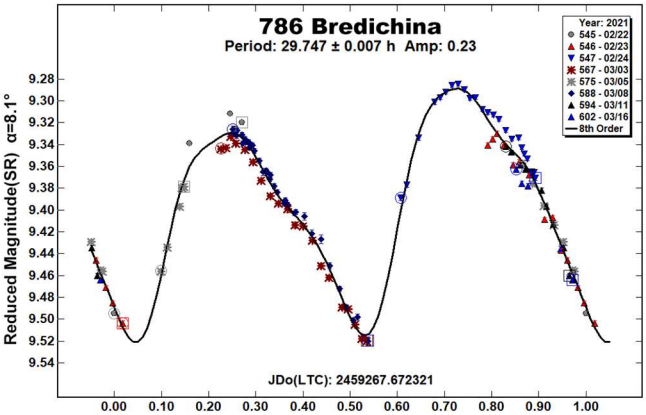

The previously reported 18.61 h is an alias of ½ period per 24 hours from our finding. The best Fourier fit for the present lightcurve has RMS error of 8 millimagnitudes and indicates *G* of roughly 0.80.

983 Gunila. Lightcurve modality for this outer main-belt asteroid has been difficult to determine with confidence. Using data from three nights, Hayes-Gehrke (2014) found a monomodal period of 8.37 h, and, from data obtainined on six consecutive nights, Polakis (2019) reported a monomodal period of 16.633 h. Our lightcurve results from nine nights' data taken over six weeks and is ambiguous between a bimodal period of 33.385(12) h or a monomodal period of half that. The low amplitude allows for either modality (Harris, 2014). Both fits yield RMS error of close to 5 millimagnitudes.

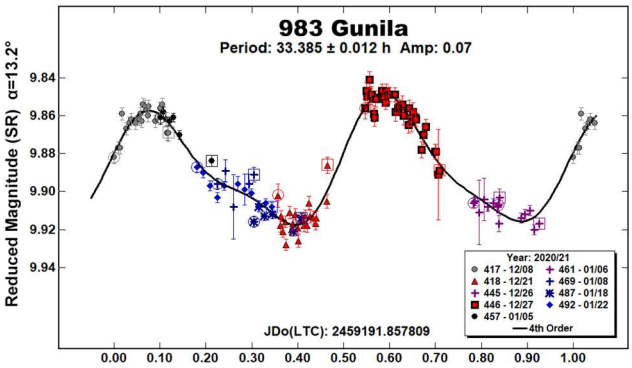

The split-halves phase plot slightly favors the bimodal period of 33.385 h as given in the figures, though the differences between halves are of low significance, being about 2 times the fit RMS error at lightcurve maximum and no perceptible difference at minimum.

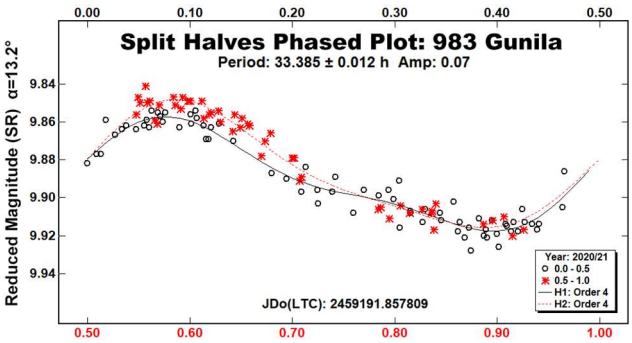

1041 Asta. Our lightcurve for this outer main-belt asteroid is complex and yields a period of 7.9775(5) h, agreeing with a previous report of 7.99 h (Carbo, 2009), but differing from a separate report of 7.554 h (Behrend, 2010web), which is entirely absent from our period spectrum. Our Fourier fit has RMS error of 7 millimagnitudes and indicates *G* value of about 0.03.

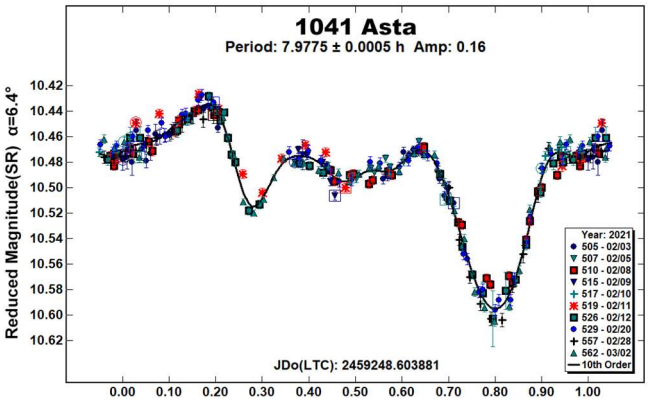

1591 Baize. One goal of our evolving data-reduction program is to improve acquisition of very low-amplitude lightcurves. Our latest such effort resulted in this lightcurve for 1591 Baize, from which we obtained an unambiguous period even with amplitude of 0.04 magnitudes. Our period of 7.808(2) h is comparable to previous reports of 7.78 h (Garlitz, 2013web), 7.788 h (Bentz, 2018) and 7.794 h (Mas, 2018), but differs from an earlier report of 10 h (Barucci, 1994). We found no previous report of amplitude smaller than 0.19 magnitudes, so we may well have observed 1591 Baize from a viewing angle near its pole. Indeed, the very largest magnitude reported to date was determined from a phase angle bisector nearly perpendicular to ours. RMS error of our Fourier fit is 7 millimagnitudes, and *G* values near 0.55 optimize the fit.

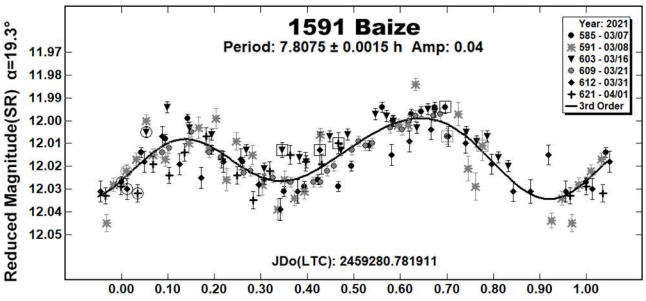

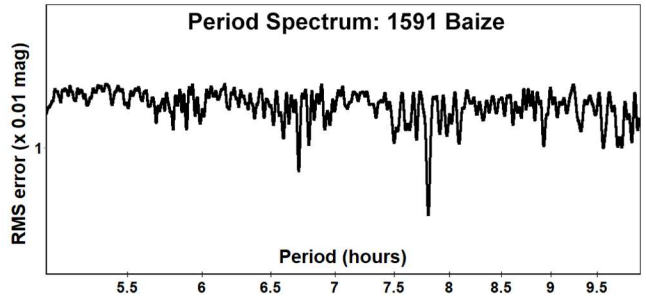

These 1591 Baize data were reduced with three experimental improvements to our session workflow: non-circular photometric apertures for asteroids, elongated in direction and extent to account for asteroid motion; unconditional exclusion of comp stars having any catalog indication of nearby flux; and iterative statistical treatment of comp-star and asteroid photometric annuli, to get much more robust estimates of sky background brightness and uncertainty.

2180 Marjaleena. This Eos-family asteroid was found to have a clearly bimodal lightcurve with period 7.7025(5) h, in agreement with previous reports of 7.703 h (Waszczak, 2015) and 7.717 h (Polakis, 2020), but differing from reports of 7.396 (Behrend, 2014web), 6.702 h (Waszczak, 2015), and 8.346 h (Hanuš, 2018a). Our RMS error is 19 millimagnitudes; the best *G* estimate is 0.12.

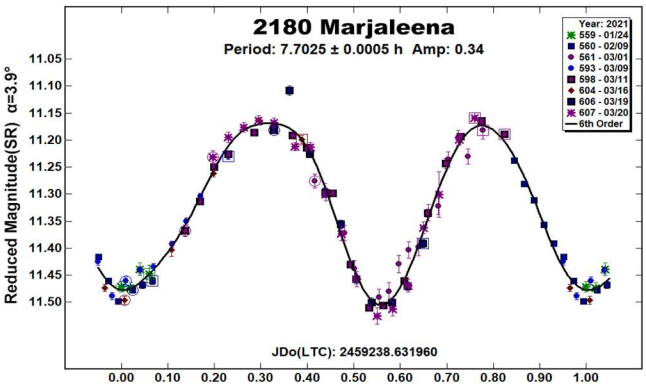

2288 Karolinum. Observations over 13 nights have been combined to make the first known complete lightcurve for this asteroid of undetermined type. We find a period of 43.151(8) h, agreeing generally with previous reports of 42.16 h (Warner, 2006) and 42.8335 h (Pál, 2020), but not with a reported 23.31 h (Behrend, 2006web). Our RMS error is 9 millimagnitudes, and *G* of 0.30 improved the Fourier fit over the default *G* value of 0.15.

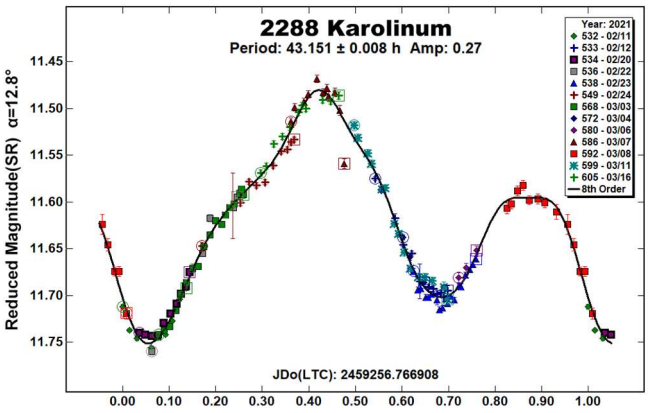

3061 Cook. This asteroid of undetermined type was found in images targeting (2689) Bruxelles (Dose, 2021), and then followed in its own right. We report here a period of 135.25(8) h; no tumbling was apparent from the lightcurve.

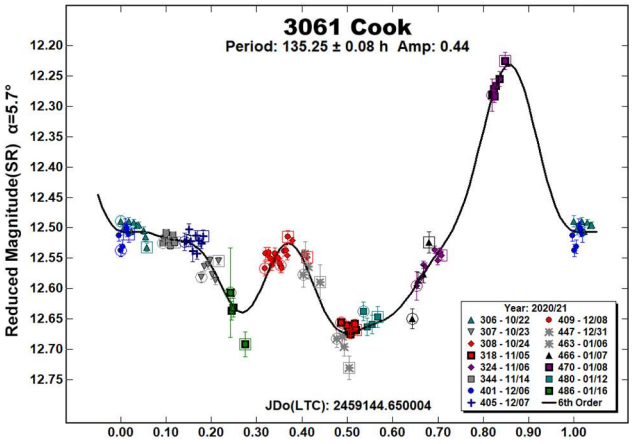

No previous reports of rotation period were found. RMS error is 19 millimagnitudes. A *G* value of 0.03 minimized fit errors; our *G* value differs from one previous survey-derived report of 0.472 (Vereš, 2015).

Even with 15 nights of observations, the lightcurve still suffers unfortunate gaps, especially in allowing for only one night near the apparent maximum (phase 0.85 in the phase plot), but the Fourier fit is close throughout, and the period spectrum shows no prominent aliases or other signals, so we assess the proposed period as likely correct. Confirming observations are encouraged.

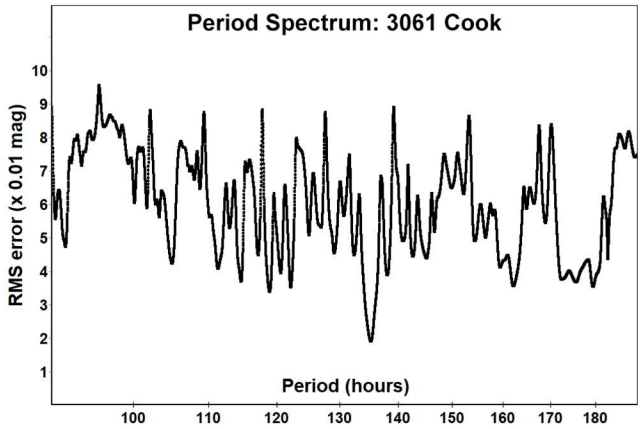

9563 Kitty. This asteroid, whose orbit is characteristic of the Eunomia family, was found to have period 5.3825(5) h, in agreement with previous reports of 5.36 h (Chang, 2015), 5.367 h (Waszczak, 2015), and 5.38191 (Hanuš, 2018b). The asteroid was faint during this apparition, leading to significant observational noise, but the large lightcurve amplitude somewhat compensated for this. RMS error is 61 millimagnitudes, best *G* value is 0.38.

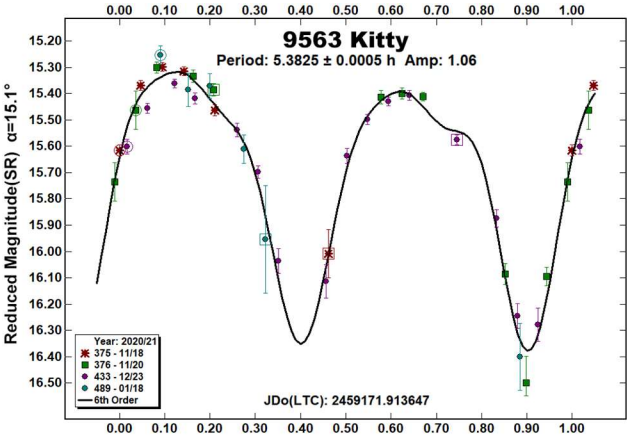

16452 Goldfinger. This high-albedo Vestoid was found to have period 3.8835(5) h.

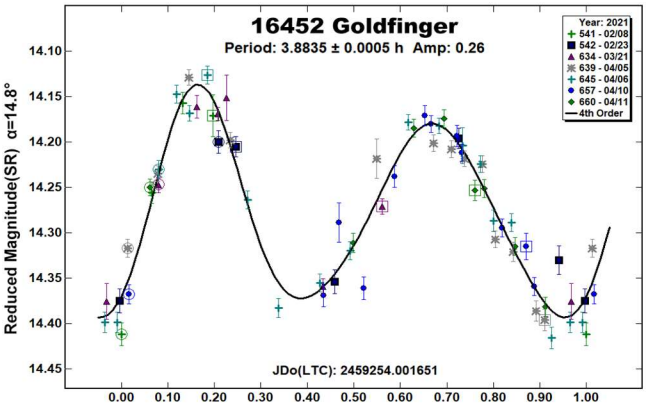

No previous period reports are known to the author. RMS error is 24 millimagnitudes; a *G* value of 0.35 markedly improved the Fourier fit over the standard 0.15 value.

Acknowledgements

The author thanks all authors of the ATLAS paper (Tonry et al, 2018) and numerous contributors for providing without cost the ATLAS refcat2 release catalog and its technical descriptions.

This project makes extensive use of the python language interpreter and of several supporting packages (notably: pandas, ephem, matplotlib, requests, astropy, and statsmodels), all provided without cost, and without which this work would have been infeasible.

References

Alvarez, E.M. (2012). "Period Determination for 414 Liriope." *Minor Planet Bull.* **39**, 21-22.

Barucci, M.A.; di Martino, M.; Dotto, E.; Fulchignoni, M.; Rotundi, A.; Burchi, R. (1994). "Rotational Properties of Small Asteroids: Photoelectric Observations of 16 Asteroids." *Icarus* **109**, 267-273.

Behrend, R. (2003web, 2006web, 2007web, 2010web, 2014web, 2019web). Observatoire de Geneve web site. *http://obswww.unige.ch/~behrend/page_cou.html*

Benishek, V. (2018). "Lightcurve and Rotation Period Determinations for 29 Asteroids." *Minor Planet Bull.*, **45**, 82-91.

Bentz, M.C.; Abbott, C.; Agudelo, S.; Dassing, S.; Flynn, W.; Gibbs, A.; Gonzalez, L.; Kim, B.; Paredes, L.; Toben, C.; Vrijmoet, E.H.; Yep, A. (2018). "Filtered Photometric Monitoring of 1591 Baize." *Minor Planet Bull.* **45**, 311-312.

Carbo, L.; Kragh, K.; Krotz, J.; Meiers, A.; Shaffer, N.; Torno, S.; Sauppe, J.; Ditteon, R. (2009). "Asteroid Lightcurve Analysis at the Oakley Southern Sky Observatory and Oakley Observatory: 2008 September and October." *Minor Planet Bull.* **36**, 91-94.

Chang, C.-K.; Ip, W.-H; Lin, H.-W.; Cheng, Y.-C.; Ngeow, C.-C.; Yang, T.-C.; Waszczak, A.; Kulkarni, S.R.; Levitan, D.; Sesar, B.; Laher, R.; Surace, J.; Prince, T.A. (2015). "Asteroid Spin-State Study Using the Intermediate Palomar Transient Factory." *Astrophys. J. Suppl. Series* **219**, 27.

Colazo, L.M.; Fornari, C.; Santucho, M., Mottino, A.; Colazo, C.; Melia, R.; Suarez, N.; Vasconi, N.; Arias, D.; Stechina, A.; Scotta, D.; Garcia, J.; Pittari, C.; Ferrero, G. (2020). "Asteroid Photometry and Lightcurve Analysis at Gora's Observatories - Part II." *Minor Planet Bull.* **47**, 337-339.

Dose, E. (2020a). "A New Photometric Workflow and Lightcurves of Fifteen Asteroids." *Minor Planet Bull.* **47**, 324-330.

Dose, E. (2020b). "Lightcurves of Nineteen Asteroids." *Minor Planet Bull.* **48**, 69-76.

Dose, E. (2021). "Lightcurves of Eighteen Asteroids." *Minor Planet Bull.* **48**, 125-131.

Florczak, M.; Dotto, E.; Barucci, M.A.; Birlan, M.; Erikson, A.; Fulchignoni, M.; Nathues, A.; Perret, L.; Thebault, P. (1997). "Rotational properties of main belt asteroids: photoelectric and CCD observations of 15 objects." *Planetary Space Sci.* **14**, 1423-1435.

Garcerán, A.C.; Macías, A.A.; Mansego, E.A.; Rodriquez, P.B.; de Haro, J.L. (2015). "Lightcurve Analysis of Six Asteroids." *Minor Planet Bull.* **42**, 235-237.

Garlitz, J. (2013web). Submission to CALL database, February 7, 2013.

Gil-Hutton, R.; Cañada, M. (2003). "Photometry of Fourteen Main Belt Asteroids." *Rev. Mex. de Astron. y Astrofís.* **39**, 69-76.

Hanuš, J.; Delbo, M.; Alí-Lagoa, V.; Bolin, B.; Jedicke, R.; Ďurech, J.; Cibulková, H.; Pravec, P.; Kušnirák, P.; Behrend, R.; Marchis, F.; Antonini, P.; Arnold, L.; Audejean, M.; Bachschmidt, M.; Bernasconi, L.; Brunetto, L.; Casulli, S.; Dymock, R.; Esseiva, N.; Esteban, M.; Gerteis, O.; de Groot, H.; Gully, H.; Hamanowa, H.; Hamanowa, H.; Krafft, P.; Lehký, M.; Manzini, F.; Michelet, J.; Morelle, E.; Oey, J.; Pilcher, F.; Reignier, F.; Roy, R.; Salom, P.A.; Warner, B.D. (2018a). "Spin States of Asteroids in the Eos Collisional Family." *Icarus* **299**, 84-96.

Hanuš, J.; Ďurech, J.; Oszkiewicz, D.A.; Behrend, R.; Carry, B.; Delbo, M.; Adam, O.; Afonina, V.; Anquetin, R.; Antonini, P.; Arnold, L.; Audejean, M.; Aurard, P.; Bachschmidt, M.; Baduel, B.; Barbotin, E.; Barroy, P.; Baudouin, P.; Berard, L.; Berger, N. Bernasconi, L.; Bosch, J.-G.; Bouley, S.; Bozhinova, I.; Brinsfield, J.; Brunetto, L.; Canaud, G.; Caron, J.; Carrier, F.; Casalnuovo, G.; Casulli, S.; Cerda, M.; Chalamet, L.; Charbonnel, S.; Chinaglia, B.; Cikota, A.; Colas, F.; Coliac, J.-F.; Collet, A.; Coloma, J.; and 128 colleagues (2018b). "New and updated convex shape models of asteroids based on optical data from a large collaboration network." *Astron. Astrophys.* **586**, A108.

Harris, A.W.; Young, J.W.; Scaltriti, F.; Zappala, V. (1984). "Lightcurves and phase relations of the asteroids 82 Alkmene and 444 Gyptis." *Icarus* **57**, 251-258.

Harris, A.W.; Pravec, P.; Galád, A.; Skiff, B.A.; Warner, B.D.; Világi, J.; Gajdoš, Š.; Carbognani, A.; Hornoch, K.; Kušnirák, P.; Cooney, W.R.; Gross, J.; Terrell, D.; Higgins, D.; Bowell, E.; Koehn, B.W. (2014). "On the maximum amplitude of harmonics on an asteroid lightcurve." *Icarus* **235**, 55-59.

Hayes-Gehrke, M.; Berenhaus, J.; Mascone, A.; Lopez-Lahocki, M.; Levantis, G.; Haigh, E.; Yang, Z.; Guerci, J.; Wasli, Z.; Koester, K. (2014). "Rotation Period of 983 Gunila." *Minor Planet Bull.* **41**, 77.

Lagerkvist, C.-I.; Magnusson, P.; Debehogne, H.; Hoffman, M.; Erikson, A.; De Campos, A.; Cutispoto, G. (1992). "Physical Studies of Asteroids. XXV: Photoelectric Photometry of Asteroids obtained at ESO and Hoher List Observatory." *Astron. Astrophys. Suppl. Series* **95**, 461-470.

Mas, V.; Fornas, G.; Lozano, J.; Rodrigo, O.; Fornas, A.; Carreño, A.; Arce, E.; Brines, P.; Herrero, D. (2018). "Twenty-one Asteroid Lightcurves at Asteroids Observers (OBAS) - MPPD: Nov 2016 - May 2017." *Minor Planet Bull.* **45**, 76-82.

Pál, A.; Szakáts, R.; Kiss, C.; Bódi, A.; Bognár, Z.; Kalup, C.; Kiss, L.L.; Marton, G.; Molnár, L.; Plachy, E.; Sárneczky, K.; Szabó, G.M.; Szabó, R. (2020). "Solar System Objects Observed with TESS - First Data Release: Bright Main-belt and Trojan Asteroids from the Southern Survey." *Astrophys. J. Suppl. Series* **247**, 26.

Pilcher, F. (2017). "Rotation Period Determinations for 49 Pales, 96 Aegle, 106 Dione, 375 Ursula, and 576 Emanuela." *Minor Planet Bull.* **44**, 249-251.

Pilcher, F. (2018), "Reexamining the Rotation Period of 576 Emanuela." *Minor Planet Bull.* **45**, 18-19.

Pilcher, F. (2020). "Lightcurves and Rotation Periods of 10 Hygiea, 47 Aglaja, 455 Bruchsalia, 463 Lola, and 576 Emanuela." *Minor Planet Bull.* **47**, 133-135.

Polakis, T.; Skiff, B.A. (2017). "Lightcurve Analysis for 341 California, 594 Mireille, 1115 Sabauda, 1504 Lapeenranta, and 1926 Demiddelaer." *Minor Planet Bull.* **44**, 299-302.

Polakis, T. (2018). "Lightcurve Analysis for Eleven Main-Belt Minor Planets." *Minor Planet Bull.* **45**, 269-273.

Polakis, T. (2019). "Lightcurve Analysis for Seven Main-Belt Minor Planets." *Minor Planet Bull.* **46**, 78-80.

Polakis, T. (2020). "Photometric Observations of Twenty-three Minor Planets." *Minor Planet Bull.* **47**, 94-101.

Tonry, J.L.; Denneau, L.; Flewelling, H.; Heinze, A.N.; Onken, C.A.; Smartt, S.J.; Stalder, B.; Weiland, H.J.; Wolf, C. (2018). "The ATLAS All-Sky Stellar Reference Catalog." *Astrophys. J.* **867,** A105, 1-16.

Vereš, R.; Jedicke, R.; Fitzsimmons, A.; Denneau, L.; Granvik, M.; Bolin, B.; Chastel, S.; Wainscoat, R.J.; Burgett, W.S.; Chambers, K.C.; Flewelling, H.; Kaiser, N.; Magnier, E.A.; Morgan, J.S.; Price, P.A.; Tonry, J.L.; Waters, C. (2015). "Absolute Magnitudes and Slope Parameters for 250,000 Asteroids Observed by Pan-STARRS PS1 - Preliminary Results." *Icarus* **261**, 34-47.

Warner, B.D. (2006). "Asteroid Lightcurve Analysis at the Palmer Divide Observatory - February-March 2006." *Minor Planet Bull.* **33**, 82-84.

Warner, B.D.; Harris, A.W.; Pravec, P. (2009). "The asteroid lightcurve database." *Icarus* **202**, 134-146. Updated 2020 August. *http://www.minorplanet.info/lightcurvedatabase.html*

Warner, B.D. (2018). *MPO Canopus* Software, version 10.7.12.9. BDW Publishing. *http://www.bdwpublishing.com*

Waszczak, A.; Chang, C.-K.; Ofek, E.O.; Laher, R.; Masci, F.; Levitan, D.; Surace, J.; Cheng, Y.-C.; Ip, W.-H.; Kinoshita, D.; Helou, G.; Prince, T.A.; Kulkarni, S. (2015). "Asteroid Light Curves from the Palomar Transient Factory Survey: Rotation Periods and Phase Functions from Sparse Photometry." *Astron. J.* **150**, 75.

Wetterer, C.J.; Saffo, C.R.; Majcen, S.; Tompkins, J. (1999). "CCD Photometry of Asteroids at the US Air Force Academy Observatory During 1998." *Minor Planet Bull.* **26**, 30-31.

Wisniewski, W.Z. (1991). "Physical studies of small asteroids: I. Lightcurves and taxonomy of 10 asteroids." *Icarus* **90**, 117-122.

Zappalá, V.; Cellino, A.; Barucci, A.M.; Fulchignoni, M.; Lupishko, D.F (1990). "An analysis of the amplitude-phase relationship among asteroids." *Astron. Astrophys.* **231**, 548-560.

357 NININA AND 748 SIMEISA – TWO ASTEROIDS WITH EARTH COMMENSURATE ROTATION PERIODS

Frederick Pilcher
Organ Mesa Observatory (G50)
4438 Organ Mesa Loop
Las Cruces, NM 88011 USA
fpilcher35@gmail.com

Lorenzo Franco
Balzaretto Observatory (A81), Rome, ITALY

Alessandro Marchini
Astronomical Observatory, DSFTA - University of Siena (K54)
Via Roma 56, 53100 - Siena, ITALY

Julian Oey
Blue Mountains Observatory (Q68)
94 Rawson Pde. Leura, NSW 2780, AUSTRALIA

(Received: 2021 March 30)

A global collaboration of observers from Australia, Europe, and North America found synodic rotation periods and amplitudes for 357 Ninina 35.983 ± 0.001 h, 0.11 ± 0.01 magnitudes; 748 Simeisa 11.903 ± 0.001 h, 0.08 ± 0.01 magnitudes.

Observations to produce the results reported in this paper have been contributed by Frederick Pilcher in the USA, Lorenzo Franco and Alessandro Marchini in Italy, and Julian Oey in Australia. Equipment details are on Table II. Image photometric measurement and lightcurve construction were done by *MPO Canopus* software. To reduce the number of data points on the lightcurves and make them easier to read, data points have been binned in sets of 5 with maximum time difference 10 minutes.

357 Ninina. Previously published rotation periods for 357 Ninina are by Tedesco (1979), > 20 h; Behrend (2005), 35.98h; Oey (2014), 35.9 h in year 2007 observations and 36.0105 h in year 2013 observations. Twenty sessions of new observations 2020 Dec. 7 - 2021 Feb. 13 provide a good fit to a period of 35.983 ± 0.001 h, amplitude 0.11 ± 0.01 magnitudes.

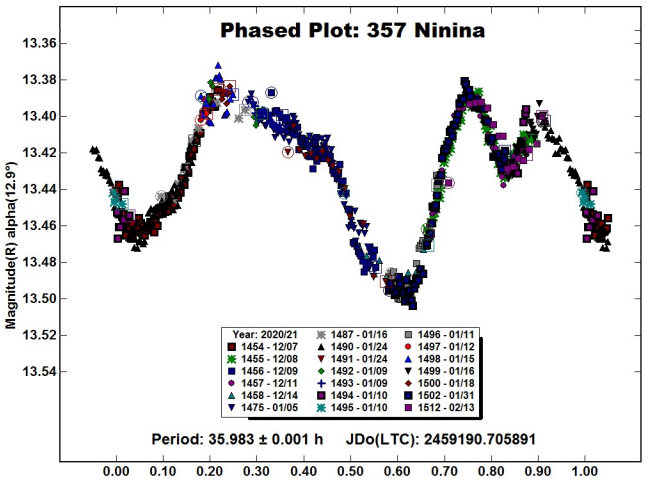

A split-halves plot of the double period is shown. About 90% of both halves of the double period are covered by the data. The segments covered by both halves of the split halves plot are nearly identical. The new result is compatible with previous determinations.

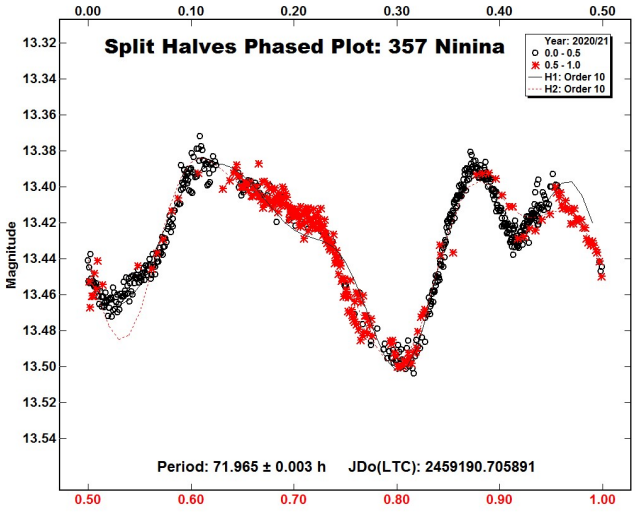

748 Simeisa. This object is a Hilda-type asteroid with orbit in the 3:2 resonance with Jupiter. Previously published rotation periods and amplitudes for 748 Simeisa are by Behrend (2011), 2011 Oct. 4-14, 11.919 h, 0.36 magnitudes, celestial longitude 345º; and Dahlgren et al. (1998), 1995 Aug 31-Sept. 2, 11.88 h, >0.22 magnitudes, celestial longitude 327º. Both observations sets were from a single observatory and show only about 8 hours, or 2/3 phase coverage. Being obtained at similar celestial longitudes, both published lightcurves show a single double-humped maximum rising about 0.2 magnitudes above nearly equal minima about 6 hours apart and a rise toward a second and perhaps higher maximum in the missing segment of the lightcurve. Warner and Stephens (2021) with data obtained at the same opposition as the data used in this paper, 2020 Oct. 30-Nov. 12, 23.633h, 0.10 magnitudes, with nearly 12 hours of their 23.633-hour lightcurve covered.

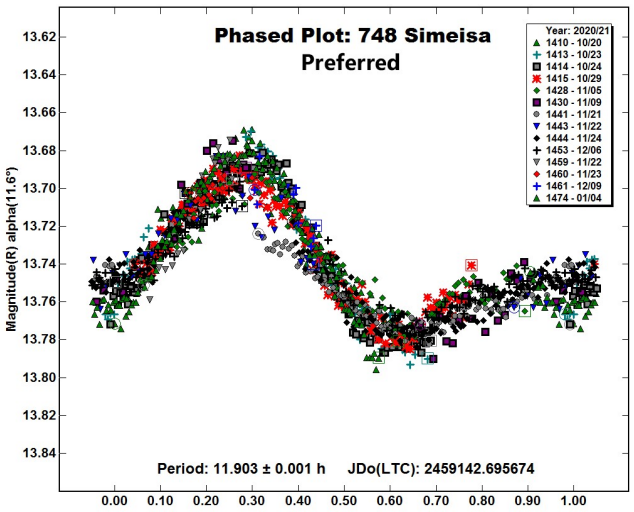

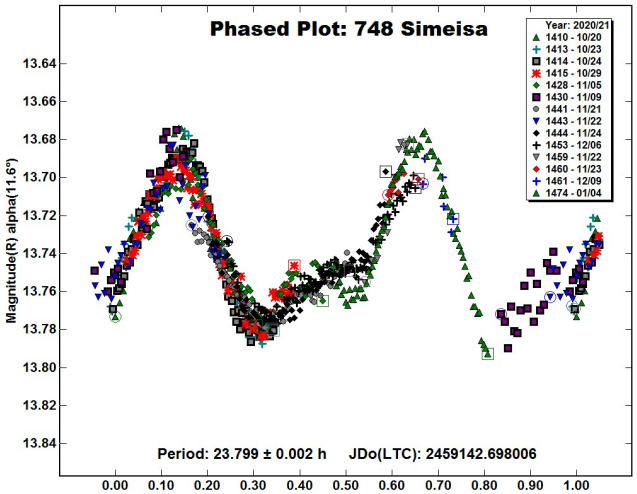

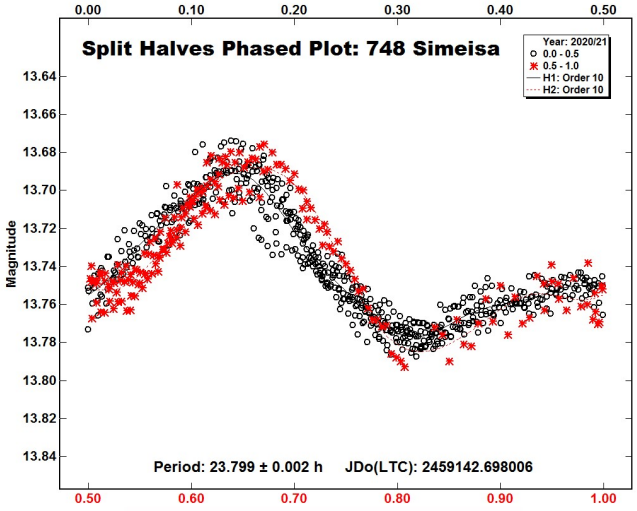

The authors of this paper obtained fourteen sessions of new observations 2020 Oct. 20 - 2021 Jan. 4 from their respective widely separated longitudes. Our data provide equally good fits to periods of 11.903 ± 0.001 hours with one maximum and minima per rotational cycle and 23.799 ± 0.002 hours with two symmetric maxima and minima, both with full phase coverage and amplitude 0.08 ± 0.01 magnitudes.

A split-halves plot of the double period shows that the two halves of the double period are nearly identical. Careful inspection of the split halves lightcurve shows that the segment between phases 0.7 and 0.8, obtained 2021 Jan. 4 at phase angle 12.6º, is slightly higher than the segments between phases 0.2 and 0.3 obtained more than one month earlier at smaller phase angles. We believe that the small discrepancy is caused by a change of lightcurve shape with changing phase angle, observed in many asteroids, and is not an indication that the double period is correct. It commonly occurs that asteroids with bimodal lightcurves at near equatorial aspect show only one maximum and minimum at a near polar aspect. Comparison of the large amplitudes found in apparently bimodal lightcurves at celestial longitudes 327º and 345º, respectively, with the much smaller amplitude of the current observations near celestial longitude 63º, suggests that our observations are within 20º to 25º of polar aspect.

Number	Name	yyyy/mm/dd	Phase	L_{PAB}	B_{PAB}	Period(h)	P.E	Amp	A.E.
357	Ninina	2020/12/07-2021/02/13	*12.9,11.6	112	-8	35.983	0.001	0.11	0.01
748	Simeisa	2020/10/20-2021/01/04	*11.6,12.6	63	1	11.903	0.001	0.08	0.01

Table I. Observing circumstances and results. The phase angle is given for the first and last date, where the * indicates that minimum phase angle occurred between these dates. L_{PAB} and B_{PAB} are the approximate phase angle bisector longitude and latitude at mid-date range (see Harris *et al.*, 1984).

Observer Observatory (MPC code)	Telescope	CCD	Filter	Observed Asteroids
Frederick Pilcher Organ Mesa Observatory (G50)	0.35-m SCT f/10.0	SBIG STL-1001E	C	357,748
Lorenzo Franco Balzaretto Observatory (A81)	0.20-m SCT f/5.0	SBIG ST7-XME	R	357,748
Alessandro Marchini Astronomical Observatory of the University of Siena(K54)	0.30-m MCT f/5.6	SBIG STL-6303e (bin 2x2)	R	357
Julian Oey Blue Mountains Observatory (Q68)	0.35-m SCT Edge f/7.0 0.35-m SCT f/5.9	SBIG STF-1603W SBIG ST-8XME	C	357,748

Table II. Observing equipment. MCT: Maksutov-Cassegrain, SCT: Schmidt-Cassegrain.

Like the authors of this paper, Warner and Stephens (2021) have published lightcurves for periods near both 12 hours and 24 hours. Their 12-hour lightcurve has a considerably different shape from ours despite having been obtained in the same time frame and leads them to favor the longer period. We are unable to explain the difference in the lightcurves. We invite interested readers to peruse the Warner and Stephens paper and evaluate the different conclusions of this paper and theirs according to their own good judgments. Following the conclusion of the 2020-2021 observing window for 748 Simeisa, we must conclude that the period remains ambiguous. The next opposition of 748 Simeisa occurs in 2022 February near declination +12º. Based on the lightcurves of Behrend (2011) and Dahlgren et al. (1995), a much larger amplitude is expected and globally distributed observations should resolve the ambiguity definitively.

Acknowledgments

First author Pilcher thanks Alan Harris and Brian Warner for helpful and productive discussions of the differences in their respective lightcurves and preferred rotation periods.

References

Behrend, R. (2005, 2011). Observatoire de Geneve web site. *http://*obswww.unige.ch/*~behrend/page_cou.html*

Dahlgren, M.; Lahulla, J.F.; Lagerkvist, C.-I.; Lagerros, J.; Mottola, S.; Erikson, A.; Gonano-Beurer, M.; Di Martino, M. (1998). "A Study of Hilda Asteroids. V. Lightcurves of 47 Hilda Asteroids." *Icarus* **133**, 247-285.

Harris, A.W.; Young, J.W.; Scaltriti, F.; Zappala, V. (1984). "Lightcurves and phase relations of the asteroids 82 Alkmene and 444 Gyptis." *Icarus* **57**, 251-258.

Oey, J. (2014). "Lightcurve analysis of asteroids from Blue Mountains Observatory in 2013." *Minor Planet Bull.* **41**, 276-281.

Tedesco, E.F. (1979). Ph. D. Dissertation, New Mexico State University.

Warner, B.D.; Stephens, R.D. (2021). "Lightcurve analysis of Hilda asteroids at the center for Solar System Studies, 2020 October-December." *Minor Planet Bull.* **48**, 164-165.

LIGHTCURVE ANALYSIS OF TEN ASTEROIDS

Larry E. Owings
Barnes Ridge Observatory
23220 Barnes Lane
Colfax, CA 95713
lowings1953@gmail.com

(Received: 2021 February 2, Revised: 2021 May 1)

Lightcurves for ten main-belt asteroids were obtained at the Barnes Ridge Observatory from 2019 July 24 through 2020 November 05. Synodic rotation periods and amplitudes are found for nine of the ten main-belt asteroids. Their synodic rotation periods and lightcurve amplitudes are: 2158 Tietjen, 8.65742 h, 0.41 mag; 3313 Mende, 13.3354 h, 0.26 mag; 3989 Odin, 5.3220 h, 0.16 mag; 4021 Dancey, 4.1085 h, 0.15 mag; 4103 Chahine, 104.9519 h, 0.80 mag; 5996 Julioangel, 9.7435 h, 0.26 mag; 7527 Marples, 9.0899 h, 0.49 mag; 9545 Petrovedmosti, 5.6649 h, 0.28 mag; 21242 1995 WZ41, 5.45303 h, 0.43 mag.

Photometric data for nine asteroids were obtained at Barnes Ridge Observatory located in northern California, USA, using a 0.43-m PlaneWave f/6.8 corrected Dall-Kirkham astrograph and Apogee U9 camera. The camera was binned 2×2 with a resulting image scale of 1.26 arcsec per pixel. All image exposures were 210-s taken through a photometric C filter. All images were obtained with *MaxIm DL* V6 driven by *ACP* V8 and analyzed using *MPO Canopus* v10.8.1.1 (Warner, 2019). The *MPO Canopus* Comp Star Selector feature was used to select comparison stars. All comparison stars and asteroid targets had an SNR of at least 100.

2158 Tietjen. Data were collected from July 24 through September 21 resulting in 36 nights and 1333 data points. 2158 Tietjen was tracked through 163.442 revolutions from phase angles of 0.99 through 20.11 deg. A period of 8.65742 ± 0.00009 h was calculated with a peak-to-peak amplitude of 0.41 ± 0.05 mag. Observations at small phase angles allowed calculation of H-G values of 11.811 ± 0.012 mag and 0.077 ± 0.019 respectively. A search of the Asteroid Lightcurve Database (or other resources) did not find any previously reported results for asteroid 2158.

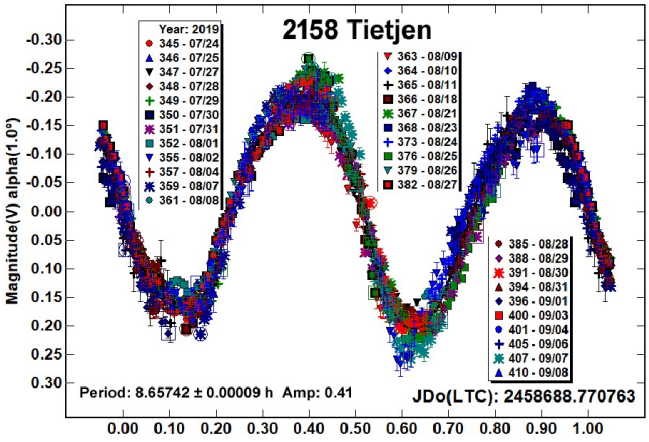

2831 Stevin. Data were collected from December 4 through January 6 2021 resulting in 17 nights and 1006 data points. A period could not be determined since data for all nights lie within ± 0.3 mag of each other. It was felt that adjusting delta comps to try and determine a period was not feasible.

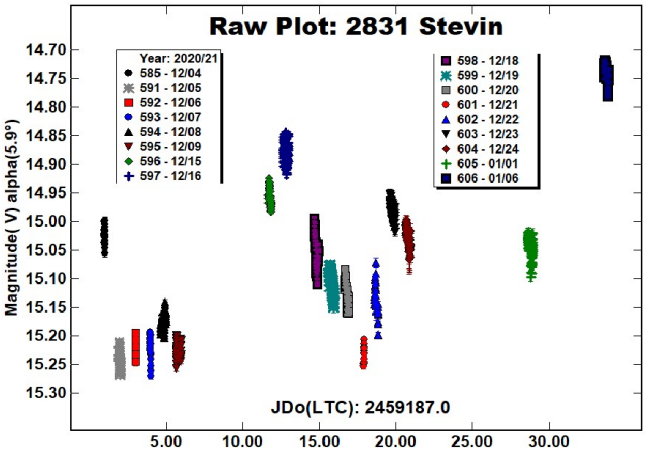

3313 Mendel. Data were collected from July 21 through August 15 2020, resulting in 20 nights and 737 data points. 3313 Mendel was tracked through 57.384 revolutions from phase angles of -3.63 through 13.71 deg. A period of 13.3354 ± 0.0006 h was calculated with a peak-to-peak amplitude of 0.26 ± 0.02 mag. Observations at small phase angles allowed calculation of H-G values of 10.122 ± 0.031 mag and 0.620 ± 0.73 respectively. Data were previously reported by Pal et. al. (2020) with a period of 13.2848 ± 0.0005 h and amplitude of 0.22 ± 0.04 mag.

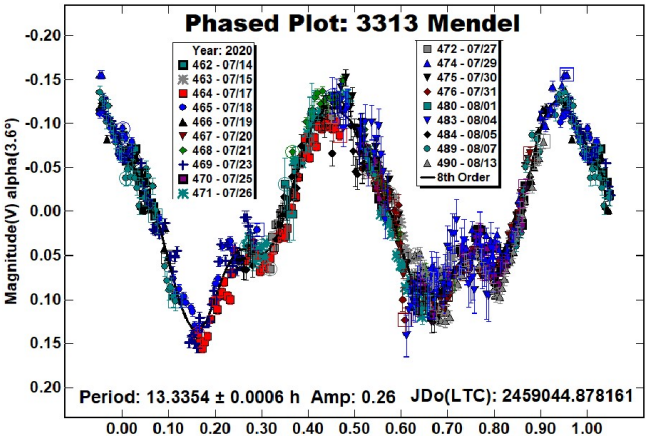

3989 Odin. Data were collected from September 24 through October 25, 2020 resulting in 17 nights and 743 data points. 3989 Odin was tracked through 139.346 revolutions from phase angles of -6.30 through 14.05 deg. A period of 5.3220 ± 0.0003 h was calculated with a peak-to-peak amplitude of 0.16 ± 0.02 mag. Observations at small phase angles allowed calculation of H-G values of 13.219 ± 0.100 mag and 0.545 ± 0.167 respectively. Data were previously reported in the LCDB with a period of 5.3229 ± 0.0002 h and amplitude of 0.16 ± 0.01 mag.

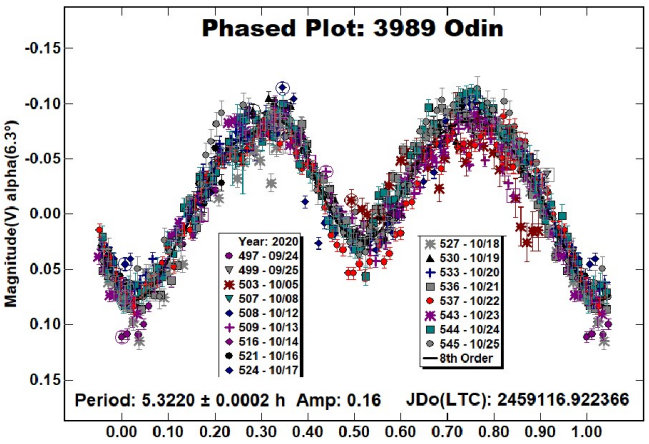

4021 Dancey. Data were collected from September 22 through October 23 2019, resulting in 6 nights and 205 data points. 4021 Dancey was tracked through 180.049 revolutions from phase angles of -3.14 through 17.23 deg. A period of 4.1085 ± 0.0002 h was calculated with a peak-to-peak amplitude of 0.15 ± 0.35 mag. Observations at small phase angles allowed calculation of H-G values of 12.802 ± 0.017 mag and 0.499 ± 0.035 respectively. A search of the Asteroid Lightcurve Database (or other resources) did not find any previously reported results for asteroid 4021.

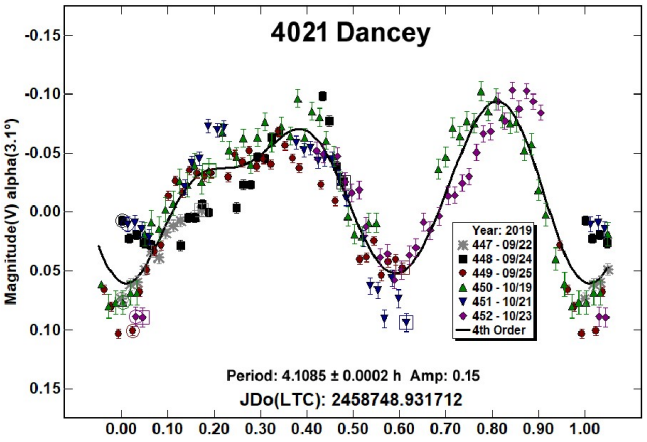

4103 Chahine. Data were collected from October 15 through December 1st 2020 resulting in 30 nights and 2143 data points. 4103 Chahine was tracked through 10.713 revolutions from phase angles of 11.9 through 18.4 deg. A period of 104.9519 ± 0.0057 h was calculated with a peak-to-peak amplitude of 0.80 ± 0.03 mag. Because of the long period only short segments of data were collected each night and it was not possible to derive H-G values. Data were previously reported by Pal et. al. (2020) with a period of 105.161 ± 0.005 h and amplitude of 0.52 ± 0.10 mag.

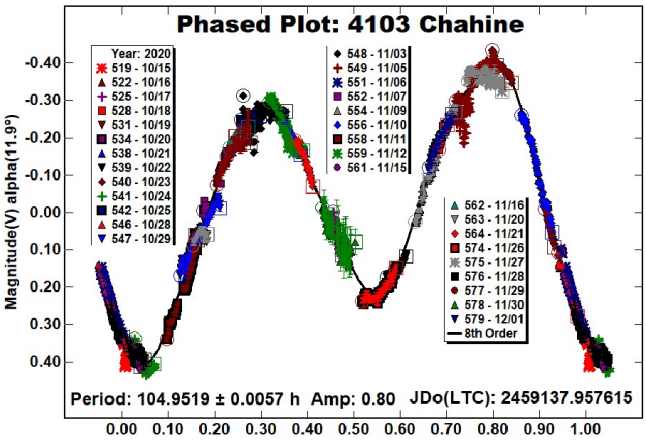

5996 Julioangel. Data were collected from September 23 through October 20 2020, resulting in 14 nights and 1067 data points. 5996 Julioangel was tracked through 67.001 revolutions from phase angles of 11.35 through 20.03 deg. A period of 9.7435 ± 0.0003 h was calculated with a peak-to-peak amplitude of 0.26 ± 0.02 mag. Since observations were started at a phase angle of greater than seven deg. a value of 0.150 was used for H-G calculation resulting in a value for H of 10.329 ± 0.157 mag. Data were previously reported by Durkee (2018) with a period of 9.74 ± 0.01 h and an amplitude of 0.34 ± 0.07 mag.

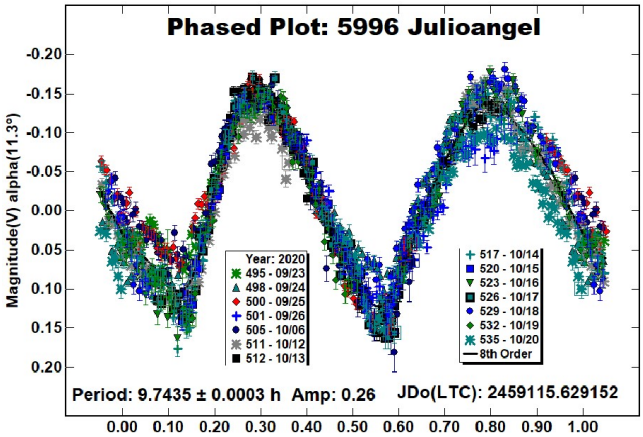

7527 Marples. Data were collected from August 24 through September 21 2019 resulting in 20 nights and 843 data points. 7527 Marples was tracked through 74.225 revolutions from phase angles of -18.9 through -3.95 deg. A period of 9.0899 ± 0.0003 h was calculated with a peak-to-peak amplitude of 0.49 ± 0.03 mag. Observations at small phase angles allowed calculation of H-G values of 14.615 ± 0.077 mag and 0.259 ± 0.088 respectively. Data were previously reported by Benishek (2020) with a period of 9.098 ± 0.004 h and amplitude of 0.54 ± 0.02 mag.

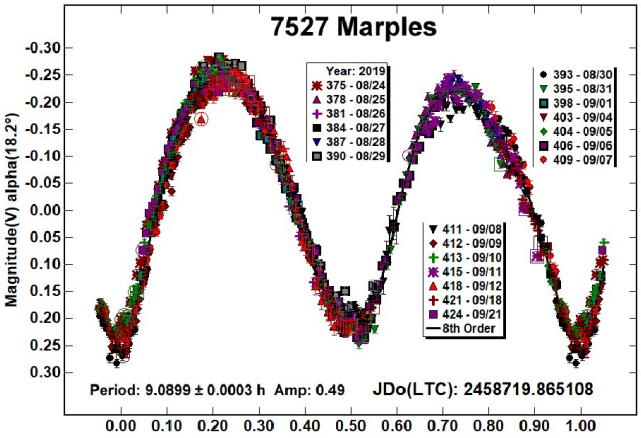

9545 Petrovedomosti. Data were collected from July 27 through August 15 2020, resulting in 10 nights and 215 data points. 9545 Petrovedomosti was tracked through 80.254 revolutions from phase angles of 3.91 through 10.91 deg. A period of 5.6649 ± 0.0003 h was calculated with a peak-to-peak amplitude of 0.28 ± 0.03 mag. Observations at small phase angles allowed calculation of H-G values of 12.185± 0.067 mag and 0.406 ± 0.138 respectively. A search of the Asteroid Lightcurve Database (and other resources) did not find any previously reported results for asteroid 9545.

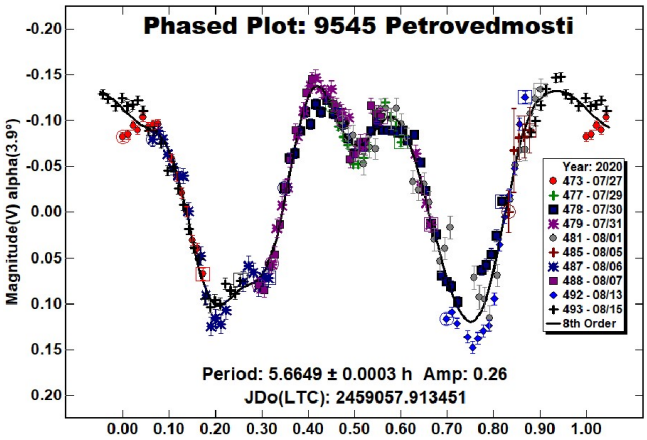

21242 1995 WZ41. Data were collected from November 5 through December 7 2020, resulting in 15 nights and 1014 data points. 21242 1995 WZ41 was tracked through 140.572 revolutions from phase angles of -10.45 through 6.00 deg. A period of 5.45303 ± 0.00005 h was calculated with a peak-to-peak amplitude of 0.43 ± 0.03 mag. Observations at small phase angles allowed calculation of H-G values of 13.469 ± 0.066 mag and 0.870 ± 0.203 respectively. A search of the Asteroid Lightcurve Database (and other resources) did not find any previously reported results for asteroid 21242.

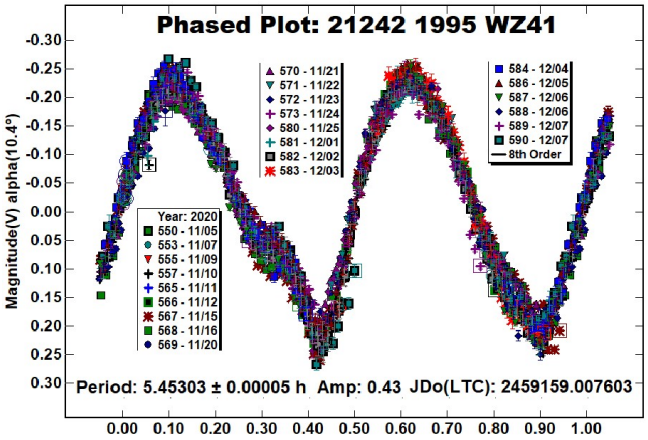

Acknowledgements

The author would like to thank Brian Warner for support of his *MPO Canopus* software package.

References

Benishek, V. (2020). "Photometry of 39 Asteroids at SOPOT Astronomical Observatory: 2019 September - 2020 March." *Minor Planet Bull.* **47**, 231-241.

Durkee, R.I. (2018). "Neglected Lightcurves from the Shed of Science." *Minor Planet Bull.* **45**, 333-335.

Harris, A.W.; Young, J.W.; Scaltriti, F.; Zappala, V. (1984). "Lightcurves and phase relations of the asteroids 82 Alkmene and 444 Gyptis." *Icarus* **57**, 251-258.

LCDB: *http://www.minorplanet.info/lightcurvedatabase.html*

Pal, A.; Szakáts, R.; Kiss, C.; Bódi, A.; Bognár, Z.; Kalup, C.; Kiss, L.L.; Marton, G.; Molnár, L.; Plachy, E.; Sárneczky, K.; Szabó, G.M.; Szabó, R. (2020). "Solar System Objects Observed with TESS - First Data Release: Bright Main-belt and Trojan Asteroids from the Southern Survey." *Ap. J. Supl. Ser.* **247**, 26-34.

Warner, B.D. (2019). *MPO Canopus* software Version 10.8.1.1. BDW Publishing. *http://www.MinorPlanetObserver.com/*

Number	Name	yyyy mm/dd	Phase	L_{PAB}	B_{PAB}	Period(h)	P.E.	Amp	A.E.
2158	Tietjen	2019 07/24-09/22	0.99,20.11	303.35	1.65	8.65742	0.00009	0.40	0.05
2831	Stevin	2020 12/04-2021 01/06		82.65	0.25				
3313	Mendel	2020 07/14-08/15	-3.63,13.71	295.75	6.80	13.3354	0.0006	0.26	0.02
3989	Odin	2020 09/24-10/25	-6.30,14.05	11.05	3.80	5.3220	0.0003	0.16	0.02
4021	Dancey	2019 09/22-10/23	-3.14,17.23	1.85	-3.65	4.1085	0.0002	0.15	0.02
4103	Chahine	2020 10/15-12/01		39.95	12.40	104.9519	0.0057	0.80	0.02
5996	Julioangel	2020 09/23-10/20	11.35,20.03	344.60	12.85	9.7435	0.0003	0.26	0.02
7527	Marples	2019 08/24-09/21	-18.19,-3.95	358.15	3.85	9.0899	0.0003	0.49	0.03
9545	Petrovedomosti	2020 07/27-08/15	3.91,10.91	305.85	4.65	5.6649	0.0003	0.28	0.02
21242	1995 WZ41	2020 11/05-12/07	-10.45,6.00	56.75	-0.40	5.4530	0.00005	0.43	0.02

Table I. Observing circumstances and results. The phase angle is given for the first and last date. If preceded by an asterisk, the phase angle reached an extrema during the period. L_{PAB} and B_{PAB} are the approximate phase angle bisector longitude/latitude at mid-date range (see Harris et al., 1984).

PERIOD DETERMINATIONS FOR TWENTY MINOR PLANETS

Tom Polakis
Command Module Observatory
121 W. Alameda Dr.
Tempe, AZ 85282
tpolakis@cox.net

(Received: 2021 March 22)

Phased lightcurves and synodic rotation periods for 20 main-belt asteroids are presented, based on CCD observations made from 2020 December through 2021 February. All the data have been submitted to the ALCDEF database.

CCD photometric observations of 20 main-belt asteroids were performed at Command Module Observatory (MPC V02) in Tempe, AZ. Images were taken using a 0.32-m f/6.7 Modified Dall-Kirkham telescope, SBIG STXL-6303 CCD camera, and a 'clear' glass filter. Exposure time for all the images was 2 minutes. The image scale after 2×2 binning was 1.76 arcsec/pixel. Table I shows the observing circumstances and results. All of the images for these asteroids were obtained between 2020 December and 2021 February.

Images were calibrated using a dozen bias, dark, and flat frames. Flat-field images were made using an electroluminescent panel. Image calibration and alignment was performed using *MaxIm DL* software.

The data reduction and period analysis were done using *MPO Canopus* (Warner, 2020). The 45′×30′ field of the CCD typically enables the use of the same field center for three consecutive nights. In these fields, the asteroid and three to five comparison stars were measured. Comparison stars were selected with colors within the range of 0.5 < B-V < 0.95 to correspond with color ranges of asteroids. In order to reduce the internal scatter in the data, the brightest stars of appropriate color that had peak ADU counts below the range where chip response becomes nonlinear were selected. *MPO Canopus* plots instrumental vs. catalog magnitudes for solar-colored stars, which is useful for selecting comp stars of suitable color and brightness.

Since the sensitivity of the KAF-6303 chip peaks in the red, the clear-filtered images were reduced to Sloan r′ to minimize error with respect to a color term. Comparison star magnitudes were obtained from the ATLAS catalog (Tonry et al., 2018), which is incorporated directly into *MPO Canopus*. The ATLAS catalog derives Sloan griz magnitudes using a number of available catalogs. The consistency of the ATLAS comp star magnitudes and color-indices allowed the separate nightly runs to be linked often with no zero-point offset required or shifts of only a few hundredths of a magnitude in a series.

A 9-pixel (16 arcsec) diameter measuring aperture was used for asteroids and comp stars. It was typically necessary to employ star subtraction to remove contamination by field stars. For the asteroids described here, I note the RMS scatter on the phased lightcurves, which gives an indication of the overall data quality including errors from the calibration of the frames, measurement of the comp stars, the asteroid itself, and the period-fit. Period determination was done using the *MPO Canopus* Fourier-type FALC fitting method (cf. Harris et al., 1989). Phased lightcurves show the maximum at phase zero. Magnitudes in these plots are apparent and scaled by *MPO Canopus* to the first night.

Most asteroids were selected from the CALL website (Warner, 2011) using the criteria of magnitude brighter than 15.5 and quality of results, U, less than 2+. In this set of observations, 5 of the 21 asteroids had no previous period analysis, 14 had U = 2, and one was U = 3. The Asteroid Lightcurve Database (LCDB; Warner et al., 2009) was consulted to locate previously published results. All the new data for these asteroids can be found in the ALCDEF database.

684 Hildburg lies in the inner main belt. It was discovered by August Kopff at Heidelberg in 1909. Binzel (1987) published a rotational period of 11.92 h, Ferrero (2014) computed 15.89 ± 0.01 h, and Behrend (2018) shows 14.2 ± 0.1 h. A total of 277 images were gathered over the course of three nights, producing a period of 11.91 ± 0.02 h, agreeing with Binzel's value. The lightcurve has an amplitude of 0.23 mag. with an RMS error of 0.026 mag.

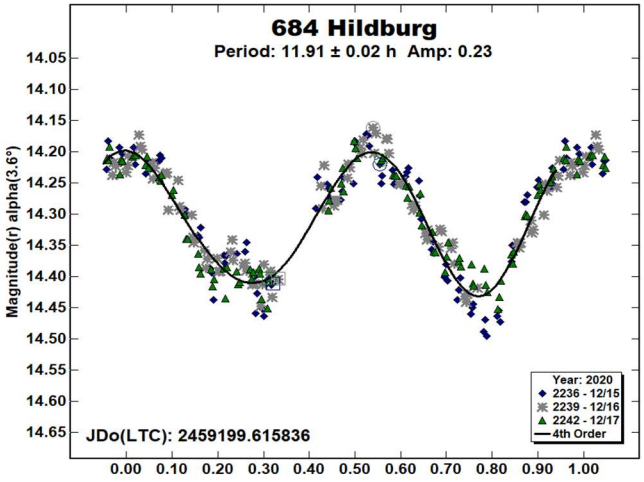

702 Alauda. This outer main-belt asteroid was discovered at Heidelberg in 1922 by Joseph Helffrich. Multiple, similar period solutions have been published. They include Benishek and Protitch-Benishek (2008), 8.3539 ± 0.0007 h; Alkema (2014), 8.3531 ± 0.0004 h; and Polakis (2020), 8.333 ± 0.006 h. Behrend (2019) indicates double this period: 16.7072 ± 0.0003 h. In four nights, 315 data points were used to calculate a period of 16.65 ± 0.02 h, with an amplitude of 0.07 ± 0.014 mag. This agrees with Behrend's solution, although the small amplitude results in some uncertainty. The period spectrum is presented to show the fit error for both periods. Note the weak signal at the half period.

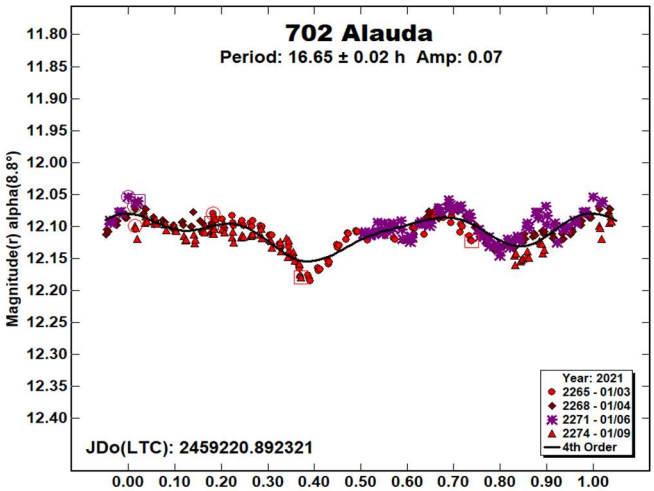

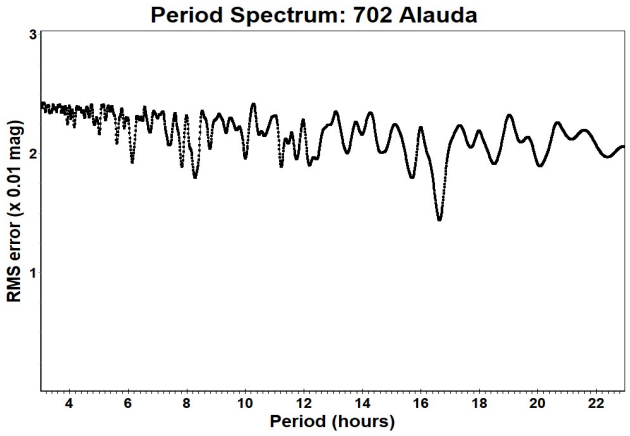

1128 Astrid was discovered in 1929 by Eugène Delporte. Among the period solutions in the LCDB are that of Behrend (2005), 10.228 ± 0.002 h; Waszczak et al. (2015), 10.229 ± 0.0031 h, and Ditteon et al. (2018), 14.552 ± 0.011 h. A total of 206 data points obtained during three nights were used to calculate a period solution of 10.25 ± 0.02 h, agreeing with Behrend and Waszczak. The amplitude of the lightcurve is 0.19 ± 0.034 mag.

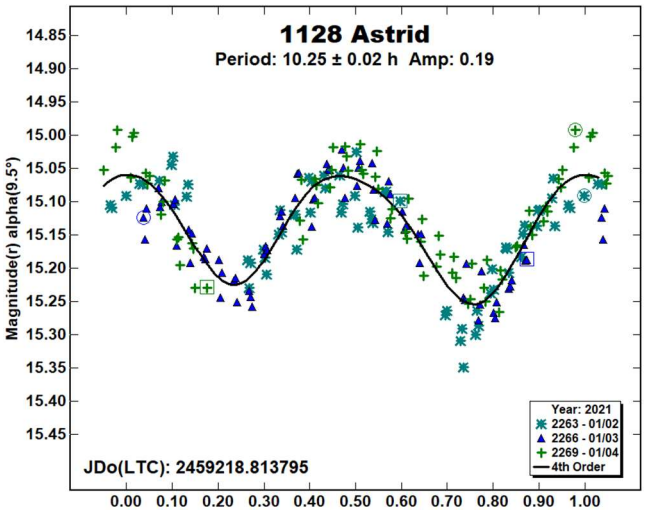

1228 Scabiosa. This outer main belt asteroid was discovered at Heidelberg in 1931 by Karl Reinmuth. The LCDB shows no period solutions. Data was gathered on seven nights, but a 13-day interval was required due to its rotation period being nearly commensurate with that of the earth. The 417 images were used to compute a period solution of 22.71 ± 0.01 h, and an amplitude of 0.61 ± 0.037 mag.

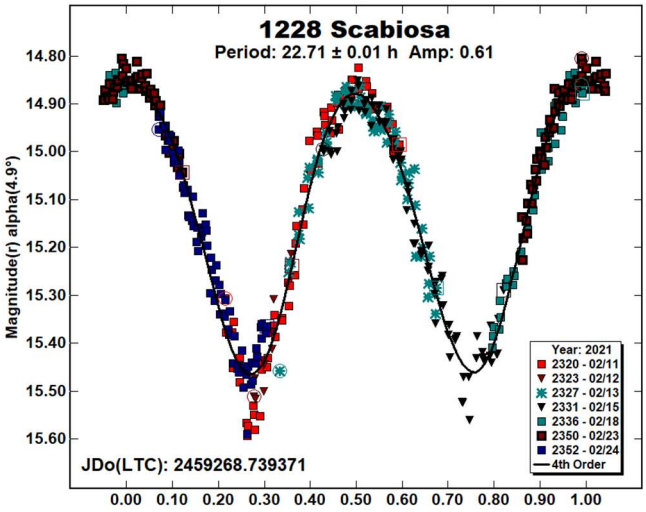

1442 Corvina is a member of the Koronis family. It was discovered at Budapest in 1937 by György Kulin. No periods are shown in the LCDB. During four nights, 339 images were gathered, producing a period solution of 31.36 ± 0.13 h. The RMS scatter on the fit of 0.056 mag. is high relative to the amplitude of 0.19 mag.

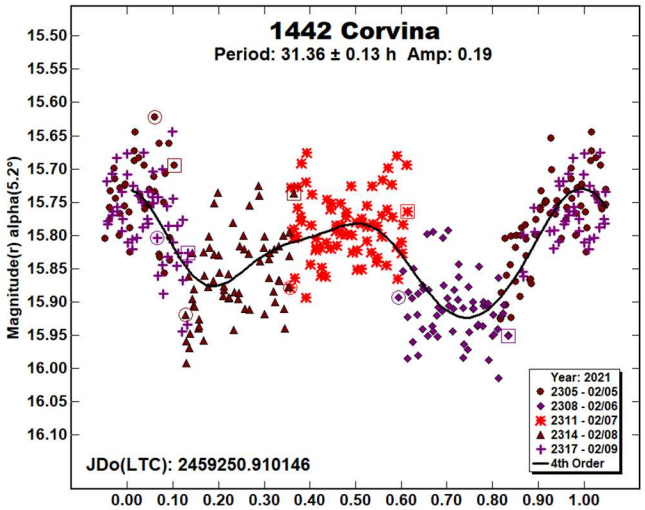

1513 Matra is a Flora-family asteroid, discovered at Budapest in 1940, also by György Kulin. Rowe (2019) published a period of 34.48 ± 0.02 h. During a nine-night interval, 607 images were obtained, yielding a synodic period of 127.5 ± 0.3 h, which disagrees with Rowe's period. The amplitude is 0.54 mag., and the RMS error on the fit is 0.061 mag. Misaligned points against the Fourier fit indicate tumbling.

Number	Name	yy/mm/dd	Phase	L_{PAB}	B_{PAB}	Period(h)	P.E.	Amp	A.E.	Grp
684	Hildburg	20/12/15-12/17	3.6,4.0	81	7	11.91	0.02	0.23	0.03	MB-I
702	Alauda	21/01/03-01/09	8.8,10.4	79	11	16.65	0.02	0.07	0.01	MB-O
1128	Astrid	21/01/02-01/04	9.5,10.2	78	1	10.25	0.02	0.19	0.03	MB-O
1228	Scabiosa	21/02/11-02/24	*4.9,1.4	153	-2	22.71	0.01	0.61	0.04	MB-O
1442	Corvina	21/02/05-02/09	5.2,6.7	123	-2	31.36	0.13	0.19	0.06	KOR
1513	Matra	21/02/11-02/21	*3.7,2.8	148	1	127.5	0.3	0.64	0.06	FLOR
1574	Meyer	21/01/09-01/12	4.3,4.9	101	-11	18.36	0.04	0.19	0.03	MB-O
1612	Hirose	21/02/07-02/13	2.3,0.7	144	-2	12.28	0.01	0.27	0.03	MB-O
1844	Susilva	21/01/13-01/14	2.1,2.5	101	3	5.423	0.011	0.18	0.03	EOS
2035	Stearns	21/01/02-01/12	15.3,19.7	75	5	132.7	1.1	0.22	0.04	H
2045	Peking	21/02/07-02/20	5.1,10.3	133	8	158.7	0.3	0.83	0.06	V
2437	Amnestia	20/12/15-12/22	5.9,9.3	75	-3	82.7	0.2	0.51	0.05	FLOR
2533	Fechtig	21/01/10-01/14	0.9,2.3	109	-2	15.41	0.04	0.16	0.04	THM
2655	Guangxi	21/02/05-02/06	9.5,9.8	117	12	11.06	0.04	0.34	0.06	MB-O
2746	Hissao	21/01/13-01/14	5.3,5.7	106	-5	3.185	0.003	0.34	0.06	FLOR
2950	Rousseau	20/12/18-12/22	4.5,5.8	83	-6	36.27	0.12	0.12	0.02	MB-O
3935	Toatenmongakkai	20/12/15-12/23	5.1,7.1	83	8	104.6	0.69	0.69	0.05	MB-I
3955	Bruckner	21/01/15-01/17	5.9,6.2	110	13	7.566	0.008	0.25	0.04	EOS
4612	Greenstein	21/02/05-02/06	5.3,5.7	129	6	3.006	0.002	0.24	0.04	MB-I
4632	Udagawa	21/02/05-02/06	3.6,4.5	112	4	3.572	0.001	0.64	0.06	FLOR

Table I. Observing circumstances and results. The phase angle is given for the first and last date. If preceded by an asterisk, the phase angle reached an extrema during the period. L_{PAB} and B_{PAB} are the approximate phase angle bisector longitude/latitude at mid-date range (see Harris et al., 1984). Grp is the asteroid family/group (Warner et al., 2009).

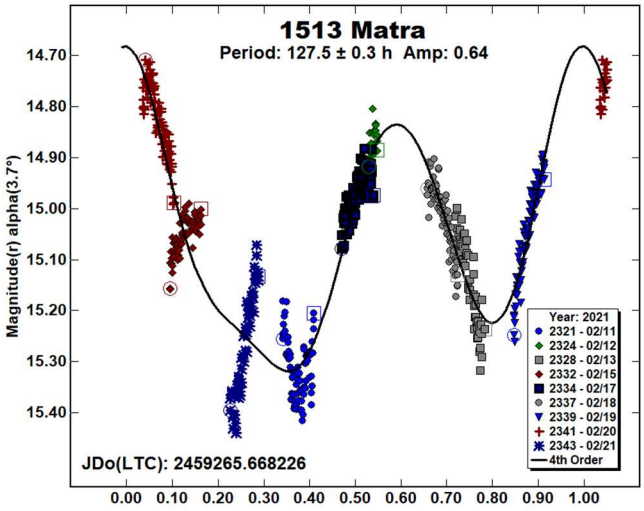

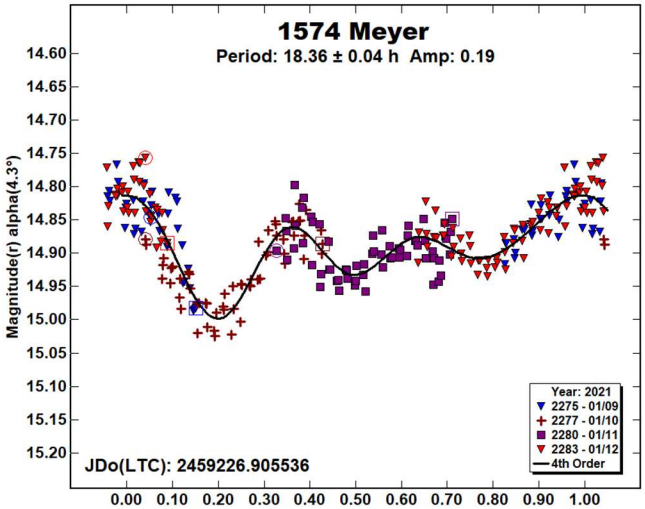

1574 Meyer, an outer main belt minor planet, was discovered by Louis Boyer at Algiers in 1949. The only entry in the LCDB is that of Carbo (2009), who shows a period of 12.64 ± 0.05 h. The asteroid was observed on four nights, and 259 images were obtained. The period spectrum showed a deep minimum at 18.36 ± 0.04 h, disagreeing with Carbo's result. The amplitude is 0.19 mag., with an RMS error on the fit of 0.029 mag.

1612 Hirose. Karl Reinmuth discovered this asteroid at Heidelberg in 1950. Waszczak et al. (2015) produced the only period solution, 12.295 ± 0.0028 h. After five nights, 321 images were sufficient to produce a period solution of 12.28 ± 0.01 h, agreeing with Waszczak's analysis. The lightcurve has an amplitude of 0.27 ± 0.031 mag.

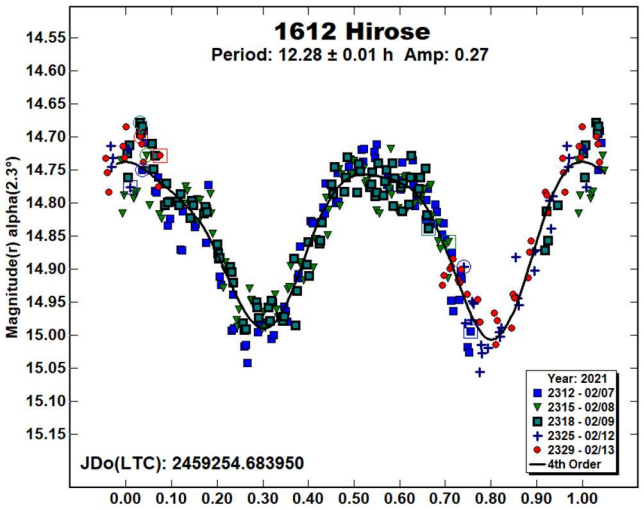

1844 Susilva. This EOS-family minor planet was discovered in 1972 by Paul Wild at Zimmerwald. Pál et al. (2020) shows a synodic period of 5.39557 ± 0.00005 h. During two nights, 143 images were secured, resulting in a period solution of 5.423 ± 0.011 h, and an amplitude of 0.18 ± 0.033 mag.

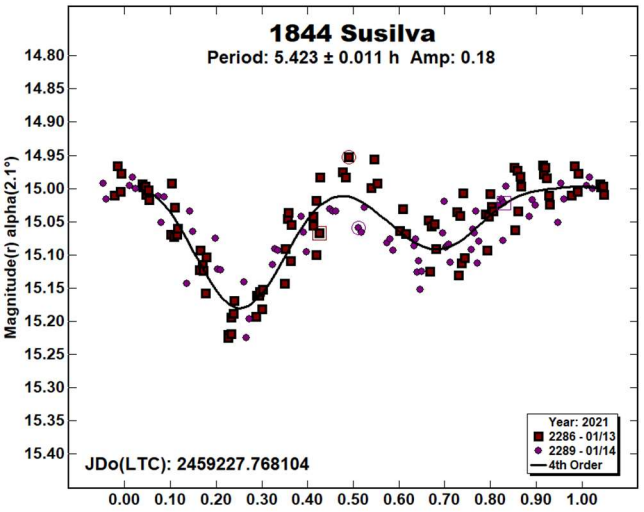

2035 Stearns is a Hungaria asteroid in a highly inclined orbit, discovered by James Gibson at El Leoncity in 1973. Among the discordant period solutions are Warner et al. (2010), 51.89 ± 0.20 h; Stephens (2014), 93 ± 1 h; and Behrend (2019), 20.79 ± 0.06 h. A total of 517 observations were made in eight nights, yielding a period of 132.7 ± 1.1 h. The amplitude is 0.22 ± 0.041 mag.

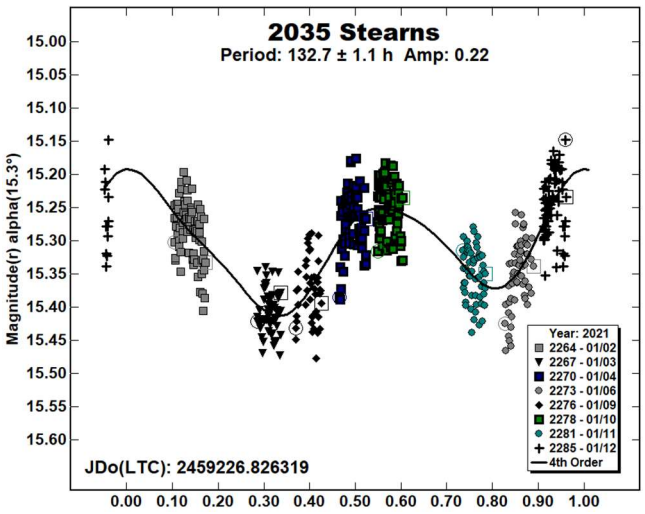

2045 Peking was discovered at Purple Mountain Observatory in Nanking in 1964. Stephens (2017) computed a period of 82.4 ± 1.0 h, and Behrend (2019) calculated 52.43 ± 0.05 h. During 13 nights, 239 images were taken. While the fit is crude, the two deep minima indicate a period of 158.7 ± 0.7 h, disagreeing with previous results. The lightcurve has an amplitude of 0.83 mag., and an RMS error on the fit of 0.064 mag.

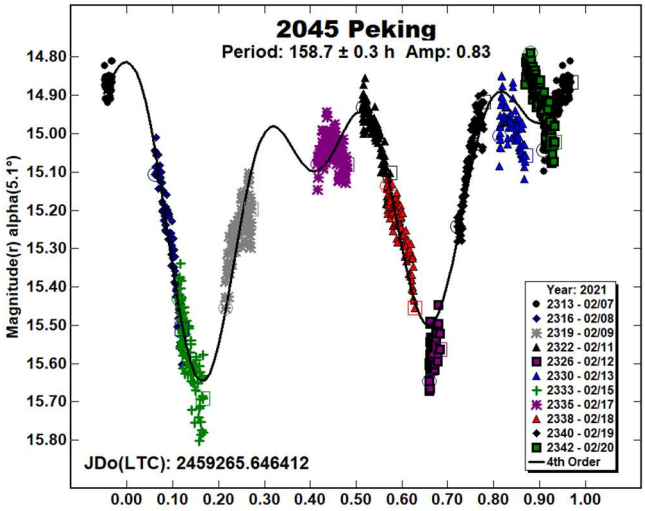

2437 Amnestia. Yrjö Väisälä discovered this Flora-family asteroid from Turku in 1942. Ruthroff (2011) calculated a period of 85 ± 5 h. It was observed on eight consecutive nights, and 615 images were taken. The best solution appears at 82.7 ± 0.2 h. The lightcurve has an amplitude of 0.51 ± 0.052 mag. The stray points are an indication of tumbling.

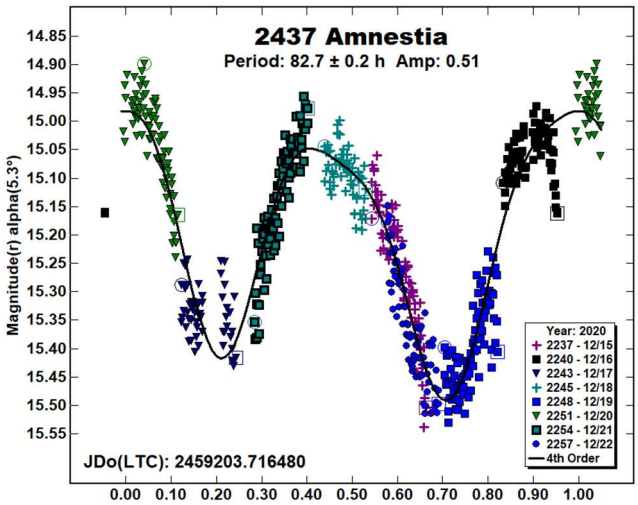

2533 Fechtig was discovered in 1905 by Max Wolf at Heidelberg. The LCDB shows no period solutions. A total of 353 images were taken during three nights. The synodic period is 15.41 ± 0.04 h, and the amplitude is 0.16 ± 0.042 mag.

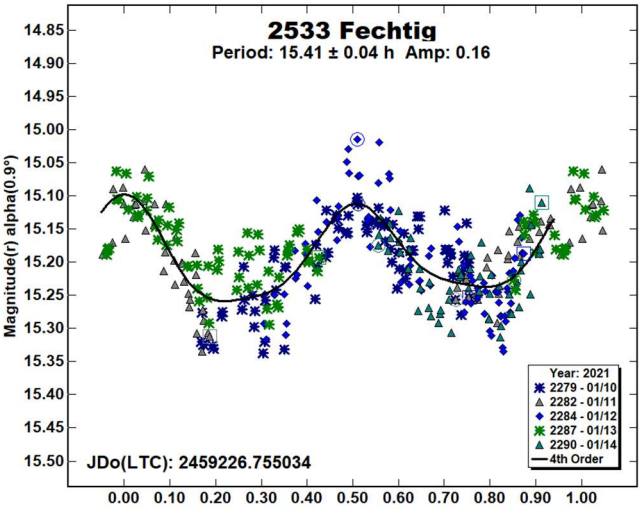

2655 Guangxi. This outer main-belt minor planet was discovered in 1974 at Purple Mountain Observatory in Nanking. No period solutions have been published. During two nights, 160 images were obtained, which produced a synodic period solution of 11.06 ± 0.04 h, and an amplitude of 0.34 ± 0.056 mag.

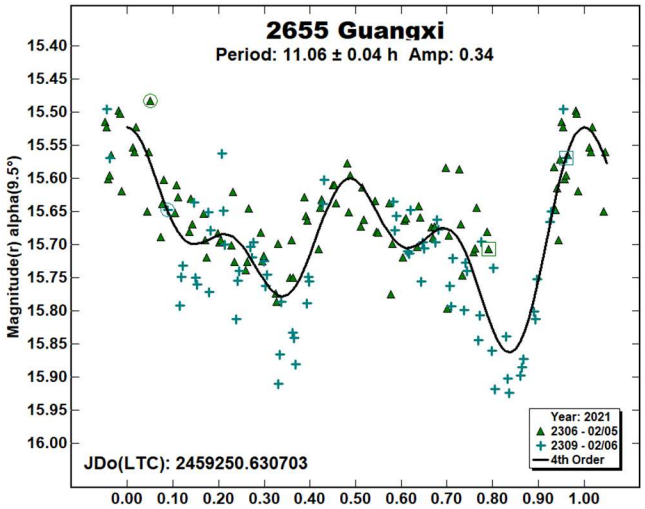

2746 Hissao. Nikolai Chernykh discovered this Flora-family asteroid at Nauchnyj in 1979. Three similar period solutions are in the LCDB: Loera-Gonzalez et al. (2019), 3.1848 ± 0.0015 h; Zeigler et al. (2019), 3.18 ± 0.01 h, and Erasmus et al. (2020), 3.185 ± 0.001 h. Two nights and 130 images provided sufficient coverage to calculate a period of 3.185 ± 0.003 h, agreeing with previous assessments. The lightcurve has an amplitude of 0.34 mag, and an RMS fit error of 0.056 mag.

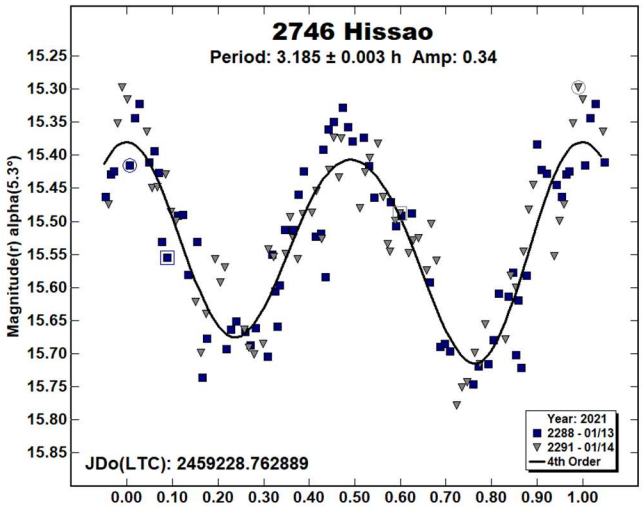

2950 Rousseau is an outer main-belt asteroid, discovered by Paul Wild at Zimmerwald in 1974. Its highly eccentric orbit brought it to a favorable 2020 opposition. Behrend (2012) shows a period of 18.228 ± 0.003 h. After five nights, 383 data points were used to determine a period of 36.27 ± 0.12 h, and an amplitude of 0.12 ± 0.018 mag.

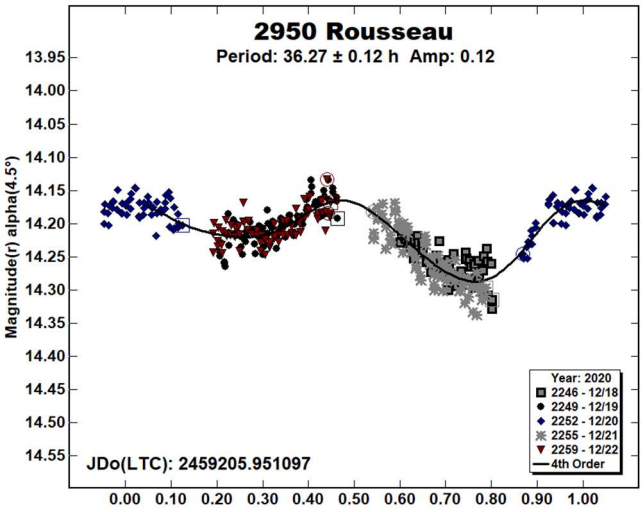

3935 Toatenmongakkai. Is an inner main-belt asteroid in an eccentric orbit. Its discovery was made by Tsutomu Seki in 1987 at Geisei. Behrend (2005) shows a rotational period of 106.3 h. The asteroid was observed on nine consecutive nights, and 875 data points were acquired. A period solution of 104.6 ± 0.2 h was obtained, agreeing with Behrend. The amplitude is 0.69 mag, and the RMS error is 0.049 mag.

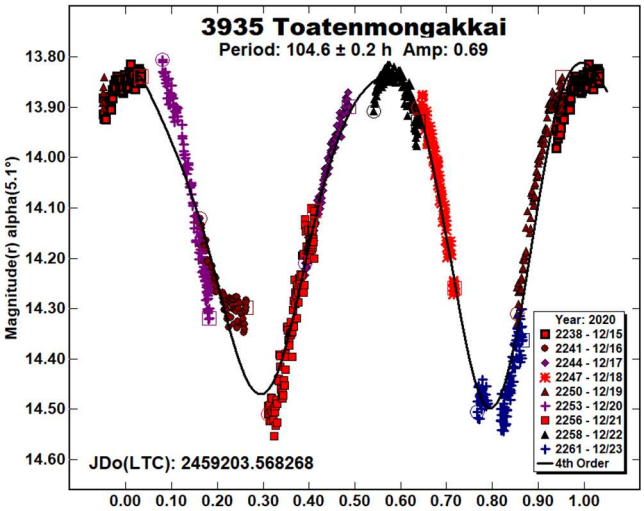

3955 Bruckner was discovered by Freimut Börngen in 1988 from Tautenberg. No period solutions for it appear in the LCDB. During three nights, 246 images were sufficient to determine a rotation period of 7.566 ± 0.008 h. The amplitude of the lightcurve is 0.25 ± 0.039 mag.

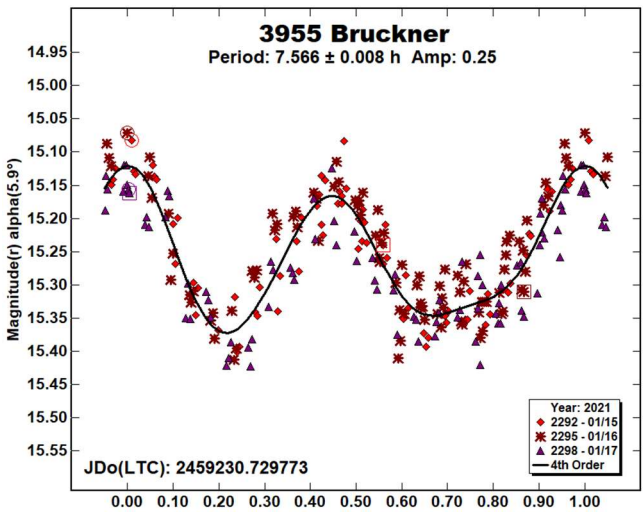

4612 Greenstein. This inner main-belt minor planet was discovered in 1989 at Palomar by Eleanor Helin. No period solutions for it have been published. A total of 167 images were taken in two nights, yielding a synodic period of 3.006 ± 0.002 h, and an amplitude of 0.24 ± 0.038 mag.

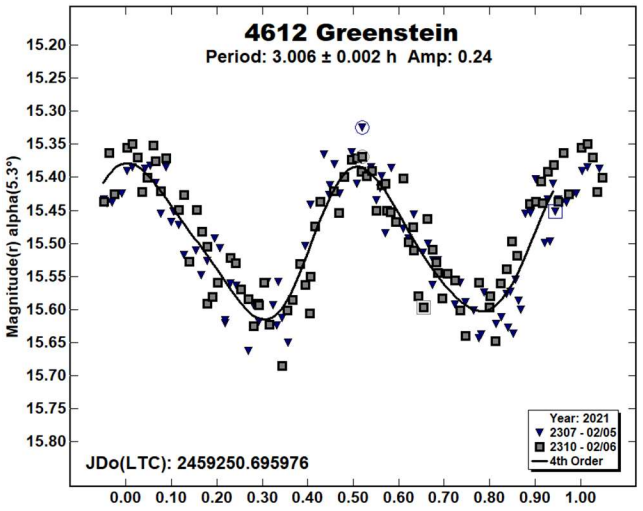

4632 Udagawa is a Flora-family asteroid, discovered at Chiyoda by Takuo Kojima in 1987. Erasmus et al. (2020) shows a period of 3.570 ± 0.001 h. It was observed for three nights, during which 243 images were acquired. The computed synodic period is 3.572 ± 0.001 h, and the amplitude is 0.64 ± 0.061 mag.

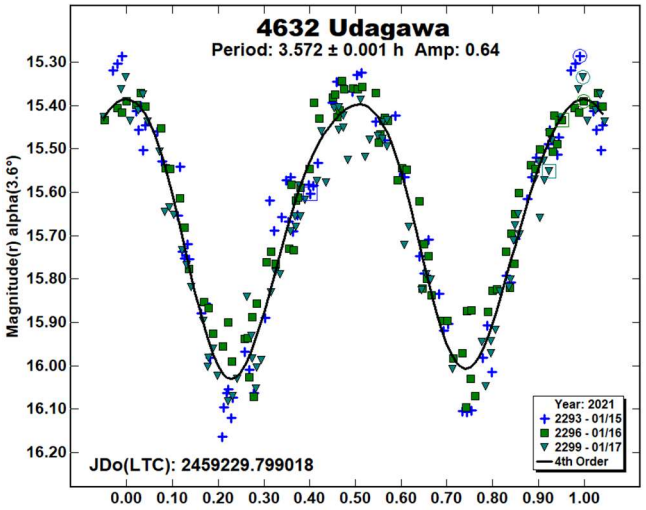

Acknowledgements

The author would like to express his gratitude to Brian Skiff for his indispensable mentoring in data acquisition and reduction. Thanks also go out to Brian Warner for support of his *MPO Canopus* software package.

References

Alkema, M.S. (2014). "Asteroid Lightcurve Analysis at Elephant Head Observatory: 2013 October-November." *Minor Planet Bull.* **41**, 186-187.

Behrend, R. (2005, 2012, 2018, 2019). Observatoire de Geneve web site. *http://obswww.unige.ch/~behrend/page_cou.html*

Benishek, V.; Protitch-Benishek, V. (2008). "CCD Photometry of Seven Asteroids at the Belgrade Astronomical Observatory." *Minor Planet Bull.* **35**, 28-30.

Binzel, R.P. (1987). "A photoelectric survey of 130 asteroids." *Icarus* **72**, 135-208.

Carbo, L.; Green, D.; Kragh, K.; Krotz, J.; Meiers, A.; Patino, B.; Pligge, Z.; Shaffer, N.; Ditteon, R. (2009). "Asteroid Lightcurve Analysis at the Oakley Southern Sky Observatory: 2008 October thru 2009 March." *Minor Planet Bull*. **36**, 152-157.

Ditteon, R.; Adam, A.; Doyel, M.; Gibson, J.; Lee, S.; Linville, D.; Michalik, D.; Turner, R.; Washburn, K. (2018). "Lightcurve Analysis of Minor Planets Observed at the Oakley Southern Sky Observatory: 2016 October - 2017 March." *Minor Planet Bull*. **45**, 13-16.

Erasmus, N.; Navarro-Meza, S.; McNeill, A.; Trilling, D.E.; Sickafoose, A.A.; Denneau, L.; Flewelling, H.; Heinze, A.; Tonry, J.L. (2020). "Investigating Taxonomic Diversity within Asteroid Families through ATLAS Dual-band Photometry." *Ap. J. Suppl. Ser.* **247**, A13.

Ferrero, A. (2014). "Period Determination of Six Main Belt Asteroids." *Minor Planet Bull*. **41**, 184-185.

Harris, A.W.; Young, J.W.; Scaltriti, F.; Zappala, V. (1984). "Lightcurves and phase relations of the asteroids 82 Alkmene and 444 Gyptis." *Icarus* **57**, 251-258.

Harris, A.W.; Young, J.W.; Bowell, E.; Martin, L.J.; Millis, R.L.; Poutanen, M.; Scaltriti, F.; Zappala, V.; Schober, H.J.; Debehogne, H.; Zeigler, K.W. (1989). "Photoelectric Observations of Asteroids 3, 24, 60, 261, and 863." *Icarus* **77**, 171-186.

Loera-Gonzalez, P.; Olguin, L.; Saucedo, J.C.; Nunez-Lopez, R.; Yahia-Keith, N.A. (2019). "Lightcurve Based Rotational Period Determination for Asteroids at Unison Observatory: First Half of 2018." *Minor Planet Bull.* **46**, 97-98.

Pál, A.; Szakáts, R.; Kiss, C.; Bódi, A.; Bognár, Z.; Kalup, C.; Kiss, L.L.; Marton, G.; Molnár, L.; Plachy, E.; Sárneczky, K.; Szabó, G.M.; Szabó, R. (2020). "Solar System Objects Observed with TESS – First Data Release: Bright Main-belt and Trojan Asteroids from the Southern Survey." *Ap. J. Suppl Ser*. **247**, id. 26.

Polakis, T. (2020). "Photometric Observations of Twenty-Three Minor Planets." *Minor Planet Bull.* **47**, 94-101.

Rowe, B. (2019). "Lightcurve Analysis of 6 Asteroids from RMS Observatory." *Minor Planet Bull.* **46**, 92-94.

Ruthroff, J.C. (2011). "Lightcurve Analysis of Eight Main-belt Asteroids and a Revised Period for 185 Eunike." *Minor Planet Bull.* **38**, 86-88.

Stephens, R.D. (2014). "Asteroids Observed from CS3: 2014 April-June." *Minor Planet Bull.* **41**, 226-230.

Stephens, R.D. (2017). "Asteroids Observed from CS3: 2016 October - December." *Minor Planet Bull.* **44**, 120-122.

Tonry, J.L.; Denneau, L.; Flewelling, H.; Heinze, A.N.; Onken, C.A.; Smartt, S.J.; Stalder, B.; Weiland, H.J.; Wolf, C. (2018). "The ATLAS All-Sky Stellar Reference Catalog." *Astrophys. J.* **867**, A105.

Warner, B.D.; Harris, A.W.; Pravec, P. (2009). "The Asteroid Lightcurve Database." *Icarus* **202**, 134-146. Updated 2020 Aug. *http://www.minorplanet.info/lightcurvedatabase.html*

Warner, B.D.; Sada, P.V.; Pollock, J.; Reichart, D.; Ivarsen, I.; Haislip, J.; Lacluyze, A.; Nysewander, M. (2010). "Lightcurve Analysis of 932 Hooveria." *Minor Planet Bull.* **37**, 139.

Warner, B.D. (2011). Collaborative Asteroid Lightcurve Link website. *http://www.minorplanet.info/call.html*

Warner, B.D. (2020). *MPO Canopus* software. *http://bdwpublishing.com*

Waszczak, A.; Chang, C.-K.; Ofek, E.O.; Laher, R.; Masci, F.; Levitan, D.; Surace, J.; Cheng, Y.-C.; Ip, W.-H.; Kinoshita, D.; Helou, G.; Prince, T.A.; Kulkarni, S. (2015). "Asteroid Light Curves from the Palomar Transient Factory Survey: Rotation Periods and Phase Functions from Sparse Photometry." *Astron. J.* **150**, A75.

Zeigler, K.; Barnhart, T.; Moser, A.; Duval, N. (2019). "CCD Photometric Observations of Asteroids 2746 Hissao, 2884 Reddish and 3394 Banno." *Minor Planet Bull.* **46**, 11-12.

MAIN-BELT ASTEROIDS OBSERVED FROM CS3: 2021 JANUARY TO MARCH

Robert D. Stephens
Center for Solar System Studies (CS3) / MoreData!
11355 Mount Johnson Ct., Rancho Cucamonga, CA 91737 USA
rstephens@foxandstephens.com

Daniel R. Coley
Center for Solar System Studies (CS3)
Corona, CA

Brian D. Warner
Center for Solar System Studies (CS3) / MoreData!
Eaton, CO

(Received: 2021 April 7)

CCD photometric observations of 24 main-belt asteroids were obtained at the Center for Solar System Studies (CS3) from 2021 January to March. In addition, 15 datasets dating back to 2013, thought to have been lost to a crashed hard drive, were recovered when a USB drive containing the reduced measurements was found. Finally, 8 pole/shape models are presented.

The Center for Solar System Studies (CS3) has nine telescopes which are normally used in program asteroid family studies. The focus is on near-Earth asteroids, but when suitable targets are not available, Jovian Trojans and Hildas are observed. When a nearly full moon is too close to the family targets being studied, targets of opportunity amongst the main-belt families were selected.

Table I lists the telescopes and CCD cameras that were used to make the observations. Images were unbinned with no filter and had master flats and darks applied. The exposures depended upon various factors including magnitude of the target, sky motion, and Moon illumination.

Telescope	Camera
0.30-m f/6.3 Schmidt-Cass	SBIG 1001E
0.35-m f/9.1 Schmidt-Cass	FLI Microline 1001E
0.35-m f/9.1 Schmidt-Cass	FLI Microline 1001E
0.35-m f/9.1 Schmidt-Cass	FLI Microline 1001E
0.35-m f/10 Schmidt-Cass	SBIG 1001E
0.35-m f/10 Schmidt-Cass	FLI Proline 1001E
0.40-m f/10 Schmidt-Cass	FLI Proline 1001E
0.40-m f/10 Schmidt-Cass	FLI Proline 1001E
0.50-m F8.1 R-C	FLI Proline 1001E

Table I: List of CS3 telescope/CCD camera combinations.

Image processing, measurement, and period analysis were done using *MPO Canopus* (Bdw Publishing), which incorporates the Fourier analysis algorithm (FALC) developed by Harris (Harris et al., 1989). For the images reduced in 2021, the Comp Star Selector feature in *MPO Canopus* was used to limit the comparison stars to near solar color. Night-to-night calibration was done using field stars from the ATLAS catalog (Tonry et al., 2018), which has Sloan *griz* magnitudes that were derived from the GAIA and Pan-STARR catalogs and are "native" magnitudes of the catalog. Those adjustments are usually ≤ ±0.03 mag. The rare greater corrections may have been related in part to using unfiltered observations, poor centroiding of the reference stars, and not correcting for second-order extinction. For the recovered measurements dating back to 2013, most used field stars from the MPOSC3 catalog, which is based on the 2MASS catalog *(http://www.ipac.caltech.edu/2mass)* but with magnitudes converted from J-K to BVRI using formulae developed by Warner (2007). The nightly zero points using this catalog have been found to be consisted to about ± 0.05 magnitude, but are occasionally higher.

The Y-axis values are ATLAS SR "sky" or Johnson V (catalog) magnitudes. The two values in the parentheses are the phase angle (a) and the value of *G* used to normalize the data to the comparison stars used in the earliest session. This, in effect, made all the observations seem to be made at a single fixed date/time and phase angle, leaving any variations due only to the asteroid's rotation and/or albedo changes. The X-axis shows rotational phase from –0.05 to 1.05. If the plot includes the amplitude, e.g., "Amp: 0.65", this is the amplitude of the Fourier model curve and *not necessarily the adopted amplitude for the lightcurve*.

For brevity, only some of the previously reported rotational periods may be referenced. A complete list is available at the asteroid lightcurve database (LCDB; Warner et al., 2009).

279 Thule. This is the first of several asteroids we were able to recover from an old crashed computer hard drive. A number of results prior to 2010 for this outer main-belt asteroid can be found in the LCDB. There is some uncertainty as to the period (Behrend, 2008web; Pravec et al., 2008web; Satō, 2015) and the suspicion of a satellite (Hamanowa and Hamanowa, 2010). We observed in 2010 (Warner et al., 2010), finding a period of 15.96 h. However, we noted due to the low amplitude the possibility of a 7.979 h period.

Subsequent to our 2010 observations, observations of Thule from 2008 by Pilcher (2014) were reported again with ambiguous periods of 7.970 h or 15.960 h. Then Marciniak et al. (2016) reported a period of 23.896 h, a 3:1 alias of the previously reported 7.9 h periods and 3:2 alias of the reported 15.9 h periods.

Our recovered 2013 data did not solve the enigmatic period. The period spectrum again shows possible periods near 8 h, 16 h, and 24 h, of near equal weighting. Because the 24 h period is commensurate with an Earth's day, a complete lightcurve cannot be obtained from a single longitude. Because the 2010 campaign involved observers from widely separated longitudes and excluded a 24 h period as a possibility, we still favor the 15.94 h period as being the most likely.

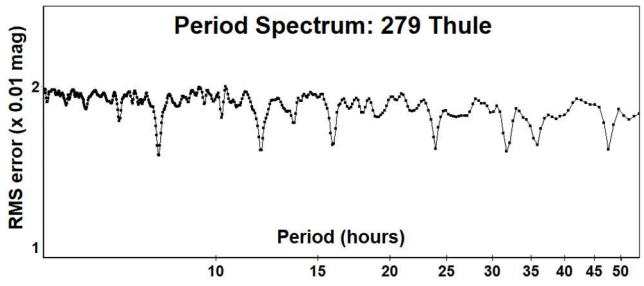

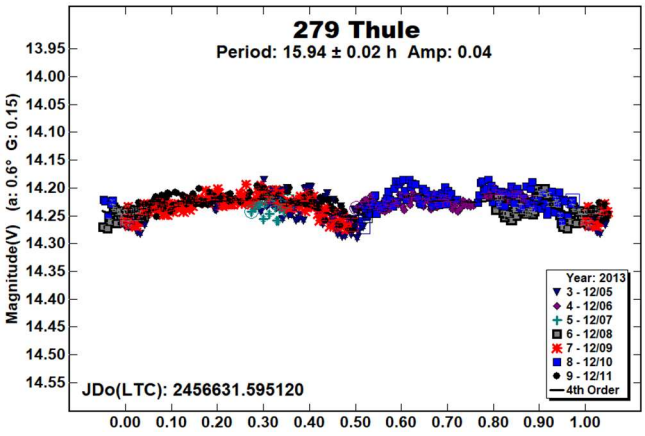

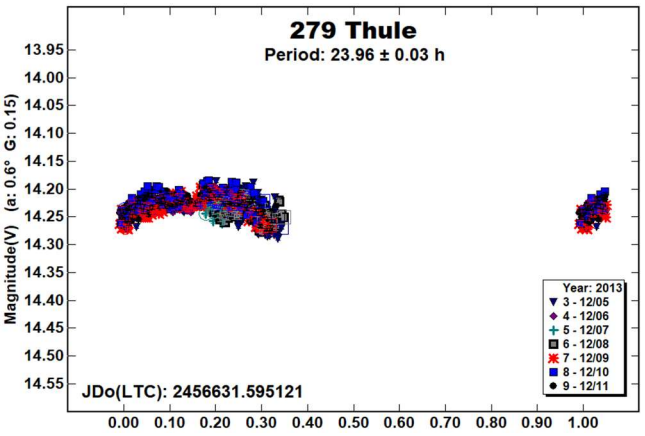

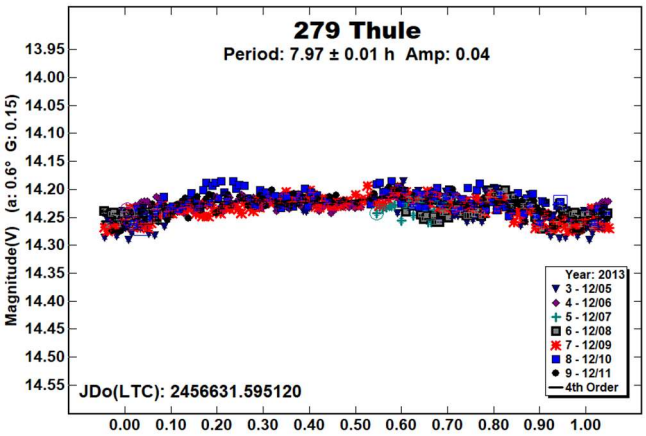

341 California. This member of the Flora family/group was another of the recovered datasets. Prior to the recovery of our data, two groups published results showing California to be a long period asteroid which was tumbling. Using observations from 2014 to 2016, Polakis and Skiff. (2017) found a primary period of 317 h with obvious signs of tumbling. Pilcher et al. (2017), using 117 sessions between 2016 June and December found a primary period of 318 h and a candidate for a secondary period of 250 h.

Our six-week run starting in 2016 January also showed signs of tumbling. Using the rules of thumb for tumbling damping time (Pravec et al., 2014; 2005), the diameter and periods make this a good candidate for tumbling. The best single period fit was 310 h. *MPO Canopus* cannot properly handle the data from a tumbling asteroid since it does not do a simultaneous search for two periods. We attempted a dual period search using the 318/250 h periods found by Pilcher et al., but the result was not an improvement over our single period search.

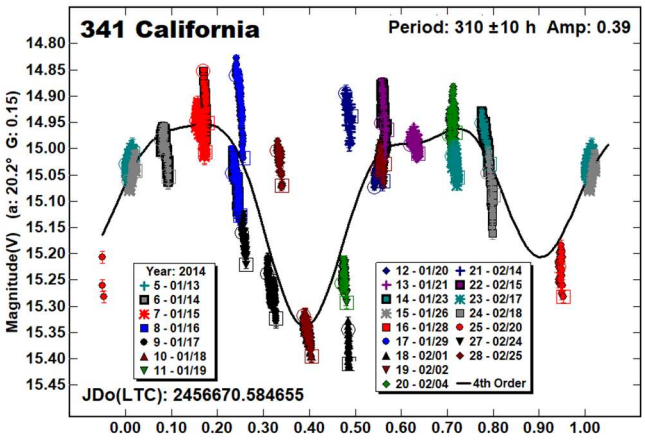

1164 Kobolda. This member of the Phocaea family/group was observed several times in the past. Higgins and Oey (2007), Sauppe et al. (2007), Higgins (2011), and Warner (2014a) each found a period near 4.14 h. Our result this year is in good agreement.

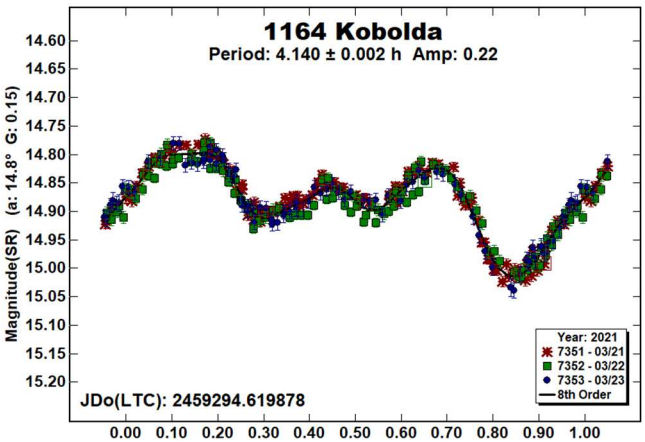

Because of the availability of the dense data from Higgins et al. and Warner in the Asteroid Lightcurve Data Exchange Format database (ALCDEF, 2020) and sparse data at the Asteroids - Dynamic web site (AstDyS-2, 2020), we attempted to solve for the sidereal period and pole position and create a shape model. These data were combined using *MPO LCInvert* (Bdw Publishing). This Windows-based program incorporates the algorithms developed by Kaasalainen and Torppa (2001) and Kaasalainen et al (2001) and converted by Josef Ďurech from the original FORTRAN to C. A period search was made over a sufficiently wide range to assure finding a global minimum in χ^2 values. We found one possible pole solution; (λ, β, P) = (270°, -61°, 4.141699 h). The full set of inversion graphics are at the end of this paper.

1331 Solvejg. This outer main-bet asteroid was observed by Garceran et al. (2016) who reported a period of 19.30 h. Using data from the Palomar Transient Factory Survey, Waszczak et al. (2015) found a period of 19.288 h. Using data from WISE and the Lowell Photometric Database, Ďurech et al. (2018a) found two possible pole solutions 180° apart: (λ, β, P) = (69°, -46°, 19.2892 h) and (248°, -41°, 19.2892 h). Their preferred solution is (69°, -46°). We recovered this dataset from 2014, finding a period of 19.33 h, consistent with those prior results.

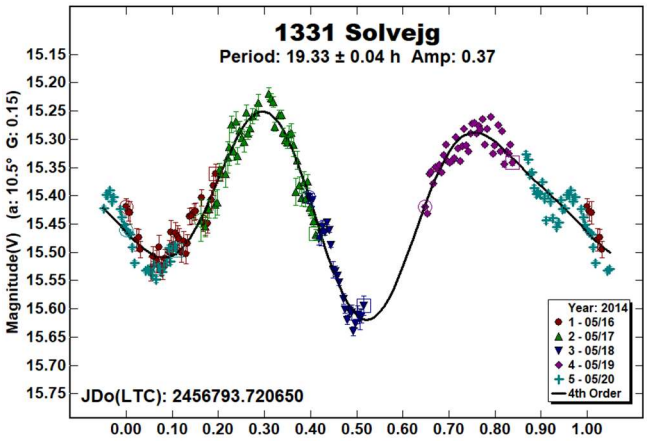

1413 Roucarie. We originally observed this member of the EOS family/group in 2011 April finding a period of 6.357 h (Coley, 2012). We observed it again in 2021 February finding a period of 6.532 h. We also recovered more data from 2013 which are consistent with the 2021 result. This caused us to revisit the 2011 period. In 2011, we only obtained two sessions, 20 days apart. Therefore, there were a many possible aliases, all of equal weight. A period of 6.530 h fits the 2011 data as well as any of the other aliases. In light of the more recent results, we are adopting that as our preferred period for the 2011 data.

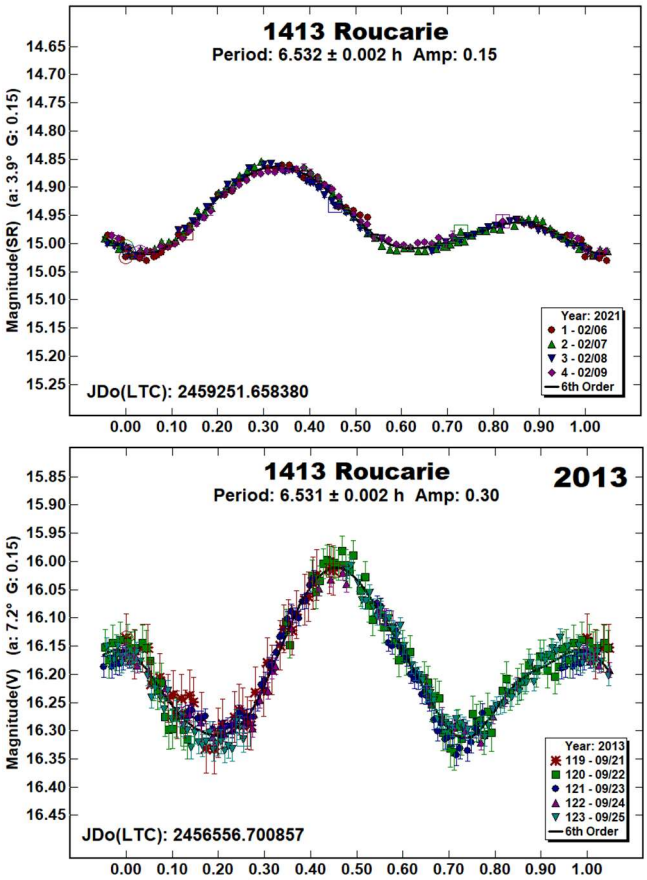

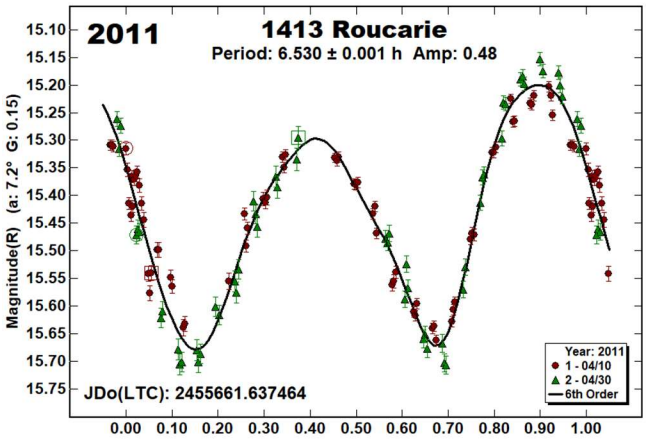

Using sparse data from the Lowell Photometric Database and WISE data, Ďurech et al. (2018a) reported a spin axis model with (λ, β) = (124°, 5°) or (310°, 5°) and a sidereal period of 6.53058 h. In addition to our dense data from the three apparitions, we used sparse data from the AstDyS-2 (2020) site to solve for the sidereal period and pole position and create a shape model.

We found two possible pols solutions 180° apart: (λ, β, *P*) = (122°, 10°, 6.530557 h) and (311°, 37°, 6.530558 h). Our preferred solution is (122°, 10°). This is in very good agreement with the Ďurech et al. model. The full set of inversion graphics are elsewhere this paper.

1568 Aisleen. This member of the Phocaea family/group was observed by Malcolm (2001) who found a period of 6.68 h. We observed it (Warner, 2014a) finding a period of 6.683 h. Finally, Behrend (2020web) reported a period of 6.6746 h. Our period this year is in good agreement with those prior results. Hanuš et al. (2011) reported a spin axis model with (λ, β) = (109°, -68°) or (310°, 5°) and a sidereal period of 6.67597 h.

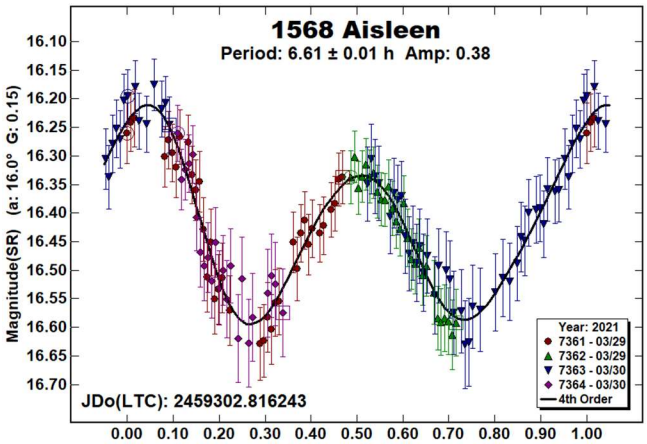

1920 Sarmiento. We have observed this member of the Hungaria family/group three times in the past (Warner, 2007; 2015; Stephens et al., 2014), each time finding a period near 4.05 h. The period we found this year is in good agreement with our prior results.

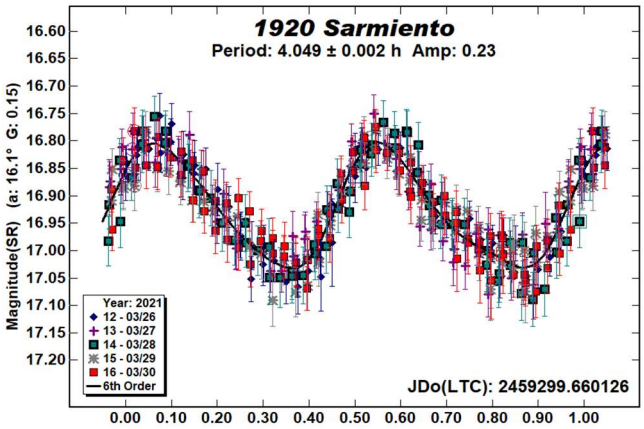

1998 Titius. We observed this Vestoid twice before (Stephens, 2016; 2017), finding periods near 6.13 h. Using data from TESS, McNeil et al. (2019) and Pál et al. (2020) found periods near 6.13 h. Our results this year are in good agreement.

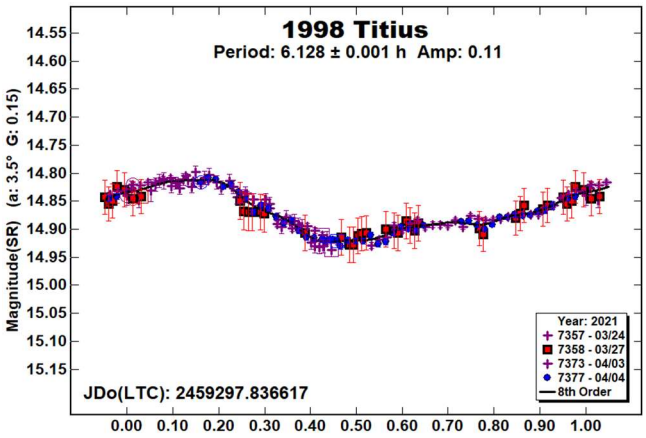

In addition to our dense data from the three apparitions, we used sparse data from the AstDyS-2 (2020) site to solve for the sidereal period and pole position and create a shape model. Our pole model showed two solutions 180° apart: (λ, β, *P*) = (236°, 2°, 6.126051 h) and (54°, 16°, 6.126052 h). Our preferred solution is (236°, 2°). The full set of inversion graphics are given elsewhere this paper.

2233 Kuznetsov. This member of the Flora family/group was observed by Ditteon and West (2011) who found a period of 5.030 h and by Stephens (2017) finding a period of 5.031 h. This year's result is in good agreement.

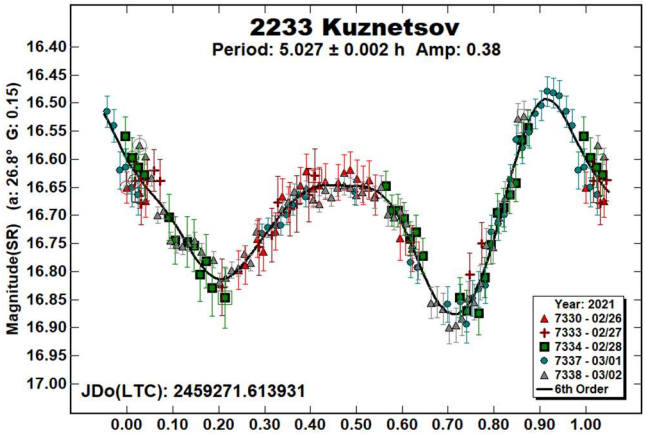

In addition to our dense data from the two apparitions, we used sparse data from the AstDyS-2 (2020) site to solve for the sidereal period and pole position and create a shape/pole model, using *MPO LCInvert* (Bdw Publishing).

Our pole model showed two possible solutions 180° apart; (λ, β, *P*) = (13°, 8°, 5.029548 h) and (192°, 1°, 5.029547 h). Our preferred solution is (13°, 8°), where the a/c ratio is 1.3 and the b/c ratio 1.2. The other solution has similar ratios.

2253 Espinette. This Mars-crosser was observed several times in the past. Behrend (2005web) reported a period of 7.440 h, Stephens (2016) reported 7.442 h, and Skiff et al. (2019) reported a period of 7.4409 h. Our result this year confirms those prior results.

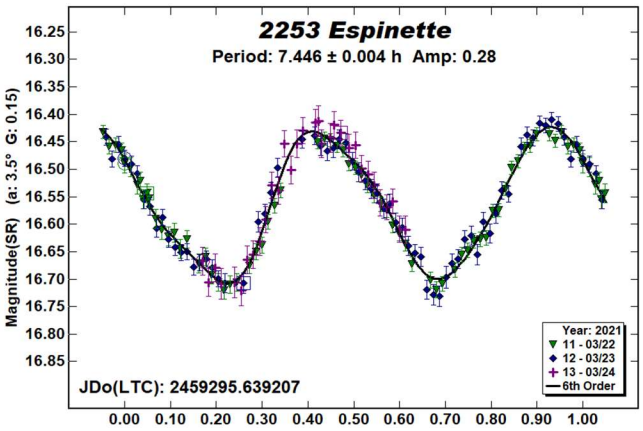

2468 Repin. This member of the Flora family/group has been observed twice in the past. We observed it (Stephens, 2016) finding a period of 4.122 h. Oey et al. (2017) did an extensive observing campaign due to its asymmetrical lightcurve, finding periods of 5.1196 h, 5.1191 h, 5.11920 h, and 5.1200 h over a four-month campaign. Our results this year is in good agreement with those prior results. In all these cases, the secondary minimum is substantially less than the primary minimum.

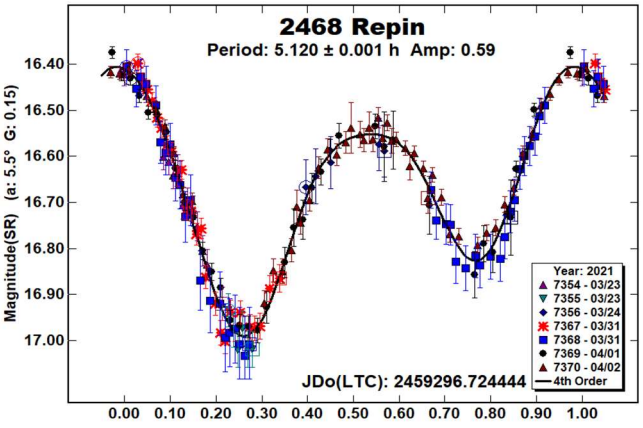

2511 Patterson. There are numerous results posted in the LCDB for this this 6 km sized member of the Vestoid family/group. Juarez et al. (2005) seems to be the first to have determined its rotational period as 4.141 h. Hasegawa et al. (2012) found a period of 4.141 h. With substantially sparser data, Waszczak et al. (2015) found a similar period. Ďurech et al. (2018b) report a sidereal period of 4.14065 h using spare and dense data. Finally, we (Stephens and Warner, 2020a) found a period of 4.139 h. The results we found this year are in good agreement.

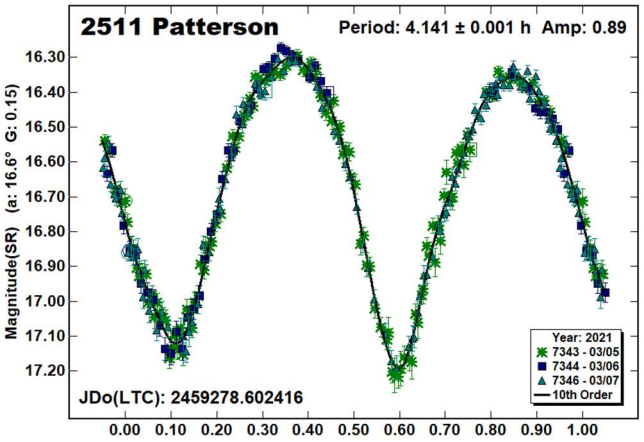

The Ďurech et al. sideral period results from a spin axis model with (λ, β) = (194°, 50°) or (10°, 31°). That model used sparse data in publicly available databases and dense data from a single night in 2016 December from the BlueEye600 robotic observatory.

In addition to our dense data from the two apparitions, we used sparse data from the AstDyS-2 (2020) site to solve for the sidereal period and pole position and to create a shape model, using *MPO LCInvert* (Bdw Publishing). We narrowed the period search based on the Ďurech et al. sideral period.

Our pole model showed two possible solutions 180° apart: (λ, β, *P*) = (215°, -80°, 4.140798 h) and (64°, -81°, 4.140797 h). Our preferred solution is (215°, -80°), where the a/c ratio is 2.75 and the b/c ratio 1.65. The other solution is similar with an a/c ratio of 2.0.

Although our sidereal period is close to the Ďurech et al. result, their latitude is substantially different, being closer to the equator. The discrepancy might result from our denser datasets, which cover seven nights over two apparitions, whereas the BlueEye600 robotic observatory was obtained on a single night. We encourage reanalysis in the future with more dense data and sparse data from ongoing surveys. The full set of inversion graphics are given at the end of this paper.

3029 Sanders. There are two periods reported in the LCDB for his member of the Flora family/group. Erasmus et al. (2020) reported a period of 3.068 h and Benishek (2020a) reported a period of 3.064 h. The period we found this year is in good agreement with those prior results.

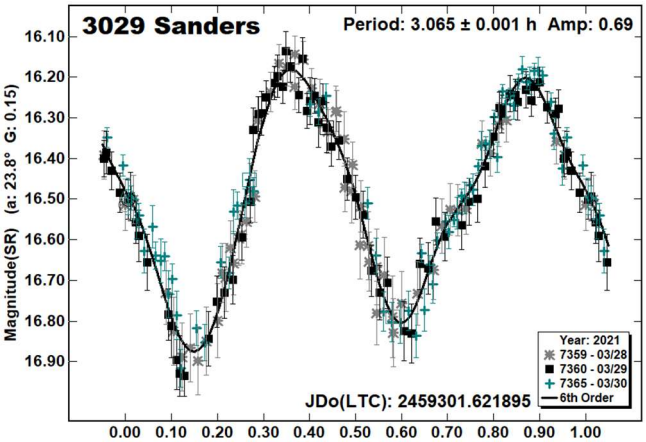

3084 Kondratyuk. This was another case of recovered data. We observed it in 2011 obtaining a partial lightcurve, by itself not sufficient to determine the period.

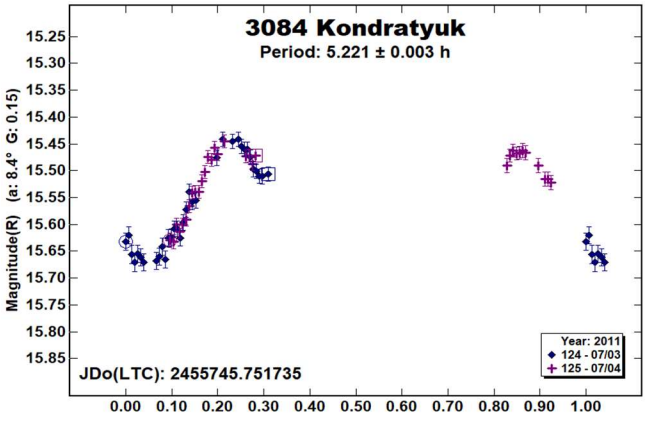

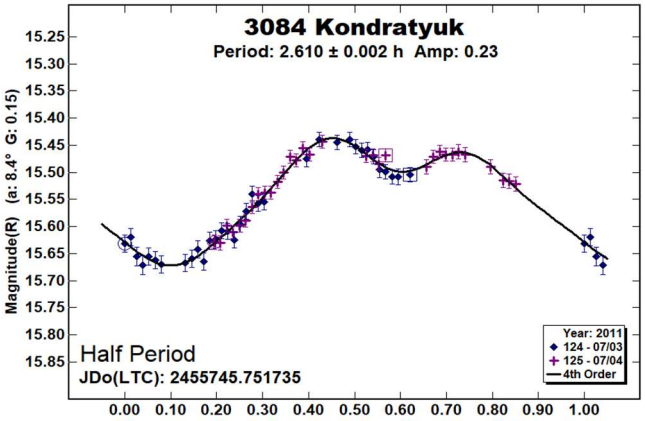

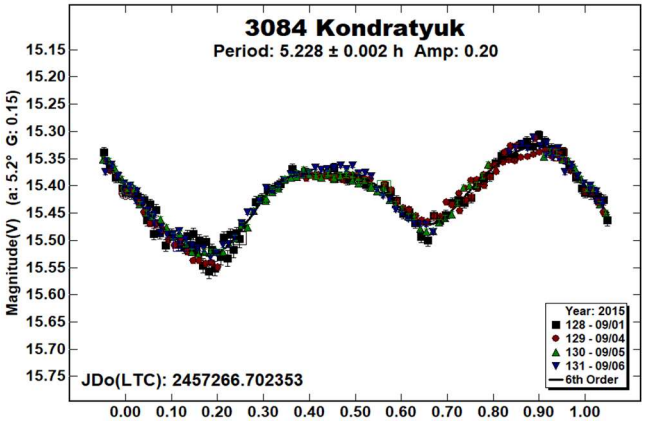

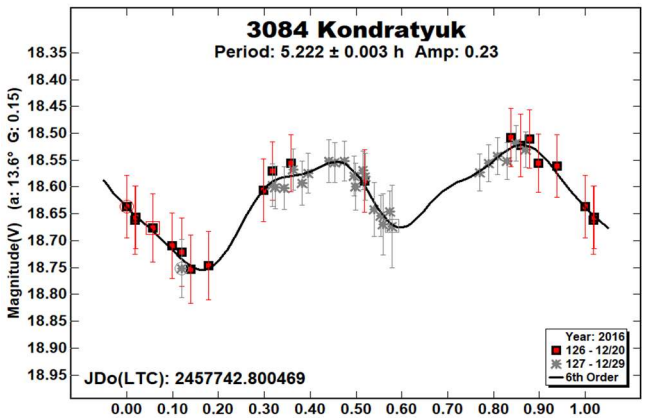

However, we were able to plot a half period of 2.610 h and therefore determine the period for the 2011 data to be 5.221 h. We reobserved it in 2015 and 2016, finding periods near 5.22 h. We plotted the 2011 data to the periods found in 2015 and 2016.

3198 Wallonia. This Mars-crosser has periods reported in the LCDB three times in the past (Behrend, 2005web, 7.58 h; Warner, 2008, 7.54 h; Stephens, 2018, 7.569 h). Our result this year is in good agreement with the previous results.

Using our prior dense datasets from 2008 and 2018 and sparse data at the Asteroids - Dynamic web site (AstDyS-2, 2020), we attempted to solve for the sidereal period and pole position and to create a shape model. A period search was made over a sufficiently wide range to assure finding a global minimum in χ^2 values.

Our pole model showed two possible solutions 180° apart: (λ, β, P) = (115°, -47°, 7.565854 h) and (253°, -45°, 7.565858 h). Our preferred solution is (115°, -47°). The full set of inversion graphics are given at the end of this paper.

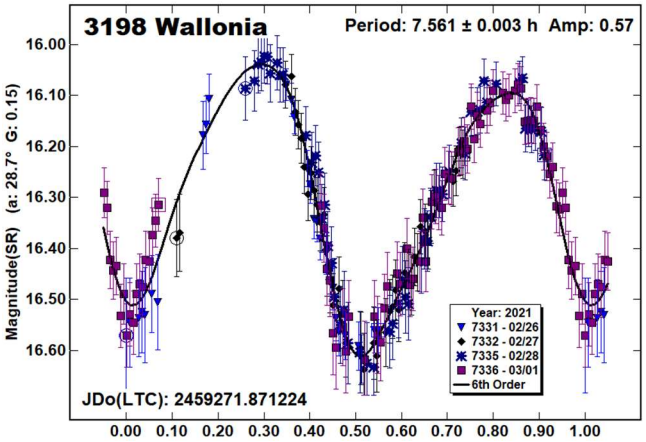

3248 Farinella. This outer main-belt asteroid has been observed many times. Ditteon et al. (2012) originally found a period of 6.676 h. However, upon reobservation, Ditteon et al. (2019) concluded a half period of 3.339 h was a better fit. Using data from TESS, Pál et al. (2020) found a period of 6.6749 h. Our result this year is a good match to the original Ditteon et al. period and the Pál et al. result.

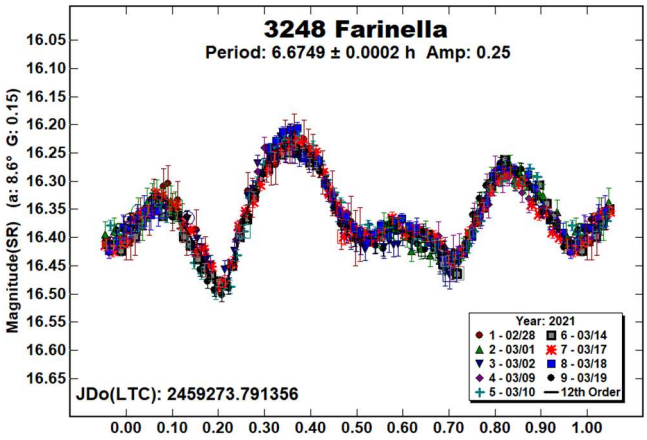

3339 Treshnikov. This outer main-belt asteroid was last observed in 2012 June (Owings, 2013), who found a period of 18.2947 h. We were able to recover this data from 2017, which is consistent with the Owings result.

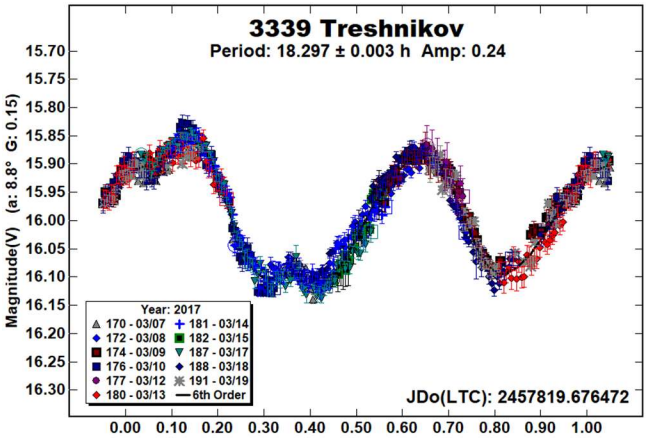

3506 French. This member of the EOS family/group was another 'dusty file cabinet' find, having been observed in 2013 October. Later, Waszczak et al. (2015) reported a period of 16.756 h using sparse data from the Palomar Transient Factory Survey. The Waszczak et al. data was coincidently obtained two weeks after our data. Our denser data and 14th order lightcurve resulted in an amplitude 0.3 magnitude higher than the Waszczak et al. result, which only used two orders in their analysis.

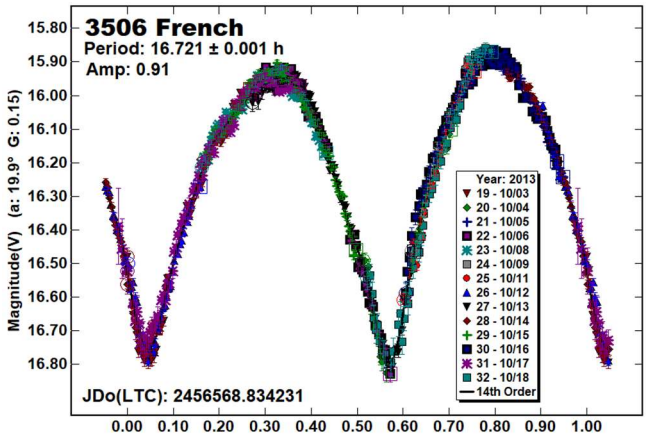

5040 Rabinowitz. This member of the Phocaea family/group was observed three times in the past. Pravec (2013web) reported a period of 4.6901 h. We observed it in 2013 (Stephens and Coley, 2013) finding a period of 4.691 h.

Finally, Clark (2014) observed it in 2013 finding a period of 4.472 h. The Clark observations were obtained over a six-week span and showed substantial changes in the amplitude of the lightcurve, perhaps explaining the difference in the rotational period from the other results. These data from 2016 were part of the recovered dataset. The period we found for 2016 agrees with Pravec's and our previous result.

Because of our dense data, and the availability of some dense data from Klinglesmith in the Asteroid Lightcurve Data Exchange Format database (ALCDEF, 2020) and sparse data at the Asteroids - Dynamic web site (AstDyS-2, 2020), we attempted to solve for the sidereal period and pole position and to create a shape model. We found one possible pole: (λ, β, P) = (101°, 48°, 4.690155 h).

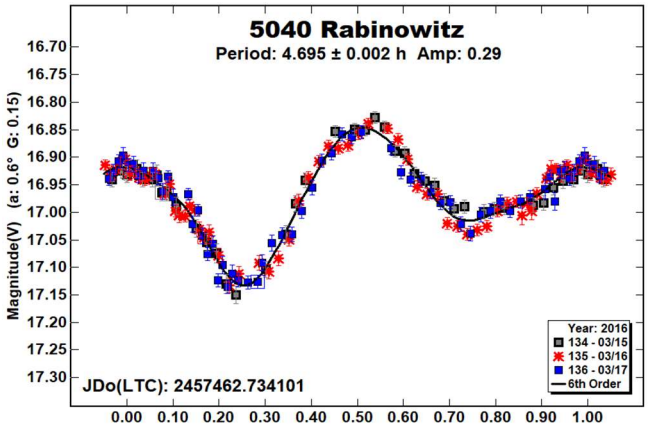

5096 Luzin. This Vestoid has been observed three times in the past; Klinglesmith et al. (2013), Benishek (2020b), and Stephens and Warner (2020b), each time finding a rotational period near 3.05 h. The result we found this year is in good agreement.

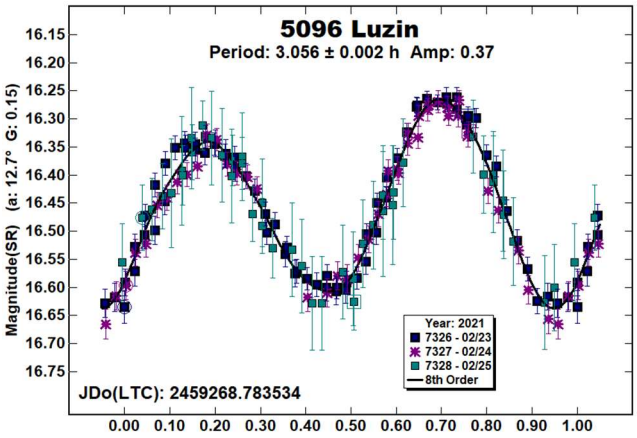

Because of the availability of the Klinglesmith et al. and Benishek data in the Asteroid Lightcurve Data Exchange Format database (ALCDEF, 2020), sparse data at the Asteroids - Dynamic web site (AstDyS-2, 2020), and our dense data from two apparitions, we attempted to solve for the sidereal period and pole position and to create a shape model.

Our pole model showed two possible solutions 180° apart: (λ, β, P) = (75°, 54°, 3.054594 h) and (249°, 35°, 3.054594 h). Our preferred solution is (75°, 54°).

(5747) 1991 CO3. Our recovered data files included this member of the Phocaea family. We observed it once before (Warner, 2009) reporting a period of 38.6 h with an amplitude of 0.30 mag. That lightcurve had only partial coverage from six sessions over 14 nights. This much more complete dataset has 23 sessions spanning a month. Several of those sessions have an amplitude exceeding the amplitude of our original lightcurve. Although the magnitudes at the time were determined using field stars converted to approximate Johnson V magnitudes based on 2MASS J-K colors (Warner, 2007), very few zero-point adjustments were needed to determine the period to be 196.45 h. With this in mind, we reanalyzed our 2008 dataset. We found many zero-point adjustments were applied to the nightly sessions. Upon removing those, we found a large amplitude, slowly rotating asteroid. The 2008 run was not long enough complete the lightcurve, but we were able to determine the half period, which gives us a period of 197.9 h.

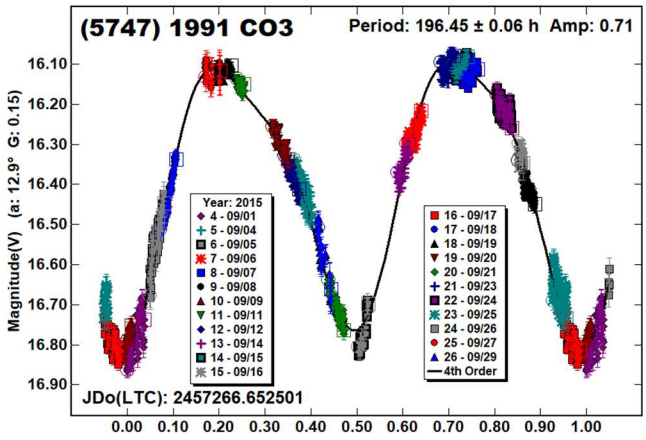

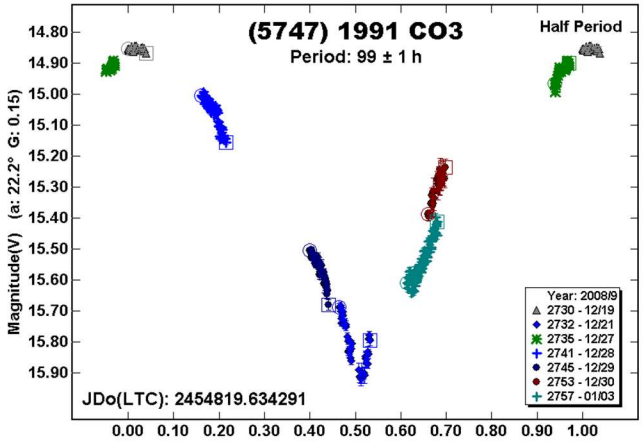

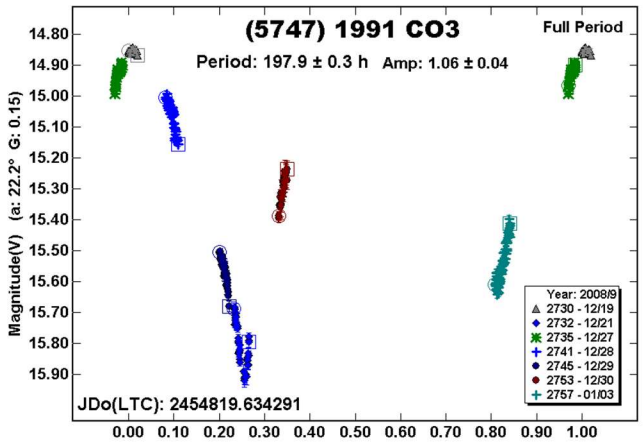

Although this asteroid is a good candidate for tumbling according to the rules of thumb for tumbling damping time (Pravec et al., 2014; 2005), there are no obvious signs of tumbling in either the 2008 or 2016 lightcurves.

6859 Datemasamune. It has always been a problem determining the rotational period of this member of the Hungaria family/group because its amplitude never exceeds 0.12 mag. We observed Datemasamune in 2006, 2009, 2011, 2016, and 2019 (Stephens and Warner, 2019 and references therein), resulting in an ambiguous lightcurve with possible periods between 5.90 h and 9.95 h, with 5.944 h being our preferred period. We recovered additional data from 2014, which did not solve the discrepancy. With only three nights of data from 2014, the period error spans most of these possible periods.

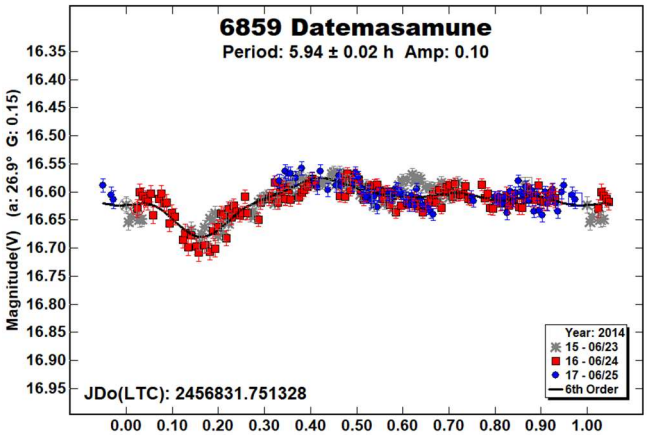

6901 Roybishop. We observed this member of the Hungaria family/group in 2008, 2011, 2015, and 2019 (Stephens and Warner, 2020a and references therein), finding ambiguous solutions as a result of its low amplitude (0.04-0.09 mag.) lightcurves. We subsequently recovered more data from 2016, which did not solve the ambiguity. Although our preferred period of 4.766 h agrees with our 2019 results, it is only a partial lightcurve. Our alternative 2019 result of 9.533 h still cannot be ruled out.

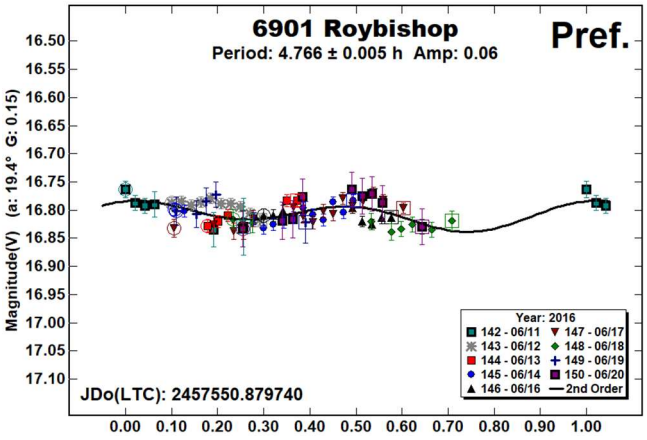

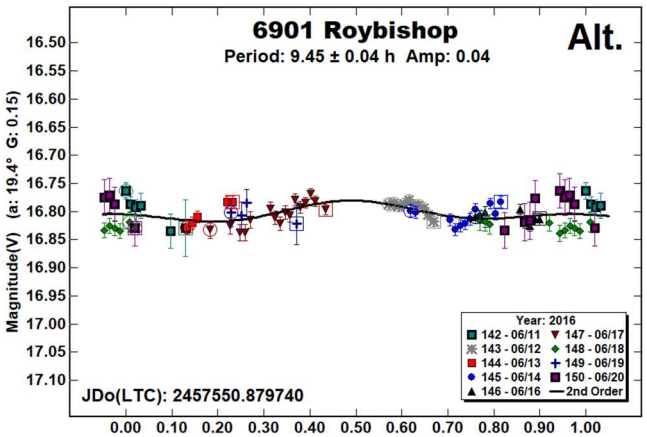

7660 Alexanderwilson. We observed this member of the Hungaria family/group four times in the past (Stephens et al., 2014; Warner, 2012a; 2014b; 2016), each time finding a period near 5.92 h. We recovered data from 2016, which led to a period that is in good agreement with the previous results. Hanuš et al. (2018) reported a spin axis model with (λ, β, *P*) = (321°, 15°) and a sidereal period of 5.91818 h.

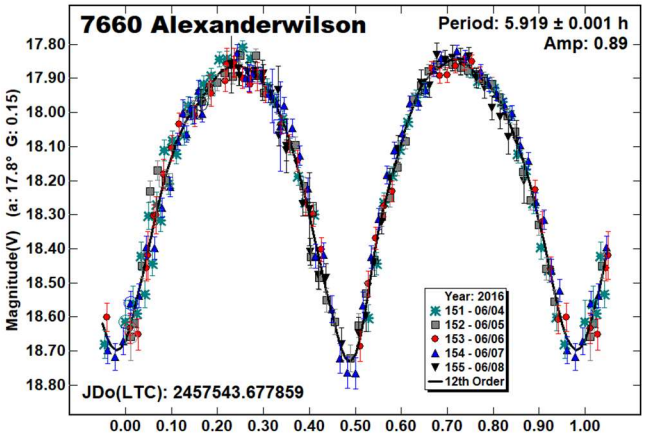

(15123) 2000 EP36. We could not find any periods posted in the LCDB for this member of the Themis family/group. This was another recovered dataset from 2017.

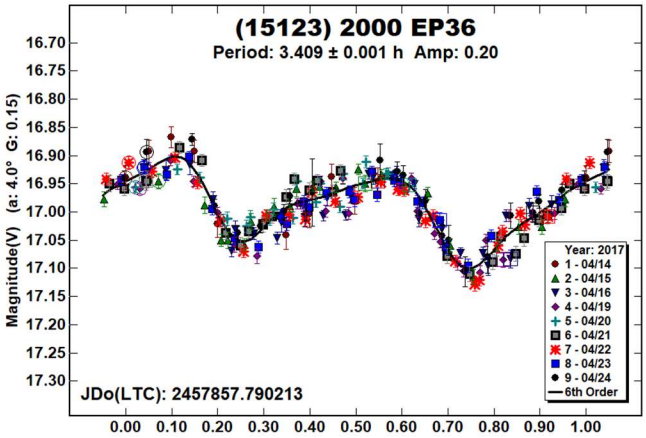

17823 Bartels. This inner main-belt asteroid was observed by the Palomar Transient Factory Survey (Waszczak et al., 2015) who found a period of 3.800 h. Pál el al. (2020), using data from TESS, found a period pf 11.3946 h. We were able to recover much denser datasets from 2013 which shows the period to be 3.784 h, close to the sparser Palomar data.

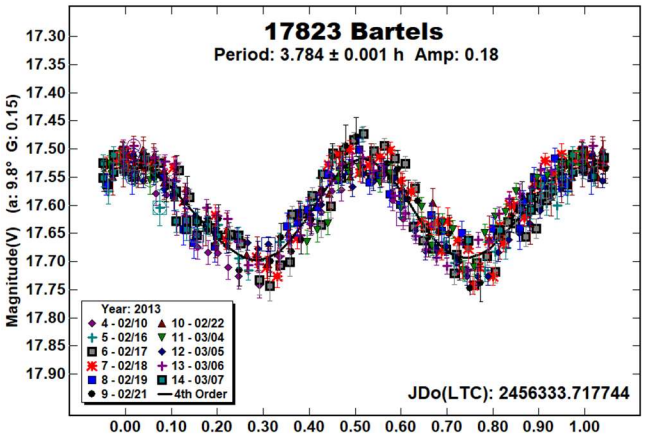

(19979) 1989 VJ. Han et al. (2013) reported a period of 7.568 h for this Vestoid. Our result this year is in good agreement.

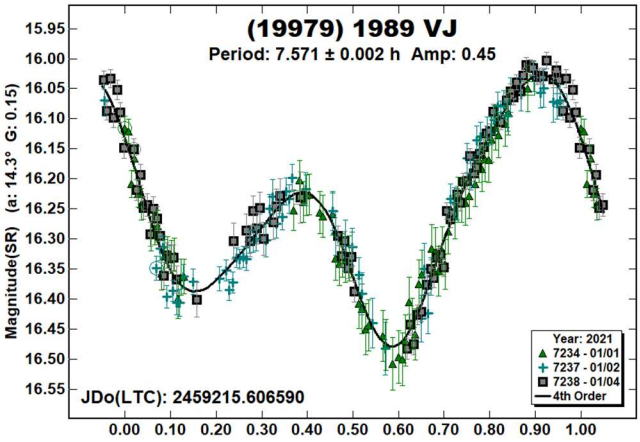

(26895) 1995 MC. We could not find any periods posted in the LCDB for this outer main-belt asteroid. This dataset was recovered from 2012. This target was followed for a month due to its low amplitude and period being commensurate with one half an Earth's day.

The solution produced a bimodal lightcurve, but the period spectrum shows the possibility of a monomodal or quadrimodal lightcurve. Given the relatively low and amplitude, a bimodal solution is not assured (Harris et al., 2014).

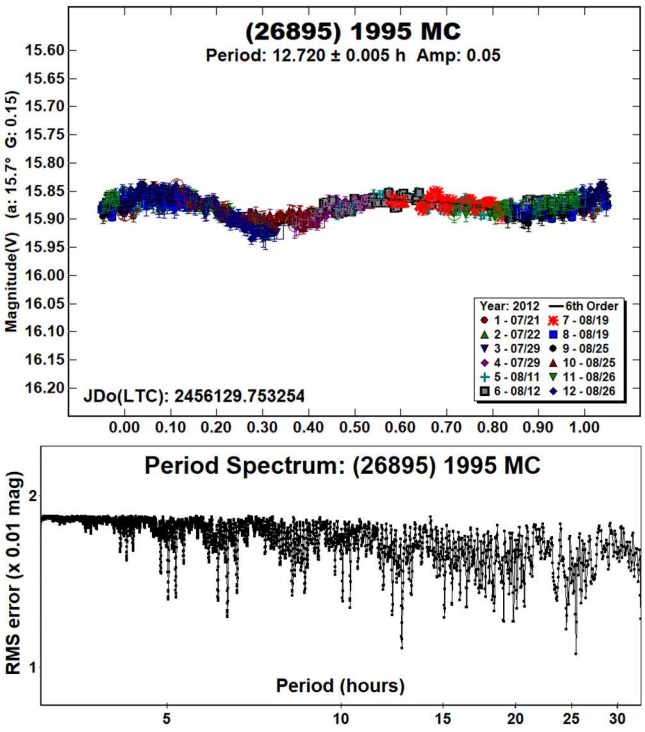

(27011) 1998 FU22. There are no entries in the LCDB for this member of the Flora family/group. It was a target of opportunity in the field of (7458) 1984 DE1 for only three nights. The slope of the individual nights suggests a long period asteroid. There were insufficient data to definitely find a period, but a half period of 37 h points to a full period of 73.4 h.

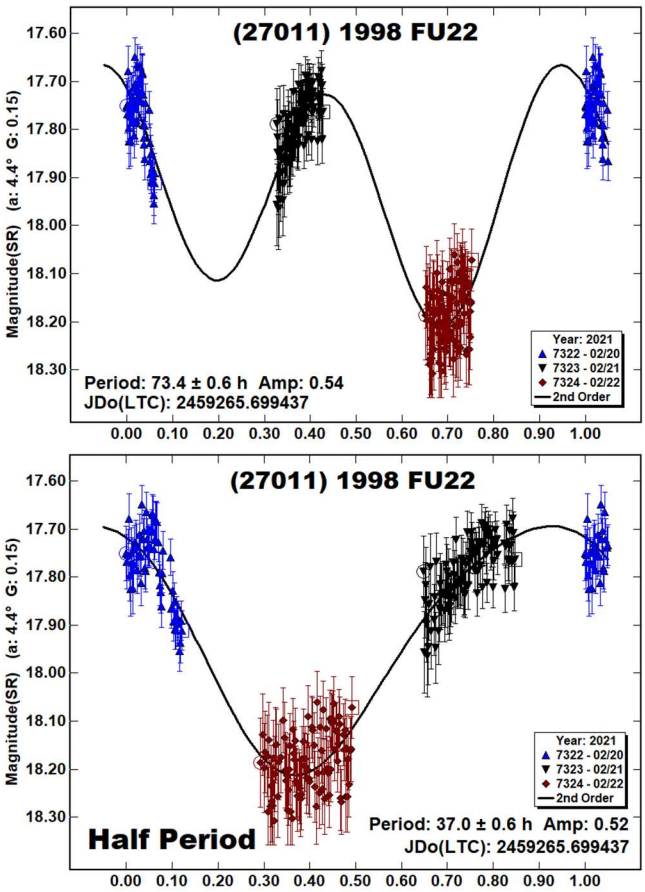

(30781) 1988 CR2. This member of the Flora family/group was observed by Chang et al. (2015) and Waszczak et al. (2015) using the Palomar Transient Factory Survey, each finding periods near 5.82 h. We recovered this dense data from 2015, finding a period near those prior results.

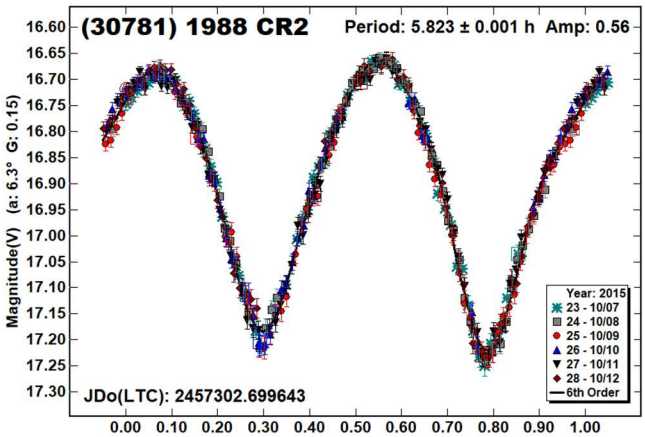

34817 Shiominemoto. We have observed this member of the Hungaria family/group four times in the past (Warner, 2007; 2011; 2012b; Stephens, 2015), each time finding a period near 6.38 h. We recovered this data from 2016, which produced a period that is in good agreement with our prior results. Ďurech et al. (2018b) reported a spin axis model with (λ, β, *P*) = (201°, 36°, 6.37750 h).

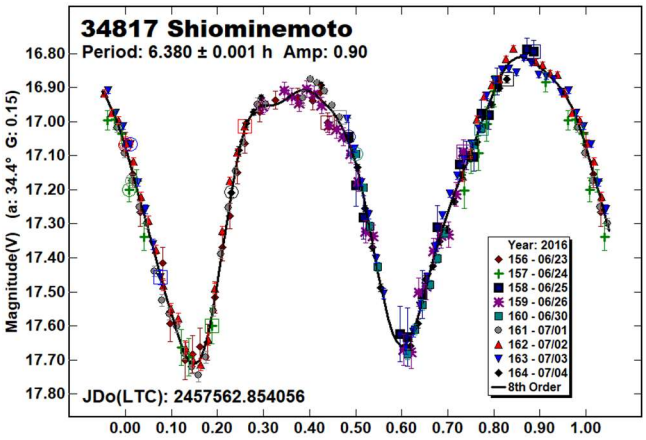

(35194) 1994 ET3. We observed this member of the Hungaria family/group once in the past (Stephens et al., 2014) finding a period of 8.912 h. Since then, we have recovered observations from 2016 and 2019. Along with our new 2021 results, all have a rotational period in good agreement with the 2014 result.

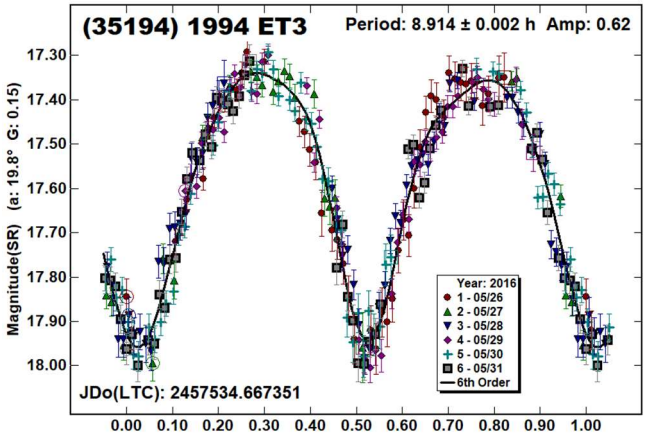

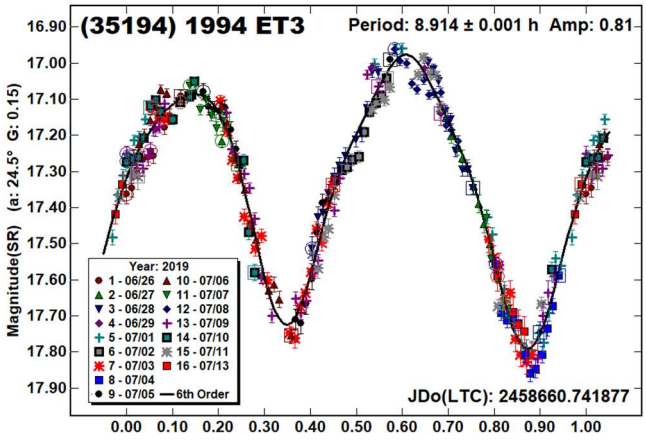

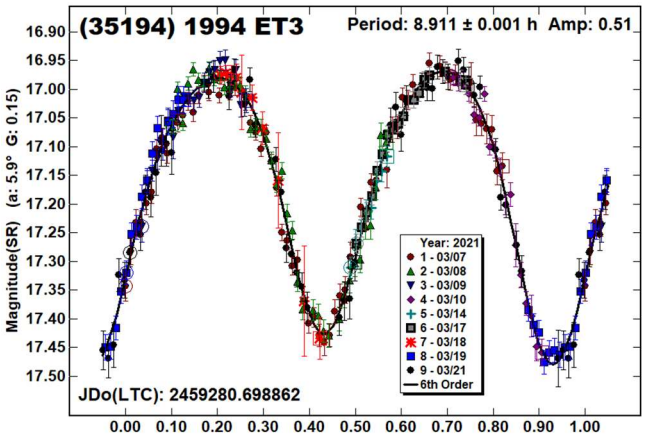

(45068) 1999 XA34. This member of the EOS family/group was observed by Waszczak et al. (2015) using the Palomar Transient Factory Survey, finding a period of 5.043 h. Our result this year is in agreement.

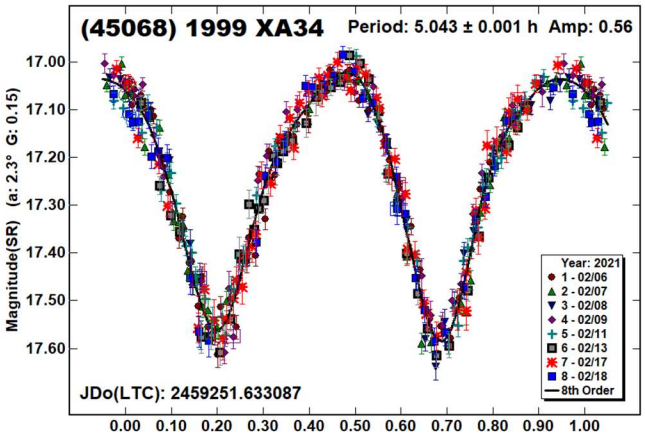

(46598) 1993 FT2. This Mars-crosser was observed in 2007 by Pray et al. (2008) who found a period of 4.86 h. Our result this year is in good agreement.

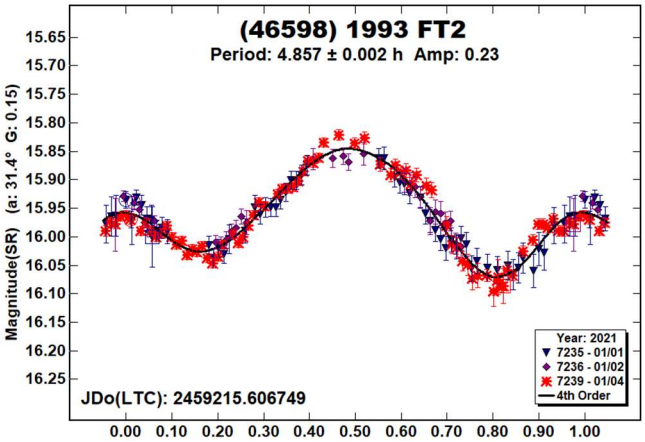

169078 Chuckshaw. There are no entries in the LCDB for this member of the Eunomia family/group. This was another set of recovered data originally obtained in 2014 May.

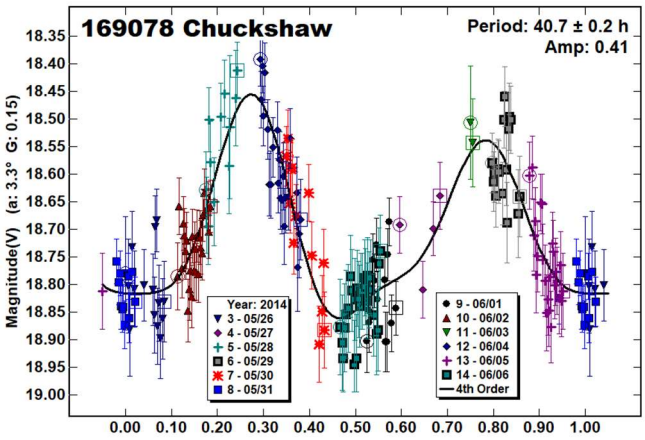

Acknowledgements

Observations at CS3 and continued support of the asteroid lightcurve database (LCDB; Warner et al., 2009) are supported by NASA grant 80NSSC18K0851.

This work includes data from the Asteroid Terrestrial-impact Last Alert System (ATLAS) project. ATLAS is primarily funded to search for near earth asteroids through NASA grants NN12AR55G, 80NSSC18K0284, and 80NSSC18K1575; byproducts of the NEO search include images and catalogs from the survey area. The ATLAS science products have been made possible through the contributions of the University of Hawaii Institute for Astronomy, the Queen's University Belfast, the Space Telescope Science Institute, and the South African Astronomical Observatory.

The authors gratefully acknowledge Shoemaker NEO Grants from the Planetary Society (2007, 2013). These were used to purchase some of the telescopes and CCD cameras used in this research.

References

ALCDEF (2020). Asteroid Lightcurve Data Exchange Format database. *http://www.alcdef.org/*

AstDys-2 (2020). Asteroids - Dynamic site. *https://newton.spacedys.com/astdys/*

Behrend, R., (2005web, 2008web, 2020web). Observatoire de Geneve web site. *http://obswww.unige.ch/~behrend/page_cou.html*

Benishek, V. (2020a). "Asteroid Photometry at Sopot Astronomical Observatory: 2019 June-October." *Minor Planet Bull.* **47**, 75-83.

Benishek, V. (2020b). "Photometry of 39 Asteroids at Sopot Astronomical Observatory: 2019 September - 2020 March." *Minor Planet Bull.* **47**, 231-241.

Chang, C.-K., Ip, W.-H., Lin, H.-W., Cheng, Y.-C., Ngeow, C.-C., Yang, T.-C., Waszczak, A., Kulkarni, S.R., Levitan, D., Sesar, B., Laher, R., Surace, J., Prince, T.A. (2015). "Asteroid Spin-rate Study Using the Intermediate Palomar Transient Factory." *Ap. J. Suppl. Ser.* **219**, A27.

Clark, M. (2014). "Asteroid Photometry from the Preston Gott Observatory." *Minor Planet Bull.* **41**, 100-101.

Coley, D. (2012). "Asteroid Lightcurve Analysis at the Danhenge Observatory Apr - Aug 2011." *Minor Planet Bull.* **39**, 13-24.

Ditteon, R.; West, J. (2011). "Asteroid Lightcurve Analysis at the Oakley Southern Observatory: 2011 January thru April." *Minor Planet Bull.* **38**, 214-217.

Ditteon, R.; Horn, L.; Kamperman, A.; Vorjohan, B.; Kirkpatrick, E. (2012). "Asteroid Lightcurve Analysis at the Oakley Souther Sky Observatory: 2011 April-May." *Minor Planet Bull.* **39**, 26-28.

Ditteon, R.; Johnson, D.; Lin, W.; Wang, Z.; Zhao, B. (2019). "Lightcurve Analysis of Minor Planets Observed at the Oakley Southern Sky Observatory: 2018 August-September." *Minor Planet Bull.* **46**, 280-282.

Ďurech, J.; Hanuš, J.; Alí-Lagoa, V. (2018a). "Asteroid models reconstructed from the Lowell Photometric Database and WISE data." *Astron. Astrophys.* **617**, A57.

Ďurech, J.; Hanuš, J.; Broz, M.; Lehky, M.; Behrend, R.; Antonini, P.; Charbonnel, S.; Crippa, R.; Dubreuil, P.; Farroni, G.; Kober, G.; Lopez, A.; Manzini, F.; Oey, J.; Poncy, R.; Rinner, C.; Roy, R. (2018b). "Shape models of asteroids based on lightcurve observations with BlueEye600 robotic observatory." *Icarus* **304**, 101-109.

Erasmus, N.; Navarro-Meza, S.; McNeill, A.; Trilling, D.E.; Sickafoose, A.A.; Denneau, L.; Flewelling, H.; Heinze, A.; Tonry, J.L. (2020). "Investigating Taxonomic Diversity within Asteroid Families through ATLAS Dual-band Photometry." *Ap. J.* **247**, A13.

Garceran, A.C.; Aznar, A.; Mansego, E.A.; Rodriguez, P.B.; de Haro, J.L.; Silva, A.F.; Silva, G.F.; Martinez, V.M.; Chiner, O.R. (2016). "Nineteen Asteroids Lightcurves at Asteroids Observers (OBAS) - MPPD: 2015 April - September." *Minor Planet Bull.* **43**, 92-97.

Hamanowa, H., Hamanowa, H. (2010). Hamanowa Astronomical Obs. Web site. *http://www2.ocn.ne.jp/~hamaten/astcjata.htm*

Han, X.L.; Li, B.; Zhao, H.; Liu, W.; Sun, L.; Shi, J.; Gao, S.; Wang, S.; Pan, X.; Jiang, P.; Zhou, H. (2013). "Photometric Observations of 782 Montefiore, 3842 Harlansmith 5542 Moffatt, 6720 Gifu, and (19979) 1989 VJ." *Minor Planet Bull.* **40**, 99-100.

Hanuš, J.; Ďurech, J.; Brož, M.; Warner, B.D.; Pilcher, F.; Stephens, R.; Oey, J.; Bernasconi, L.; Casulli, S.; Behrend, R.; Polishook, D.; Henych, T.; Lehký, M.; Yoshida, F.; Ito, T. (2011). "A study of asteroid pole-latitude distribution based on an extended set of shape models derived by the lightcurve inversion method." *Astron. Astrophys.* **530**, A134.

Hanuš, J.; Ďurech, J.; Oszkiewicz, D.A.; Behrend, R.; Carry, B.; Delbo, M.; Adam, O.; Afonina, V.; Anquetin, R.; Antonini, P.; Arnold, L.; Audejean, M.; Aurard, P.; Bachschmidt, M.; Baduel, B.; Barbotin, E.; Barroy, P.; Baudouin, P.; Berard, L.; Berger, N. (2018). "New and updated convex shape models of asteroids based on optical data from a large collaboration network." *Astron. Astrophys.* **586**, A108.

Harris, A.W.; Young, J.W.; Scaltriti, F.; Zappala, V. (1984). "Lightcurves and phase relations of the asteroids 82 Alkmene and 444 Gyptis." *Icarus* **57**, 251-258.

Number	Name	21yy/mm/dd	Phase	L_{PAB}	B_{PAB}	Period(h)	P.E.	Amp	A.E.	Grp
279	Thule	13/12/05-12/11	0.6,2.2	71		15.94	0.02	0.04	0.02	MB-O
						7.97	0.03	0.04	0.02	
						23.96	0.03			
341	California	14/01/13-02/25	20.2,24.4	72	5	310	10	0.43	0.10	FLOR
1164	Kobolda	03/21-03/23	14.8,15.9	160	7	4.140	0.002	0.22	0.02	PHO
1331	Solvejg	05/16-05/20	10.5,11.8	208	4	19.33	0.04	0.37	0.02	MB-O
1413	Roucarie	11/04/10-04/30	7.3,13.7	182	2	6.530	0.001	0.48	0.02	MB-O
		13/09/21-09/25	7.3,8.5	339	3	6.531	0.002	0.30	0.02	
		02/06-02/09	3.9,4.3	135	-9	6.532	0.002	0.15	0.01	
1568	Aisleen	03/29-03/30	16.0,15.9	224	28	6.61	0.01	0.38	0.02	PHO
1920	Sarmiento	03/26-03/30	16.1,16.2	184	28	4.049	0.002	0.23	0.02	H
1998	Titius	03/24-04/04	*3.5,3.3	189	-3	6.128	0.001	0.11	0.02	V
2233	Kuznetsov	02/26-03/02	26.8,27.0	91	-2	5.027	0.002	0.38	0.02	FLOR
2253	Espinette	03/22-03/24	3.7,4.6	174	3	7.446	0.004	0.28	0.02	MC
2468	Repin	03/23-04/02	5.6,9.8	172	-5	5.120	0.001	0.59	0.02	FLOR
2511	Patterson	03/05-03/07	16.6,17.2	129	8	4.141	0.001	0.89	0.02	V
3029	Sanders	03/28-03/30	23.8,24.3	140	-1	3.065	0.001	0.69	0.02	FLOR
3084	Kondratyuk	11/07/03-07/04	*9.1,8.6	293	6	5.221	0.003	0.23	0.02	MB-I
		15/09/01-09/06	5.2,2.4	345	2	5.228	0.002	0.20	0.02	MB-I
		16/12/20-12/29	13.6,10.7	125	-5	5.222	0.003	0.23	0.03	
3198	Wallonia	02/26-03/01	28.7,28.0	205	23	7.561	0.003	0.57	0.03	MC
3248	Farinella	02/28-03/19	8.6,12.5	132	10	6.6749	0.0002	0.25	0.02	MB-O
3339	Treshnikov	17/03/07-03/19	8.8,11.1	157	21	18.297	0.003	0.24	0.03	MB-O
3506	French	13/10/03-10/18	19.9,17.2	69	10	16.721	0.001	0.91	0.02	EOS
5040	Rabinowitz	03/15-03/17	*0.6,0.4	176	0	4.695	0.002	0.29	0.02	PHO
5096	Luzin	02/23-02/25	12.8,11.9	180	-5	3.056	0.002	0.37	0.02	V
5747	1991 CO3	08/12/19-01/03	*22.6,26.8	59	20	197.9	0.3	1.05	0.10	PHO
		15/09/01-09/29	*12.8,18.0	337	28	196.45	0.06	0.71	0.02	
6859	Datemasamune	14/12/31-12/31	*26.9,26.3	306	23	5.94	0.02	0.10	0.02	H
6901	Roybishop	16/06/11-06/20	19.5,15.5	294	0	4.766	0.005	0.06	0.02	H
						9.45	0.01	0.06	0.02	
7660	Alexanderwilson	16/06/04-06/08	17.8,17.8	258	32	5.919	0.001	0.89	0.02	H
15123	2000 EP36	17/04/14-04/24	4.0,8.1	195	1	3.409	0.001	0.20	0.02	MB-O
17823	Bartels	13/02/10-03/07	*9.8,5.5	158	5	3.784	0.001	0.18	0.02	MB-I
19979	1989 VJ	01/01-01/04	14.4,15.6	74	0	7.571	0.002	0.45	0.02	V
26895	1995 MC	07/21-08/12	15.7,8.1	327	10	12.720	0.005	0.05	0.02	MB-M
27011	1998 FU22	02/20-02/22	*4.5,3.0	160	-1	73.4	0.6	0.54	0.10	FLOR
30781	1988 CR2	10/07-10/12	6.3,7.8	10	-9	5.823	0.001	0.56	0.02	FLOR
34817	Shiominemoto	06/23-07/04	34.4,33.0	328	14	6.380	0.001	0.90	0.02	MC
35194	1994 ET3	16/05/26-05/31	*19.8,20.4	241	34	8.914	0.002	0.62	0.02	H
		19/06/26-07/13	24.4,23.1	304	26	8.914	0.001	0.81	0.02	
		03/07-03/21	*5.9,6.8	174	8	8.911	0.001	0.51	0.02	
45068	1999 XA34	02/06-02/18	2.3,7.0	132	1	5.043	0.001	0.56	0.02	EOS
46598	1993 FT2	01/01-01/04	31.4,32.0	62	29	4.857	0.002	0.23	0.02	MC
169078	Chuckshaw	05/26-06/06	*3.3,3.1	250	-2	40.7	0.2	0.41	0.05	MB-M

Table III. Observing circumstances and results. The phase angle is given for the first and last date. If preceded by an asterisk, the phase angle reached an extrema during the period. L_{PAB} and B_{PAB} are the approximate phase angle bisector longitude/latitude at mid-date range (see Harris et al., 1984). Grp is the asteroid family/group (Warner et al., 2009): ERI, Erigone; EUN, Eunomia; FLOR, Flora; H, Hungaria; KOR, Koronis; MC, Mars-crosser; PHO, Phocaea.

Harris, A.W.; Young, J.W.; Contreiras, L.; Dockweiler, T.; Belkora, L.; Salo, H.; Harris, W.D.; Bowell, E.; Poutanen, M.; Binzel, R.P.; Tholen, D.J.; Wang, S. (1989). "Phase relations of high albedo asteroids: The unusual opposition brightening of 44 Nysa and 64 Angelina." *Icarus* **81**, 365-374.

Harris, A.W., Pravec, P., Galad, A., Skiff, B.A., Warner, B.D., Vilagi, J., Gajdos, S., Carbognani, A., Hornoch, K., Kusnirak, P., Cooney, W.R., Gross, J., Terrell, D., Higgins, D., Bowell, E., Koehn, B.W. (2014). "On the maximum amplitude of harmonics on an asteroid lightcurve." *Icarus* **235**, 55-59.

Hasegawa, S.; Miyasaka, S.; Mito, H.; Sarugaku, Y.; Ozawa, T.; Kuroda, D.; Nishihara, S.; Harada, A.; Yoshida, M.; Yanagisawa, K.; Shimizu, Y.; Nagayama, S.; Toda, H.; Okita, K.; Kawai, N.; Mori, M.; Sekiguchi, T.; Ishiguro, M.; Abe, M. (2012). "Lightcurve Survey of V-Type Asteroids. Observations Until 2005." *ACM 2012, Proceedings of the conference held May 16-20, 2012* Id. 6281.

Higgins, D.; Oey, J. (2007). "Asteroid Lightcurve Analysis at Hunters Hill Observatory and Collaborating Stations - December 2006 - April 2007." *Minor Planet Bull.* **34**, 79-80.

Higgins, D. (2011). "Period Determination of Asteroid Targets Observed at Hunters Hill Observatory: May 2009 - September 2010." *Minor Planet Bull.* **38**, 41-46.

Juarez, R.A.; Martinez, C.T.; Ryan, W.H.; Ryan, E.V. (2005). "Physical Properties of the Vesta family asteroid 2511 Patterson." *Bulletin of Amer. Astron. Soc.* **37**, 1155.

Number	Name	λ	β	Period	λ	β	Period	a/b ratio	a/c ratio
1164	Kobolda	**270°**	**-61°**	**4.141699 h**				**1.5**	**1.4**
1413	Roucarie	**122°**	**10°**	**6.530557 h**	311°	37°	6.530558 h	**1.5**	**1.7**
1998	Titius	**236°**	**2°**	**6.126051 h**	54°	16°	6.126052 h	**1.2**	**2.4**
2233	Kuznetsov	**13°**	**8°**	**5.029548 h**	192°	1°	5.029547 h	**1.2**	**1.3**
2511	Patterson	**215°**	**-80°**	**4.140798 h**	64°	-81°	4.140797 h	**1.7**	**2.8**
3198	Wallonia	**115°**	**-47°**	**7.565854 h**	253°	-45°	7.565858 h	**1.4**	**1.7**
5040	Rabinowitz	**101°**	**48°**	**4.690155 h**				**1.1**	**1.8**
5096	Luzin	**75°**	**54°**	**3.054594 h**	249°	35°	3.054594 h	**1.4**	**1.8**

Table IV. Results of Pole/Shape modeling. The preferred solution is listed first in bold text.

Kaasalainen, M.; Torppa, J. (2001). "Optimization Methods for Asteroid Lightcurve Inversion. I. Shape Determination." *Icarus* **153**, 24-36.

Kaasalainen, M.; Torppa J.; Muinonen, K. (2001). "Optimization Methods for Asteroid Lightcurve Inversion. II. The Complete Inverse Problem." *Icarus* **153**, 37-51.

Klinglesmith III, D.A.; Hanowell, J.; Risley, E.; Turk, J.; Vargas, A.; Warren, C.A. (2013). "Asteroid Synodic Periods from Etscorn Campus Observatory." *Minor Planet Bull.* **40**, 65-67.

Malcolm, G. (2001). "Rotational Periods and Lightcurves of 1166 Sakuntala and 1568 Aisleen." *Minor Planet Bull.* **28**, 64.

Marciniak, A.; Pilcher, F.; Oszkiewicz, D.; Bartczak, P.; Santana-Ros, T.; Kamiński, K.; Urakawa, S.; Ogłoza, W.; Fauvaud, S.; Kankiewicz, P.; Kudak, V.; Żejmo, M.; Nishiyama, K.; Okumura, S.; Nimura, T.; Hirsch, R.; Konstanciak, I.; Tychoniec, Ł.; Figas, M. (2016) "Difficult cases in photometric studies of asteroids." *Proceedings of the Polish Astronomical Society* **3**, 84-87.

McNeill, A.; Mommert, M.; Trilling, D.E.; Llama, J.; Skiff, B. (2020). "Asteroid Photometry from the Transiting Exoplanet Survey Satellite: A Pilot Study." *Ap. J.* **245**, A29.

Oey, J.; Williams, H.; Groom, R.; Pray, D.; Benishek, V. (2017). "Lightcurve Analysis of Binary and Potential Binary Asteroids in 2015." *Minor Planet Bull.* **44**, 193-199.

Owings, L. (2013). "Lightcurves for 1896 Beer, 2574 Ladoga, 3301 Jansje, 3339 Treshnikov 3833 Calingasta, 3899 Wichterle, 4106 Nada, 4801 Ohre, 4808 Ballaero, and (8487) 1989 SQ." *Minor Planet Bull*. **40**, 8-10.

Pál, A.; Szakáts, R.; Kiss, C.; Bódi, A.; Bognár, Z.; Kalup, C.; Kiss, L.L.; Marton, G.; Molnár, L.; Plachy, E.; Sárneczky, K.; Szabó, G.M.; Szabó, R. (2020). "Solar System Objects Observed with TESS - First Data Release: Bright Main-belt and Trojan Asteroids from the Southern Survey." *Ap. J.* **247**, A26.

Pilcher, F. (2014). "New Photometric Observations of 279 Thule." *Minor Planet Bull*. **41**, 73-75.

Pilcher, F.; Franco, L.; Pravec, P. (2017). "319 Leona and 341 California - Two Very Slowly Rotating Asteroids." *Minor Planet Bull*. **44**, 87-90.

Polakis, T.; Skiff, B.A. (2017). "Lightcurve Analysis for 341 California, 594 Mireille, 1115 Sabauda 1504 Lappeenranta, and 1926 Demiddelaer." *Minor Planet Bull*. **44**, 299-302.

Pravec, P.; Harris, A.W.; Scheirich, P.; Kušnirák, P.; Šarounová, L.; Hergenrother, C.W.; Mottola, S.; Hicks, M.D.; Masi, G.; Krugly, Yu.N.; Shevchenko, V.G.; Nolan, M.C.; Howell, E.S.; Kaasalainen, M.; Galád, A.; Brown, P.; Degraff, D.R.; Lambert, J.V.; Cooney, W.R.; Foglia, S. (2005). "Tumbling asteroids." *Icarus* **173**, 108-131.

Pravec, P.; Wolf, M.; Sarounova, L. (2008web, 2010web, 2013web). *http://www.asu.cas.cz/~ppravec/neo.htm*

Pravec, P.; Scheirich, P.; Durech, J.; Pollock, J.; Kusnirak, P.; Hornoch, K.; Galad, A.; Vokrouhlicky, D.; Harris, A.W.; Jehin, E.; Manfroid, J.; Opitom, C.; Gillon, M.; Colas, F.; Oey, J.; Vrastil, J.; Reichart, D.; Ivarsen, K.; Haislip, J.; LaCluyze, A. (2014). "The tumbling state of (99942) Apophis." *Icarus* **233**, 48-60.

Pray, D.P.; Galad, A.; Husarik, M.; Oey, J. (2008). "Lightcurve Analysis of Fourteen Asteroids." *Minor Planet Bull*. **35**, 34-36.

Satō, I.; Hamanowa, H.; Tomioka, H.; Uehara, S. (2015). "Possible Duplicities of Five Asteroids." *Intl J. Astr. Ap.* **5**, 193-207.

Sauppe, J.; Torno, S.; Lemke-Oliver, R.; Ditteon, R. (2007). "Asteroid Lightcurve Analysis at the Oakley Observatory - March/April 2007." *Minor Planet Bull.* **34**, 119-122.

Skiff, B.A.; McLelland, K.P.; Sanborn, J.J.; Pravec, P.; Koehn, B.W. (2019). "Lowell Observatory Near-Earth Asteroid Photometric Survey (NEAPS): Paper 3." *Minor Planet Bull.* **43**, 52-56.

Stephens, R.D. (2015). "Asteroids Observed from CS3: 2015 January - March." *Minor Planet Bull.* **42**, 200-203.

Stephens, R.D. (2016). "Asteroids Observed from CS3: 2015 July - September." *Minor Planet Bull.* **43**, 52-56.

Stephens, R. (2017). "Asteroids Observed from CS3: 2016 - September." *Minor Planet Bull*. **44**, 49-52.

Stephens, R. (2018). "Asteroids Observe from CS3: 2018 April - June." *Minor Planet Bull*. **45**, 353-355.

Stephens, R.D.; Coley, D. (2013). "A Plethora of Phocaea Asteroids." *Minor Planet Bull.* **40**, 203-204.

Stephens, R.D.; Coley, D.; Warner, B.D. (2014). "Collaborative Asteroid Lightcurve Analysis at the Center for Solar System Studies: 2013 April-June." *Minor Planet Bull.* **41**, 8-13.

Stephens, R.D.; Warner, B.D. (2019). "Main-belt Asteroids Observed from CS3: 2019 April to June." *Minor Planet Bull.* **46**, 449-456.

Stephens, R.D.; Warner, B.D. (2020a). "Main-belt Asteroids Observed from CS3: 2019 July to September." *Minor Planet Bull.* **47**, 50-60.

Stephens, R.D.; Warner, B.D. (2020b). "Main-Belt Asteroids Observed from CS3: 2019 October to December." *Minor Planet Bull.* **47**, 125-133.

Tonry, J.L.; Denneau, L.; Flewelling, H.; Heinze, A.N.; Onken, C.A.; Smartt, S.J.; Stalder, B.; Weiland, H.J.; Wolf, C. (2018). "The ATLAS All-Sky Stellar Reference Catalog." *Astrophys. J.* **867**, A105.

Warner, B.D. (2007). "Initial Results from a Dedicated H-G Project." *Minor Planet Bull*. **37**, 57-64.

Warner, B.D. (2008). "Asteroid Lightcurve Analysis at the Palmer Divide Observatory: February-May 2008." *Minor Planet Bull*. **35**, 163-166.

Warner, B.D. (2009). "Asteroid Lightcurve Analysis at the Palmer Divide Observatory: 2008 December - 2009 March." *Minor Planet Bull.* **36**, 109-116.

Warner, B.D. (2011). "Upon Further Review: V. An Examination of Previous Lightcurve Analysis from the Palmer Divide Observatory." *Minor Planet Bull.* **38**, 63-65.

Warner, B.D. (2012a). "Asteroid Lightcurve Analysis at the Palmer Divide Observatory: 2011 June - September." *Minor Planet Bull.* **39**, 16-21.

Warner, B.D. (2012b). "Asteroid Lightcurve Analysis at the Palmer Divide Observatory: 2011 September - December." *Minor Planet Bull.* **39**, 69-80.

Warner, B.D. (2014a). "Asteroid Lightcurve Analysis at CS3-Palmer Divide Station: 2014 March-June." *Minor Planet Bull.* **41**, 235-241.

Warner, B.D. (2014b). "Asteroid Lightcurve Analysis at CS3-Palmer Divide Station: 2014 June-October." *Minor Planet Bull.* **42**, 54-60.

Warner, B.D. (2015). "Asteroid Lightcurve Analysis at CS3-Palmer Divide Station: 2014 October-December." *Minor Planet Bull.* **42**, 108-114.

Warner, B.D. (2016). "Asteroid Lightcurve Analysis at CS3-Palmer Divide Station: 2016 April-July." *Minor Planet Bull.* **43**, 300-304.

Warner, B.D.; Harris, A.W.; Pravec, P. (2009). "The Asteroid Lightcurve Database." *Icarus* **202**, 134-146. Updated 2020 Oct. *http://www.minorplanet.info/lightcurvedatabase.html*

Warner, B.D.; Harris, A.W.; Coley, D.; Stephens, R.D.; Allen, B.; Higgins, D. (2010). "Lightcurve Analysis of 279 Thule." *Minor Planet Bull*. **37**, 168-169.

Waszczak, A.; Chang, C.-K.; Ofek, E.O.; Laher, R.; Masci, F.; Levitan, D.; Surace, J.; Cheng, Y.-C.; Ip, W.-H.; Kinoshita, D.; Helou, G.; Prince, T.A.; Kulkarni, S. (2015). "Asteroid Light Curves from the Palomar Transient Factory Survey: Rotation Periods and Phase Functions from Sparse Photometry." *Astron. J.* **150**, A75.

SPIN/SHAPE MODEL FOR 1164 Kobolda

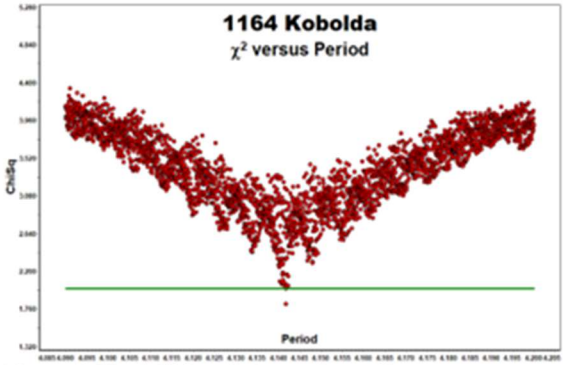

Figure 1. The initial period search results.

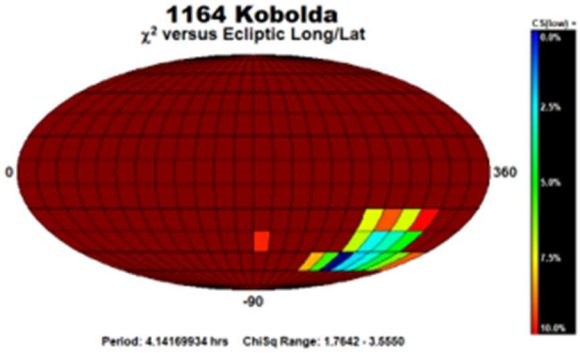

Figure 2. The pole search found two probable solutions.

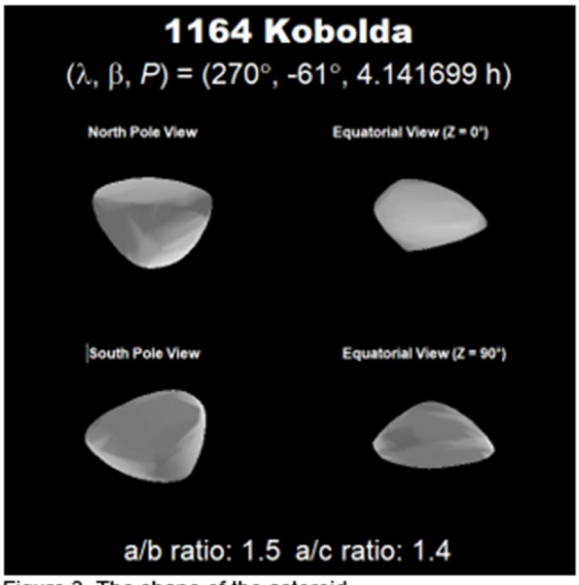

Figure 3. The shape of the asteroid.

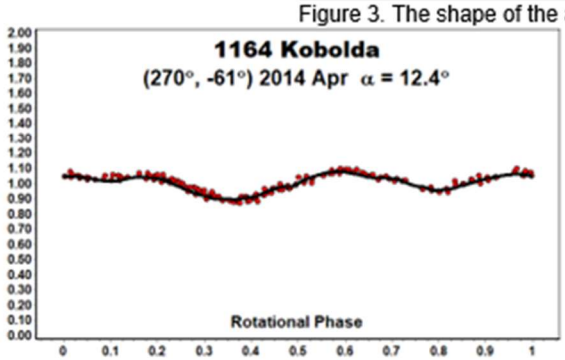

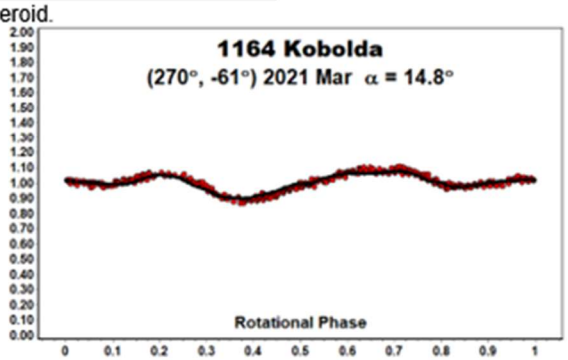

Figure 4/5. The comparison plots are against the preferred pole solution. The red dots indicate the data used for modeling while the black line is the smoothed lightcurve for generated by the shape at the time of the observations. The match is very close on both occasions, which gives confidence in the shape/spin axis model.

SPIN/SHAPE MODEL FOR 1413 Roucarie

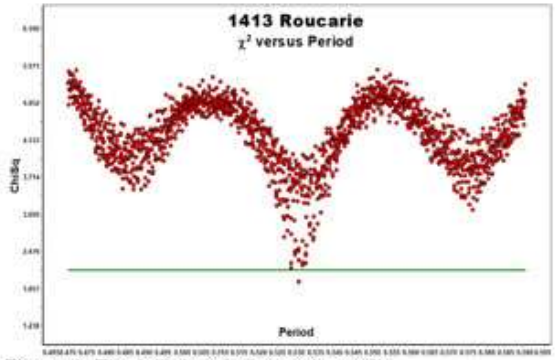

Figure 1. The initial period search results.

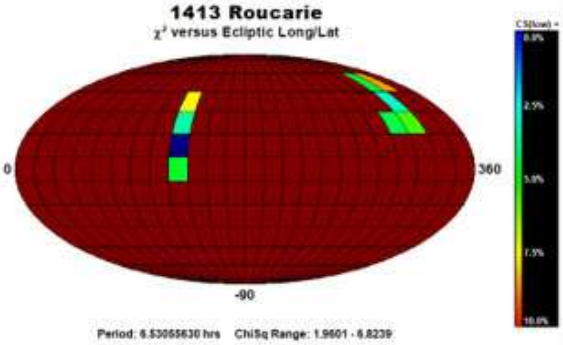

Figure 2. The pole search found two probable solutions.

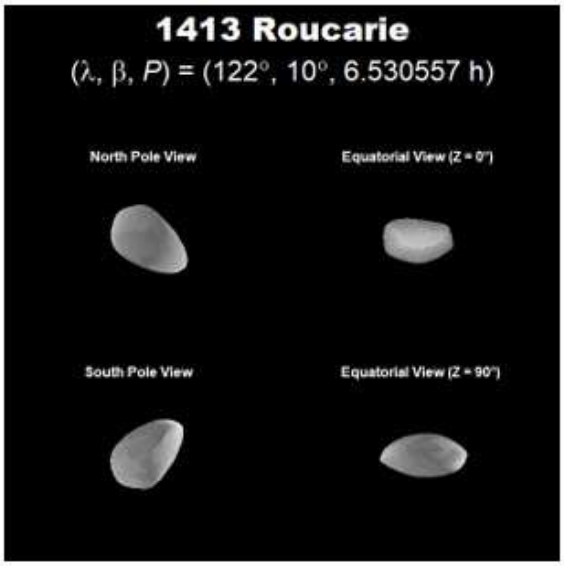

Figure 3. The shape of the asteroid based on the preferred solution.

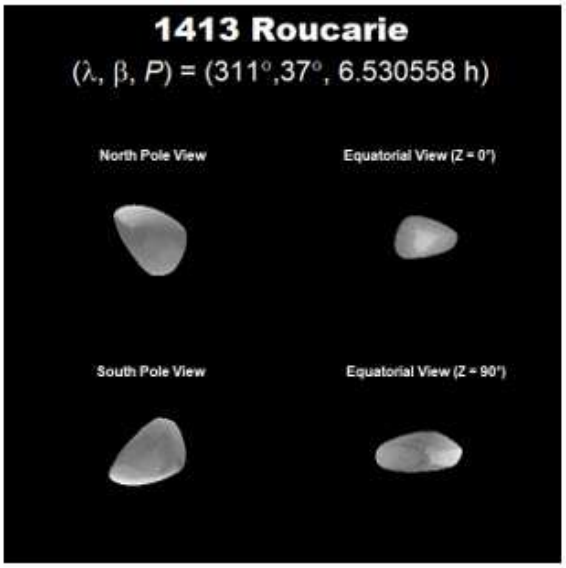

Figure 4. The shape of the asteroid based upon the secondary solution.

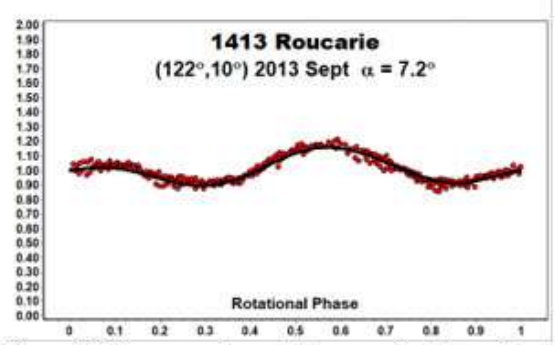

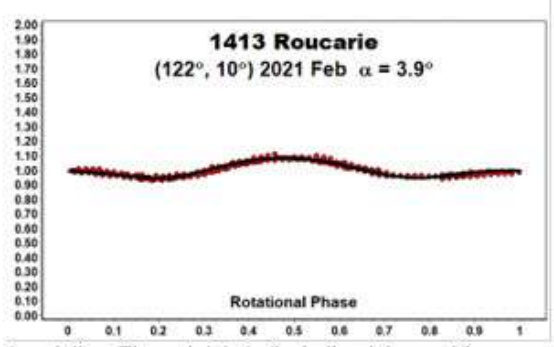

Figure 5/6. The comparison plots are against the preferred pole solution. The red dots indicate the data used for modeling while the black line is the smoothed lightcurve for generated by the shape at the time of the observations. The match is very close on both occasions, which gives confidence in the shape/spin axis model.

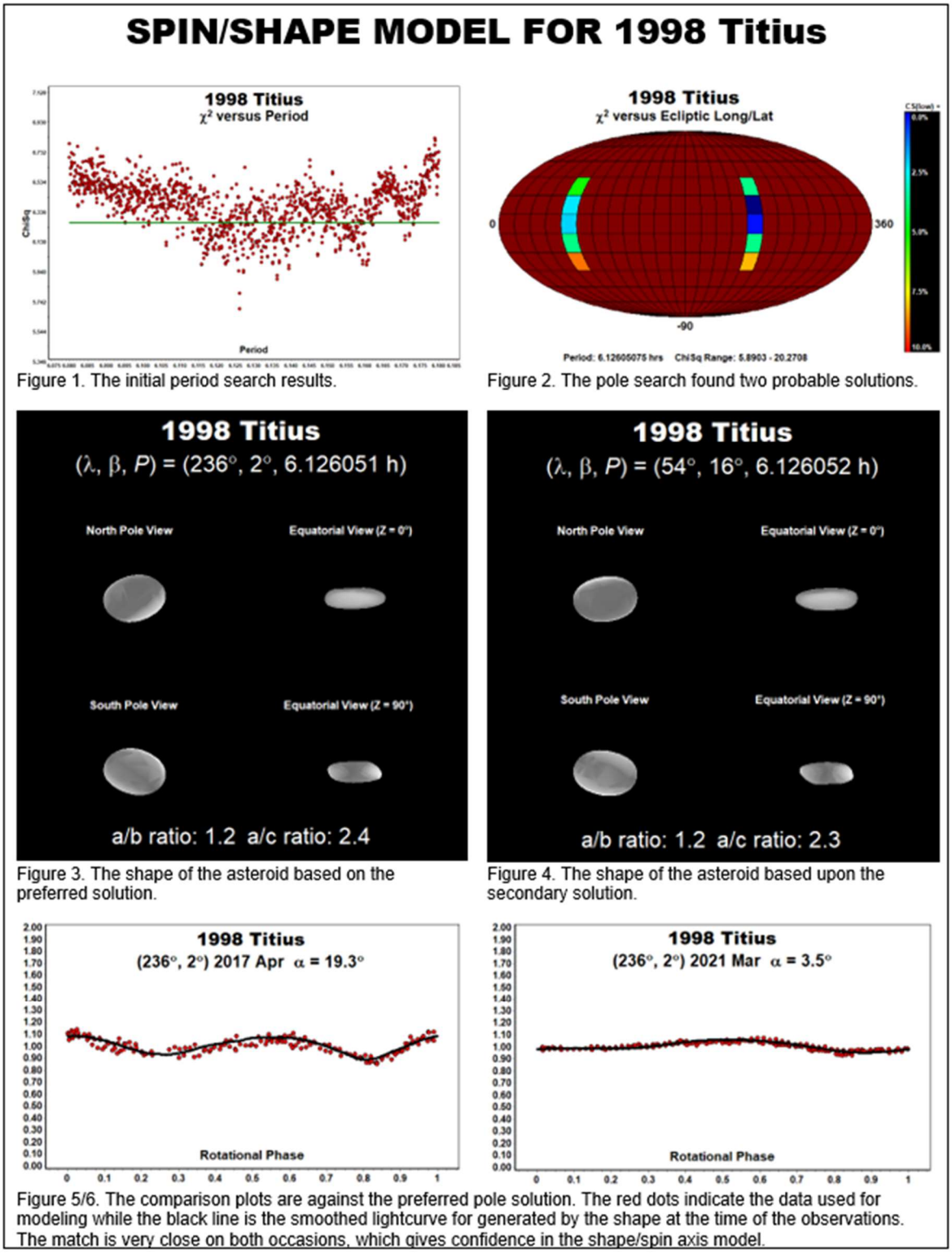

Figure 1. The initial period search results.

Figure 2. The pole search found two probable solutions.

Figure 3. The shape of the asteroid based on the preferred solution.

Figure 4. The shape of the asteroid based upon the secondary solution.

Figure 5/6. The comparison plots are against the preferred pole solution. The red dots indicate the data used for modeling while the black line is the smoothed lightcurve for generated by the shape at the time of the observations. The match is very close on both occasions, which gives confidence in the shape/spin axis model.

SPIN/SHAPE MODEL FOR 2233 Kuznetsov

Figure 1. The initial period search results.

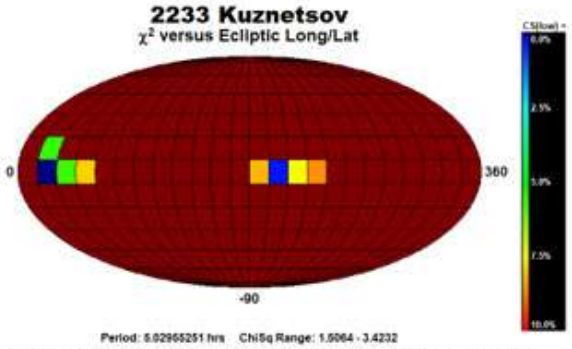

Figure 2. The pole search found two probable solutions.

Figure 3. The shape of the asteroid based on the preferred solution.

Figure 4. The shape of the asteroid based upon the secondary solution.

Figure 5/6. The comparison plots are against the preferred pole solution. The red dots indicate the data used for modeling while the black line is the smoothed lightcurve for generated by the shape at the time of the observations. The match is very close on both occasions, which gives confidence in the shape/spin axis model.

SPIN/SHAPE MODEL FOR 2511 Patterson

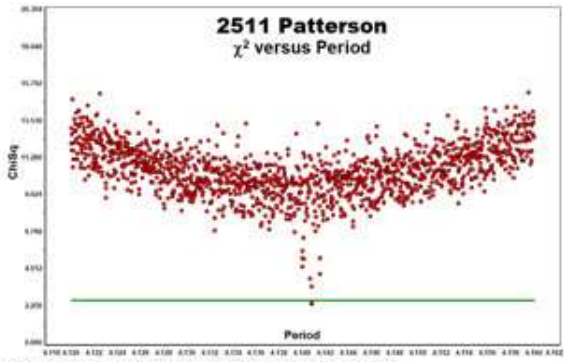

Figure 1. The initial period search results.

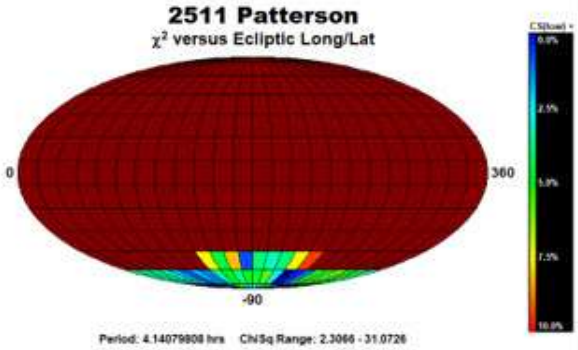

Figure 2. The pole search found two probable solutions.

Figure 3. The shape of the asteroid based on the preferred solution.

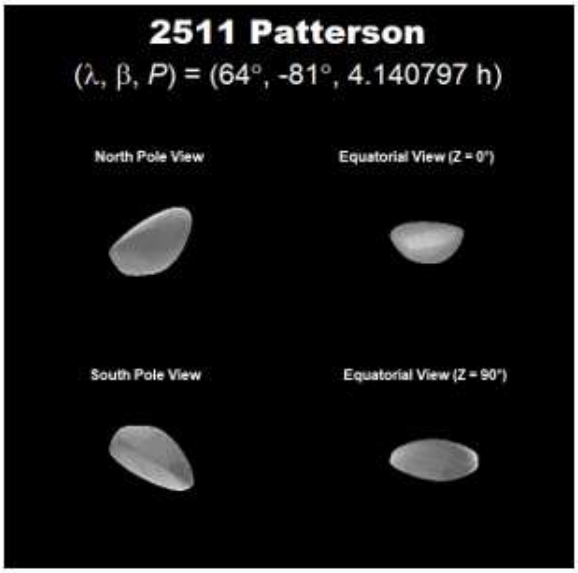

Figure 4. The shape of the asteroid based upon the secondary solution.

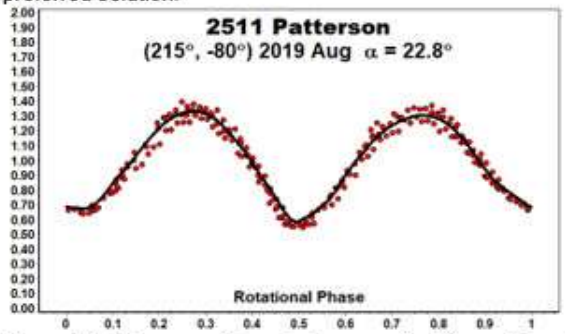

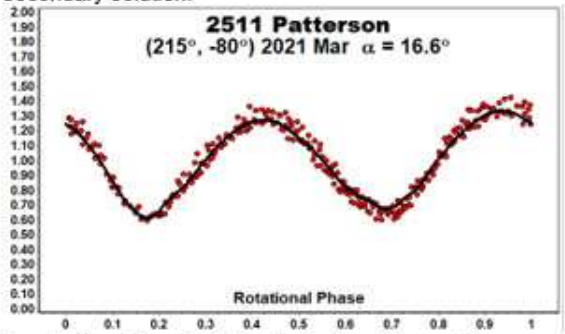

Figure 5/6. The comparison plots are against the preferred pole solution. The red dots indicate the data used for modeling while the black line is the smoothed lightcurve for generated by the shape at the time of the observations. The match is very close on both occasions, which gives confidence in the shape/spin axis model.

SPIN/SHAPE MODEL FOR 3198 Wallonia

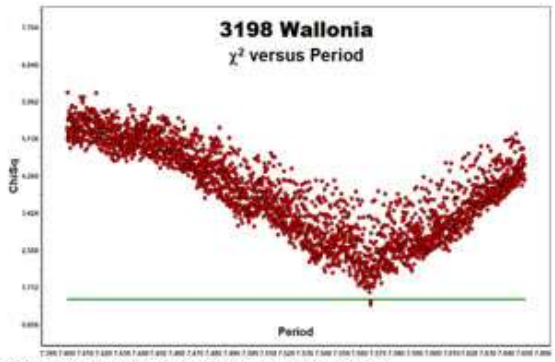

Figure 1. The initial period search results.

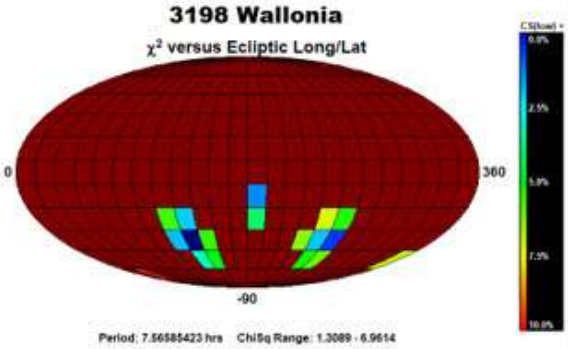

Figure 2. The pole search found two probable solutions.

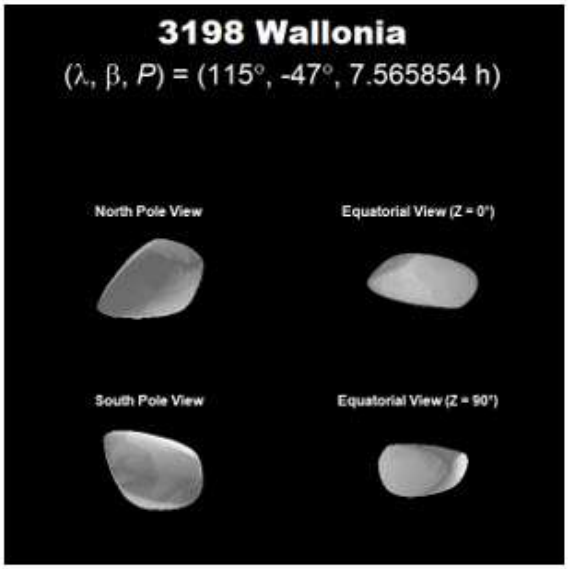

Figure 3. The shape of the asteroid based on the preferred solution.

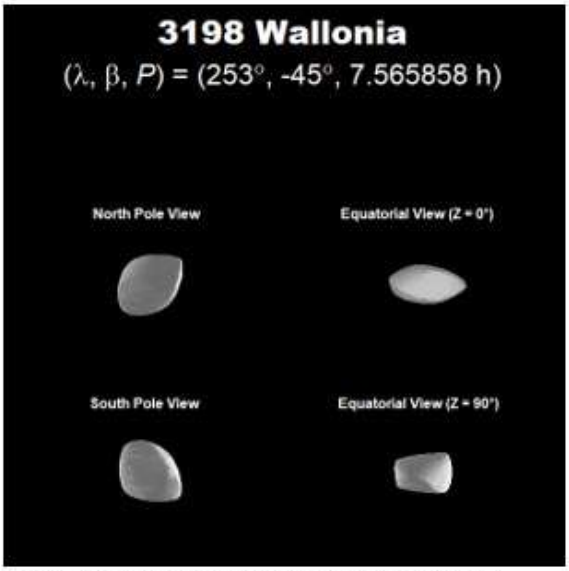

Figure 4. The shape of the asteroid based upon the secondary solution.

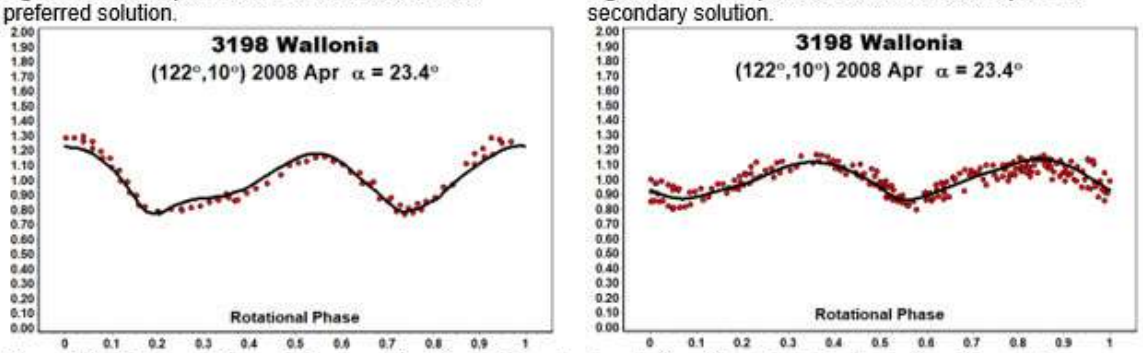

Figure 5/6. The comparison plots are against the preferred pole solution. The red dots indicate the data used for modeling while the black line is the smoothed lightcurve for generated by the shape at the time of the observations. The match is very close on both occasions, which gives confidence in the shape/spin axis model.

SPIN/SHAPE MODEL FOR 5040 Rabinowitz

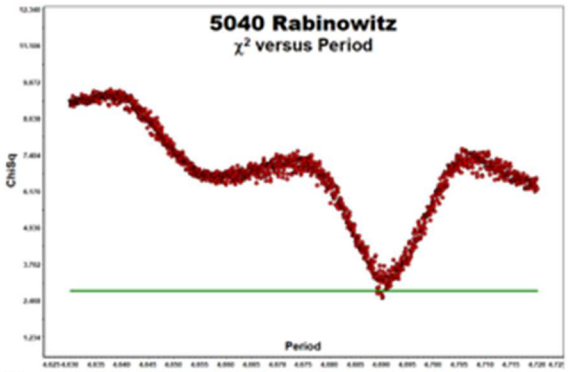

Figure 1. The initial period search results.

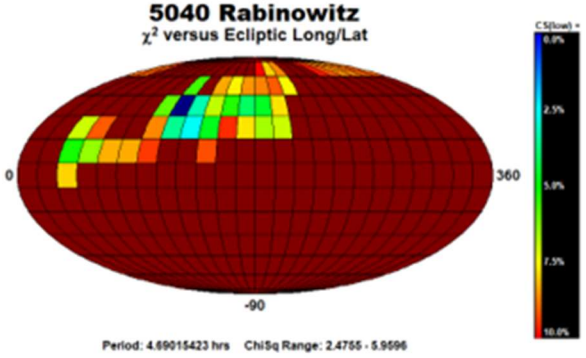

Figure 2. The pole search found two probable solutions.

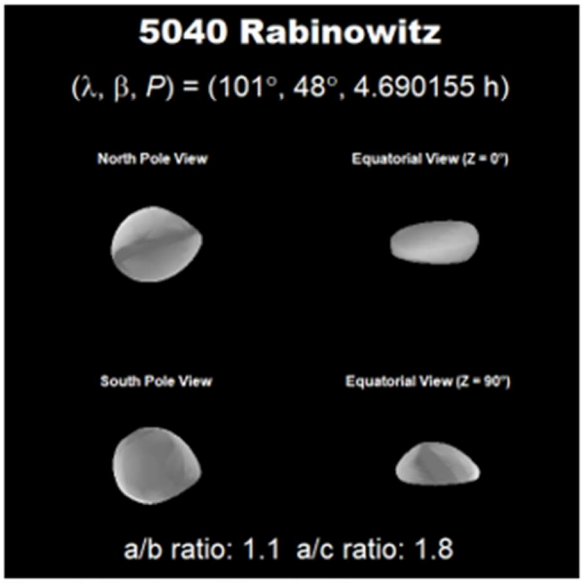

Figure 3. The shape of the asteroid.

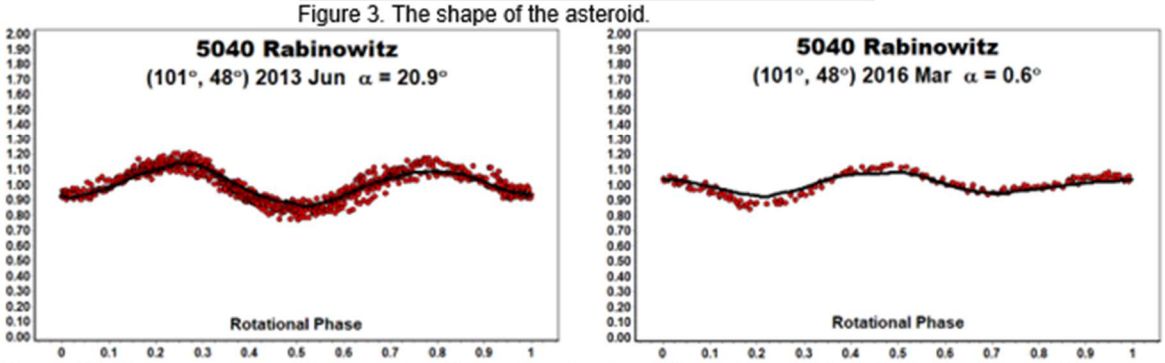

Figure 4/5. The comparison plots are against the preferred pole solution. The red dots indicate the data used for modeling while the black line is the smoothed lightcurve for generated by the shape at the time of the observations. The match is very close on both occasions, which gives confidence in the shape/spin axis model.

SPIN/SHAPE MODEL FOR 5096 Luzin

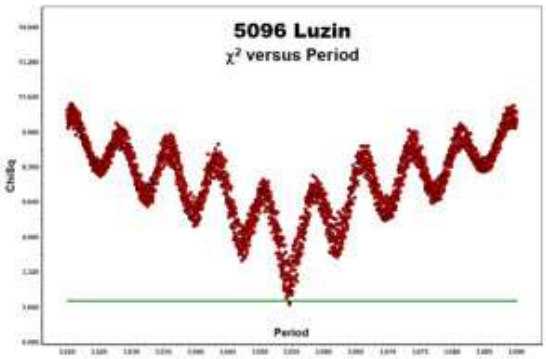

Figure 1. The initial period search results.

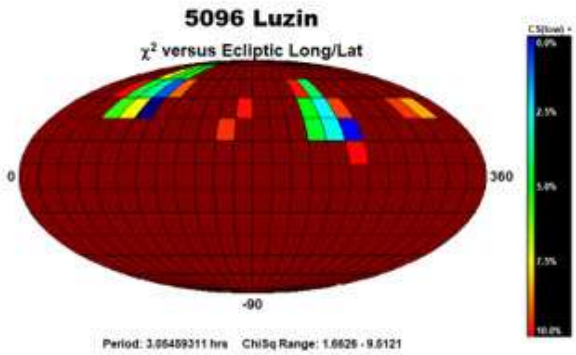

Figure 2. The pole search found two probable solutions.

Figure 3. The shape of the asteroid based on the preferred solution.

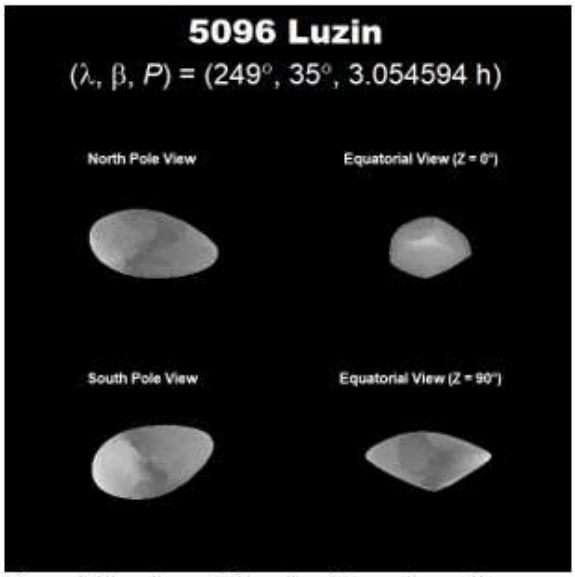

Figure 4. The shape of the asteroid based upon the secondary solution.

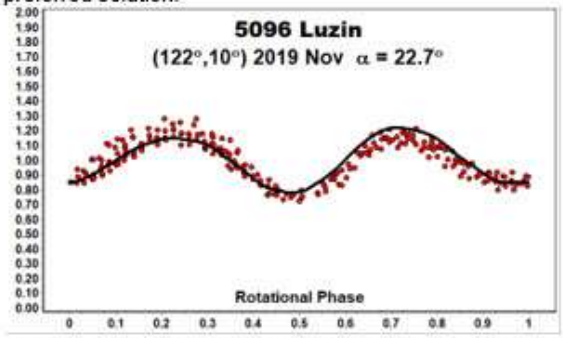

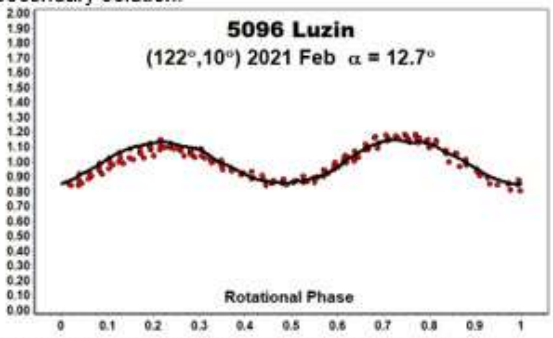

Figure 5/6. The comparison plots are against the preferred pole solution. The red dots indicate the data used for modeling while the black line is the smoothed lightcurve for generated by the shape at the time of the observations. The match is very close on both occasions, which gives confidence in the shape/spin axis model.

LIGHTCURVES AND SPIN RATES OF EARTH CO-ORBITAL ASTEROIDS

Galin Borisov
Armagh Observatory and Planetarium, College Hill, BT61 9DG
Armagh, Northern Ireland, United Kingdom
Galin.Borisov@Armagh.ac.uk

Apostolos A. Christou
Armagh Observatory and Planetarium
Armagh, Northern Ireland, United Kingdom

Stefano Bagnulo
Armagh Observatory and Planetarium
Armagh, Northern Ireland, United Kingdom

Alberto Cellino
INAF–Osservatorio Astrofisico di Torino, Turin, Italy

Aldo Dell'oro
INAF–Osservatorio Astrofisico di Arcetri, Florence, Italy

(Received: 2021 February 19, Revised: 2021 May 1)

We present photometric optical lightcurves and derived rotation periods for a sample of seven Earth co-orbital asteroids: 2008 WM64 (2.356 ± 0.033 h), 2016 AU8 (4.698 ± 0.013 h), 2000 EE104 (13.324 ± 1.135 h), 2018 EB (2.600 ± 0.437 h), 2014 KZ44 (2.797 ± 0.596 h), 2016 JP (3.288 ± 0.224 h), and 2014 KQ76 (2.953 ± 0.063 h). These observations were carried out at the Bulgarian National Astronomical Observatory - Rozhen using the FoReRo2 instrument attached on the 2mRCC telescope.

Asteroids co-orbital with the Earth - broadly defined as those with an average heliocentric distance of 1 au - present special challenges to surveys. Because of the very slow net Earth-relative motion from one revolution to the next, they can remain far from our planet and close to the Sun's location in the sky for many decades. As a result, observational completeness for this type of orbit is generally lower than for other near-Earth asteroids (Tricarico, 2017). When an object of this type is discovered, it typically offers a few brief annually-recurring apparitions when it is bright enough to allow physical characterisation. Afterwards, the accumulated Keplerian drift will place it out of reach of observational scrutiny for many decades hence.

Photometric observations of selected Earth co-orbital asteroids were carried out from the Bulgarian National Astronomical Observatory - Rozhen. We used the Focal Reducer Rozhen or "FoReRo2" instrument attached on the 2-m RCC telescope. The asteroid targets and their observational circumstances are presented in Table 1.

The data were reduced by applying standard bias and flat-field corrections followed by aperture photometry to produce the lightcurve for each object shown in Fig. 1. To determine their periods and amplitudes, we fit the lightcurves from single or multiple nights to Fourier series of different orders, typically between 3 and 5, using Levenberg-Marquardt nonlinear least-squares minimisation (Press et al., 1992) and assuming a double-peaked lightcurve. Zero-point offsets for different nights and different filters were included as free parameters in the fit to allow us to adjust more precisely the different parts of the lightcurves and determine more accurately the amplitude. A refined period search was then performed over a narrow range around the initial solution to estimate more accurately the period. In the following, we present an object-by-object analysis of our photometric data.

(418849) 2008 WM64 (H=20.6) is an Apollo asteroid. It has a previously published rotation period of P=2.40 ± 0.02 h (Rowe, 2018; Warner, 2018a). Our analysis of the new observations shows a period of P=2.356 ± 0.033 h, consistent with the previous estimate given the statistical uncertainty. The $\chi 2$ period search clearly shows only one minimum suggesting a unique period solution from our data.

(512245) 2016 AU8 (H=19.9) is an Aten asteroid with a previously published rotation period of P=4.516 ± 0.002 h (Warner and Stephens, 2019a). Our analysis of the new observations yields a period of P=4.698 ± 0.013 h. The new solution has a small uncertainty even though it is based on partial lightcurve coverage and is slightly longer than the previous estimate. The $\chi 2$ period search shows only one minimum which again suggests a unique period solution.

(138175) 2000 EE104 (H=20.4) is an Apollo asteroid suspected to have boulders with diameters of larger than 10 m distributed along its orbit (Lai et al., 2017). Jewitt (2020) finds no evidence for co-moving companions or a dust particle trail and report a B-V colour of 1.16 ± 0.04 which they interpret as intermediate between C-class and S-class asteroids. The mean B-R colour is consistent with that measured for Jovian Trojan and D-type asteroids. Asteroids can shed material from their surface and onto heliocentric orbit if they rotate once every few hours or faster (Pravec et al., 2010; Jacobson and Scheeres, 2011). Here we obtained a rotational period of P=13.324 ± 1.135 h using data from 3 observing nights in 2018 and 2019. We employed the period search routine within the DAMIT software package (Durech et al., 2010) to combine observations from the different nights taking into account the mutual positions of the Sun, the Earth and the object for each individual measurement. The obtained period for this object is quite slow and far from the spin-barrier (Pravec and Harris, 2000), and it is therefore unlikely that spin-induced mass shedding due to the asteroid's present rotational state is responsible for any existing orbit-sharing material.

Number	Name	yyyy mm/dd	Phase	L_{PAB}	B_{PAB}	Period(h)	P.E.	Amp	A.E.	Grp
418849	2008 WM64	2017 12/25	36.9	96	19	2.356	0.033	0.62	-	APO
512245	2016 AU8	2018 01/19	42.5	90	6	4.698	0.013	0.39	-	ATE
138175	2000 EE104	2018 11/09	66.3	100	8	-	-	-	-	APO
138175	2000 EE104	2019 01/01	19.5	108	14	-	-	-	-	APO
138175	2000 EE104	2020 01/02	17.9	104	14	13.324	1.135	0.82	-	APO
	2018 EB	2018 10/06	75.6	52	-10	2.600	0.437	-	-	APO
468909	2014 KZ44	2019 05/30	47.0	254	43	2.797	0.596	-	-	ATE
522684	2016 JP	2020 04/25,27	53.3	240	21	3.288	0.224	0.23	-	ATE
468910	2014 KQ76	2020 04/25	44.7	228	25	2.953	0.063	0.12	-	APO

Table I. Observing circumstances and results. The phase angle is given for the first date. L_{PAB} and B_{PAB} are the approximate phase angle bisector longitude/latitude at mid-date range (see Harris et al., 1984). **Grp** is the asteroid family/group (APO-Apollo, ATE-Aten).

2018 EB (H=21.9) is an Apollo asteroid. It has a previously published rotation period of P=3.16 ± 0.01 h (Warner and Stephens, 2019b). Our analysis of the new observed lightcurve shows a period of P=2.600 ± 0.437 h. This is based on partial lightcurve coverage which, together with the large scatter in the data, is responsible for the relatively high uncertainty. Nevertheless, the $\chi 2$ period search shows only one deep minimum which suggests a unique solution for the period.

(468909) 2014 KZ44 (H=20.4) is an Aten asteroid with no previously published rotation period. Our analysis of the new photometric data shows a period of P=2.797 ± 0.596 h. The large uncertainly is due to high photometric scatter as well as less-than-full lightcurve coverage. Its $\chi 2$ period search shows one single-peaked solution but a poorly-defined double-peaked solution. Here we present the double-peaked lightcurve obtained from the Fourier fitting routine.

(522684) 2016 JP (H=21.1) is a small Aten-class asteroid. There are two series of observations published previously which yielded quite different rotation periods. The first photometric observations suggested a very long period of 37.4 ± 0.1h (Warner, 2018b) but more recent observations (Pravec, 2019) yield a much shorter period, 3.2905 ± 0.0003h. Our observations show a period of P=3.288 ± 0.224h thus strongly supporting the latter estimate. The $\chi 2$ period search shows multiple minima between values of 3 and 5 h. We chose the optimal solution by visual inspection of all individual lightcurves with different period solutions and by using as criteria the better overlapping of the different nights for a double-peaked lightcurve.

(468910) 2014 KQ76 (H=21.5) is an Apollo asteroid. It has no previously published rotation period. Our analysis of the new observations shows a period of P=2.953 ± 0.063 h. The $\chi 2$ period search shows only one deep minimum which suggests a unique solution from our data.

Acknowledgements

This work was supported via grant ST/R000573/1 from the UK Science and Technology Facilities Council. The authors gratefully acknowledge observing grant support from the Institute of Astronomy and National Astronomical Observatory, Bulgarian Academy of Sciences. Astronomical research at the Armagh Observatory and Planetarium is grant-aided by the Northern Ireland Department for Communities (DfC). The authors also acknowledge DfC for the FoReRo2 instrument development contribution from the Armagh Observatory & Planetarium toward the new CCD camera Andor iKon-L used in this study.

References

Durech, J.; Sidorin, V.; Kaasalainen, M. (2010). "DAMIT: a database of asteroid models." *A&A* **513**, A46.

Harris, A.W.; Young, J.W.; Scaltriti, F.; Zappala, V. (1984). "Lightcurves and phase relations of the asteroids 82 Alkmene and 444 Gyptis." *Icarus* **57**, 251-258.

Jacobson, S.A.; Scheeres, D.J. (2011). "Dynamics of rotationally fissioned asteroids: Source of observed small asteroid systems." *Icarus* **214**, 161-178.

Jewitt, D. (2020). "138175 (2000 EE104) and the source of interplanetary field enhancements." *The Planetary Science Journal* **1**, 33.

Lai, H.R.; Russell, C.T.; Wei, H.Y.; Connors, M.; Delzanno, G.L. (2017). "Possible potentially threatening co-orbiting material of asteroid 2000EE104 identified through interplanetary magnetic field disturbances." *Meteoritics and Planetary Science* **52**, 1125-1132.

Pravec, P.; Harris, A.W. (2000). "Fast and slow rotation of asteroids." *Icarus* **148**, 12-20.

Pravec, P. and 25 colleagues (2010). "Formation of asteroid pairs by rotational fission." *Nature* **466**, 1085-1088.

Pravec, P. (04.06.2019). Ondrejov Asteroid Photometry Project. *http://www.asu.cas.cz/~ppravec/newres.txt*

Press, W.H.; Teukolsky, S.A.; Vetterling, W.T.; Flannery, B.P. (1992). "Nonlinear Models." In *Numerical recipes in C. The art of scientific computing*, 681–688. Cambridge University Press, New York.

Rowe, B. (2018). *Minor Planet Bull.* **45**, 292-294.

Tricarico, P. (2017). "The Near-Earth asteroid population from two decades of observations." *Icarus* **284**, 416–423.

Warner, B.D. (2018a). *Minor Planet Bull.* **45**, 138-147.

Warner, B.D. (2018b). *Minor Planet Bull.* **45**, 366-379.

Warner, B.D.; Stephens, R.D. (2019a). *Minor Planet Bull.* **46**, 144-152.

Warner, B.D.; Stephens, R.D. (2019b). *Minor Planet Bull.* **46**, 423-438.

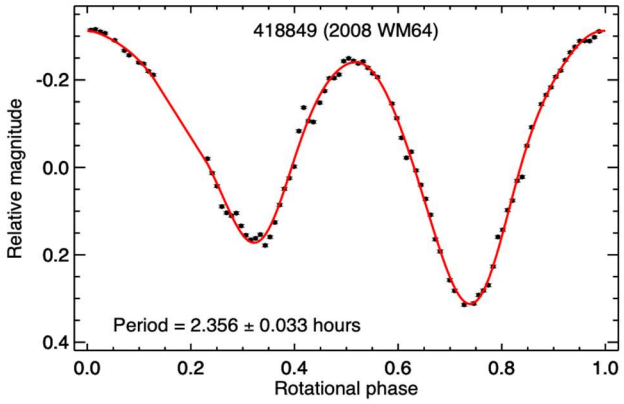
418849 (2008 WM64)
Relative magnitude
Rotational phase
Period = 2.356 ± 0.033 hours

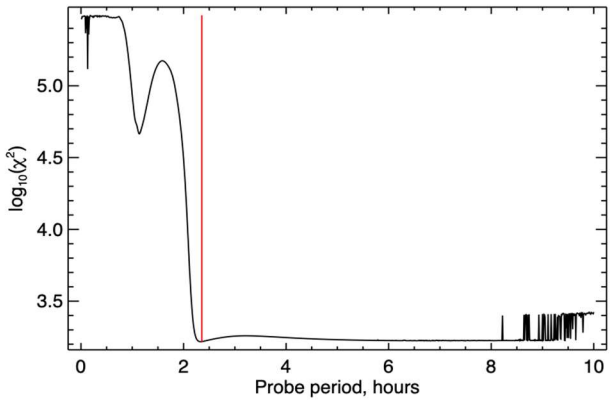
log10(χ2)
Probe period, hours

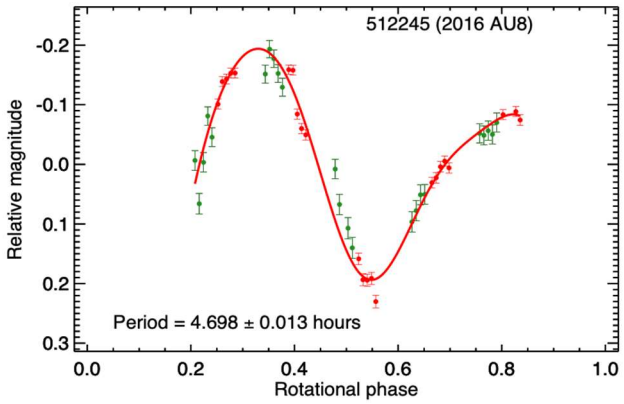
512245 (2016 AU8)
Relative magnitude
Rotational phase
Period = 4.698 ± 0.013 hours

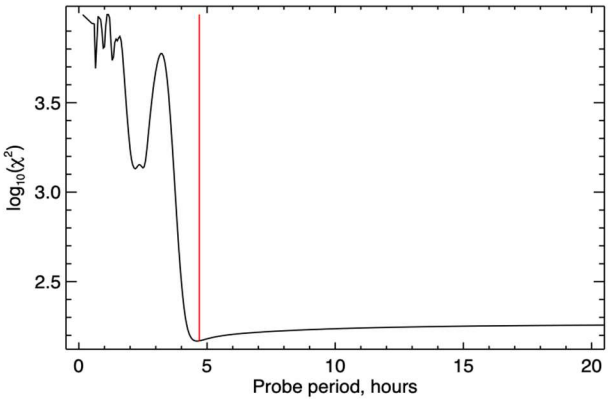
log10(χ2)
Probe period, hours

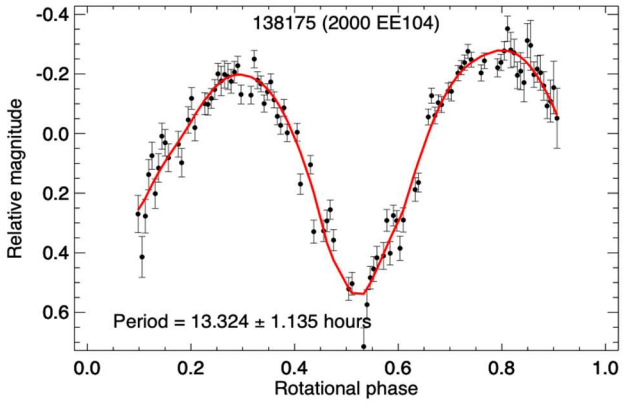
138175 (2000 EE104)
Relative magnitude
Rotational phase
Period = 13.324 ± 1.135 hours

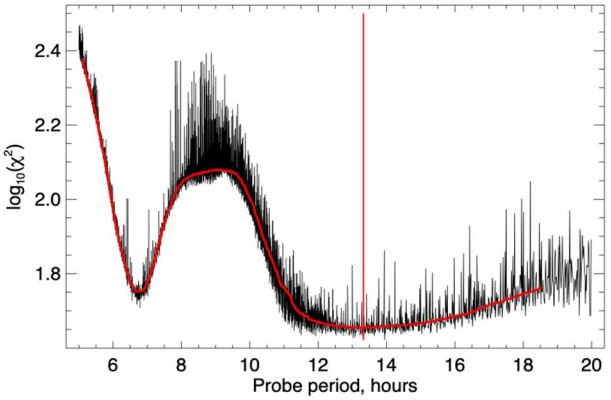
log10(χ2)
Probe period, hours

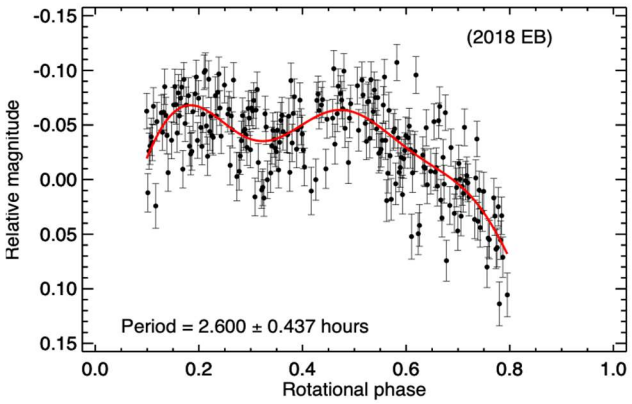
(2018 EB)
Relative magnitude
Rotational phase
Period = 2.600 ± 0.437 hours

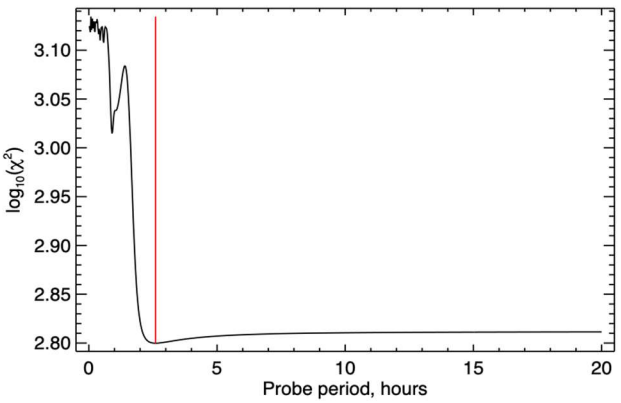
log10(χ2)
Probe period, hours

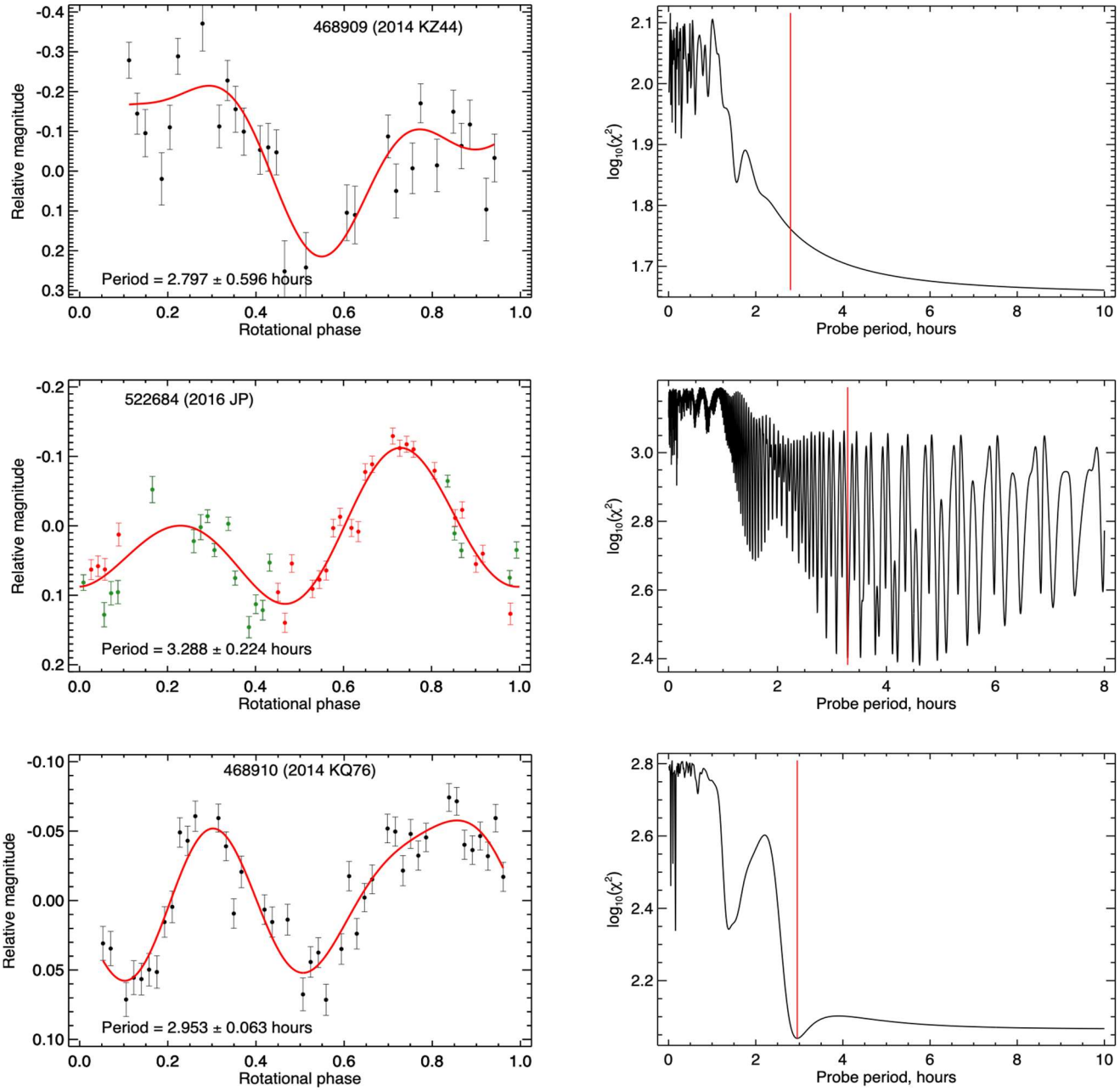

Figure 1: ***The left column*** presents the lightcurves of observed Earth co-orbitals asteroids. Different colours represent data obtained on different nights except for 2016 AU8 where they represent different filters - Sloan g′ and r′. The Fourier fit is presented with a red line. For 2000 EE104 we present the observations only for one night (2020 01/02) with the fit computed using all 3 nights. ***The right column*** presents the χ^2 period search. The preferred solution is marked with a vertical red line. For 2000 EE104 we did running average smoothing and found the global minimum of the χ^2 hence the solution of the period.

1803 ZWICKY
A CONFIRMED BINARY ASTEROID

Tom Polakis
Command Module Observatory
121 W. Alameda Dr.
Tempe, AZ 85282
tpolakis@cox.net

Robert D. Stephens
Center for Solar System Studies / MoreData!
Rancho Cucamonga, CA 91730

(Received: 2021 March 25, Revised: 2021 May 1)

Observations made from February through March 2021 led to the discovery that 1803 Zwicky is an asynchronous binary system. The primary body has a rotation period of 2.7329 ± 0.0002 h, and the orbital period is 28.46 ± 0.02 h. The small lightcurve amplitude suggests a spherical shape. From the mutual event depths we infer a minimum secondary-to-primary mean diameter ratio of 0.26 ± 0.02.

During the course of CCD photometric observations of 21 main-belt minor planets from 2020 December through 2021 March, 1803 Zwicky stood out with data points that departed from a typical rotational phased lightcurve. An inspection of a raw lightcurve from TESS satellite data published by Pal et al. (2020) showed periodic sharp drops in brightness. This led to four additional nights of observations, during which the asteroid's binary nature was confirmed, and rotation and revolution periods computed.

Observations were performed at Command Module Observatory (MPC V02) in Tempe, AZ and the Center for Solar System Studies (MPC U81) in California. Images were taken at V02 using a 0.32-m f/6.7 Modified Dall-Kirkham telescope, SBIG STXL-6303 CCD camera, and a 'clear' glass filter. Exposure time for all the images was 2 minutes. The image scale after 2×2 binning was 1.76 arcsec/pixel. Images at U81 were taken with a 0.40-m f/10 Schmidt-Cassegrain telescope and FLI Proline 1001 camera, also with a clear filter. Those frames have an image scale of 1.22 arcsec/pixel.

Table I shows the observing circumstances and results.

The data reduction and period analysis were done using *MPO Canopus* (Warner, 2020). For each set of images, the asteroid and five comparison stars were measured. Comparison stars were selected with colors within the range of 0.5 < B-V < 0.95 to correspond with color ranges of asteroids. *MPO Canopus* plots instrumental vs. catalog magnitudes for solar-colored stars, which is useful for selecting comp stars of suitable color and brightness.

Clear-filtered images were reduced to Sloan r′ to minimize error with respect to a color term. Comparison star magnitudes were obtained from the ATLAS catalog (Tonry et al., 2018), which is incorporated directly into *MPO Canopus*. The ATLAS catalog derives Sloan griz magnitudes using a number of available catalogs. The consistency of the ATLAS comp star magnitudes and color-indices allowed the separate nightly runs to be linked with no zero-point offset.

It was typically necessary to employ star subtraction to remove contamination by field stars. Initial period determination was done using the *MPO Canopus* Fourier-type FALC fitting method (cf. Harris et al., 1989). Magnitudes in these plots are apparent and scaled by MPO Canopus to the first night. After reaching a satisfactory rotation and orbit solution, data files were sent to Petr Pravec, who refined the results.

The Asteroid Lightcurve Database (LCDB; Warner et al., 2009) was consulted to locate previously published results. New data for this asteroid can be found in the ALCDEF database.

1803 Zwicky was discovered by Paul Wild at Zimmerwald in 1967. This Phocaea-family asteroid has a high eccentricity of 0.247, and a large inclination of 22º. The only period in the LCDB is that of Pal et al. (2020), 2.73364 ± 0.00005 h. A simple period analysis using V02 data from 2021 February 21 through 24 yielded a rotation period of 2.732 ± 0.001 h. Data points from February 22 showed a troublesome departure from the lightcurve that could not be explained by any data-gathering anomalies.

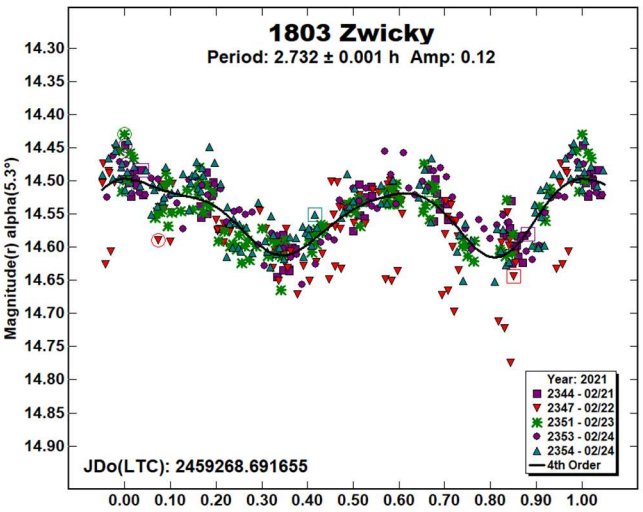

The raw lightcurve for 1803 Zwicky provided with the Pal et al. (2020) paper revealed deep, evenly spaced minima overlaid on a shorter cycle with smaller amplitude.

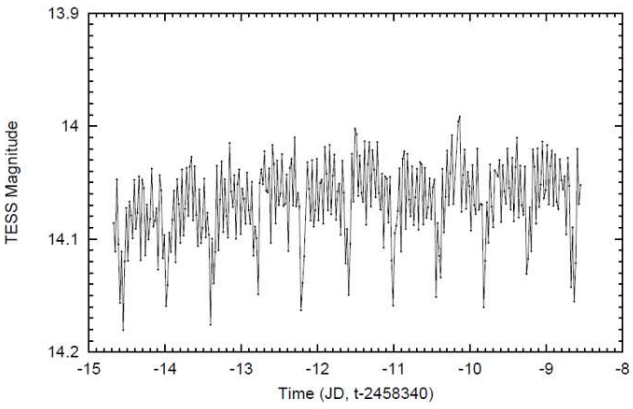

Their phased lightcurve also features data points displaced downward that mimic the rotational lightcurve.

Number	Name	yy/mm/dd	Phase	L_{PAB}	B_{PAB}	Period(h)	P.E.	Amp	A.E.	Grp
1803	Zwicky	21/02/21-03/04	5.3,10.9	145	4	2.7329	0.0002	0.14	0.01	MB-O
						28.46	0.02	0.14	0.01	

Table I. Observing circumstances and results. Period is rotation and orbital for each body. The first line gives the primary period for the system. The second line gives the secondary period. The phase angle is given for the first and last date. If preceded by an asterisk, the phase angle reached an extrema during the period. L_{PAB} and B_{PAB} are the approximate phase angle bisector longitude/latitude at mid-date range (see Harris et al., 1984). Grp is the asteroid family/group (Warner et al., 2009).

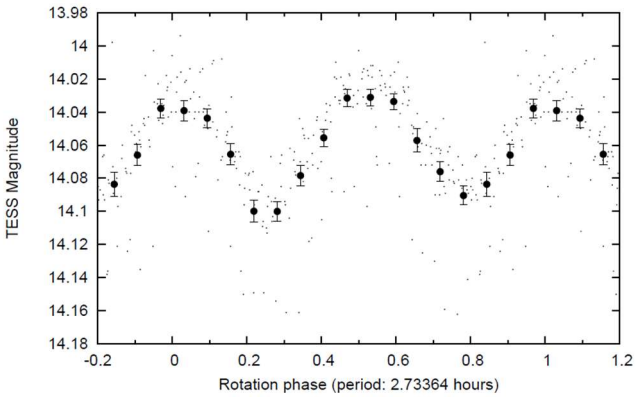

Additional dense photometric data was taken at V02 during three full nights from 2021 March 1 through 3, and at U81 on March 4. All of the data was sent to Petr Pravec, who determined the rotation period of 2.7329 +/- 0.0002 h for the primary body and orbital period of 28.46 ± 0.02 h for the secondary. Mutual event depths are 0.07 and 0.14 mag., suggesting a minimum secondary-to-primary mean diameter ratio of 0.26. Phased lightcurves for rotation and orbital periods are shown.

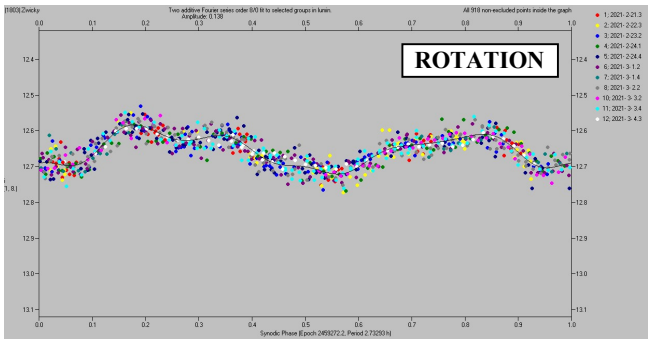

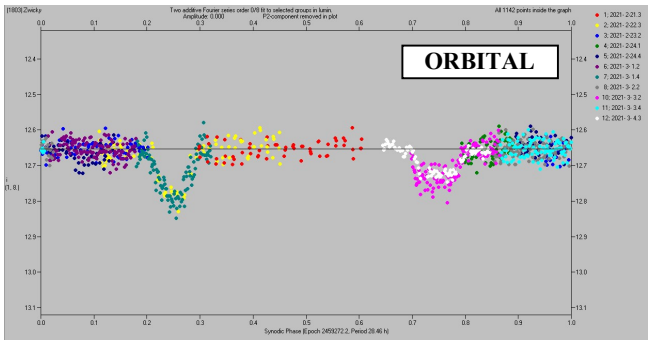

Acknowledgements

The author would like to express his gratitude to Petr Pravec for his indispensable data reduction effort. Thanks also go out to Brian Warner for his helpful advice relating to binary asteroids and support of his MPO Canopus software package.

References

Harris, A.W.; Young, J.W.; Scaltriti, F.; Zappala, V. (1984). "Lightcurves and phase relations of the asteroids 82 Alkmene and 444 Gyptis." *Icarus* **57**, 251-258.

Harris, A.W.; Young, J.W.; Bowell, E.; Martin, L.J.; Millis, R.L.; Poutanen, M.; Scaltriti, F.; Zappala, V.; Schober, H.J.; Debehogne, H.; Zeigler, K.W. (1989). "Photoelectric Observations of Asteroids 3, 24, 60, 261, and 863." *Icarus* **77**, 171-186.

Pal, A.; Szakáts, R.; Kiss, C.; Bódi, A.; Bognár, Z.; Kalup, C.; Kiss, L.L.; Marton, G.; Molnár, L.; Plachy, E.; Sárneczky, K.; Szabó, G.M.; Szabó, R. (2020). "Solar System Objects Observed with TESS - First Data Release: Bright Main-belt and Trojan Asteroids from the Southern Survey." *Ap. J. Supl. Ser.* **247**, 26-34.

Tonry, J.L., Denneau, L., Flewelling, H., Heinze, A.N., and five additional co-authors. (2018). "The ATLAS all-sky stellar reference catalog." *Astrophys. J.* **867**, 105.

Warner, B.D.; Harris, A.W.; Pravec, P. (2009). "The Asteroid Lightcurve Database." *Icarus* **202**, 134-146. Updated 2020 Aug. *http://www.minorplanet.info/lightcurvedatabase.html*

Warner. B.D. (2020). *MPO Canopus* software. *http://bdwpublishing.com*

ON CONFIRMED AND SUSPECTED BINARY ASTEROIDS OBSERVED AT THE CENTER FOR SOLAR SYSTEM STUDIES

Brian D. Warner
Center for Solar System Studies / MoreData!
446 Sycamore Ave.
Eaton, CO 80615 USA
brian@MinorPlanetObserver.com

Robert D. Stephens
Center for Solar System Studies / MoreData!
Rancho Cucamonga, CA 91730

Daniel R. Coley
Center for Solar System Studies
Corona, CA

(Received: 2021 April 8)

Using data from observations made at the Center for Solar System Studies from 2021 January through March along with recovered legacy data, we report on the analysis of confirmed and suspected binary asteroids 2419 Moldavia, 2873 Binzel, 3561 Devine, 4383 Suruga, 4666 Dietz, 16525 Shumarinaiko, (88188) 2000 XH44, (416694) 2004 YR32, and 1999 RM45.

Data from CCD photometric observations made at the Center for Solar System Studies in 2021 January through March along with legacy data recovered following a hard drive failure were used to look for indications of an asteroid being binary. Confirmed binaries are those that show mutual events (occultations/eclipses) while suspected binaries include those with two periods, no obvious mutual events, and periods consistent with binary asteroids (Pravec et al., 2018, Figure 14).

Table I lists the telescopes and CCD cameras that were combined to make the observations. All the cameras use CCD chips from the KAF blue-enhanced family and so have essentially the same response. The pixel scales ranged from 1.24-1.60 arcsec/pixel.

Telescopes	Cameras
0.30-m f/6.3 Schmidt-Cass	SBIG STL-1001E
0.35-m f/9.1 Schmidt-Cass	FLI Microline 1001E
0.35-m f/9.1 Schmidt-Cass	FLI Microline 1001E
0.35-m f/9.1 Schmidt-Cass	FLI Microline 1001E
0.35-m f/10 Schmidt-Cass	SBIG STL-1001E
0.35-m f/10 Schmidt-Cass	FLI Proline 1001E
0.40-m f/10 Schmidt-Cass	FLI Proline 1001E
0.40-m f/10 Schmidt-Cass	FLI Proline 1001E
0.50-m f/8.1 Ritchey-Chrétien	FLI Proline 1001E

Table I. List of available telescopes and CCD cameras at CS3. The exact combination for each telescope/camera pair can vary due to maintenance or specific needs.

All lightcurve observations were unfiltered since a clear filter can cause a 0.1-0.3 mag loss. The exposure duration varied depending on the asteroid's brightness and sky motion. Guiding on a field star sometimes resulted in a trailed image for the asteroid.

Measurements were made using *MPO Canopus*. The Comp Star Selector utility in *MPO Canopus* found up to five comparison stars of near solar-color for differential photometry. To reduce the number of adjusted nightly zero points and their amounts, the analysis of the 2021 data used the ATLAS catalog r´ (SR) magnitudes (Tonry et al., 2018). The rare zero-point adjustments ≥ ±0.03 mag may be related in part to using unfiltered observations, poor centroiding of the reference stars, not correcting for second-order extinction, or selecting a star that is an unresolved pair.

The Y-axis shows the catalog ("sky") magnitudes for the "primary" period (P_1) while the "secondary" (P_2) plots give the differential from the average magnitude in the P_1 plot. "SR" indicates that the ATLAS catalog was used. "V" or "R" came from other catalogs, e.g., APASS (Henden et al., 2009) or MPOSC3 that converted 2MASS J-K to BVRI (Warner, 2007).

The two values in the parentheses are the phase angle (a) and the value of *G* used to normalize the data to the comparison stars used in the earliest session as well as the mid-date/time of that session. Ideally, this leaves any variations due only to the asteroid's rotation and/or albedo changes. The X-axis shows rotational phase from -0.05 to 1.05. If the plot includes the amplitude, e.g., "Amp: 0.65", this is the amplitude of the Fourier model curve and *not necessarily the adopted amplitude for the lightcurve*.

From here on, "LCDB" refers to the asteroid lightcurve database (Warner et al., 2009).

2419 Moldavia (Flora). Birlan et al. (1996) found a period of 2.412 h. Our data from 2020/21 found a very similar period for a primary period derived from a dual-period search in *MPO Canopus*. We also found a secondary period of 10.154 h. The LCDB includes three confirmed binaries with $10.5 \le P_{ORB} \le 11$ h. If confirmed, this would be the shortest orbital period and, to be consistent with Pravec et al. (2018), have the satellite diameter be $Ds < 0.3Dp$.

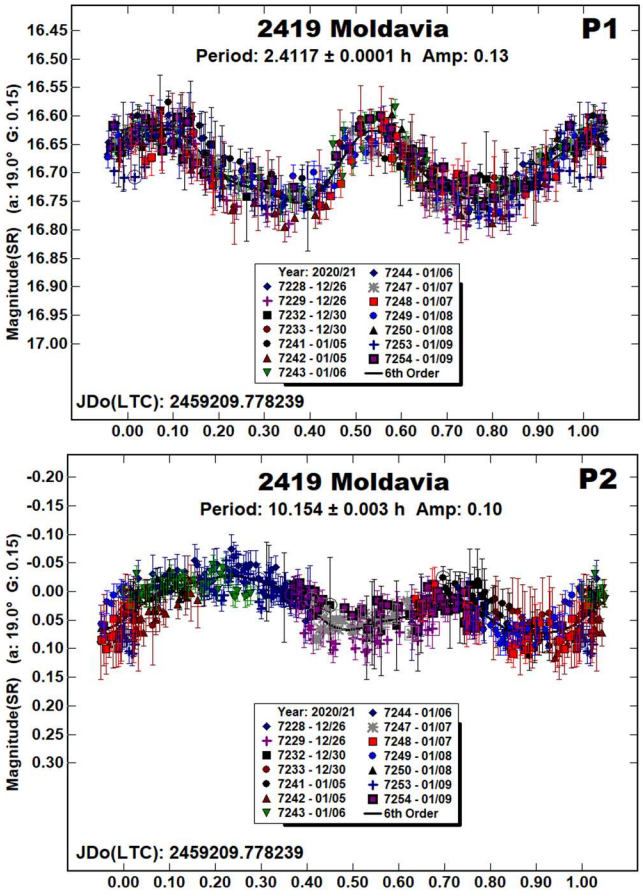

2873 Binzel. Vachier et al. (2019) discovered this Flora asteroid to be binary, finding P_1 = 2.70371 h and P_{ORB} = 44.58 h. The estimated the effective diameters ratio to be $Ds/Dp \geq 0.25$. We were able to recover data obtained in 2013. There dataset was insufficient to confirm the Vachier et al. results. The two plots show the data forced to those earlier results. From the nearly flat P_2 plot, it appears that the asteroid was out of *eclipse season*.

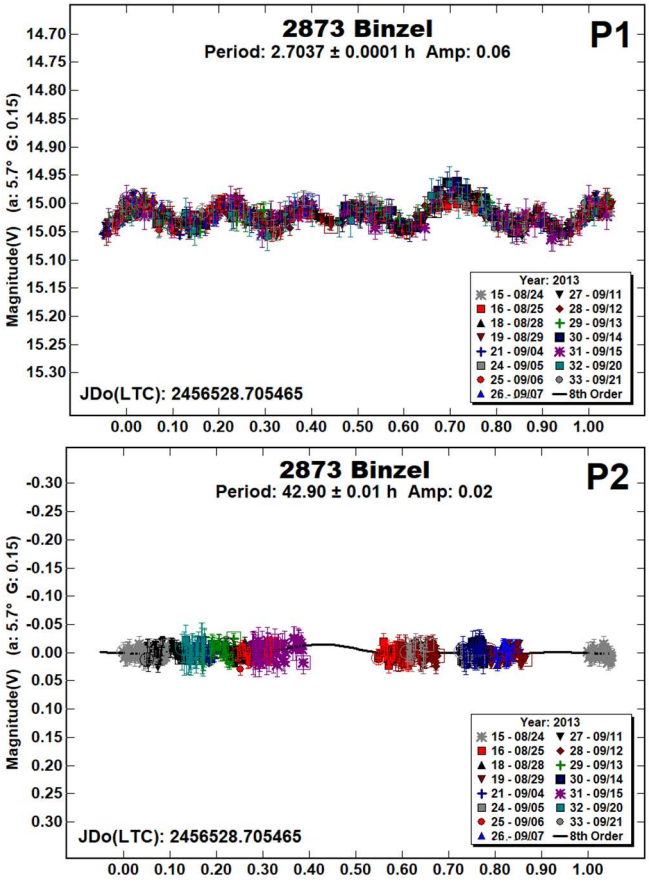

3561 Devine. Binzel et al. (1992) reported a period of 2.81 h for this Hilda asteroid. Analysis of our 2021 data initially found a period near 40 h. Using this as the initial value in a dual-period search, we eventually found a somewhat weak, but obvious, shorter period component with a lightcurve amplitude of 0.05 mag. Given the absence of mutual events, our conclusion is that P_2 = 39.20 h is most likely the orbital period of an elongated satellite (a/b ~ 1.18:1).

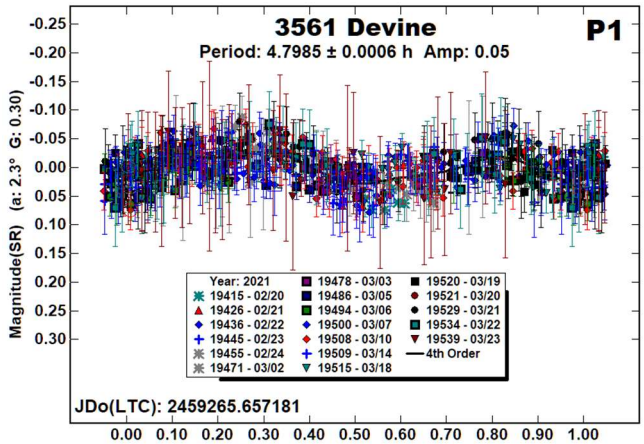

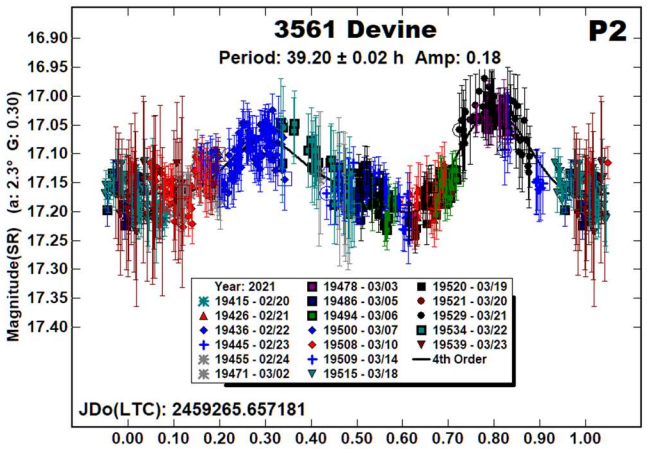

4383 Suruga. Warner (2013) first reported the binary status of this asteroid, finding P_1 = 3.4069 h and P_{ORB} = 16.386 h. The diameters ratio was $Ds/Dp \geq 0.22$. The extracted legacy data from 2015 confirms the initial results, including the size ratio.

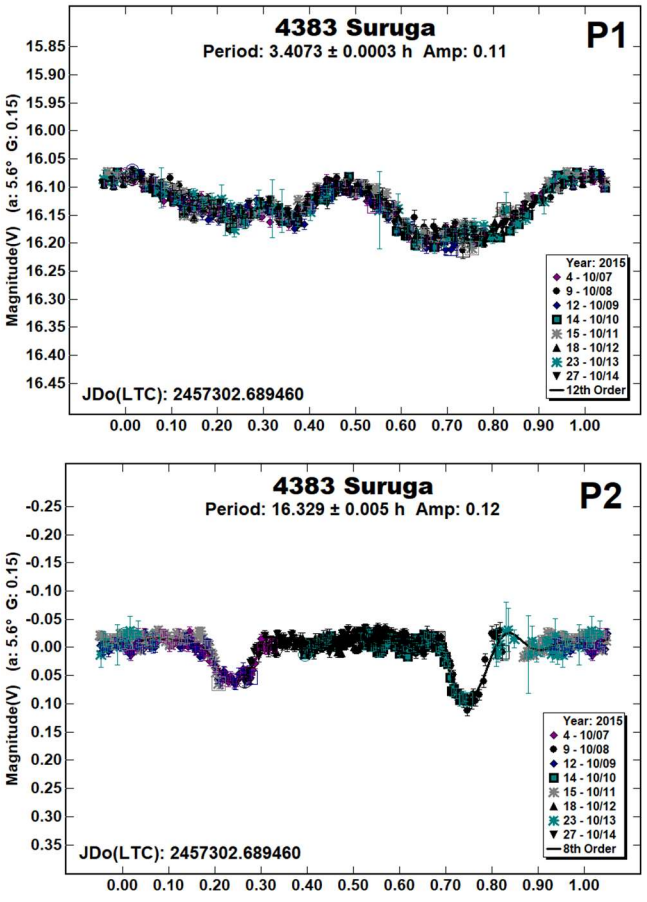

4666 Dietz. There are several entries in the LCDB giving a primary (or sole period if not said to be binary) close to 2.95 h (e.g., Behrend, 2011web, 2.9528 h; Pravec et al., 2011web, 2.95184 h). From observations in 2015, Pravec et al. (2015web) suspected the asteroid to be binary, finding a tentative P_{ORB} = 16.64 h. Adding the Pravec et al. data from 2011 and 2015, Oey et al. (2018) found P_{ORB} = 33.2 h and $Ds/Dp \geq 0.34$. There was also a possibility for a third period.

Stephens (this work) observed at the same time in 2018. His data yield essentially the same results: P_1 = 2.9525 h, P_{ORB} = 33.08 h, and $Ds/Dp \geq 0.38$.

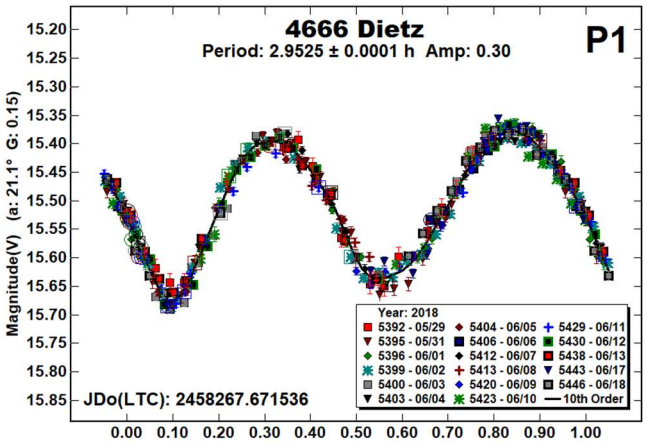

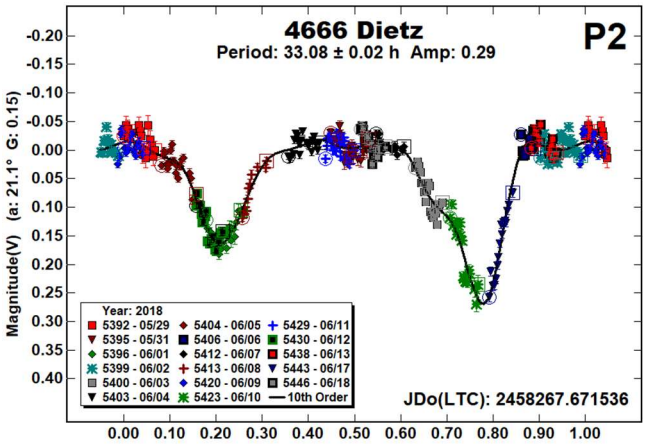

The extracted legacy data from 2011 showed that the binary discovery might have been possible in 2011. The "2011 P1" plot shows the final result of a dual-period search on the dataset that spanned only three days. Note that even after refining P_{ORB} to 16 h or 33 h, there are signs of a third period. However, the dataset was too sparse to make a useful search.

There are two plausible solutions for *PORB*. One, P_{ORB17} = 17.41 h, is somewhat near that reported by Pravec et al. (2015web). The alternate solution was forced to near the Oey et al. (2018) result, giving P_{ORB33} = 33.4 h.

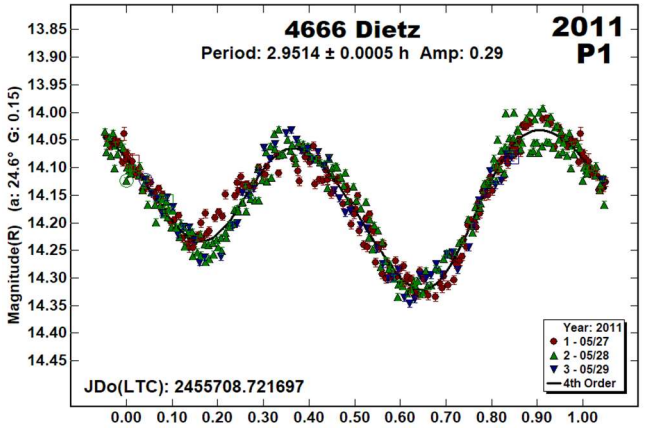

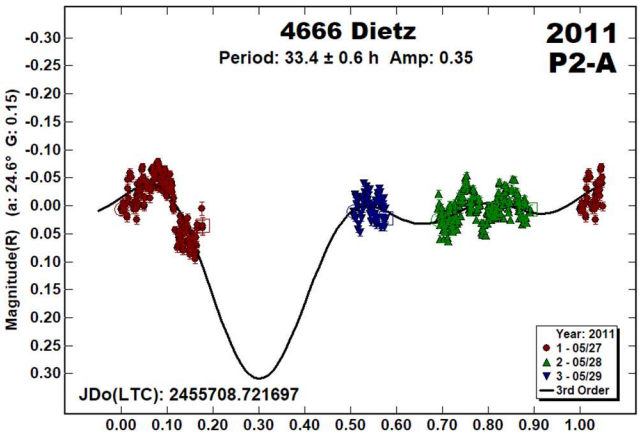

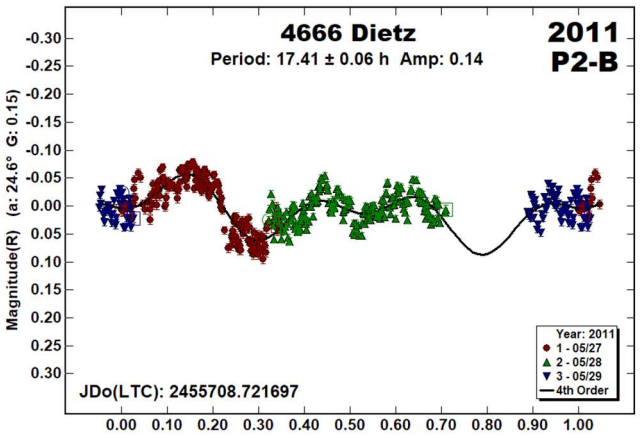

The shorter 17-h lightcurve could have easily been interpreted as showing mutual events, leading to $Ds/Dp \geq 0.31$. Given the near commensurability of both potential orbital solutions with an Earth day, a more extended dataset might have been able to confirm the binarity and remove the ambiguity for P_{ORB}, especially with help from an observer at a different longitude.

16525 Shumarinaiko. Warner and Coley (2013) reported this inner main-belt asteroid to be binary, finding P_1 = 2.5932 h and P_{ORB} = 14.409 h. There were signs of mutual events, but mainly the P_{ORB} lightcurve showed the typical "bowed" shape of a tidally-locked and elongated satellite.

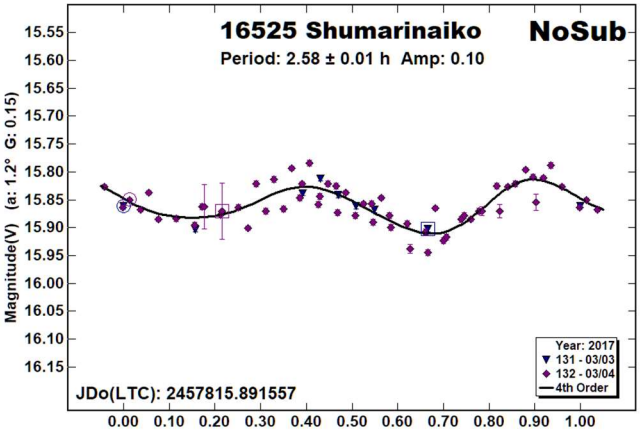

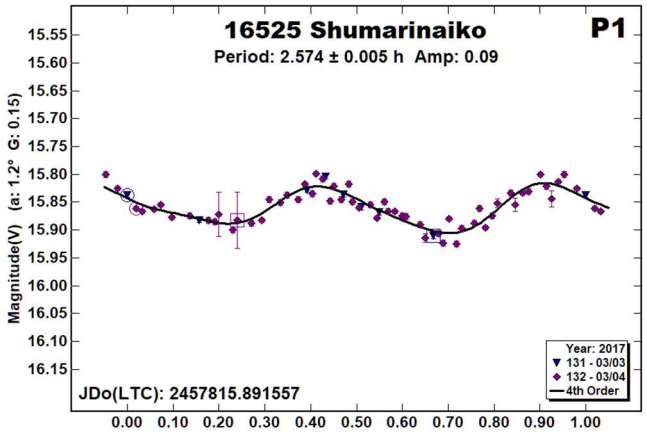

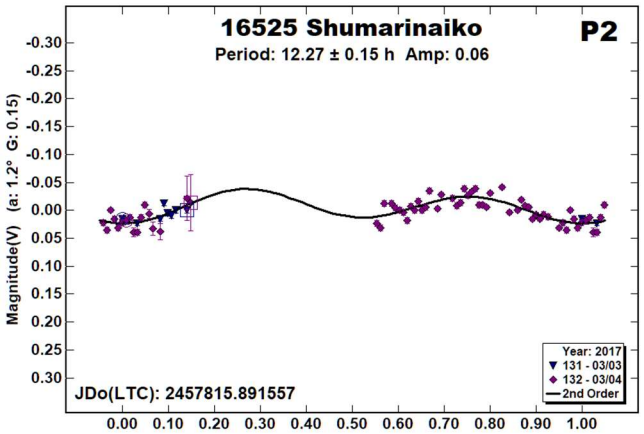

We were able to extract a very limited dataset from 2017 with fewer than 100 data points obtained over two nights. Even so, we attempted to duplicate the results from the 2013 observations. While the "NoSub" plot seemed to show an attenuation and we did eventually extract a similar primary period of P_1 = 2.58 h, the dataset was too sparse to find an accurate solution for the orbital period. The P_2 plot shows the best fit that we could find using a second-order Fourier fit.

(88188) 2000 XH44. Behrend (2004web) reported a period of 5.16 h, but it is rated as unreliable in the LCDB. Galad et al. (2005) reported a reliable period of 2.6906 h.

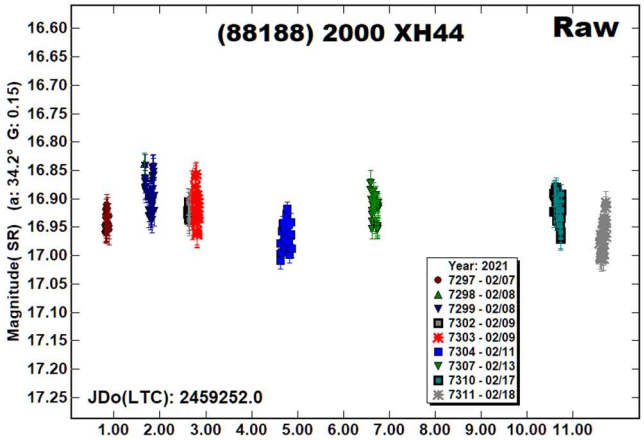

The raw plot of our 2021 data seemed to show a long-period component after resetting the zero-point adjustments that were made to get a single period solution back to 0. The dual-period search found a few long-period solutions; we adopted the one that fit to a bimodal lightcurve, i.e., P_1 = 189 h. This seems to fit with the raw data plot but there are caveats to that comparison that depend on the true period and the sampling rate of the sessions.

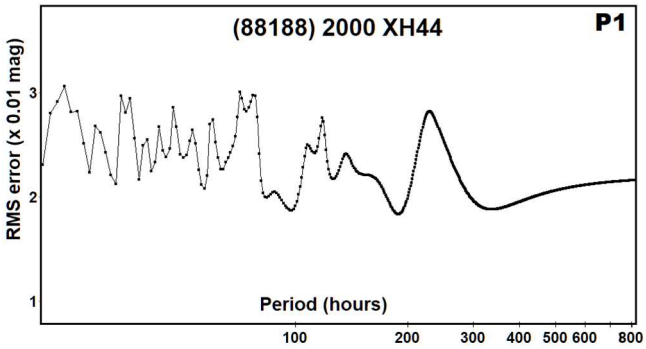

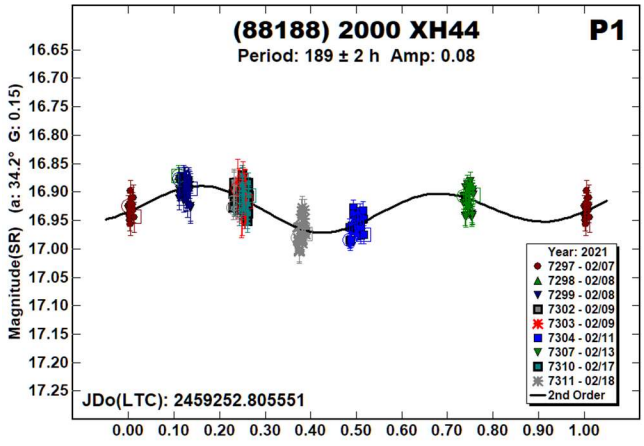

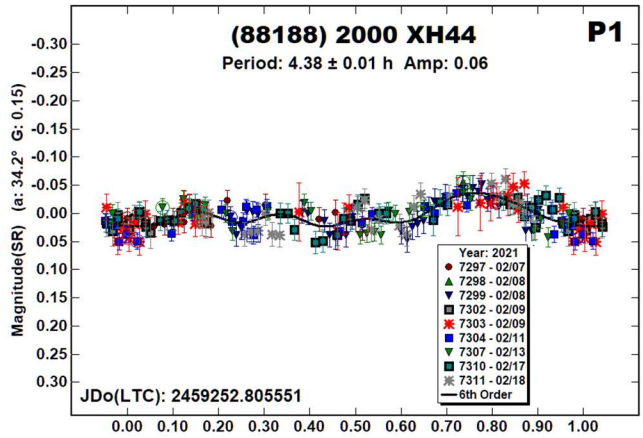

The dual-period search also found a weak P_2 = 4.38 h, but it could just as well be the result of the Fourier analysis locking onto noise in the dataset. If the period actually has a physical cause, i.e., a small satellite at a significant distance from the primary, then the asteroid would be a candidate for a *very wide binary* (see, e.g., Warner, 2016).

(416694) 2004 YR32. There were no previously reported periods in the LCDB for the near-Earth asteroid. Mainzer et al. (2019) found a diameter of 2.3 km using H = 17.6. This leads to a derived albedo of 0.03, which is atypically low for NEAs, which presumes that they are type S and have an albedo of 0.20 ± 0.11 (Warner et al., 2009). The higher albedo value would lead to a diameter of 900 m.

A plot of the raw data from our 2021 observations, not shown here, indicated that a period of about 48 h (or 24 h) was probable. Since this is in the realm for *very wide binary* asteroids (Warner, 2016), we used the dual-period search in *MPO Canopus* to see if a short period component was hiding in the data.

Despite the very noisy dataset, the effort was successful, finding a well-defined second period of P_2 = 4.076 h based on P_1 = 50.3 h. While P_1 ~ 25 h cannot be formally excluded, the resulting lightcurve would have a significantly larger amplitude, enough so that we are comfortable with adopting P_1 = 50.3 h. as the correct solution.

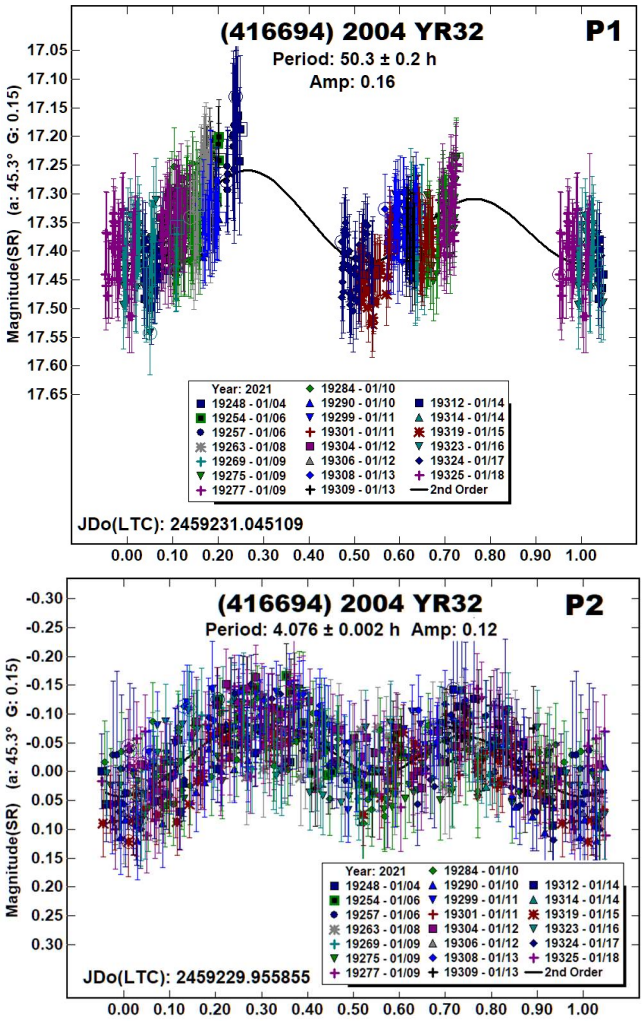

1999 RM45. Pravec et al. (2021) were first to report that this NEA is a binary asteroid. They found $P1$ = 3.0697 h, P_{ORB} = 16.445 h, and $Ds/Dp \geq 0.45$.

Our independent observations were made about the same time. The data clearly showed a period of about 16.5 h and what could be interpreted as mutual events caused by an elongated satellite. However, the dataset was insufficient to find a more refined and certain period beyond P_2 = 16.50 h.

The dataset was not only too sparse but too noisy to extract the period found by Pravec et al. (2021). A repeated iteration using our P_2 and forcing a solution near 3.07 h found two, unconvincing solutions of P_1 = 3.016 h or 3.354 h, which have a close to 10:9 ratio. The shorter P_1 = 3.016 h is close to Pravec et al. (2021) and so is labeled "P1-P" (preferred) even though the fit of our data to P_1 = 3.354 h was better.

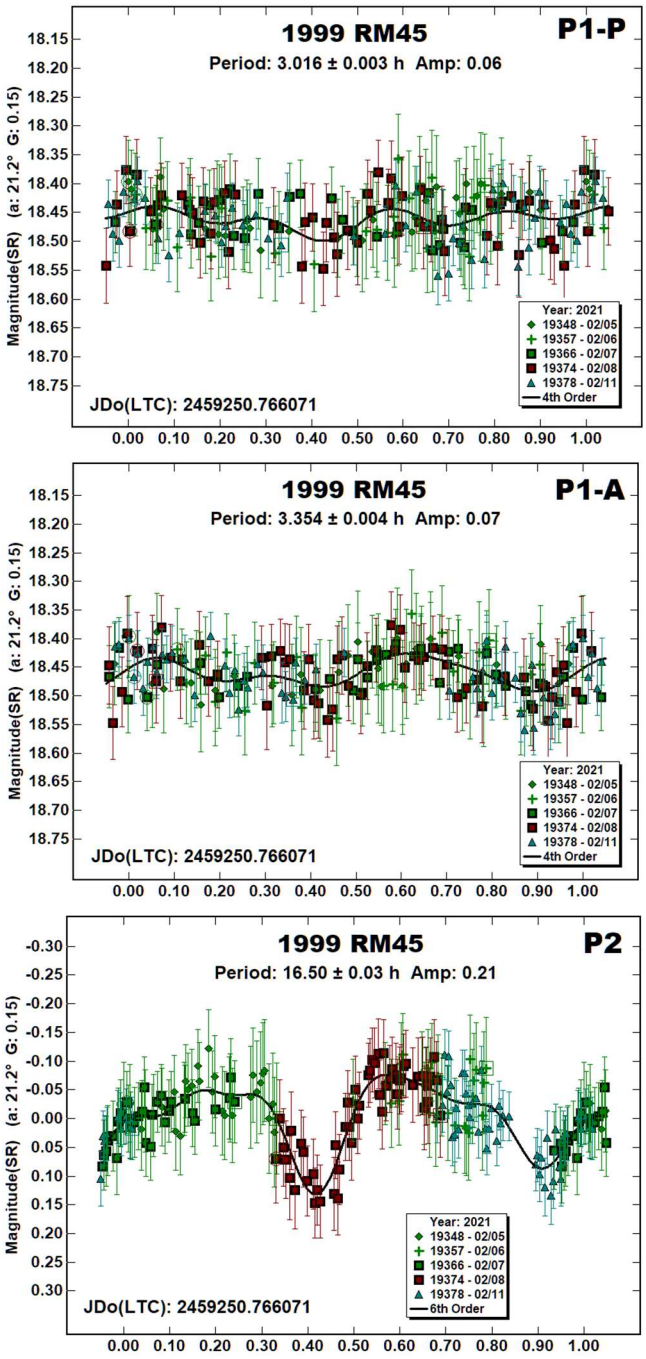

Number	Name	20yy mm/dd	Phase	L_{PAB}	B_{PAB}	Period(h)	P.E.	Amp	A.E.	Grp/Dr
2419	Moldavia	20/12/16-01/09	19.0,12.7	131	-6	2.4117	0.0001	0.13	0.01	FLOR
						10.154	0.003	0.10	0.01	<0.3
2873	Binzel	13/08/24-09/21	5.5,18.0	326	-7	[F]2.7037	0.0001	0.06	0.01	FLOR
						[F]42.90	0.01	0.02	0.01	
3561	Devine	21/02/20-03/23	2.3,8.9	144	5	4.7985	0.0006	0.05	0.01	HIL
						39.20	0.02	0.18	0.03	
4383	Suruga	15/10/07-10/14	5.6,7.8	10	-10	3.4073	0.0003	0.11	0.01	MB-I
						16.329	0.005	0.12	0.01	≥0.22
4666	Dietz	18/05/29-06/18	21.2,28.6	217	0	2.9525	0.0001	0.30	0.02	MB-I
						33.08	0.02			≥0.38
		11/05/27-05/29	10.2,10.4	250	13	2.9514	0.0005	0.29	0.03	MB-I
						[PO]17.41	0.06	0.14	0.02	≥0.31
						[F]33.4	0.6	>0.1		
16525	Shumarinaiko	17/03/03-03/04	1.3,0.9	164	1	2.574	0.005	0.09	0.01	MB-I
						12.27	0.15	0.06	0.01	
88188	2000 XH44	21/02/07-02/18	34.2,40.2	108	12	189	2	0.08	0.01	NEA
						4.38	0.01	0.06	0.01	
416694	2004 YR32	21/01/04-01/18	45.3,64.9	143	31	50.3	0.2	0.16	0.02	NEA
						4.076	0.002	0.12	0.03	
	1999 RM45	21/02/05-02/11	21.2,18.9	151	-10	[P]3.354	0.004	0.07	0.03	NEA
						[A]3.354	0.004	0.07	0.03	
						16.50	0.03	0.21	0.03	

Table II. Observing circumstances. [A]Alternate primary period. [F]Period is forced to another result. [P]Preferred primary period. [PO]Preferred orbital solution. The first line gives the primary period for the system. The second line gives the secondary period. The phase angle (α) is given at the start and end of each date range. An asterisk indicates that the phase angle reached a maximum or minimum during the period. L_{PAB} and B_{PAB} are, respectively the average phase angle bisector longitude and latitude (see Harris et al.,1984). For the Grp/Dr column, the first line gives the group/family based on Warner et al. (2009). FLOR Flora; HIL Hilda; MB-I Inner main-belt; NEA: Near-Earth asteroid. The Dr column on the second line indicates a confirmed binary and is the estimated diameter ratio of the secondary to primary (Ds/Dp).

Acknowledgements

Funding for observations at CS3 and work on the asteroid lightcurve database (Warner et al., 2009) and ALCDEF database (*alcdef.org*) are supported by NASA grant 80NSSC18K0851. The authors gratefully acknowledge Shoemaker NEO Grants from the Planetary Society (2007, 2013). These were used to purchase some of the telescopes and CCD cameras used in this research.

This work includes data from the Asteroid Terrestrial-impact Last Alert System (ATLAS) project. ATLAS is primarily funded to search for near earth asteroids through NASA grants NN12AR55G, 80NSSC18K0284, and 80NSSC18K1575; byproducts of the NEO search include images and catalogs from the survey area. The ATLAS science products have been made possible through the contributions of the University of Hawaii Institute for Astronomy, the Queen's University Belfast, the Space Telescope Science Institute, and the South African Astronomical Observatory.

References

References from web sites should be considered transitory, unless from an agency with a long lifetime expectancy. Sites run by private individuals, even if on an institutional web site, do not necessarily fall into this category.

Behrend, R. (2004web; 2011web) Observatoire de Geneve web site. *http://obswww.unige.ch/~behrend/page_cou.html*

Binzel, R.P.; Xu, S.; Bus, S.J.; Bowell, E. (1992). "Small main-belt asteroid lightcurve survey." *Icarus* **99**, 225-237.

Birlan, M.; Barucci, M.A.; Angeli, C.A.; Doressoundiram, A.; De Sanctis, M.C. (1996). "Rotational properties of asteroids: CCD observations of nine small asteroids." *Planet. Space Sci.* **44**, 555-558.

Galad, A.; Pravec, P.; Kusnirak, P.; Gajdos, S.; Kornos, L.; Vilagi, J. (2005). "Joint Lightcurve Observations of 10 Near-Earth asteroids from Modra and ONDREJOV." *Earth, Moon, and Planets* **97**, 147-163.

Harris, A.W.; Young, J.W.; Scaltriti, F.; Zappala, V. (1984). "Lightcurves and phase relations of the asteroids 82 Alkmene and 444 Gyptis." *Icarus* **57**, 251-258.

Henden, A.A.; Terrell, D.; Levine, S.E.; Templeton, M.; Smith, T.C.; Welch, D.L. (2009). *http://www.aavso.org/apass*

Mainzer, A.; Bauer, J.; Cutri, R.; Grav, T.; Kramer, E.; Masiero, J.; Sonnett, S.; Wright, E. Eds. (2019). "NEOWISE Diameters and Albedos V2.0." NASA Planetary Data System. urn:nasa:pds:neowise_diameters_albedos::2.0. *https://doi.org/10.26033/18S3-2Z54*

Oey, J.; Kusnirak, P.; Pravec, P.; Hornoch, K.; Pray, D.; Benishek, V.; Montaigut, R.; Leroy, A.; Vilagi, J. (2018). *CBET* **4536**.

Pravec, P.; Wolf, M.; Sarounova, L. (2011web, 2015web). *http://www.asu.cas.cz/~ppravec/neo.htm*

Pravec, P.; Fatka, P.; Vokrouhlicky, D.; Scheeres, D.J.; Kusnirak, P.; Hornoch, K.; Galad, A.; Vrastil, J.; Pray, D.P.; Krugly, Yu.N.; Gaftonyuk, N.M.; Inasaridze, R.Ya.; Ayvazian, V.R.; Kvaratskhelia, O.I.; Zhuzhunadze, V.T.; Husarik, M.; Cooney, W.R.; Gross, J.; Terrell, D.; Világi, J.; Kornos, L.; Gajdos, S.; Burkhonov, O.; Ehgamberdiev, Sh.A.; Donchev, Z.; Borisov, G.; Bonev, T.; Rumyantsev, V.V.; Molotov, I.E. (2018). "Asteroid clusters similar to asteroid pairs." *Icarus* **304**, 110-126.

Pravec, P.; Hornoch, K.; Fatka, P.; Kusnirak, P. (2021). *CBET* **4631**.

Tonry, J.L.; Denneau, L.; Flewelling, H.; Heinze, A.N.; Onken, C.A.; Smartt, S.J.; Stalder, B.; Weiland, H.J.; Wolf, C. (2018). "The ATLAS All-Sky Stellar Reference Catalog." *Ap. J.* **867**, A105.

Vachier, F.; Pravec, P.; Kucakova, H.; Hornoch, K.; Kusnirak, P.; Pray, D.; Cooney, W.; Gross, J.; Terrell, D.; Flanagan, B.; Pellerin, B.; Durkee, R.; Benishek, V.; Berthier, J.; Klotz, A.; Teng, J.-P.; Peyrot, A.; Thierry, P. (2019). *CBET* **4628**.

Warner, B.D. (2007). "Initial Results of a Dedicated H-G Program." *Minor Planet Bul.* **34**, 113-119.

Warner, B.D. (2013). "Lightcurve Photometry Opportunities: 2013 April-June." *Minor Planet Bull*. **40**, 119-121.

Warner, B.D. (2016). "Three Additional Candidates for the Group of Very Wide Binaries." *Minor Planet Bul.* **43**, 306-309.

Warner, B.D.; Coley, D. (2013). "16525 Shumarinaiko: A New Nysa Binary." *Minor Planet Bull*. **40**, 124-125.

Warner, B.D.; Harris, A.W.; Pravec, P. (2009). "The Asteroid Lightcurve Database." Icarus **202**, 134-146. Updated 2020 Aug. *http://www.minorplanet.info/lightcurvedatabase.html*

LIGHTCURVE AND ROTATION PERIOD DETERMINATIONS FOR 25 ASTEROIDS

Vladimir Benishek
Belgrade Astronomical Observatory
Volgina 7, 11060 Belgrade 38, SERBIA
vlaben@yahoo.com

(Received: 2021 April 15)

Lightcurves and synodic rotation periods for 25 asteroids determined from CCD photometric data acquired at Sopot Astronomical Observatory (SAO) over the time span 2020 July - 2021 April are summarized in this paper.

Photometric observations of 25 asteroids were conducted at Sopot Astronomical Observatory (SAO) from 2020 July through 2021 April in order to determine the asteroids' synodic rotation periods. For this purpose, two 0.35-m *f*/6.3 Meade LX200GPS Schmidt-Cassegrain telescopes were employed. The telescopes are equipped with a SBIG ST-8 XME and a SBIG ST-10 XME CCD cameras. The exposures were unfiltered and unguided for all targets. Both cameras were operated in 2×2 binning mode, which produces image scales of 1.66 arcsec/pixel and 1.25 arcsec/pixel for ST-8 XME and ST-10 XME cameras, respectively. Prior to measurements, all images were corrected using dark and flat field frames.

Photometric reduction was conducted using *MPO Canopus* (Warner, 2018). Differential photometry with up to five comparison stars of near solar color ($0.5 \leq$ B-V ≤ 0.9) was performed using the Comparison Star Selector (CSS) utility. This helped ensure a satisfactory quality level of night-to-night zero-point calibrations and correlation of the measurements within the standard magnitude framework. Field comparison stars were calibrated using standard Cousins R magnitudes derived from the Carlsberg Meridian Catalog 15 (VizieR, 2021) Sloan r' magnitudes using the formula: R = r' – 0.22 in all cases presented in this paper. In some instances, small zero-point adjustments were necessary in order to achieve the best match between individual data sets in terms of achieving the most favorable statistical indicators of Fourier fit goodness.

Lightcurve construction and period analysis was performed using *Perfindia* custom-made software developed in the R statistical programming language (R Core Team, 2020) by the author. The essence of its algorithm is reflected in finding the most favorable solution for rotational period by minimizing the *residual standard error* of the lightcurve Fourier fit.

The lightcurve plots presented in this paper show so-called 2% error for rotational periods, i.e., an error that would cause the last data point in a combined data set by date order to be shifted by 2% (Warner, 2012) and represented by $\Delta P = (0.02 \cdot P^2) / T$, where P and T are the rotational period and the total time span of observations, respectively. Both of these quantities must be expressed in the same units.

Some of the targets presented in this paper were observed within the Photometric Survey for Asynchronous Binary Asteroids (*BinAstPhot Survey*) under the leadership of Dr. Petr Pravec from Ondřejov Observatory, Czech Republic.

Table I gives the observing circumstances and results.

440 Theodora was a fairly bright target, favorable for observing during a waxing Moon approaching full at the end of 2021 February. A secure rotation period value has been established for it over several apparitions throughout previous decades. A search of the LCDB database (Warner et al., 2009) yielded the following previously found periods: 4.828 h (Florczak et al., 1997), a sidereal period of 4.83658 h by Hanuš et al. (2011) and two determinations by Behrend (4.82821 h, 2010; 4.83612 h, 2018). A synodic rotation period of $P = 4.835 \pm 0.007$ h, derived from the SAO data obtained over three nights is in good agreement with the previously found results.

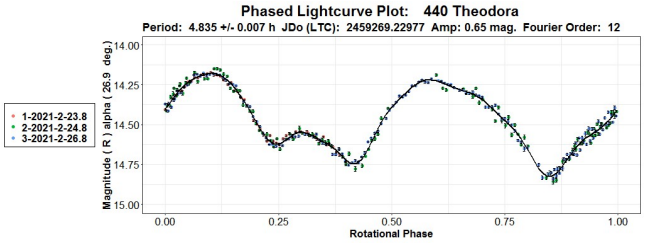

1117 Reginita. As in the preceding case, there are several fairly consistent rotation periods found over previous decades. Among some of them are 2.9463 h (Wisniewski et al., 1997), 2.9458 h (Behrend, 2007), 2.9464 h (Kryszczynska et al., 2012), 2.928 h (Waszczak et al., 2015), and 2.9467 h (Franco et al., 2018). Again, the SAO result ($P = 2.949 \pm 0.007$ h) obtained from the 2021 February observations conducted on two consecutive nights is consistent with the previous ones.

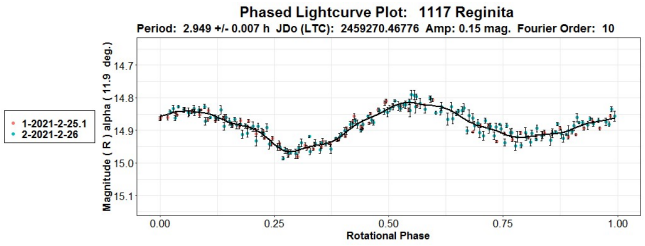

1158 Luda. Several previous rotation period results are quite uniform: 6.863 h (Behrend, 2005), 6.90 h (Warner, 2005), 6.870 h (Warner, 2011a), and 6.86 h (Kim et al., 2014). The exception is that of Alvarez-Candal et al. (7.44 h, 2004). The 2021 February SAO data collected on four consecutive nights confirm the consistent previously determined values, yielding a result of $P = 6.89 \pm 0.02$ h.

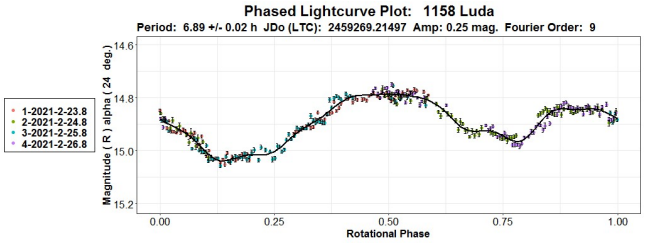

1610 Mirnaya. This was a *BinAstPhot Survey* target with no previously known rotation period. The SAO observations carried out on five nights in 2021 January-February show an unequivocal bimodal period result of $P = 4.745 \pm 0.002$ h.

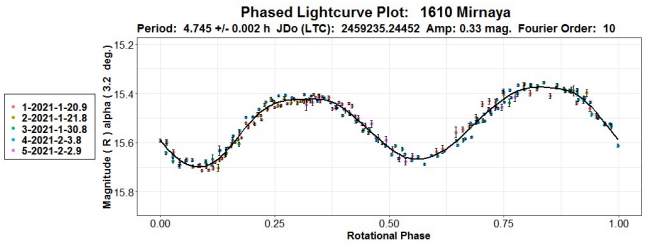

1675 Simonida. This is another minor planet with a well-established rotation period. These include 5.3 h (Wisniewski et al., 1997), 5.29 h (Behrend, 2008), 5.2885 h (Kryszczynska et al., 2012), and 5.28779 h (Pal et al., 2020). A bimodal lightcurve with a fairly large amplitude (0.46 mag.) phased to a period of $P = 5.283 \pm 0.008$ h was the result of period analysis using SAO photometric data collected on three nights in late 2021 March.

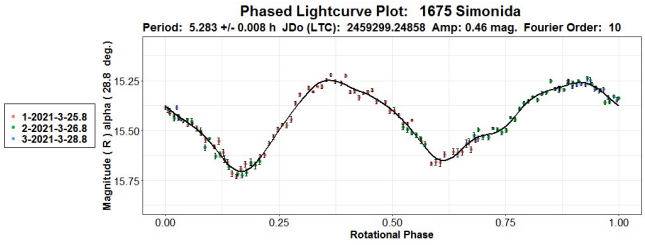

2273 Yarilo. No prior period results were known for this *BinAstPhot Survey* inner main-belt target. Period analysis upon four photometric data sets obtained at SAO in 2021 February-March led to a synodic rotational period of $P = 2.8200 \pm 0.0006$ h.

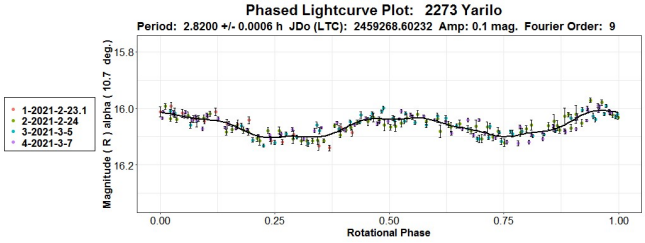

2438 Oleshko. The only previously found rotation periond by Behrend (2011) of 3.227 h is corroborated by the SAO rotation period determination ($P = 3.2253 \pm 0.0008$ h) based on five datasets obtained in 2021 February-March.

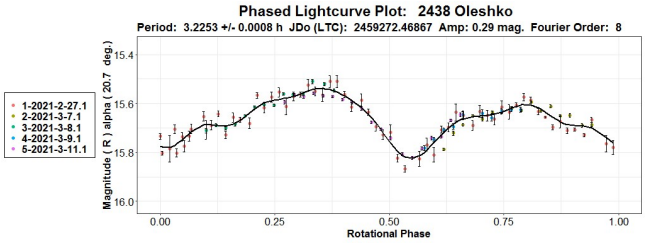

2712 Keaton. The only previously found rotation period by Chang et al. (5.87 h, 2019) significantly differs from the new result derived from dense SAO photometry that indicates an unambiguous period of $P = 6.720 \pm 0.005$ h. As a program target within *BinAstPhot Survey*, this inner main-belt asteroid was observed on five nights in early 2021 April.

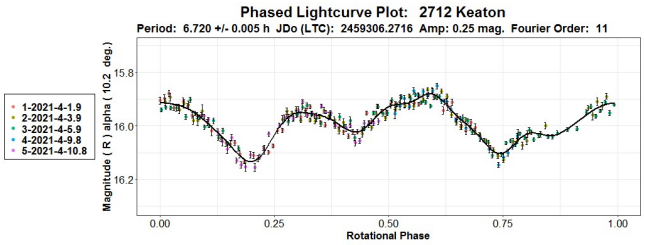

2961 Katsurahama. Several consistent previously found rotation periods such as those by Warner (2.936 h, 2011b) and Kryszczynska et al. (2.937 h, 2012) are in excellent agreement with a bimodal solution of P = 2.939 ± 0.004 h found from the SAO 2021 February-March data.

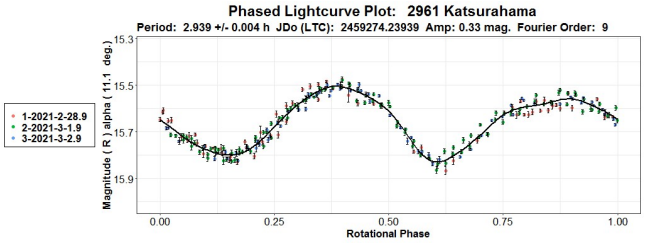

3760 Poutanen. A newly found period of P = 2.957 ± 0.007 h from the 2021 March SAO data is fully consistent with three previous results: 2.956 h (Salvaggio et al., 2017), 2.9554 h (Benishek, 2018), and 2.95588 h (Pal et al., 2020).

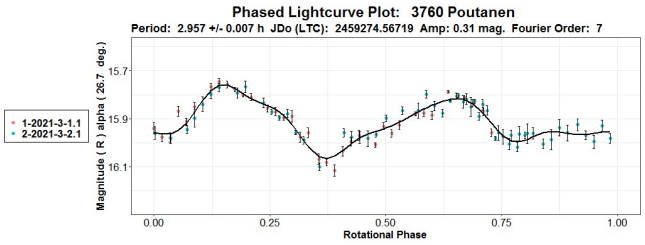

4170 Semmelweis. Data taken on three consecutive nights in late 2021 March yielded a bimodal lightcurve of fairly high amplitude (0.53 mag) and a corresponding period of P = 5.30 ± 0.02 h, which affirms previous results by Waszczak et al. (2015, 5.302 h and 5.305 h), Aznar Macias (2016, 5.31 h), and Pal et al. (2020, 5.3054 h).

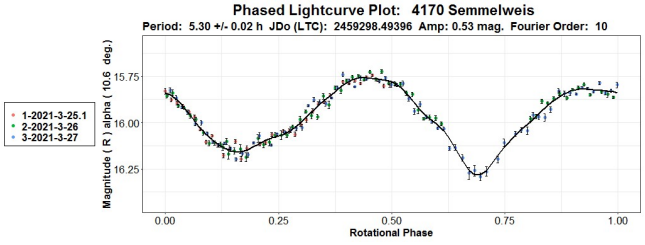

4612 Greenstein. No period results prior to this determination were found in the LCDB. Photometric observations over four nights at SAO in 2021 February-March resulted in a bimodal lightcurve phased to an unambiguous solution period of P = 3.0080 ± 0.0007 h.

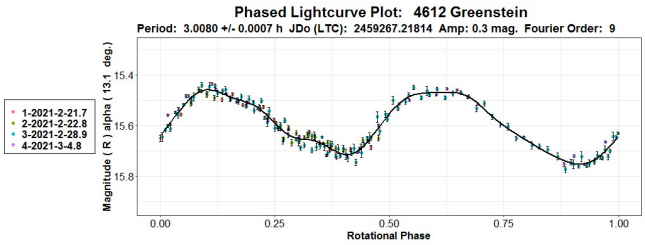

4774 Hobetsu. A bimodal period solution found from the 2021 apparition SAO data (P = 3.5770 ± 0.0004 h) slightly differs from the value determined from the 2019 SAO observations of 3.564 h (Benishek, 2020) and matches exactly the period obtained during the 2004 apparition by Pray (2005, 3.577 h).

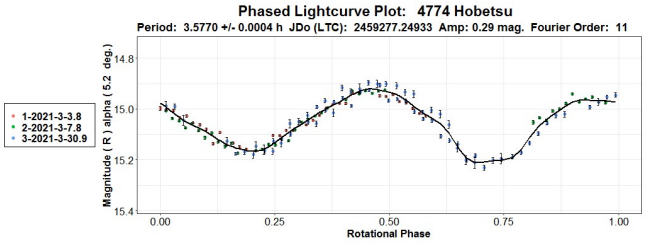

4794 Bogard. An insight into the LCDB showed this to be the very first period determination for this *BinAstPhot Survey* target. The SAO observations taken on six nights in 2021 February-March led to a period of P = 2.7350 ± 0.0004 h as the statistically most favorable one.

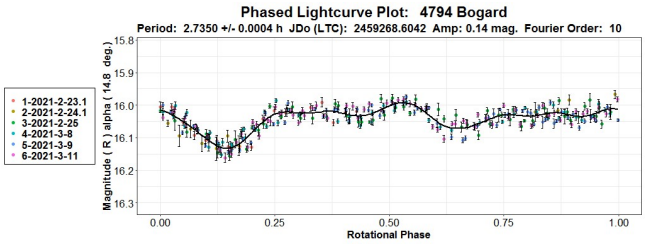

5431 Maxinehelin. The new result for synodic rotation period (P = 5.195 ± 0.003 h) obtained from the SAO observations carried out over five nights in the second half of 2020 July is identical to the previous values reported by Pravec (2013, 5.1951 h) and Stephens (2014, 5.195 h) but differs quite noticeably from the period found by Klinglesmith III et al. (2014, 4.888 h).

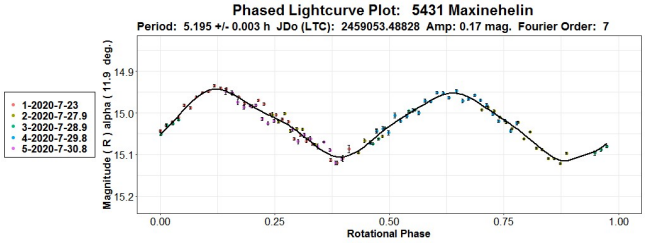

6524 Baalke. As it turned out, the rotational cycle of this inner main-belt asteroid is quite short, photometric observations at SAO on two consecutive nights in early 2021 February at low solar phase angles were sufficient to establish a lightcurve and to find a plausible rotation period. A bimodal lightcurve with an amplitude of 0.31 mag and phased to a period of P = 2.682 ± 0.005 h was constructed from the acquired data. According to the LCDB, this is the first reported rotation period this asteroid.

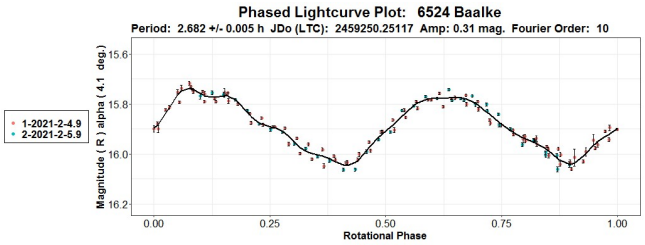

6526 Matogawa. There were no reports on rotation periods for this *BinAstPhot Survey* target prior to this work. Period analysis points to a value of $P = 3.297 \pm 0.003$ h as a reliable solution. The relevant photometric data were collected at SAO on four nights in early 2021 April.

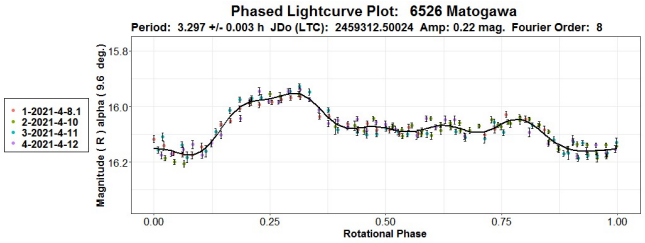

8425 Zirankexuejijin. No previous reports on rotation period determinations for this asteroid are known. Photometric data were obtained at SAO on four nights in the second half of 2021 February yielding a bimodal lightcurve phased to a period of $P = 4.011 \pm 0.003$ h and an amplitude of 0.26 mag.

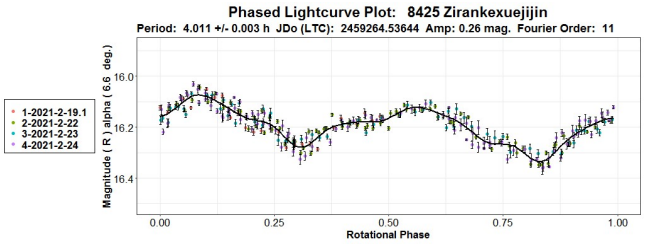

8441 Lapponica. The two previously determined periods by Behrend (2008, 3.27 h) and Clark (2008, 3.275 h) are consistent with the result of $P = 3.2856 \pm 0.0003$ h found from the SAO data collected on six nights in 2021 March-April.

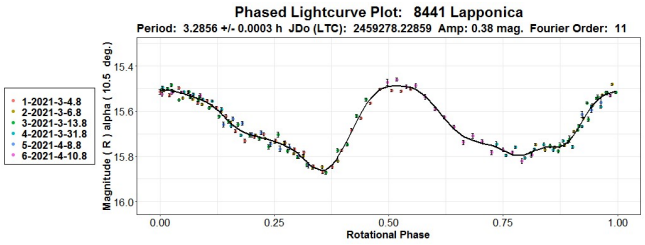

9044 Kaoru. This was a *BinAstPhot Survey* target with no previously known rotation period. Period analysis conducted over data collected on three consecutive nights in late 2021 March indicates an unambiguous rotation period solution of $P = 4.706 \pm 0.009$ h.

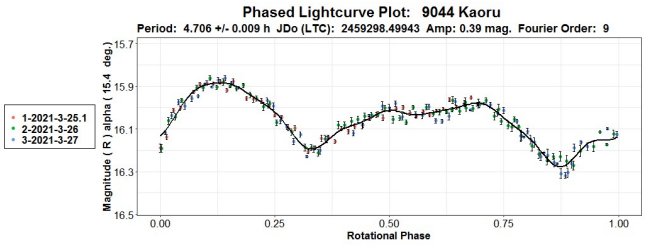

(10037) 1984 BQ. This Vesta family asteroid was also a *BinAstPhot Survey* target with no rotation period determination results in the LCDB. An unambiguous bimodal period solution of $P = 6.749 \pm 0.005$ h was found from the data collected on five nights in the first half of 2021 February.

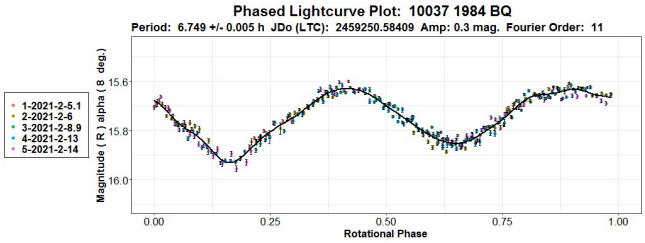

(18640) 1998 EF9. No previous rotation periods were found in this case as well. Data taken on two nights in 2021 December led to a bimodal period solution of $P = 3.7010 \pm 0.0008$ h.

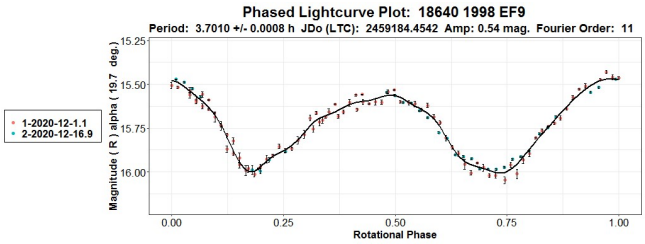

(27064) 1998 SY63. A check of the LCDB records points this to being the first rotation period determination for 1998 SY63. A unique period solution of $P = 2.971 \pm 0.003$ h was found analyzing the data collected on three nights in 2021 February.

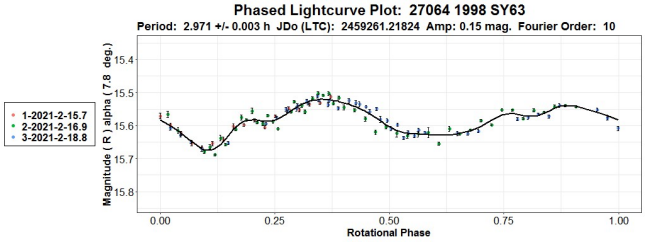

(33808) 1999 XD114. A high-amplitude (0.72 mag.) lightcurve associated with a period of $P = 7.721 \pm 0.004$ h arises as an unequivocal solution in period analysis performed upon the combined dataset made up of observations from 2021 February at low solar phase angles, shedding light for the first time at hitherto unknown spin rate of this inner main-belt asteroid.

Number	Name	20yy/mm/dd	Phase	L_{PAB}	B_{PAB}	Period (h)	P.E.	Amp	A.E.	Grp
440	Theodora	21/02/23-21/02/26	26.9,27.5	104	0	4.835	0.007	0.65	0.02	FLOR
1117	Reginita	21/02/24-21/02/26	11.9,11.4	181	3	2.949	0.007	0.15	0.02	FLOR
1158	Luda	21/02/23-21/02/26	24.0,24.2	89	15	6.89	0.02	0.25	0.03	EUN
1610	Mirnaya	21/01/20-21/02/03	3.2,10.4	116	3	4.745	0.002	0.33	0.03	FLOR
1675	Simonida	21/03/25-21/03/28	28.8,28.9	119	8	5.283	0.008	0.46	0.02	FLOR
2273	Yarilo	21/02/23-21/03/07	10.7,4.3	197	-1	2.8200	0.0006	0.10	0.02	MB-I
2438	Oleshko	21/02/26-21/03/11	20.7,16.0	196	5	3.2253	0.0008	0.29	0.03	FLOR
2712	Keaton	21/04/01-21/04/10	10.2,14.8	176	0	6.720	0.005	0.25	0.03	MB-I
2961	Katsurahama	21/02/28-21/03/03	11.1,12.1	141	-6	2.939	0.004	0.33	0.02	FLOR
3760	Poutanen	21/03/01-21/03/02	26.7,26.5	216	13	2.957	0.007	0.31	0.03	MB-I
4170	Semmelweis	21/03/24-21/03/27	10.6,9.9	211	7	5.30	0.02	0.53	0.02	EOS
4612	Greenstein	21/02/21-21/03/04	13.1,17.7	131	7	3.0080	0.0007	0.30	0.02	MB-I
4774	Hobetsu	21/03/03-21/03/30	5.2,18.8	157	-4	3.5770	0.0004	0.29	0.03	FLOR
4794	Bogard	21/02/23-21/03/11	14.8,6.0	179	0	2.7350	0.0004	0.14	0.02	FLOR
5431	Maxinehelin	20/07/22-20/07/30	11.9,10.5	314	14	5.195	0.003	0.17	0.02	PHO
6524	Baalke	21/02/04-21/02/06	4.1,4.9	128	2	2.682	0.005	0.31	0.02	MB-I
6526	Matogawa	21/04/08-21/04/12	9.7,7.8	213	7	3.297	0.003	0.22	0.03	FLOR
8425	Zirankexuejijin	21/02/19-21/02/24	6.6,3.7	161	0	4.011	0.003	0.26	0.03	FLOR
8441	Lapponica	21/03/04-21/04/10	10.5,26.7	152	6	3.2856	0.0003	0.38	0.02	FLOR
9044	Kaoru	21/03/24-21/03/27	15.4,14.5	209	7	4.706	0.009	0.39	0.02	FLOR
10037	1984 BQ	21/02/05-21/02/14	*8.0,6.0	146	11	6.749	0.005	0.30	0.02	V
18640	1998 EF9	20/11/30-20/12/16	19.7,13.1	102	6	3.7010	0.0008	0.54	0.02	PHO
27064	1998 SY63	21/02/15-21/02/18	7.8,9.1	137	10	2.971	0.003	0.15	0.02	FLOR
33808	1999 XD114	21/02/14-21/03/01	9.7,14.0	136	15	7.721	0.004	0.72	0.03	MB-I
42320	2001 XH17	21/03/03-21/03/08	7.8,9.2	156	14	4.218	0.003	0.19	0.06	MB-I

Table I. Observing circumstances and results. Phase is the solar phase angle given at the start and end of the date range. If preceded by an asterisk, the phase angle reached an extrema during the period. L_{PAB} and B_{PAB} are the average phase angle bisector longitude and latitude. Grp is the asteroid family/group (Warner *et al.*, 2009): EUN = Eunomia, FLOR = Flora, MB-I = main-belt inner, PHO = Phocaea, EOS = Eos, V = Vestoid.

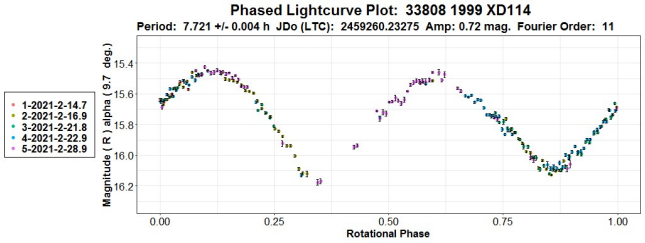

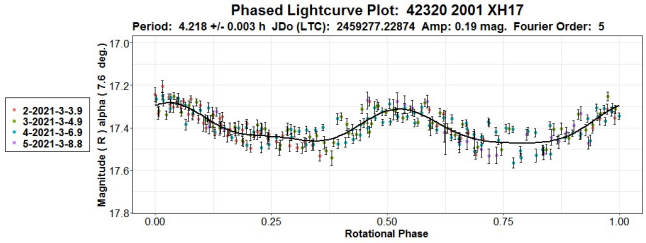

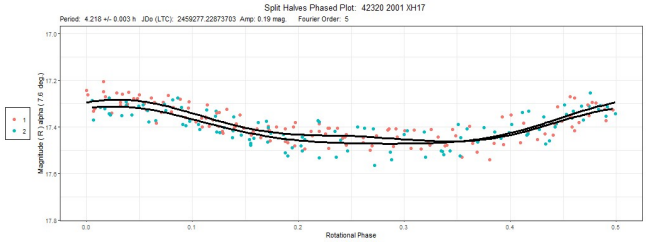

(42320) 2001 XH17 was another inner main-belt minor planet without a previously known rotation period. Despite its fairly low brightness (fainter than 17th magnitude) at the time it was observed in early 2021 March, this asteroid was selected for photometry because it was in the same CCD field of view for several nights with another much brighter newly discovered binary asteroid, 3523 Arina, and followed systematically within the *BinAstPhot Survey*.

Despite the larger data scatter, a bimodal period of P = 4.218 ± 0.003 h stands out as a statistically dominant solution in period analysis. A harmonically related half-period monomodal period value (P/2), although somewhat less statistically favorable, could not be ruled out as a possibility given the relatively small lightcurve amplitude (0.19 mag.).

This alternative solution is supported by a considerable overlap of the two lightcurve halves for the bimodal period within the data scatter, which is significant compared to the lightcurve amplitude, and so it is hard to reach a definitive conclusion based on the "split halves" test. The longer period of 4.218 h is formally adopted as a solution in this paper but further observations are highly recommended in future apparitions to verify the result.

Acknowledgements

Observational work at Sopot Astronomical Observatory is supported by a 2018 Gene Shoemaker NEO Grant from The Planetary Society.

References

Alvarez-Candal, A.; Duffard, R.; Angeli, C.A.; Lazzaro, D.; Fernandez, S. (2004). "Rotational Lightcurves of Asteroids Belonging to Families." *Icarus* **172**, 388-401.

Aznar Macias, A. (2016). "Parameters of Rotation and Shapes of Main-belt Asteroids from APT Observatory Group: Second Quarter 2016." *Minor Planet Bull.* **43**, 350-353.

Behrend, R. (2005, 2007, 2008, 2010, 2018). Observatoire de Geneve web site. *http://obswww.unige.ch/~behrend/page_cou.html*

Benishek, V. (2018). "Lightcurve and Rotation Period Determinations for 29 Asteroids." *Minor Planet Bull.* **45**, 82-91.

Benishek, V. (2020). "Asteroid Photometry at Sopot Astronomical Observatory: 2019 June-October." *Minor Planet Bull.* **47**, 75-83.

Chang, C.-K.; Lin, H.-W.; Ip, W.-H.; Chen, W.-P.; Yeh, T.-S.; Chambers, K.C.; Magnier, E.A.; Huber, M.E.; Flewelling, H.A.; Waters, C.Z.; Wainscoat, R.J.; Schultz, A.S.B. (2019). "Searching for Super-fast Rotators Using the Pan-STARRS 1." *Astrophys. J. Suppl. Series* **241**, 6.

Clark, M. (2008). "Asteroid Lightcurve Observations." *Minor Planet Bull.* **35**, 152-154.

Florczak, M.; Dotto, E.; Barucci, M.A.; Birlan, M.; Erikson, A.; Fulchignoni, M.; Nathues, A; Perret, L.; Thebault, P. (1997). "Rotational properties of main belt asteroids: photoelectric and CCD observations of 15 objects." *Planetary and Space Science*, **45**, 1423-1435.

Franco, L.; Marchini, A.; Baj, G.; Scarfi, G.; Succi, G.; Bachini, M.; Arena, C. (2018). "Lightcurves for 91 Aegina, 235 Carolina, 1117 Reginita, and (505657) 2014 SR339." *Minor Planet Bull.* **45**, 399-400.

Hanuš, J.; Durech, J.; Broz, M.; Warner, B.D.; Pilcher, F.; Stephens, R.; Oey, J.; Bernasconi, L.; Casulli, S.; Behrend, R.; Polishook, D.; Henych, T.; Lehký, M.; Yoshida, F.; Ito, T. (2011). "A study of asteroid pole-latitude distribution based on an extended set of shape models derived by the lightcurve inversion method." *Astron. Astrophys.* **530**, A134.

Kim, M.-J.; Choi, Y.-J.; Moon, H.-K.; Byun, Y.-I.; Brosch, N.; Kaplan, M.; Kaynar, S.; Uysal, O.; Guzel, E.; Behrend, R.; Yoon, J.-N.; Mottola, S.; Hellmich, S.; Hinse, T.C.; Eker, Z.; Park, J.-H. (2014). "Rotational Properties of the Maria Asteroid Family." *Astron. J.* **147**, A56.

Klinglesmith III, D.A.; Hanowell, J.; Risley, E.; Turk, J.; Vargas, A.; Warren, C.A. (2014). "Asteroid Observations at the Etscorn Campus Observatory." *Minor Planet Bull.* **41**, 82-84.

Kryszczynska, A.; Colas, F.; Polinska, M.; Hirsch, R.; Ivanova, V.; Apostolovska, G.; Bilkina, B.; Velichko, F.P.; Kwiatkowski, T.; Kankiewicz, P. and 20 colleagues. (2012). "Do Slivan states exist in the Flora family? I. Photometric survey of the Flora region." *Astron. Astrophys.* **546**, A72.

Pal, A.; Szakáts, R.; Kiss, C.; Bódi, A.; Bognár, Z.; Kalup, C.; Kiss, L.L.; Marton, G.; Molnár, L.; Plachy, E.; Sárneczky, K.; Szabó, G.M.; Szabó, R. (2020). "Solar System Objects Observed with TESS - First Data Release: Bright Main-belt and Trojan Asteroids from the Southern Survey." *Ap. J. Supl. Ser.* **247**, 26-34.

Pravec, P. (2013). Photometric Survey for Asynchronous Binary Asteroids web site. *http://www.asu.cas.cz/~ppravec/newres.txt*

Pray, D.P. (2005). "Lightcurve Analysis of Asteroids 276, 539, 1014, 1067, 3693, and 4774." *Minor Planet Bull.* **32**, 8-9.

R Core Team (2020). R: A language and environment for statistical computing. R Foundation for Statistical Computing. Vienna, Austria. *https://www.R-project.org/*

Salvaggio, F.; Marchini, A.; Papini, R. (2017). "Rotation Period Determination for 3760 Poutanen and 14309 Defoy." *Minor Planet Bull.* **44**, 354-355.

Stephens, R.D. (2014). "Asteroids Observed from CS3: 2013 July-September." *Minor Planet Bull.* **41**, 13-15.

VizieR (2021). *http://vizier.u-strasbg.fr/viz-bin/VizieR*

Warner, B.D. (2005). "Asteroid Lightcurve Analysis at the Palmer Divide Observatory - Winter 2004-2005." *Minor Planet Bull.* **32**, 54-58.

Warner, B.D.; Harris, A.W.; Pravec, P. (2009). "The Asteroid Lightcurve Database." *Icarus* **202**, 134-146. Updated 2020 Oct 22. *http://www.minorplanet.info/lightcurvedatabase.html*

Warner, B.D. (2011a). "Upon Further Review: III. An Examination of Previous Lightcurve Analysis from the Palmer Divide Observatory." *Minor Planet Bull.* **38**, 21-23.

Warner, B.D. (2011b). "Upon Further Review: V. An Examination of Previous Lightcurve Analysis from the Palmer Divide Observatory." *Minor Planet Bull.* **38**, 63-65.

Warner, B.D. (2012). The MPO Users Guide: A Companion Guide to the MPO Canopus/PhotoRed Reference Manuals. BDW Publishing, Colorado Springs, CO.

Warner, B.D. (2018). *MPO Canopus* software, version 10.7.11.3. *http://www.bdwpublishing.com*

Waszczak, A.; Chang, C.-K.; Ofek, E.O.; Laher, R.; Masci, F.; Levitan, D.; Surace, J.; Cheng, Y.-C.; Ip, W.-H.; Kinoshita, D.; Helou, G.; Prince, T.A.; Kulkarni, S. (2015). "Asteroid Light Curves from the Palomar Transient Factory Survey: Rotation Periods and Phase Functions from Sparse Photometry." *Astron. J.* **150**, A75.

Wisniewski, W.Z.; Michalowski, T.M.; Harris, A.W.; McMillan, R.S. (1997). "Photometric Observations of 125 Asteroids." *Icarus* **126**, 395-449.

LIGHTCURVE ANALYSIS FOR NINE NEAR-EARTH ASTEROIDS

Peter Birtwhistle
Great Shefford Observatory
Phlox Cottage, Wantage Road
Great Shefford, Berkshire, RG17 7DA
United Kingdom
peter@birtwhistle.org.uk

(Received: 2021 Apr 10)

Lightcurves and amplitudes for nine near-Earth asteroids observed from Great Shefford Observatory during close approaches in 2021 are reported: 2020 TB12, 2020 YE5, 2021 AU, 2021 CO, 2021 DP, 2021 DX1, 2021 EB1, 2021 EX1 and 2021 FH. All have rotation periods faster than the 2.2h spin barrier and five appear to show signs of tumbling.

Photometric observations of near-Earth asteroids during close approaches to Earth during January - March 2021 were made at Great Shefford Observatory using a 0.40-m Schmidt-Cassegrain and Apogee Alta U47+ CCD camera. All observations were made unfiltered and with the telescope operating with a focal reducer at f/6. The 1K×1K, 13-micron CCD was binned 2×2 resulting in an image scale of 2.16 arcsec/pixel. All the images were calibrated with dark and flat frames and *Astrometrica* (Raab, 2018) was used to measure photometry using APASS Johnson V band data from the UCAC4 catalogue. *MPO Canopus* (Warner, 2021), incorporating the Fourier algorithm developed by Harris (Harris et al., 1989) was used for lightcurve analysis.

All the objects were discovered on or after the last available update of the LCDB (Warner et al., 2009) and therefore no previous results for any of the objects are contained therein. Searches of the Astrophysics Data System (ADS, 2021) have also not found any previously reported results for any of the nine objects. Other sources of information for previously reported results are listed against each object where appropriate.

2020 TB12. Discovered on 2020 Oct 15 by Pan-STARRS1 (Mastaler et al., 2020), this Apollo made an approach to within 7 Lunar Distances (LD) on 2021 Feb 1 and was observed on 2021 Feb 4 for 1 hour at a range of 9 LD and at a phase angle of >90°. It is classed as a Potentially Hazardous Asteroid (PHA) by the Minor Planet Center (MPC, 2021a), PHAs defined as having a Minimum Orbit Intersection Distance (MOID) < 0.05 AU and H < 22.0. The MPC lists 2020 TB12 with MOID = 0.009 and H = 21.7, though JPL (2021) lists H as 22.16, just outside the PHA limit and the JPL value implies a diameter of ~108 m assuming a default NEO albedo of p_v = 0.20 (Warner et al., 2009).

333 usable images were collected with exposures limited to 8 s due to the sky motion of 24 arcsec/minute. Large variations in magnitude were obvious over a period no shorter than several minutes, so the individual images were stacked using *Astrometrica* into 35 groups comprising a maximum of 10 images in each to enhance the signal to noise ratio. Individual stacks contained exposures over a time span of no more than 90 s. It is apparent from the raw plot that there are 5 unequal maxima and 4 minima, Canopus manages to represent the points well with a period of 0.640 ± 0.004 h but the curve suggests the likelihood of some tumbling being present, with none of the maxima or minima repeating. From this reduction it is therefore expected to be rated as PAR = -1 (Non-Principal Axis rotation possible, but not conclusively) on the scale of Pravec et. al. (2005). The only previously reported result located for 2020 TB12 (Pravec, 2021) lists it with a rating of PAR = -2 (NPA rotation detected based on deviations from a single period but the second period is not resolved) from observations made between 2021 Jan 8 - 15 and gives P_1 = 0.6294 ± 0.0001 h with a second period P_2 = 0.41951 ± 0.00005 h. The current analysis is therefore in reasonable agreement with the primary period from the earlier study.

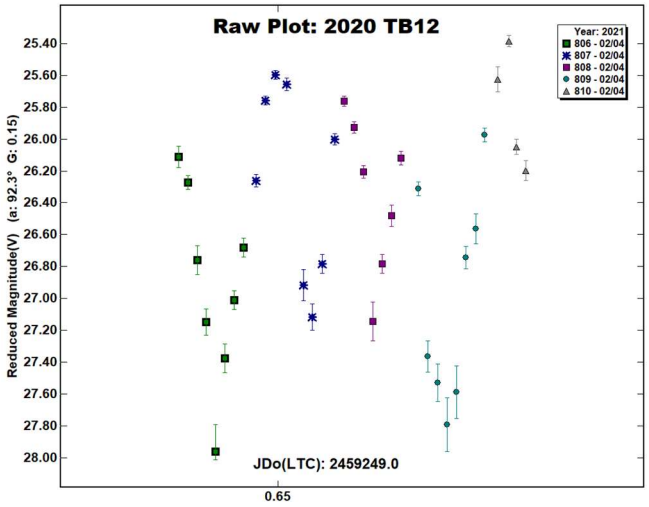

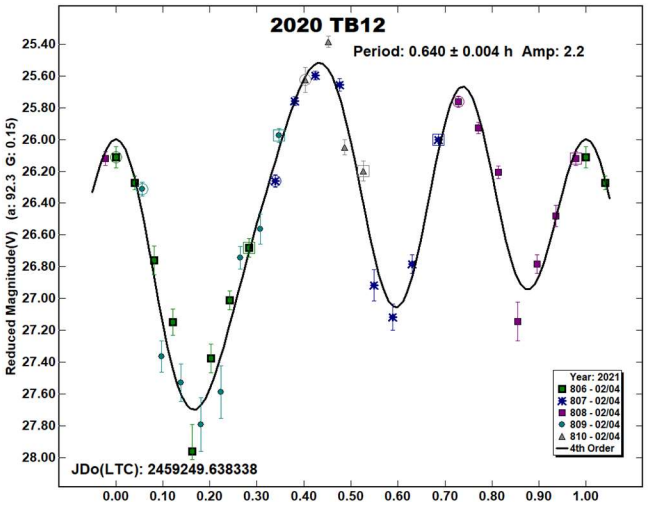

2020 YE5. This small, ~21 m diameter, Apollo object was discovered with the 6.5-m reflector at Las Campanas Observatory on 2020 Dec 18 (Sheppard et al., 2021) at mag +23 and made a close approach to 1.1 LD on 2021 Jan 22.6 UTC. It was followed during its approach, starting at 2021 Jan 21.87 UTC for 6.4 hours. During this interval its distance from Earth ranged from 2.0 to 1.6 LD and the apparent speed increased from 90 to 160 arcsec/min. Exposures were limited to a maximum of 4.1 s to keep trailing of the NEO within a 3-pixel radius annulus in *Astrometrica* and a total of 3237 measurements were made. The lightcurve is of low amplitude, implying a relatively spherical object or possibly pole-on aspect. Phase angle increased from 19° to 30° during the period observed.

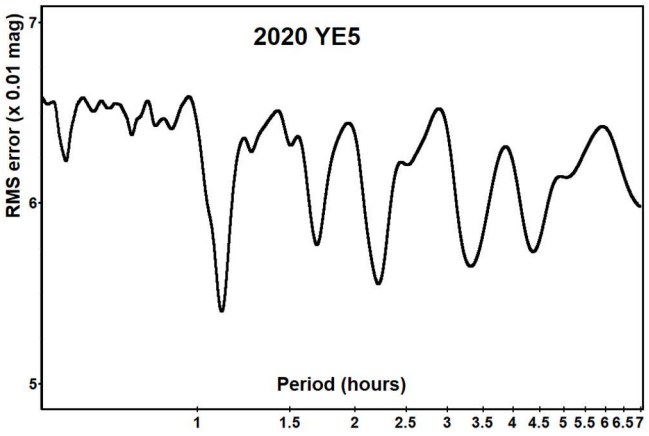

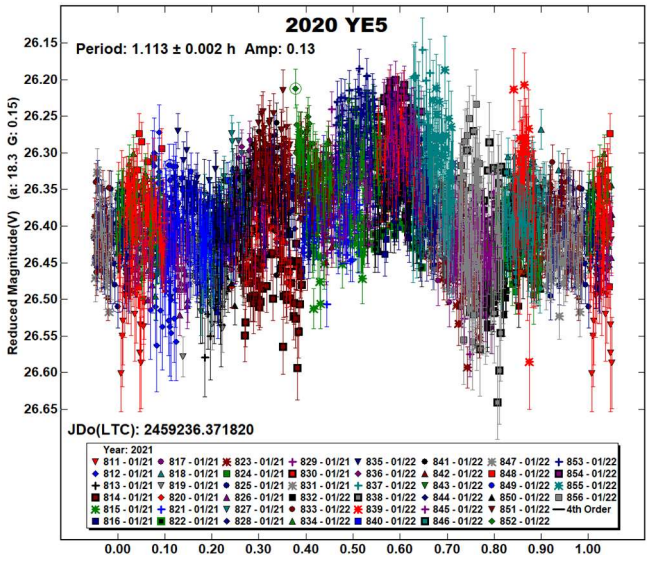

2021 AU. Another small (~39 m diameter) Apollo, discovered at 17th mag by the ATLAS 0.5-m reflector on Mauna Loa (Groeller et al., 2021) on 2021 Jan 4 and reached 15th mag during an approach to 3.5 LD on 2021 Jan 6.85 UTC. It was observed for 3 h at the point of closest approach, when the apparent speed was 114 arcsec/min and exposures were limited to 3.5 s to keep trailing short.

The raw plot from *MPO Canopus* shows 0.5 mag variations peaking every ~45 minutes and suggestive of a bimodal solution. However, the secondary maxima show significant differences in amplitude and shape of curve, especially on the descending slope, indicating that the body may be tumbling. A phased bimodal solution gives a period of 96 min, implying less than two rotations were observed, insufficient to resolve NPA rotation and so it is expected to be rated as PAR = -1.

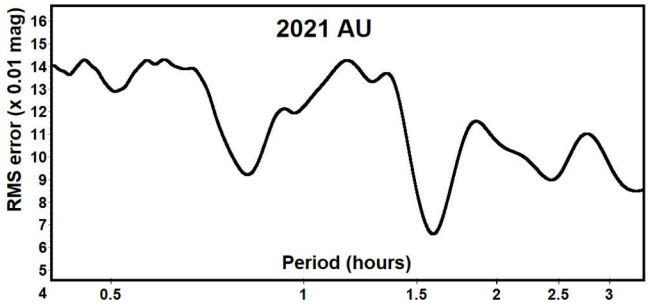

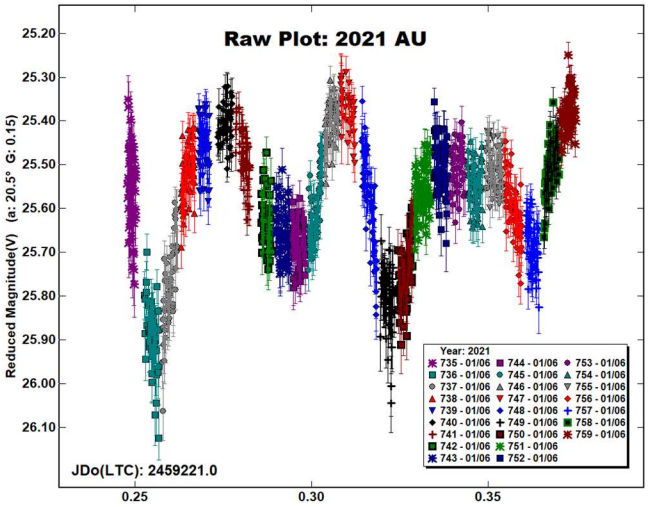

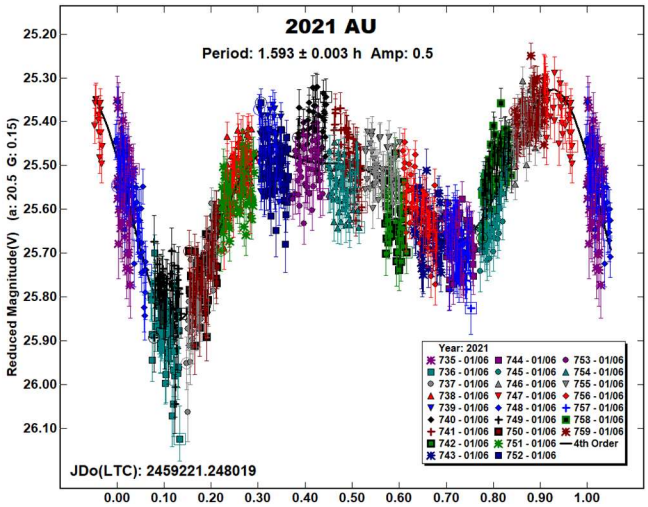

2021 CO. This was a discovery by the Catalina Sky Survey on 2021 Feb 5 (Wierzchos et al., 2021) and made a close approach to 0.95 LD on 2021 Feb 11.64 UTC. The SBDB (JPL, 2021) lists it with H = 25.3, implying a size of ~26 m. It was observed for 2.6 h from 2021 Feb 11.00 UTC when it was 14th mag and moving at 100+ arcsec/min, with exposures kept to a maximum length of 3.8 s.

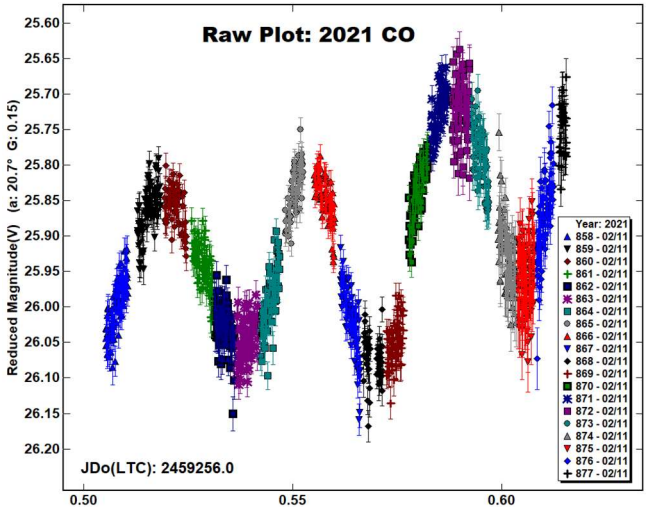

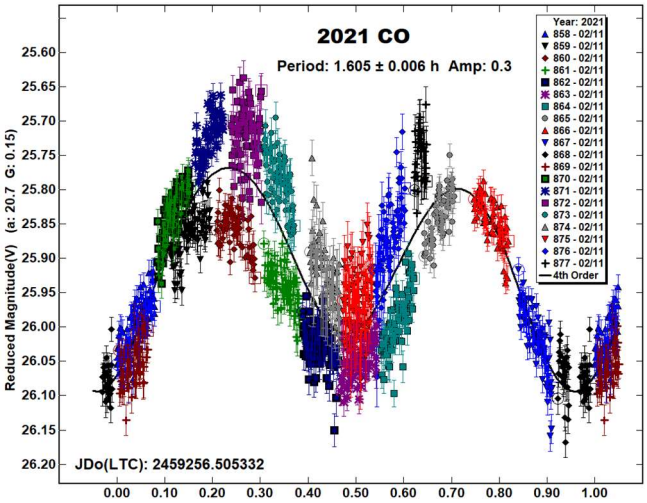

Strong variations are shown on the raw plot, but similarly to 2020 TB12 and 2021 AU, although a dominant periodic variation is evident, there are significant deviations from what would be expected if it were in simple principal axis rotation. The period of observation covers 3 maxima and minima, not enough to properly characterise the variations, therefore this is expected to be another candidate for rating as PAR = -1.

2021 DP. A ZTF team discovery from Palomar (Dupouy et al., 2021), this small ~14-m sized Apollo had passed Earth at 2.9 LD about 4 hours before discovery on 2021 Feb 18. It was under observation from Great Shefford for 61 minutes that same day, the telescope being repositioned five times due to the sky motion of 19 arcsec/min. Two hours later it was observed again for a period of 12 minutes. Large regular variations in brightness are evident in the raw plots from both periods of observation.

However, the height of maxima appears to vary semi-regularly and suggests the possibility of some non-principal axis rotation. The period spectrum indicates the dominant variation has a period of 0.11312 h and a phased plot labelled "PA rot. assumed" shows the resulting bimodal lightcurve assuming principal axis rotation, with significantly more scatter than the individual data point error bars would imply.

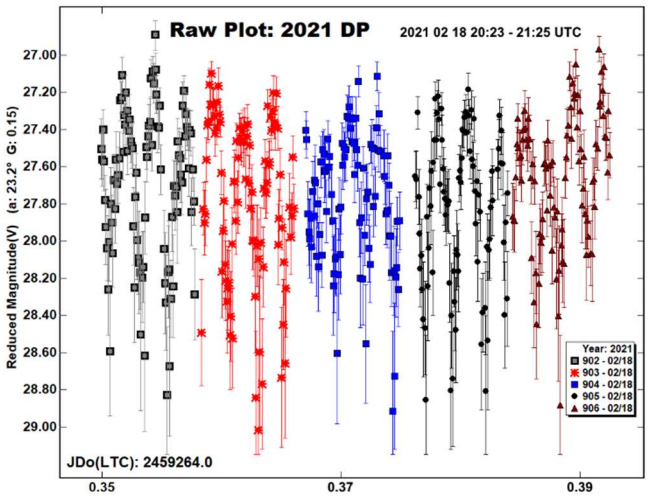

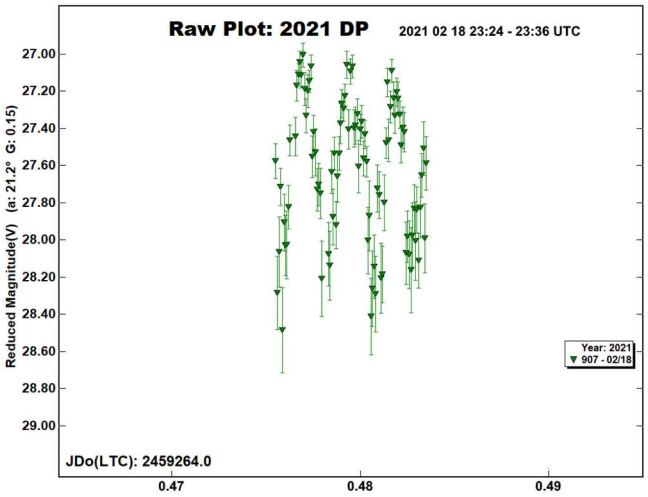

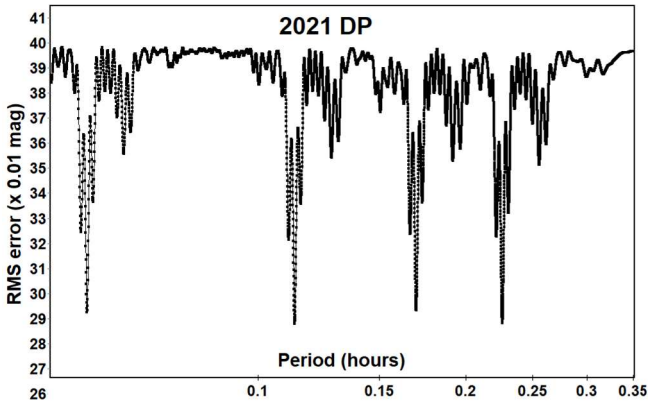

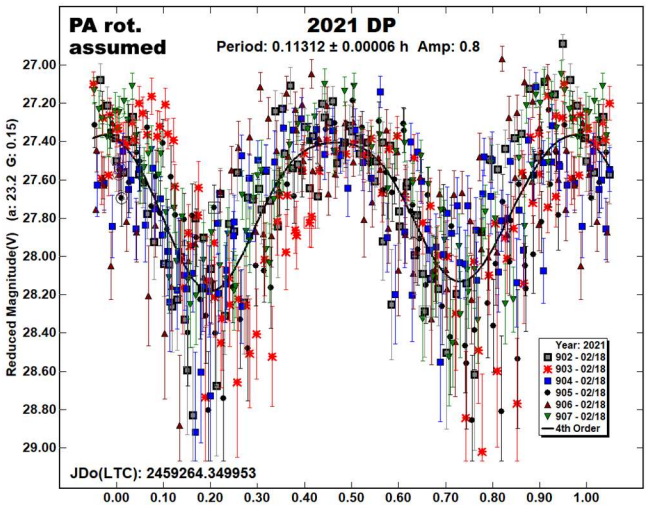

The Dual-Period Search function within *MPO Canopus* was used to see if removing the effect of the dominant lightcurve would reveal any residual NPAR periodicity. After several iterations the dominant variation was refined to 0.11297 ± 0.00004 h with an amplitude of 0.80 mags, and a second period revealed with an almost sinusoidal bimodal lightcurve with period 0.12831 ± 0.00008 h and amplitude 0.55 mags. Phased lightcurves are given for these, labelled P1 and P2.

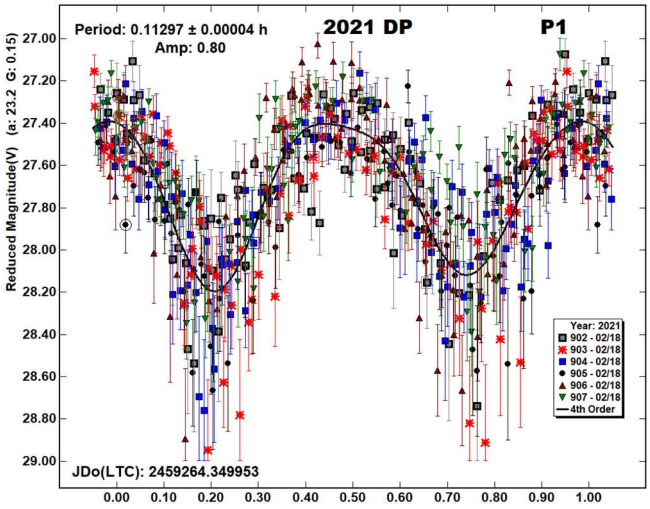

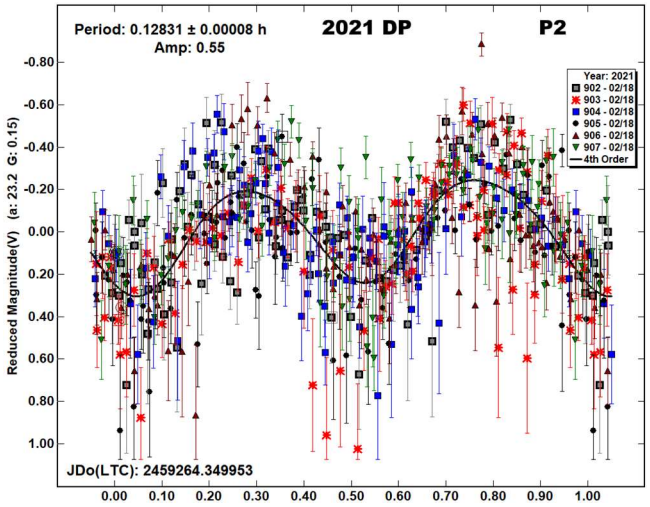

Although there is still a large amount of noise in the data points both periods are well resolved, helped by the large amplitudes and number of rotations covered. The *MPO Canopus* Dual Period Search is designed to find multiple periods in binary asteroid systems, not to determine lightcurve parameters for tumbling asteroids and the frequencies derived here may be linear combinations of the real frequencies, which would need a physical model of the NPA rotation to be constructed to properly resolve. However, this is expected to be rated as PAR = -3, i.e., NPA rotation reliably detected with the two periods resolved. There may be some ambiguities in one or both periods. (Petr Pravec, personal communication).

2021 DX1. This was a 17th mag discovery by the Catalina Sky Survey on 2021 Feb 20 (Bacci et al., 2021) which remained at a similar brightness for nearly two weeks following. With $H = 23.0$ it has an estimated diameter of ~75 m. 2021 DX1 was observed for 6.4 h starting 2021 Feb 25.9 UTC and 1087 16-s exposures were obtained. Conditions were poor, with the 98% illuminated Moon only 55° away, however, large amplitude variations over a period of tens of minutes were obvious during data collection. The raw plot shows regular variations but with significant differences in the shape of the curve and varying heights of maxima indicating non-principal axis rotation is likely.

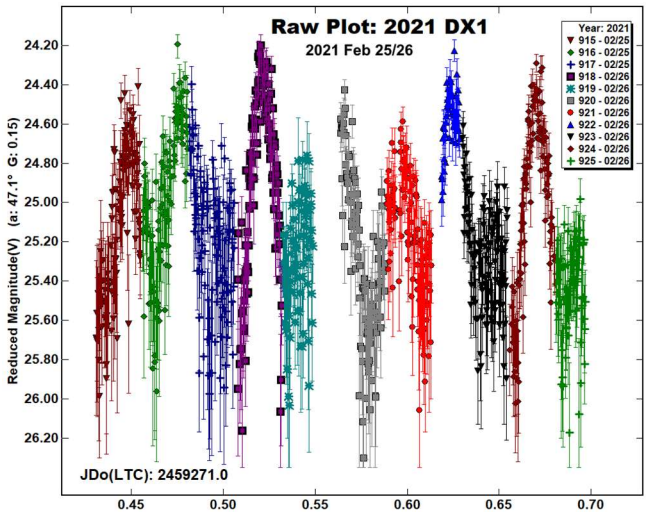

Assuming just principal axis rotation is present results in a period spectrum indicating a best fit period of 1.784 h and a bimodal phased lightcurve, labelled 'PA rot. assumed'.

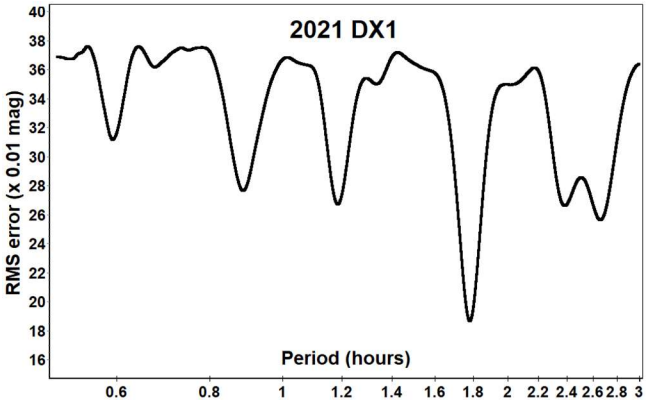

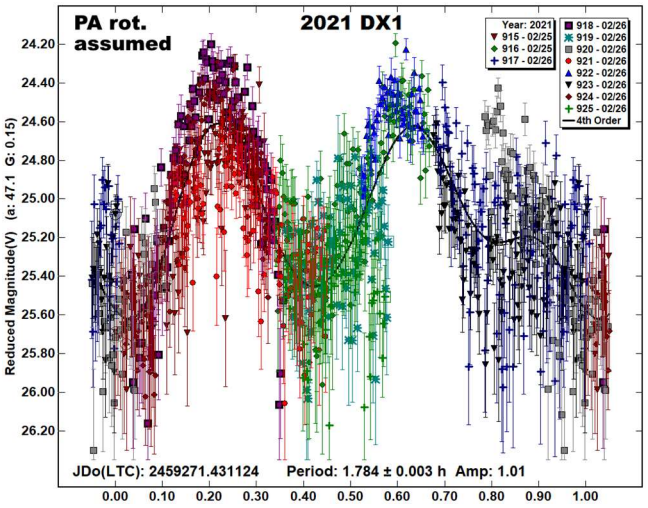

Using the *MPO Canopus* Dual-period search function designed for binary asteroids, to find one period, subtracting its effect to find a second period, then using that to refine the first period and repeating, the dominant 1 mag amplitude period was sharpened up to 1.782 h and a second period of 1.182 h revealed, with a 0.5 mag amplitude, these lightcurves labelled 'P1' and 'P2'.

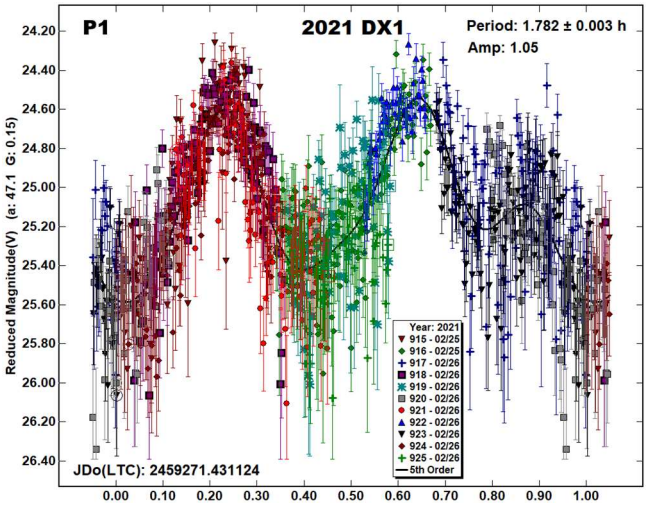

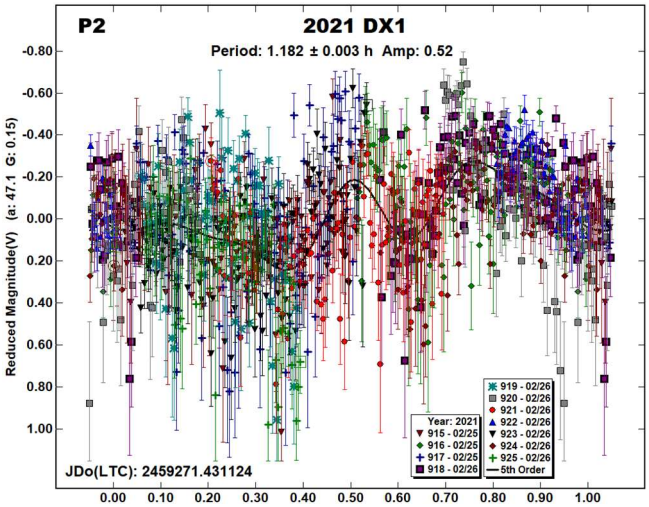

The raw lightcurve and 'PA rot. assumed' phased curve show evidence of NPA rotation and the 'P1' phased curve improves the fit of the data. However, the 2nd period is less well defined and it is expected that this will be rated as PAR = -2, i.e., NPA rotation detected based on deviations from a single period but the second period is not resolved. (Petr Pravec, personal communication).

The same issues with interpreting the *MPO Canopus* Dual-period search function for tumblers discussed for 2021 DP also apply here. It is also noted that it is likely the errors derived for the individual periods in a dual-period search are understated for tumbling objects as the periods are derived separately and sequentially, rather than the two being derived simultaneously within the same reduction.

With the large amount of noise present, especially in the P_2 curve, as an exercise, a separate determination was made by stacking the 1087 images to improve the signal to noise ratio. With both periods being > 1 h, a maximum of 10 contiguous images were combined, resulting in the longest effective elapsed time in a single data point being no greater than 2.7 minutes. Therefore, Integration time / Period = 0.04, less than the 0.185 value beyond which smearing of the lightcurve would be expected to occur (see Table I and Pravec et al., 2000). The stacking resulted in a total of 118 data points and these were used to generate equivalent plots to the unstacked reduction (raw, PA rot. assumed, P_1 and P_2), given here to demonstrate that although the underlying curves are easier to see in the stacked versions, there is no practical change to the results, differences between the best-fit periods in the stacked and unstacked results are insignificant.

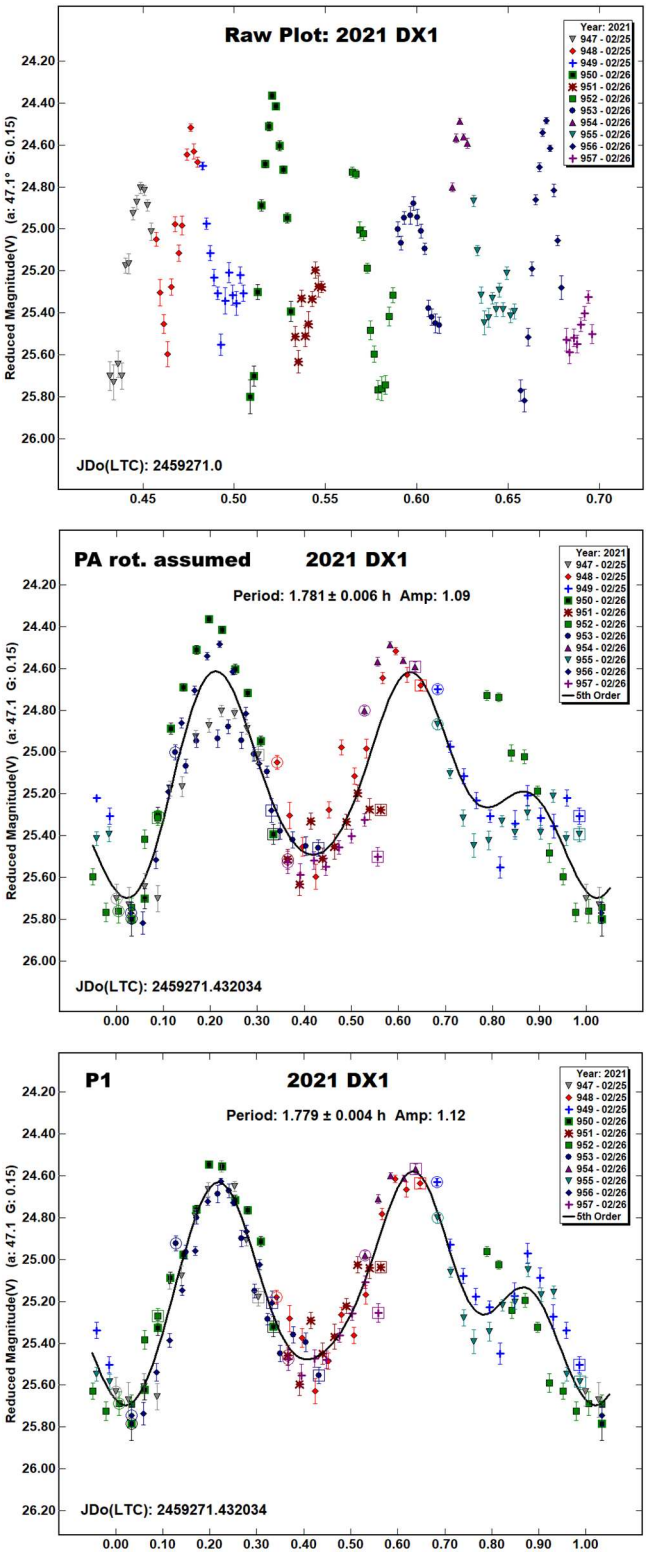

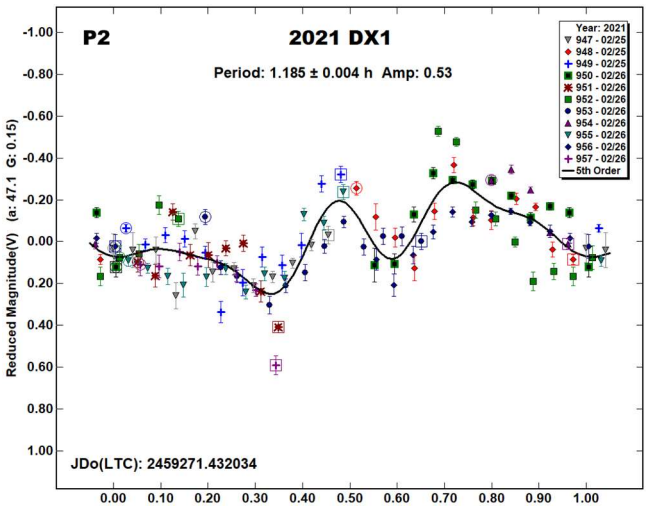

2021 DX1 is listed by Pravec (Pravec, 2021) with a rating of PAR = -3 (NPA rotation reliably detected with the two periods resolved) and gives P_1 = 1.18879 ± 0.00009 h and P_2 = 1.7678 ± 0.0002 h, from observations obtained between 2021 Mar 6-10, these periods being in good agreement with the results in this paper.

2021 EB1. This Apollo object, estimated diameter ~59 m was discovered by the Catalina Sky Survey at 19th mag on 2021 Mar 6 and announced with pre-discovery positions from Pan-STARRS1 and 2 dating back to 2021 Feb 10 (Melnikov et al., 2021). It passed Earth at 8.6 LD on 2021 Mar 11.2 UTC but due to increasing phase angle was predicted to be brightest 2 days beforehand at mag +18.8 (MPC, 2021c).

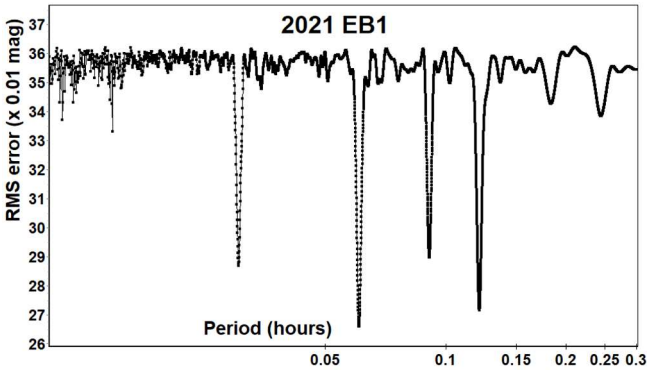

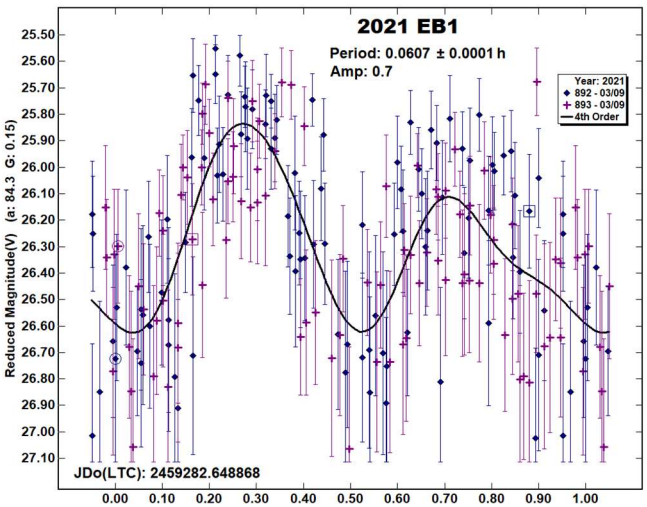

When observed on 2021 Mar 9.15 UTC it was showing large variations in magnitude, taking about 2 minutes to vary from peak to peak and at brightest was about 1 mag brighter than the ephemeris prediction. It was followed for 52 minutes and was visible throughout on individual 10-s exposures, though faint at minimum. The resulting phased lightcurve is noisy but shows a bimodal curve with a period of 3.6 minutes. It completed 14 revolutions during the period of observation.

2021 EX1. A 15th mag discovery from the Piszkés-tető Mountain Station of the Konkoly Observatory in Hungary on 2021 Mar 7.9 UTC (Foglia et al., 2021), 30 hours after passing Earth at 3 LD. Thanks to the speed with which the observers identified and reported their discovery and the effectiveness of the NEOCP system at the Minor Planet Center (MPC, 2021b), the first images at Great Shefford were obtained less than 20 minutes after the time of the first reported discovery position. Unfortunately, conditions soon deteriorated and a span of only 48 minutes of photometry was possible, with cloud interruptions. The next night 2021 EX1 had faded about 1 mag, but a more extensive set of images in better conditions was obtained. Solving the lightcurve using just the 85 measurements obtained on the first night results in a period of 0.1129 ± 0.0004 h and solving using the 475 measures from the second night gives a period of 0.1131 ± 0.0001 h. The phased lightcurve is the result of using all measures from both nights after making small adjustments to the zero points of the sessions over the two nights, with the RMS of those corrections being 0.058 mag.

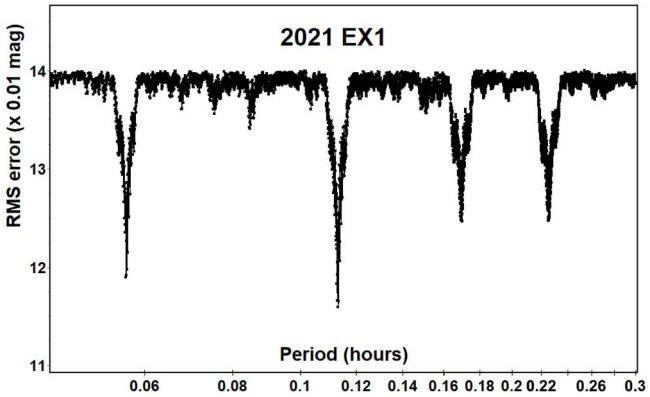

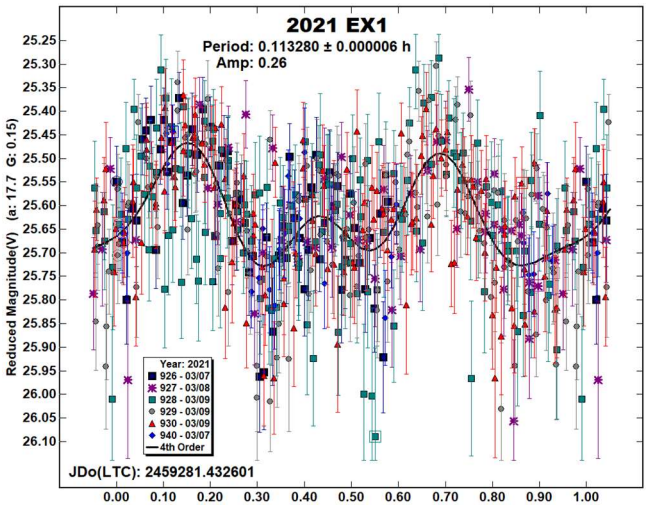

2021 FH. Another small (~14 m diameter) Apollo, discovered at Mt. Lemmon on 2021 Mar 18 (Brucker et al., 2021). 2021 FH passed Earth at 0.6 LD on 2021 Mar 23.7 UTC and was under observation from Great Shefford for 83 minutes starting at 2021 Mar 23.02 UTC when it was within 2 LD, its sky motion increased from 60 to 72 arcsec / min during the period. In case superfast rotation was present exposures were kept short, reducing from 6.5 to 5.6 s during the session, which also allowed for trailing of the target to be kept constant and within the measurement annulus in *Astrometrica*. A small amplitude, bimodal superfast rotation period of 63.5 s is evident and indicates that 78 revolutions occurred during the period of observation.

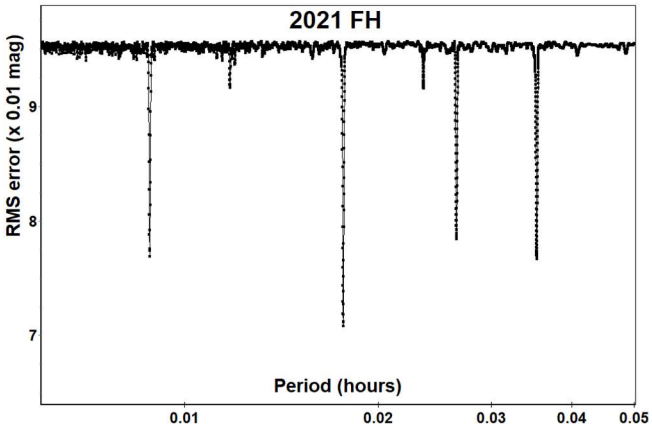

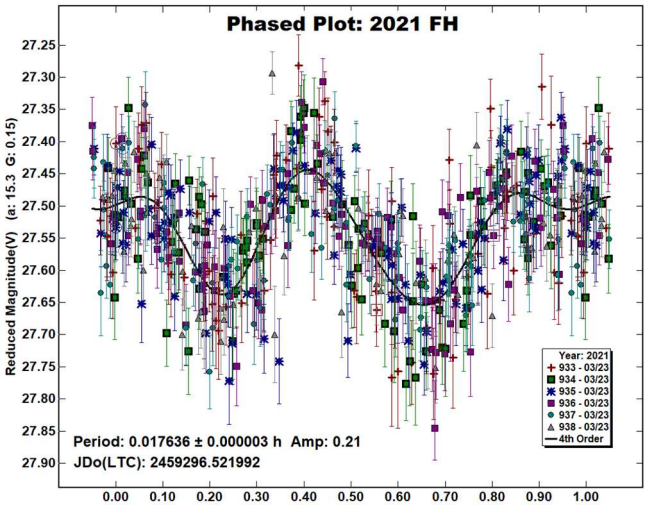

Acknowledgements

The author would like to thank Petr Pravec for his great help and much appreciated advice on the analysis of tumbling asteroids and to Brian Warner for his continued help and support.

The author also gratefully acknowledges a Gene Shoemaker NEO Grant from the Planetary Society (2005) and a Ridley Grant from the British Astronomical Association (2005) both of which facilitated upgrades to observatory equipment used in this study.

References

ADS (2021). Astrophysics Data System. *https://ui.adsabs.harvard.edu/*

Bacci, P.; Maestripieri, M.; Tesi, L.; Fagioli, G.; Groeller, H.; Christensen, E.J.; Farneth, G.A.; Fuls, D.C.; Gibbs, A.R.; Grauer, A.D.; Kowalski, R.A.; Larson, S.M.; Leonard, G.J.; Pruyne, T.A.; Rankin, D.; and 16 colleagues (2021). "2021 DX1." MPEC 2021-D75. *https://minorplanetcenter.net/mpec/K21/K21D75.html*

Brucker, M.J.; Bulger, J.; Lowe, T.; Schultz, A.; Willman, M.; Chambers, K.; Chastel, S.; de Boer, T.; Denneau, L.; Fairlamb, J.; Flewelling, H.; Huber, M.; Lin, C.-C.; Magnier, E.; Ramanjooloo, Y.; and 17 colleagues (2021). "2021 FH." MPEC 2021-F29. *https://minorplanetcenter.net/mpec/K21/K21F29.html*

Dupouy, P.; Bolin, B.T.; Bhalerao, V.; Copperwheat, C.M.; Deshmukh, K.P.; Hsu, C.-Y.; Lin, Z.-Y.; Purdum, J.; Royle, S.; Sharma, K.; Zhai, C.; Duev, D.A.; Lin, H.-W.; Masci, F.J.; Birtwhistle, P.; and 8 colleagues (2021). "2021 DP." MPEC 2021-D37. *https://minorplanetcenter.net/mpec/K21/K21D37.html*

Foglia, S.; Galli, G.; Buzzi, L.; Tichy, M.; Ticha, J.; Honkova, M.; Pettarin, E.; Robson, M.; Cloutier, W.; Leonard, G.J.; Gray, B.; Rankin, D.; Shelly, F.C.; Holmes, R.; Linder, T.; and 19 colleagues (2021). "2021 EX1." MPEC 2021-E67. *https://minorplanetcenter.net/mpec/K21/K21E67.html*

Groeller, H.; Christensen, E.J.; Farneth, G.A.; Fuls, D.C.; Gibbs, A.R.; Grauer, A.D.; Kowalski, R.A.; Larson, S.M.; Leonard, G.J.; Pruyne, T.A.; Rankin, D.; Seaman, R.L.; Shelly, F.C.; Wierzchos, K.W.; Bulger, J.; and 32 colleagues (2021). "2021 AU." MPEC 2021-A33. *https://minorplanetcenter.net/mpec/K21/K21A33.html*

Harris, A.W.; Young, J.W.; Scaltriti, F.; Zappala, V. (1984). "Lightcurves and phase relations of the asteroids 82 Alkmene and 444 Gyptis." *Icarus* **57**, 251-258.

Harris, A.W.; Young, J.W.; Bowell, E.; Martin, L.J.; Millis, R.L.; Poutanen, M.; Scaltriti, F.; Zappala, V.; Schober, H.J.; Debehogne, H.; Zeigler, K. (1989). "Photoelectric Observations of Asteroids 3, 24, 60, 261, and 863." *Icarus* **77**, 171-186.

JPL (2021). Small-Body Database Browser *https://ssd.jpl.nasa.gov/sbdb.cgi*

Kwiatkowski, T.; Buckley, D.A.H.; O'Donoghue, D.; Crause, L.; Crawford, S.; Hashimoto, Y.; Kniazev, A.; Loaring, N.; Romero Colmenero, E.; Sefako, R.; Still, M.; Vaisanen, P. (2010). "Photometric survey of the very small near-Earth asteroids with the SALT telescope - I. Lightcurves and periods for 14 objects." *Astronomy & Astrophysics* **509**, A94.

Mastaler, R.A.; Linder, T.; Holmes, R.; Bulger, J.; Lowe, T.; Schultz, A.; Willman, M.; Chambers, K.; Chastel, S.; de Boer, T.; Denneau, L.; Fairlamb, J.; Flewelling, H.; Huber, M.; Lin, C.-C.; and 18 colleagues (2020). "2020 TB12." MPEC 2020-W103. *https://minorplanetcenter.net/mpec/K20/K20WA3.html*

Name	Integration Times	Max intg./ Period	a/b	Min Points	Fields
2020 TB12	90$^{\Sigma}$	0.04	1.7	35	5
2020 YE5	1-4.1	0.001	1.1	3237	46
2021 AU	1.5,3.5	0.001	1.3	1321	25
2021 CO	2.9-3.8	0.001	1.2	1360	20
2021 DP	5.4,5.7	0.01	1.6	459	5
2021 DX1	16	0.004	1.4	1087	11
2021 EB1	10	0.05	1.2	194	2
2021 EX1	5,6,7	0.02	1.1	560	6
2021 FH	5.6-6.5	0.10	1.1	563	6

Table I. Ancillary information, listing the integration times used (seconds), the fraction of the period represented by the longest integration time (Pravec et al., 2000), the calculated minimum elongation of the asteroid (Kwiatkowski et al., 2010), the number of data points used in the analysis and the number of times the telescope was repositioned to different fields.
Note: Σ = Longest elapsed integration time for stacked images (start of first to end of last exposure used).

Name	yyyy mm/ dd	Phase		L_{PAB}	B_{PAB}	Period(h)	P.E.	Amp	A.E	PAR	H
2020 TB12	2021 02/04-02/04	92.4,92.2	138	47		0.640	0.004	2.2	0.1	-1	22.2
2020 YE5	2021 01/21-01/22	18.6,29.7	130	-9		1.113	0.002	0.13	0.07		25.8
2021 AU	2021 01/06-01/06	20.3,22.4	96	-2		1.593	0.003	0.5	0.1	-1	24.4
2021 CO	2021 02/11-02/11	20.8,25.7	131	-4		1.605	0.006	0.3	0.1	-1	25.3
2021 DP	2021 02/18-02/18	23.2,21.1	151	11		0.11297	0.00004	0.8	0.2	-3	26.6
						0.12831	0.00008	0.6	0.2		
2021 DX1	2021 02/25-02/26	47.2,45.7	170	21		1.782	0.003	1.1	0.1	-2	23.0
						1.182	0.003	0.5	0.2		
2021 EB1	2021 03/09-03/09	84.3,84.7	170	44		0.0607	0.0001	0.7	0.3		23.5
2021 EX1	2021 03/07-03/09	25.6,26.3	164	13		0.113280	0.000006	0.26	0.10		24.9
2021 FH	2021 03/23-03/23	15.2,13.9	177	4		0.017636	0.000003	0.21	0.05		26.7

Table II. Observing circumstances and results. Where two lines are given, these include two periods determined for NPA rotation. The phase angle is given for the first and last date. If preceded by an asterisk, the phase angle reached an extrema during the period. LPAB and BPAB are the approximate phase angle bisector longitude/latitude at mid-date range (see Harris et al., 1984). PAR is the expected Principal Axis Rotation quality detection code (Pravec et al., 2005) and H is the absolute magnitude at 1 au from Sun and Earth taken from the Small-Body Database Browser (JPL, 2021).

Melnikov, S.; Hoegner, C.; Laux, U.; Ludwig, F.; Stecklum, B.; Tichy, M.; Ticha, J.; Honkova, M.; Aschi, S.; Pettarin, E.; Wierzchos, K.W.; Christensen, E.J.; Farneth, G.A.; Fuls, D.C.; Gibbs, A.R.; and 36 colleagues (2021). "2021 EB1." MPEC 2021-E42. *https://minorplanetcenter.net/mpec/K21/K21E42.html*

MPC (2021a). MPC Database Search. *https://minorplanetcenter.net/db_search*

MPC (2021b). Minor Planet Center NEO Confirmation Page *https://www.minorplanetcenter.net/iau/NEO/toconfirm_tabular.html*

MPC (2021c). Minor Planet Center Minor Planet Ephemeris Service. *https://minorplanetcenter.net/iau/MPEph/MPEph.html*

Pravec, P.; Hergenrother, C.; Whiteley, R.; Sarounova, L.; Kusnirak, P.; Wolf, M. (2000). "Fast Rotating Asteroids 1999 TY2, 1999 SF10, and 1998 WB2." *Icarus* **147**, 477-486

Pravec, P.; Harris, A.W.; Scheirich, P.; Kušnirák, P.; Šarounová, L.; Hergenrother, C.W.; Mottola, S.; Hicks, M.D.; Masi, G.; Krugly, Yu.N.; Shevchenko, V.G.; Nolan, M.C.; Howell, E.S.; Kaasalainen, M.; Galád, A.; and 5 colleagues. (2005). "Tumbling Asteroids." *Icarus* **173**, 108-131.

Pravec, P. (2021). "Prepublished periods of asteroids." *http://www.asu.cas.cz/~ppravec/newres.htm*

Raab, H. (2018). *Astrometrica* software, version 4.12.0.448. *http://www.astrometrica.at/*

Sheppard, S.S.; Tholen, D.J.; Mastaler, R.A.; Wells, L. (2021). "2020 YE5." MPEC 2021-A05. *https://minorplanetcenter.net/mpec/K21/K21A05.html*

Warner, B.D.; Harris, A.W.; Pravec, P. (2009). "The Asteroid Lightcurve Database." *Icarus* **202**, 134-146. Updated 2020 Oct. *http://www.MinorPlanet.info/lightcurvedatabase.html*

Warner, B.D. (2021). MPO Software. *MPO Canopus*, v. 10.8.4.2. Bdw Publishing, Eaton, CO. *http://minorplanetobserver.com*

Wierzchos, K.W.; Christensen, E.J.; Farneth, G.A.; Fuls, D.C.; Gibbs, A.R.; Grauer, A.D.; Groeller, H.; Kowalski, R.A.; Larson, S.M.; Leonard, G.J.; Pruyne, T.A.; Rankin, D.; Seaman, R.L.; Shelly, F.C.; James, N.; and 15 colleagues (2021). "2021 CO." MPEC 2021-C34. *https://minorplanetcenter.net/mpec/K21/K21C34.html*

NEAR-EARTH ASTEROID LIGHTCURVE ANALYSIS AT THE CENTER FOR SOLAR SYSTEM STUDIES: 2021 JANUARY - MARCH

Brian D. Warner
Center for Solar System Studies / MoreData!
446 Sycamore Ave.
Eaton, CO 80615 USA
brian@MinorPlanetObserver.com

Robert D. Stephens
Center for Solar System Studies / MoreData!
Rancho Cucamonga, CA

(Received: 2021 April 15)

Lightcurves of 20 Near-Earth asteroids (NEAs) obtained at the Center for Solar System Studies (CS3) from 2021 January through March were analyzed for rotation period, peak-to-peak amplitude, and signs of satellites or tumbling.

CCD photometric observations of 20 near-Earth asteroids (NEAs) were made at the Center for Solar System Studies (CS3) from 2021 January through March. Table I lists the telescopes and CCD cameras that were combined to make observations.

Up to nine telescopes can be used for the campaign, although seven is more common. All the cameras use CCD chips from the KAF blue-enhanced family and so have essentially the same response. The pixel scales ranged from 1.24-1.60 arcsec/pixel.

Telescopes	Cameras
0.30-m *f*/6.3 Schmidt-Cass	FLI Microline 1001E
0.35-m *f*/9.1 Schmidt-Cass	FLI Proline 1001E
0.40-m *f*/10 Schmidt-Cass	SBIG STL-1001E
0.40-m *f*/10 Schmidt-Cass	
0.50-m *f*/8.1 Ritchey-Chrétien	

Table I. List of available telescopes and CCD cameras at CS3. The exact combination for each telescope/camera pair can vary due to maintenance or specific needs.

All lightcurve observations were unfiltered since a clear filter can cause a 0.1-0.3 mag loss. The exposure duration varied depending on the asteroid's brightness and sky motion. Guiding on a field star sometimes resulted in a trailed image for the asteroid.

Measurements were made using *MPO Canopus*. The Comp Star Selector utility in *MPO Canopus* found up to five comparison stars of near solar-color for differential photometry. To reduce the number of times and amounts of adjusting nightly zero points, we use the ATLAS catalog r´ (SR) magnitudes (Tonry et al., 2018). Those adjustments are usually $|\Delta| \leq 0.03$ mag. The larger corrections, which are rare, may have been related in part to using unfiltered observations, poor centroiding of the reference stars, and not correcting for second-order extinction. Another cause may be selecting what appears to be a single star but is actually an unresolved pair.

The Y-axis values are ATLAS SR "sky" (catalog) magnitudes. The two values in the parentheses are the phase angle (a) and the value of *G* used to normalize the data to the comparison stars used in the earliest session. This, in effect, had all the observations made at a single fixed date/time and phase angle, leaving any variations due only to the asteroid's rotation and/or albedo changes. The X-axis shows rotational phase from –0.05 to 1.05. If the plot includes the amplitude, e.g., "Amp: 0.65", this is the amplitude of the Fourier model curve and *not necessarily the adopted amplitude for the lightcurve*.

"LCDB" refers to Warner et al. (2009) from here on.

5879 Almeria. Warner (2017) found a period of 13.67 h based on a noisy sparse data set from 2017. Our 2021 data set (1,500 data points over 19 days) led to $P = 21.967$ h. The period spectrum using the 2021 data confirms an essentially zero chance for 13.7 h.

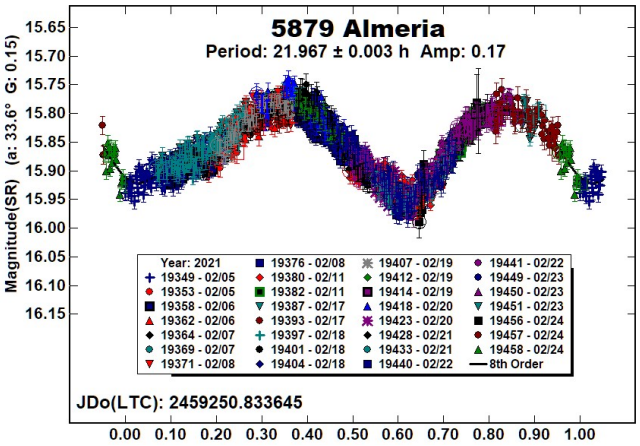

(65717) 1993 BX3. Mottola et al. (1995) found a period of 20.463 h for this 200-m NEA. Pravec et al. (2020web) reported 20.294 h. Our result is in good agreement with those earlier reports.

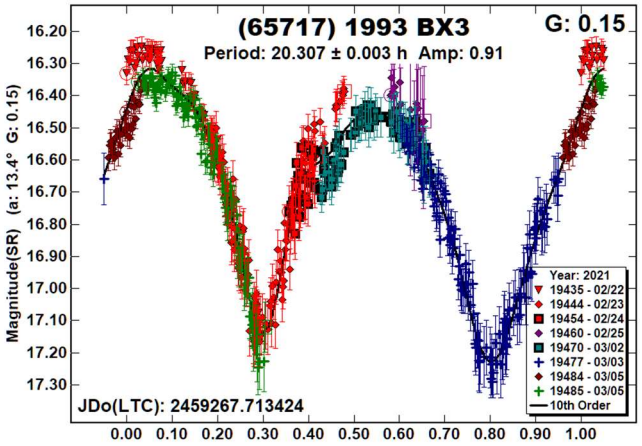

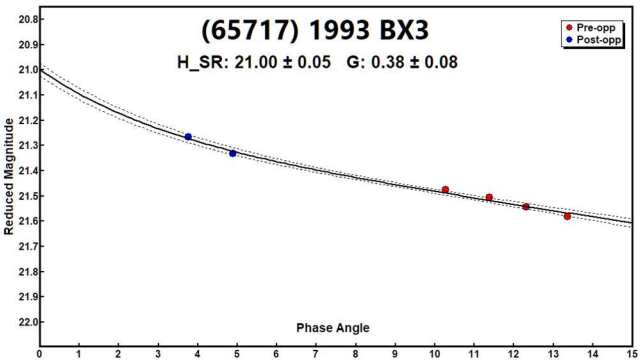

During period analysis, we found using the default of $G = 0.15$ produced an ill-fitting lightcurve. Our data covered a sufficient range of phase angles to find a new value of $G_{SR} = 0.38$. When this value was used, almost no or very small zero-point adjustments were required to produce a clean-fitting lightcurve. Assuming V-SR = 0.22 (Warner and Stephens, 2021), gives $H = 21.22$. The MPCORB catalog gives $H = 20.7$.

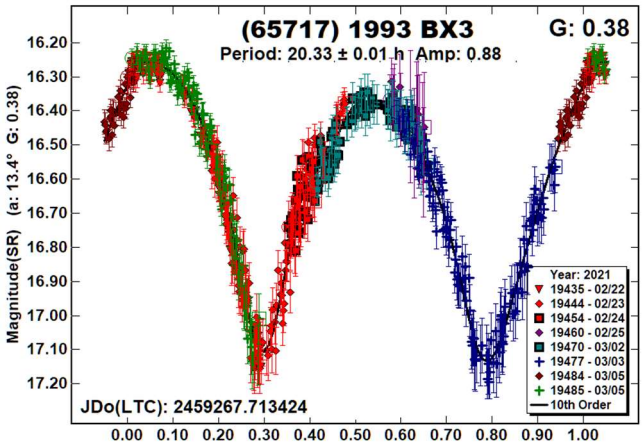

99942 Apophis. The tumbling state of Apophis was well-studied by Pravec et al. (2014). They found the strongest lightcurve amplitude was in the second harmonic of $P_1 = (P\phi^{-1} - P\psi^{-1})^{-1} = 30.56$ h. The true periods for precession and rotation are $P\phi = 27.38$ h and $P\psi = 263$ h. Our data clearly show that the asteroid is tumbling and that our result of the dominant period found by *MPO Canopus* closely matches Pravec et al. (2014).

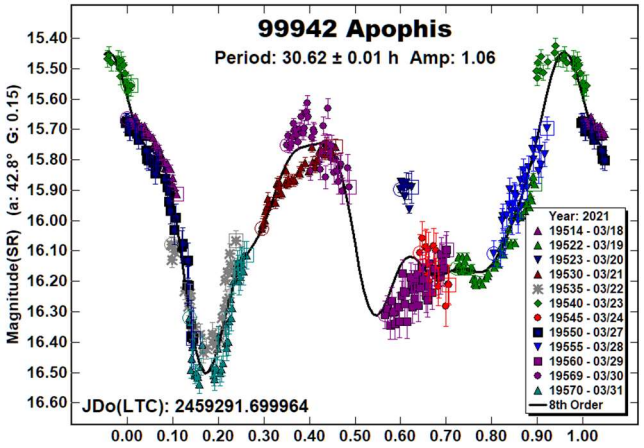

(162186) 1999 OP3. With such a flat lightcurve, our result could be the result of the Fourier analysis latching onto noise and so the period of 8.36 h is highly questionable.

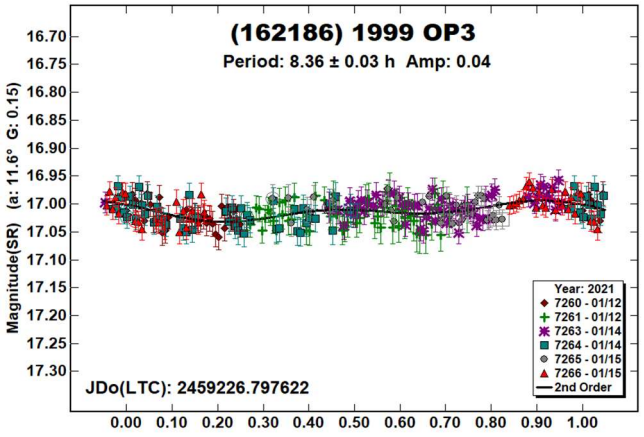

(164201) 2004 EC. Galad and Kornos (2008) found a period of 6.642 h. The period spectrum based on our data shows a weak solution near that result as well as several strong possibilities. We adopted $P = 3.909$ h, which produced a bimodal lightcurve. With such a low amplitude, a mono- or multimodal lightcurve is possible as well (Harris et al., 2014). The asymmetry of the bimodal lightcurve proved helpful in rejecting those other solutions.

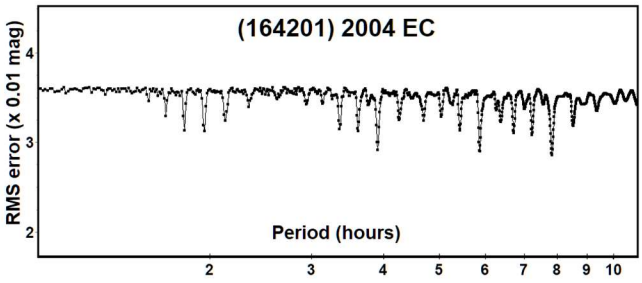

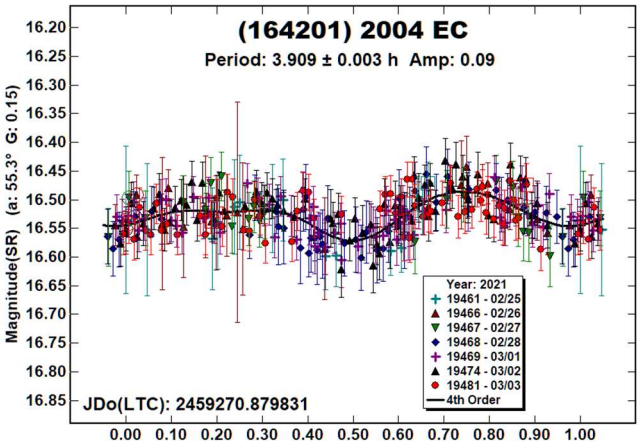

(206359) 2003 QM47. There were no previous results in the LCDB for this 750-m NEA. Despite the noisy data, we were able to find a reasonably reliable period of 45.8 h. We also tried other periods that were nearly commensurate with an Earth day. The resulting lightcurves were considered implausible.

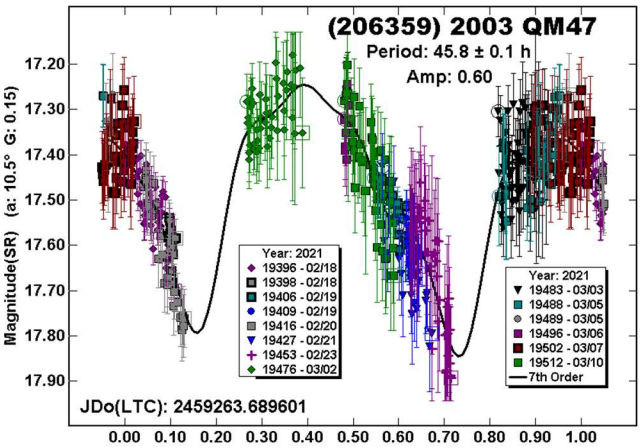

(216707) 2004 XP164. We observed this 950-m NEA for two nights. The combined lightcurve, with a single period solution, shows good overlap from the two nights in some places but considerable difference in others. Given the size and dominant period of 15.5 h, tumbling is possible, bordering on likely (Pravec et al., 2005; 2014). However, also possible is that the shape of the

lightcurve changed dramatically as the phase angle decreased from 21° to 9°. Splitting the data into individual nights shows a good fit to a single period for the February data (15.483 h). The January data set gave P = 15.52 h but wasn't able to cover a full lightcurve.

Whether or not the asteroid is in a tumbling state cannot be confirmed from our data set alone. Unfortunately, the next time 2004 XP164 is V < 18 is not until 2037 January, when it will be V ~ 17.2 at a Declination of -6°.

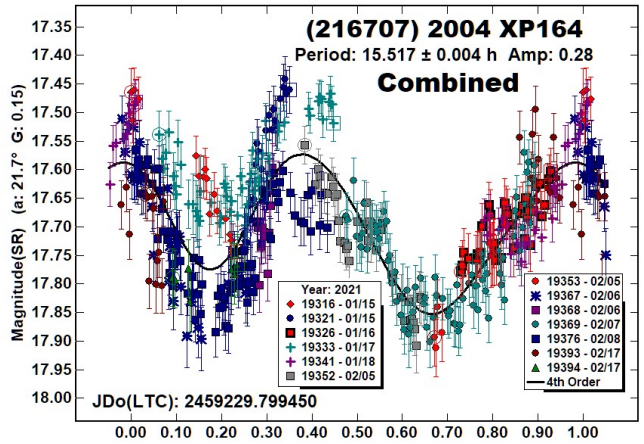

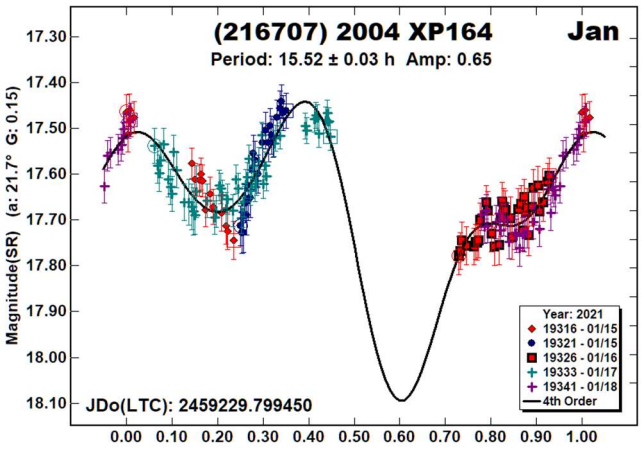

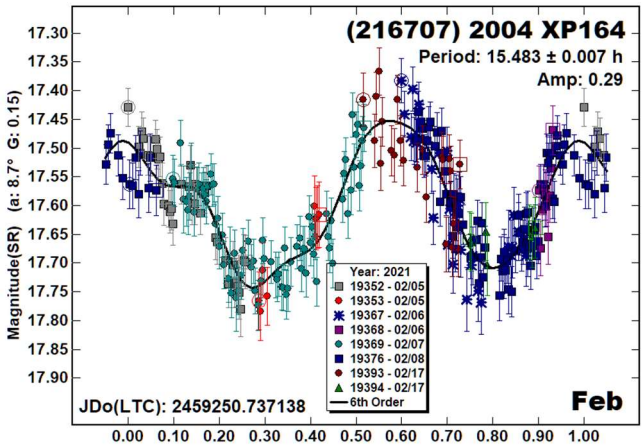

(332446) 2008 AF4. The shape of the lightcurve for this 350-m NEA also changed dramatically over the range of our observations. This is clearly shown when trying to plot the full data set to a single period. The large phase angles probably allowed shadowing effects to influence the lightcurve shape, being trimodal in the combined and Jan 9-10 plots but almost quadrimodal for Jan 11.

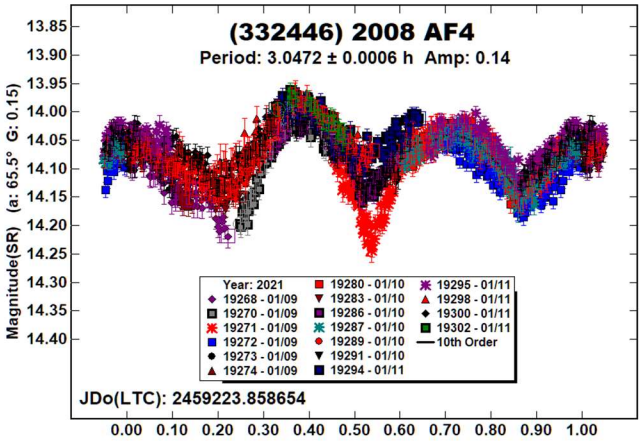

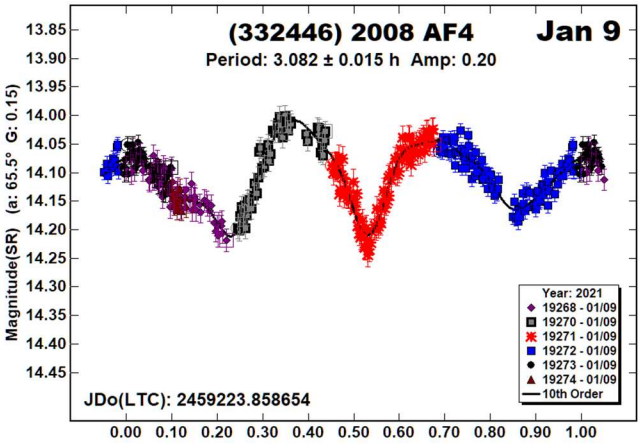

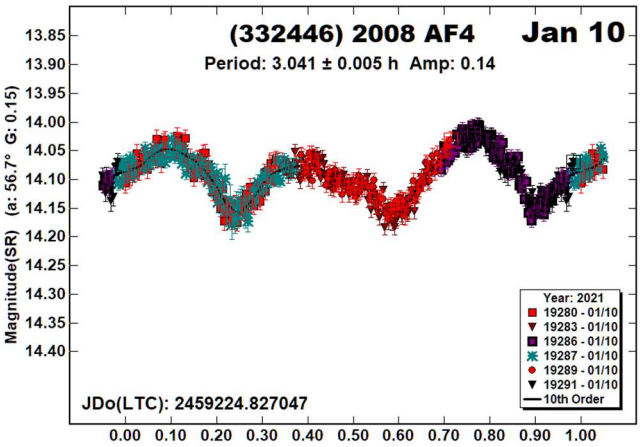

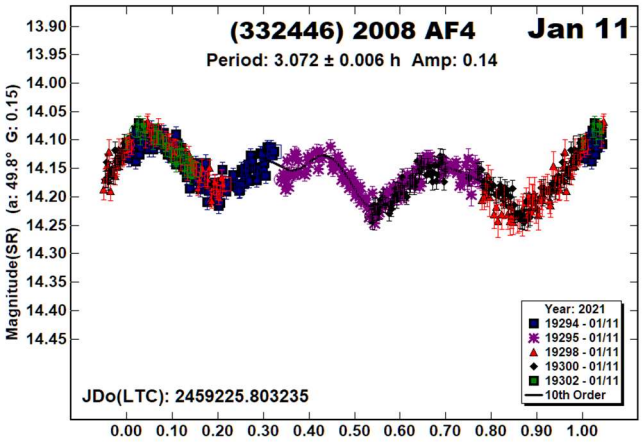

Splitting the data set into separate nights shows that the sidereal period decreased as the phase angle decreased. This is usually interpreted to mean that the asteroid rotation is prograde.

(380359) 2002 TN30. The estimated diameter for 2002 TN30 is 1 km. There were no previous entries in the LCDB. While the lightcurve shape is asymmetrical, no other period produced a plausible lightcurve.

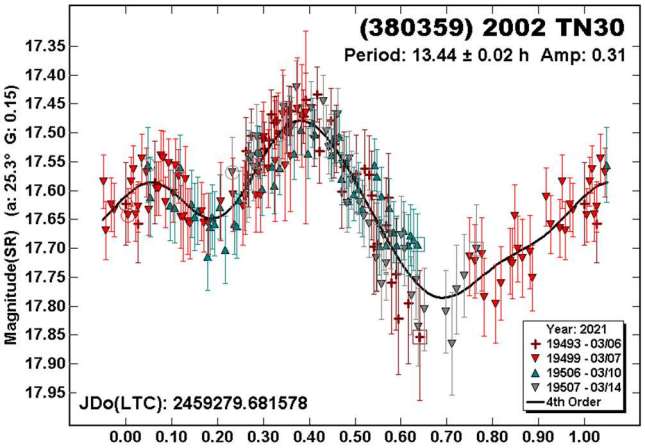

(415029) 2011 UL21. Warner (2018a) found an unreliable (U = 1) period of 1.562 h in 2017. The amplitude at that time was very low. However, observations six months later (Warner, 2018b) revealed a lightcurve with 0.32 mag amplitude and reliable period of 2.732 h. The 2021 data also produced an unreliable solution because of low amplitude. It's worth noting that the 3.31 and 2.732 h periods have a very close to 6:5 ratio.

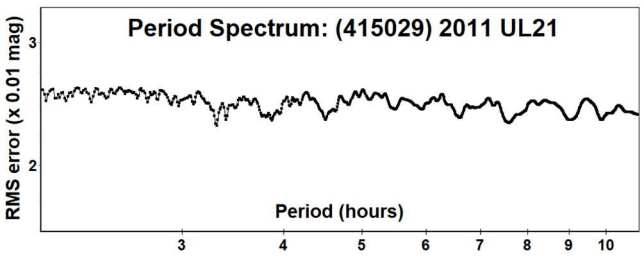

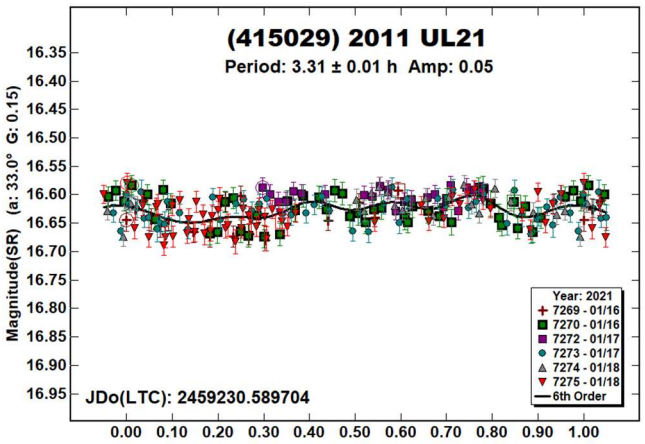

(438902) 2009 WF104. There were no previously reported rotation periods in the LCDB. Using the default albedo of 0.2 and the MPCORB $H = 17.3$ gives a diameter of 1.03 km. However, Mainzer et al. (2019) using WISE data and $H = 17.2$ found $D = 2.23$ km. This leads to a derived albedo of 0.047, which is notably darker than the typical NEA with a taxonomic class in the S complex. Such presumed interlopers are not unexpected.

The raw plot of the data shows seemingly good evidence that the asteroid is tumbling. This highly likely based on the derived period and diameter (Pravec et al., 2005; 2014). *MPO Canopus* could find only the dominant period, which is possibly the second-order harmonic of the rotation and precession frequencies (see the discussion for 99942 Apophis above).

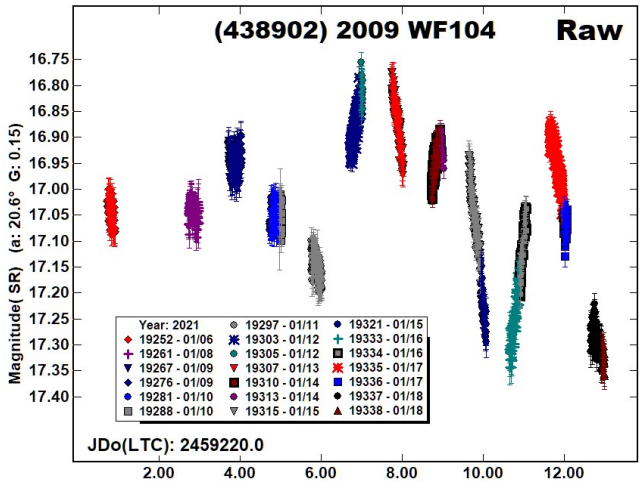

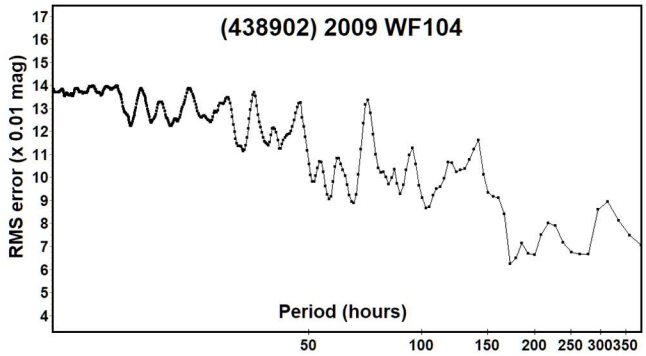

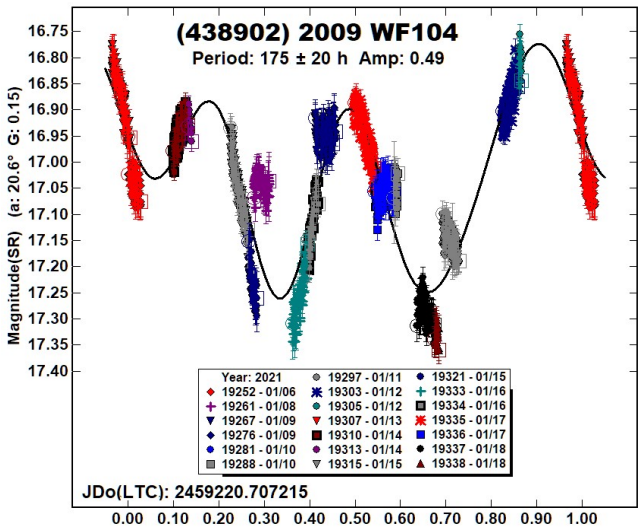

A follow-up campaign involving several observers is unlikely: the asteroid remains V < 19.5 through 2050.

2003 YM1. The estimated diameter for 2003 YM1 is 750 m. There were no previously reported periods in the LCDB.

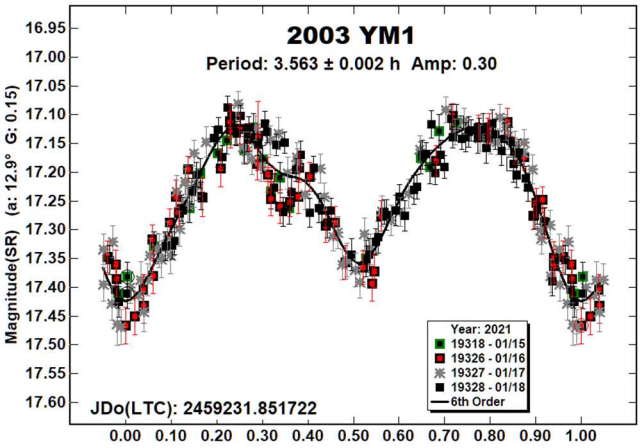

2003 AF23. There were no previous entries in the LCDB for this 180-m asteroid. It's size and the dominant period near 20 h make this a likely tumbling asteroid candidate (Pravec et al., 2014; 2005).

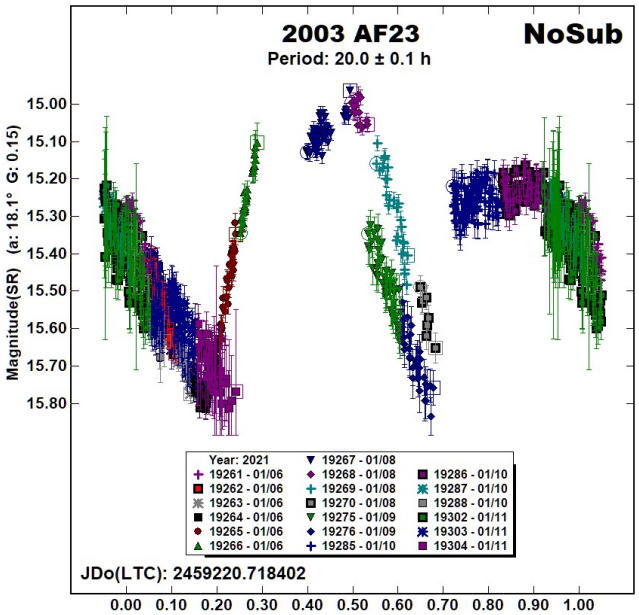

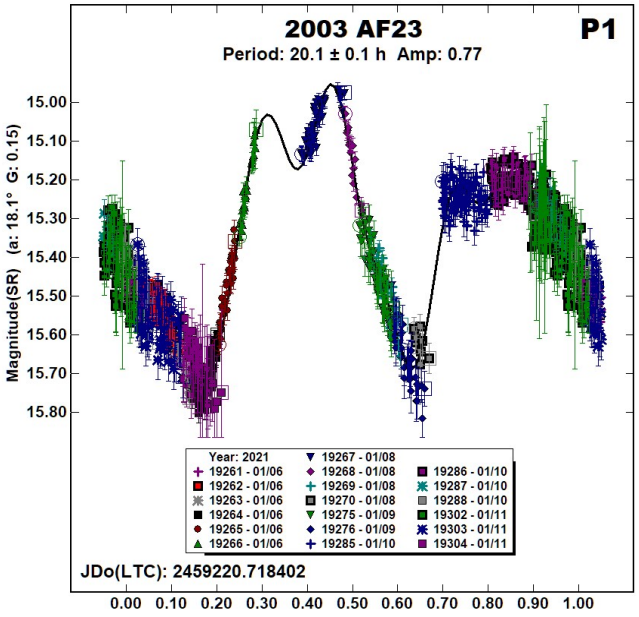

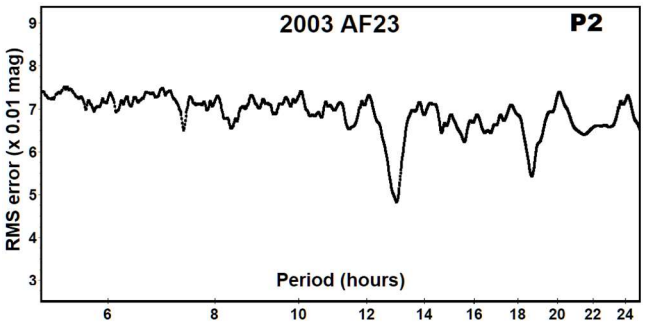

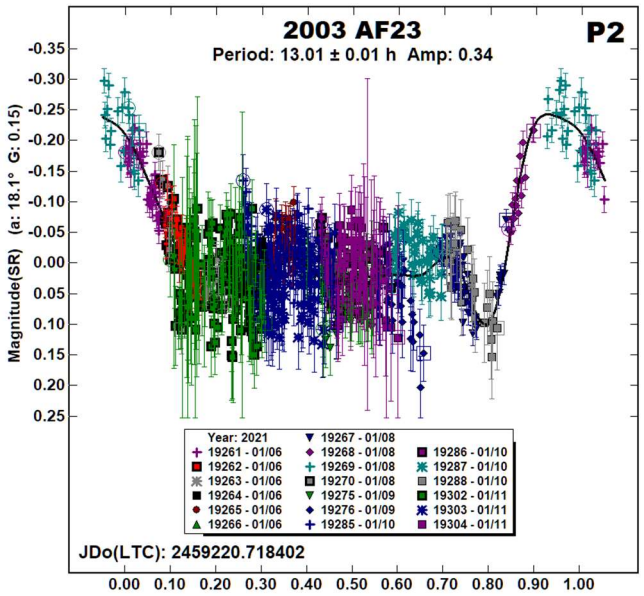

The "NoSub" plot shows that a single period solution was not going to be possible. We tried the dual-period search in *MPO Canopus* despite it not being able to handle tumbling asteroids properly. This led to a dominant period of 20.1 h but even so, the fit of the data to the model curve is marginal. The lightcurve for the second period of 13.01 h seems physically improbable, leaving it and the dominant period to be harmonics of the true periods of precession and rotation, or some unexplained systematic problem.

2004 QD3. Despite the noisy data set we were able to find a secure a result of 13.58 h for this 400-m NEA. The observations covered a sufficient range of phase angles to allow finding the H-G parameters.

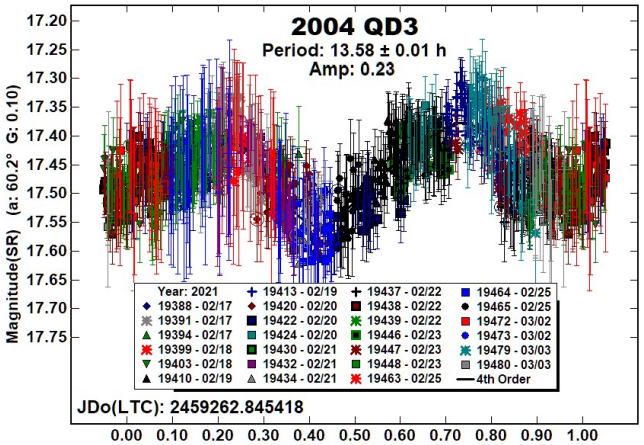

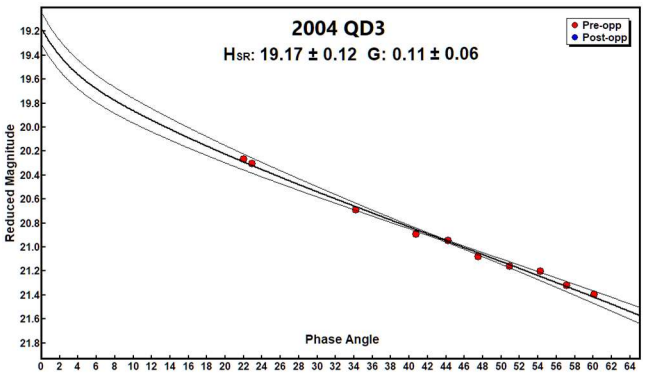

Assuming V-SR = 0.22 (Warner and Stephens, 2021) gives $H = 19.39$. This is very close to the MPCORB $H = 19.4$.

The value for G is on the lower end of those allowed for S-type asteroids. However, it's also well within the range of those for C-type asteroids (Warner et al, 2009). Barring spectroscopic or multi-color observations, the taxonomic class is uncertain. Since the average albedos for the two classes differ by 0.16, the actual diameter could range from 400 m (type S) to 700 m (type C) when using $H = 19.4$.

2008 BC22. The noisy and sparse data set for 2008 BC22, with an estimated diameter of 400 m, could produce only a marginally useful solution. Given the low phase angle and almost 0.3 mag amplitude, we opted for a bimodal lightcurve solution (Harris et al., 2014).

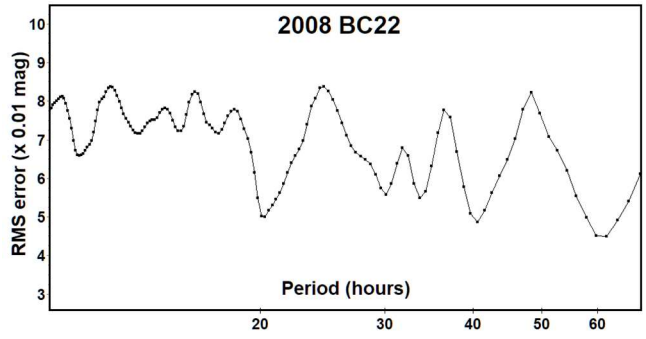

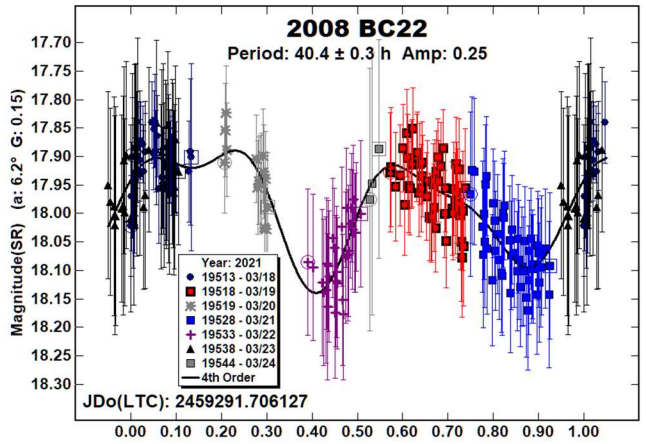

2015 AS45. Several Earth-day commensurate solutions were in the period spectrum. The lightcurve at 47.9 h is bimodal but a monomodal solution at 24 h is also possible. In that case, the amplitude would be significantly larger. The half-period (near 12 h) lightcurve was too shallow compared to the slopes of the raw data from individual nights.

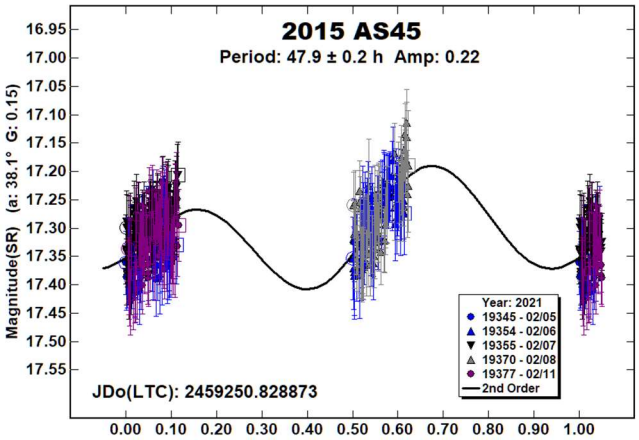

2018 PP10. Noise and low amplitude contributed to finding an uncertain solution of 6.91 h. The period spectrum showed some other, harmonically related, periods but we chose the period that gave the most probable lightcurve.

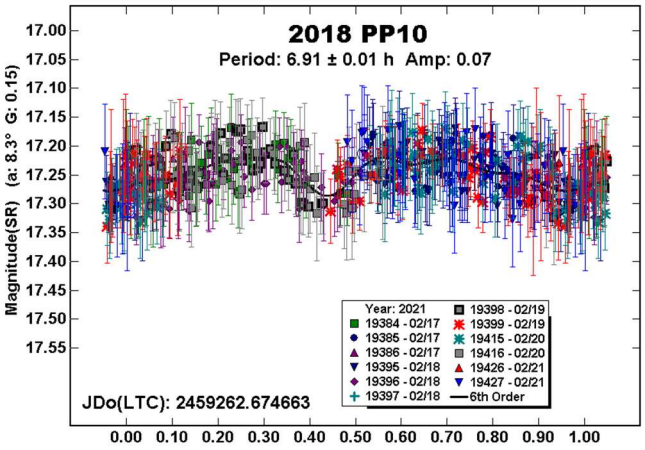

2020 WM3. There were no rotation periods found in the LCDB for the 500-m 2020 WM3. This is another asteroid with a period nearly commensurate with an Earth day. The slopes of the Fourier curve at 11.60 h were similar to those for the data on individual nights. However, the half-period at 5.8 h with a monomodal lightcurve cannot be formally excluded.

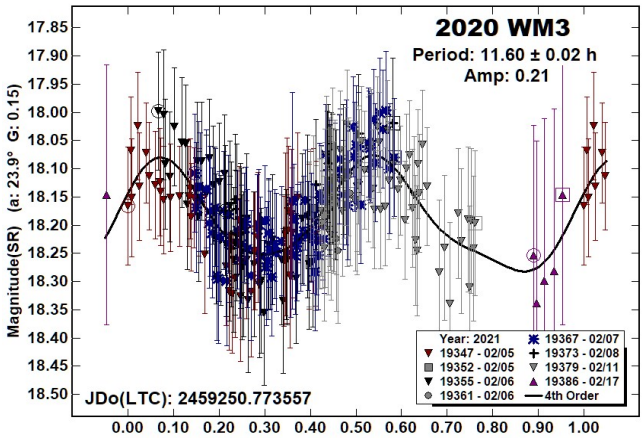

2020 YQ3. We observed 2020 YQ3 in 2021 from early to mid-January. The "NoSub" plot at a single period indicated that the asteroid was likely in a tumbling state.

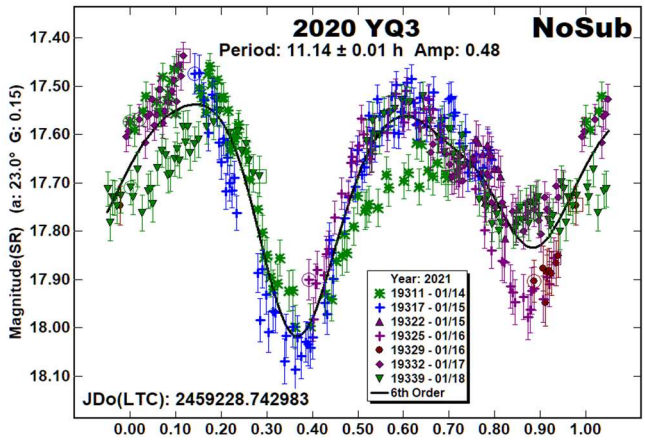

Even though *MPO Canopus* cannot properly handle tumbling asteroids, we tried the dual-period search feature since it seemed that there a was a strong dominant period in the data.

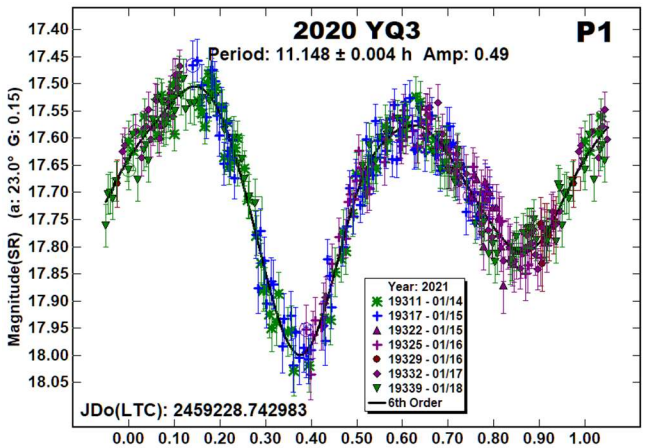

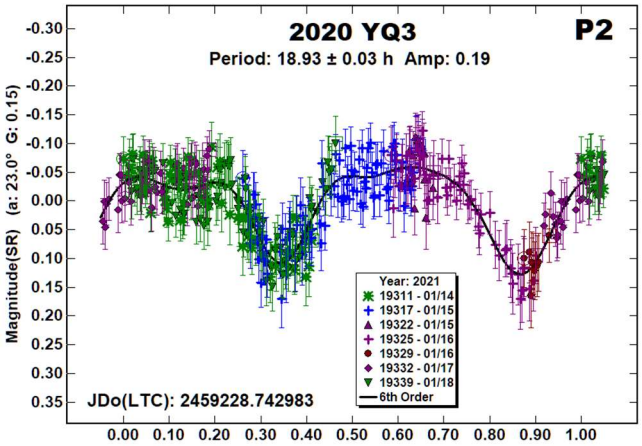

Our analysis led to P_1 = 11.148 h and P_2 = 18.93 h. Both produced good fits of the data to the Fourier curve. However, because of the limitations of the software, we forwarded our data to Petr Pravec, who incorporated our data with his obtained into mid-February. The combination of data from different longitudes and the proper software allowed him to find P_1 = 14.752 h and P_2 = 11.080 h (Pravec et al., 2021web), the latter being close to one of our periods.

Even his results should not be taken to be the definitive periods of precession and rotation. Their frequencies may be integral multiples of the ones derived here.

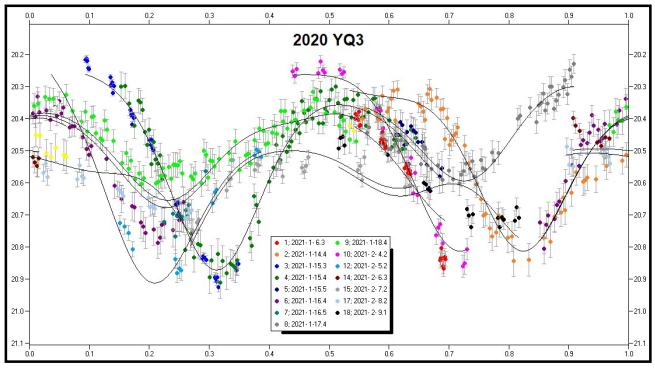

2021 DX1. Our data set led to a period of 1.189 h. However, there were signs of tumbling seen despite the noise.

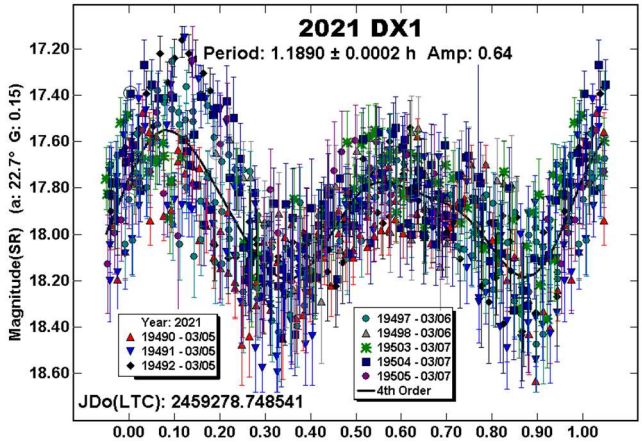

We sent our data to Petr Pravec (private communications) who confirmed that the asteroid was tumbling and that one probable period was 1.19 h. He was observing the asteroid at that time and hoped to find a more definitive result after analysis of his data.

Acknowledgements

Thanks to Petr Pravec, Ondrejov Observatory, Ondrejov, CZECH REPUBLIC, for his advice and reviewing our data of suspected tumbling asteroids. Funding for observations at CS3 and work on the asteroid lightcurve database (Warner et al., 2009) and ALCDEF database (*alcdef.org*) are supported by NASA grant 80NSSC18K0851. The authors gratefully acknowledge Shoemaker NEO Grants from the Planetary Society (2007, 2013). These were used to purchase some of the telescopes and CCD cameras used in this research.

This work includes data from the Asteroid Terrestrial-impact Last Alert System (ATLAS) project. ATLAS is primarily funded to search for near earth asteroids through NASA grants NN12AR55G, 80NSSC18K0284, and 80NSSC18K1575; byproducts of the NEO search include images and catalogs from the survey area. The ATLAS science products have been made possible through the contributions of the University of Hawaii Institute for Astronomy, the Queen's University Belfast, the Space Telescope Science Institute, and the South African Astronomical Observatory.

References

References from web sites should be considered transitory, unless from an agency with a long lifetime expectancy. Sites run by private individuals, even if on an institutional web site, do not necessarily fall into this category.

Galad, A.; Kornos, L. (2008). "A Sample of Lightcurves from Modra." *Minor Planet Bull*. **35**, 78-81.

Harris, A.W.; Young, J.W.; Scaltriti, F.; Zappala, V. (1984). "Lightcurves and phase relations of the asteroids 82 Alkmene and 444 Gyptis." *Icarus* **57**, 251-258.

Harris, A.W.; Pravec, P.; Galad, A.; Skiff, B.A.; Warner, B.D.; Vilagi, J.; Gajdos, S.; Carbognani, A.; Hornoch, K.; Kusnirak, P.; Cooney, W.R.; Gross, J.; Terrell, D.; Higgins, D.; Bowell, E.; Koehn, B.W. (2014). "On the maximum amplitude of harmonics on an asteroid lightcurve." *Icarus* **235**, 55-59.

Mainzer, A.; Bauer, J.; Cutri, R.; Grav, T.; Kramer, E.; Masiero, J.; Sonnett, S.; Wright, E.; Eds. (2019). "NEOWISE Diameters and Albedos V2.0." NASA Planetary Data System. urn:nasa:pds:neowise_diameters_albedos::2.0. *https://doi.org/10.26033/18S3-2Z54*

Mottola, S.; De Angelis, G.; Di Martino, M.; Erikson, A.; Hahn, G.; Neukum, G. (1995). "The near-earth objects follow-up program: First results." *Icarus* **117**, 62-70.

Pravec, P.; Wolf, M.; Sarounova, L. (2020web; 2021web). *http://www.asu.cas.cz/~ppravec/neo.htm*

Pravec, P.; Harris, A.W.; Scheirich, P.; Kušnirák, P.; Šarounová, L.; Hergenrother, C.W.; Mottola, S.; Hicks, M.D.; Masi, G.; Krugly, Yu.N.; Shevchenko, V.G.; Nolan, M.C.; Howell, E.S.; Kaasalainen, M.; Galád, A.; Brown, P.; Degraff, D.R.; Lambert, J.V.; Cooney, W.R.; Foglia, S. (2005). "Tumbling asteroids." *Icarus* **173**, 108-131.

Number	Name	2021 mm/dd	Phase	L_{PAB}	B_{PAB}	Period(h)	P.E.	Amp	A.E.
5879	Almeria	02/05-02/24	*33.7,30.0	164	8	21.967	0.003	0.17	0.02
65717	1993 BX3	02/22-03/05	13.5,4.0	160	-5	20.33	0.01	0.88	0.03
99942	Apophis	03/18-03/31	42.9,60.7	153	-8	30.62	0.01	1.06	0.05
162186	1999 OP3	01/12-01/15	11.6,9.9	128	6	8.36	0.03	0.04	0.01
164201	2004 EC	02/25-03/03	55.5,47.1	198	38	3.909	0.003	0.09	0.02
206359	2003 QM47	02/18-03/10	10.5,26.4	142	2	45.8	0.1	0.60	0.05
216707	2004 XP164	01/15-02/17	*20.9,13.9	138	5	15.517	0.004	0.37	0.06
		01/15-01/18	20.9,19.1	137	0	15.52	0.03	0.38	0.04
		02/05-02/17	8.7,13.9	139	0	15.483	0.007	0.32	0.03
332446	2008 AF4	01/09-01/11	65.5,49.8	139	7	3.0472	0.0006	0.14	0.02
		01/09	65.5	143	4	3.082	0.015	0.20	0.01
		01/10	56.7	140	6	3.041	0.005	0.14	0.01
		01/11	49.8	136	8	3.072	0.006	0.14	0.01
380359	2002 TN30	03/06-03/14	25.3,23.6	160	23	13.44	0.02	0.31	0.03
415029	2011 UL21	01/16-01/18	33.2,35.7	82	-5	3.31	0.01	0.05	0.02
438902	2009 WF104	01/06-01/18	20.6,29.2	116	21	175	20	0.52	0.10
	2003 YM1	01/15-01/18	12.9,12.2	126	-6	3.563	0.002	0.30	0.03
	2003 AF23	21/01/08-01/11	11.1,20.0	108	-8	T20.1	0.1	0.77	0.05
						13.01	0.01	0.34	0.10
	2004 QD3	02/17-03/03	60.4,22.0	178	11	13.58	0.01	0.23	0.05
	2008 BC22	03/18-03/24	6.2,10.9	174	-2	40.4	0.3	0.25	0.05
	2015 AS45	02/05-02/11	38.1,39.2	170	4	47.9	0.2	0.22	0.03
	2018 PP10	02/17-02/20	8.1,2.6	150	3	6.91	0.01	0.07	0.02
	2020 WM3	02/05-02/17	*24.0,25.4	155	-14	11.60	0.02	0.21	0.03
	2020 YQ3	01/14-01/18	23.1,16.8	128	7	T11.148	0.004	0.49	0.03
						18.93	0.03	0.19	0.02
Pravec	2020 YQ3	01/06-02/09	*41.4,13.0	130	6	T14.752	0.003	0.65	0.05
Pravec et al. (2021web)						11.080	0.002		
	2021 DX1	03/05-03/07	22.7,20.2	177	2	T1.1890	0.0002	0.64	0.10

Table III. Observing circumstances and analysis results. T Tumbling asteroid. The phase angle (α) is given at the start and end of each date range. If there is an asterisk before the first phase value, the phase angle reached a maximum or minimum during the period. L_{PAB} and B_{PAB} are, respectively the average phase angle bisector longitude and latitude (see Harris et al.,1984).

Pravec, P.; Scheirich, P.; Durech, J.; Pollock, J.; Kusnirak, P.; Hornoch, K.; Galad, A.; Vokrouhlicky, D.; Harris, A.W.; Jehin, E.; Manfroid, J.; Opitom, C.; Gillon, M.; Colas, F.; Oey, J.; Vrastil, J.; Reichart, D.; Ivarsen, K.; Haislip, J.; LaCluyze, A. (2014). "The tumbling state of (99942) Apophis." *Icarus* **233**, 48-60.

Tonry, J.L.; Denneau, L.; Flewelling, H.; Heinze, A.N.; Onken, C.A.; Smartt, S.J.; Stalder, B.; Weiland, H.J.; Wolf, C. (2018). "The ATLAS All-Sky Stellar Reference Catalog." *Ap. J.* **867**, A105.

Warner, B.D.; Harris, A.W.; Pravec, P. (2009). "The Asteroid Lightcurve Database." *Icarus* **202**, 134-146. Updated 2021 April. *http://www.minorplanet.info/lightcurvedatabase.html*

Warner, B.D. (2017). "Near-Earth Asteroid Lightcurves at CS3-Palmer Divide Station: 2017 April thru June." *Minor Planet Bull*. **44**, 335-344.

Warner, B.D. (2018a). "Near-Earth Asteroid Lightcurve Analysis at CS3-Palmer Divide Station: 2017 October-December." *Minor Planet Bull*. **45**, 138-147.

Warner, B.D. (2018b). "Near-Earth Asteroid Lightcurve Analysis at CS3-Palmer Divide Station: 2018 April-Jun." *Minor Planet Bull*. **45**, 366-379.

Warner, B.D.; Stephens, R.D. (2021). "On Confirmed and Suspected Binary Asteroids at the Center for Solar System Studies." *Minor Planet Bull.* **47**, 187-193.

LIGHTCURVE ANALYSIS OF HILDA ASTEROIDS AT THE CENTER FOR SOLAR SYSTEM STUDIES: 2021 JANUARY-MARCH

Brian D. Warner
Center for Solar System Studies / MoreData!
446 Sycamore Ave.
Eaton, CO 80615 USA
brian@MinorPlanetObserver.com

Robert D. Stephens
Center for Solar System Studies / MoreData!
Rancho Cucamonga, CA

Daniel R. Coley
Center for Solar System Studies
Corona, CA

(Received: 2021 April 8)

New CCD photometric observations of ten Hilda asteroid members were made from 2021 January through March: 153 Hilda, 190 Ismene, 1202 Marina, 2067 Aksnes, 3990 Heimdal, 6237 Chikushi, (7458) 1984 DE1, 8743 Keneke, and (23186) 2000 PO8. Two of the objects, 3990 Heimdal and 8743 Keneke, are suspected to be in a tumbling state.

CCD photometric observations of Hilda asteroids are made at the Center for Solar System Studies (CS3) as part of an ongoing study of this family/group that is located between the outer main-belt and Jupiter Trojans in a 3:2 orbital resonance with Jupiter. The goal is to determine the spin rate statistics of the Hildas and to find pole and shape models when possible. We also look to examine the degree of influence that the YORP (Yarkovsky-O'Keefe-Radzievskii-Paddack) effect (Rubincam, 2000) has on distant objects and to compare the spin rate distribution against the Jupiter Trojans, which can provide evidence that the Hildas are more "comet-like" than main-belt asteroids.

Table I lists the telescopes and CCD cameras that are combined to make observations. Up to nine telescopes are commonly used for observations. All the cameras use CCD chips from the KAF blue-enhanced family and so have essentially the same response. The pixel scales ranged from 1.24-1.60 arcsec/pixel. All lightcurve observations were unfiltered since a clear filter can result in a 0.1-0.3 magnitude loss. The exposures varied depending on the asteroid's brightness.

Telescopes	Cameras
0.30-m *f*/6.3 Schmidt-Cass	FLI Microline 1001E
0.35-m *f*/9.1 Schmidt-Cass	FLI Proline 1001E
0.35-m *f*/11 Schmidt-Cass	SBIG STL-1001E
0.40-m *f*/10 Schmidt-Cass	
0.50-m *f*/8.1 Ritchey-Chrétien	

Table I. List of available telescopes and CCD cameras at CS3. The exact combination for each telescope/camera pair can vary due to maintenance or specific needs.

To reduce the number of times and amounts of adjusting nightly zero points, we use the ATLAS catalog r´ (SR) magnitudes (Tonry et al., 2018). Those adjustments are usually ≤ ±0.03 mag. The rare greater corrections may have been related in part to using unfiltered observations, poor centroiding of the reference stars, and not correcting for second-order extinction. Another cause may be selecting what appears to be a single star but is actually an unresolved pair.

The Y-axis values are ATLAS SR "sky" (catalog) magnitudes. The two values in the parentheses are the phase angle (a) and the value of *G* used to normalize the data to the comparison stars used in the earliest session. This, in effect, made all the observations seem to be made at a single fixed date/time and phase angle, leaving any variations due only to the asteroid's rotation and/or albedo changes. The X-axis shows rotational phase from –0.05 to 1.05. If the plot includes the amplitude, e.g., "Amp: 0.65", this is the amplitude of the Fourier model curve and *not necessarily the adopted amplitude for the lightcurve*.

153 Hilda. There are numerous references to previous works for the namesake of the Hilda family, e.g., Warner and Stephens (2018), Pilcher and Benishek (2019), Pilcher (2020), and Warner and Stephens (2020a). For those three, the period was very close to 5.958 h and the amplitude ranged from 0.11 to 0.23 mag.

The data from 2021 observations showed a nearly flat lightcurve (0.02 mag) with a slightly longer period of 6.076 h. We used dense lightcurves from Pilcher and Benishek found on the ALCDEF web site and sparse data on the AstDys site for ATLAS, Catalina Sky Survey, and USNO-Flagstaff to generate a model. The results are shown following the references section.

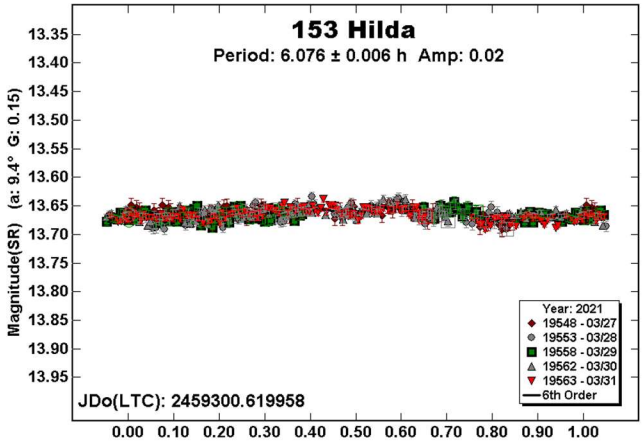

190 Ismene. Dahlgren et al. (1998) found a period of 6.52 h for this 160-km Hilda. Similar results were found by Shevchenko et al (2008) and by us using data from 2019 (Warner and Stephens, 2020a). Our result is in good agreement with those earlier works even though the lightcurve has a small gap near 0.85 rotation phase.

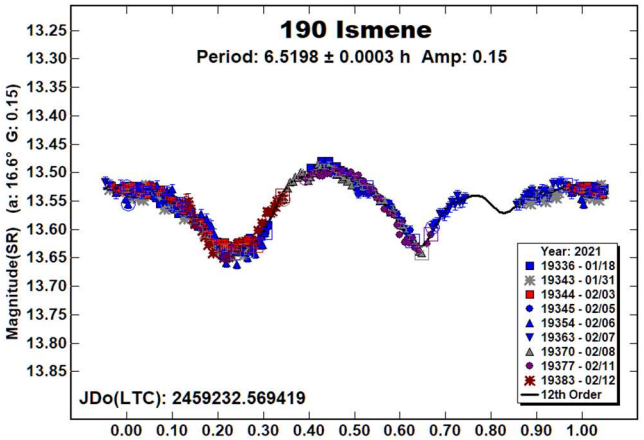

1202 Marina. Dahlgren et al. (1998) found a period of 9.45 h for Marina, which has an estimated diameter of 55 km. We observed it in 2020 and found a period of 9.558 h (Warner and Stephens, 2020b). Durech et al. (2020) derived a shape model with a sidereal period of 9.45833 h and preferred J2000 ecliptic pole of (λ,β) = (54°, -47°).

The data analysis found a period of 9.461 h, which is in better agreement with Dahlgren et al. and Durech et al. The fit of our recent data using the shorter period is greatly improved over the one forced to our result from 2020.

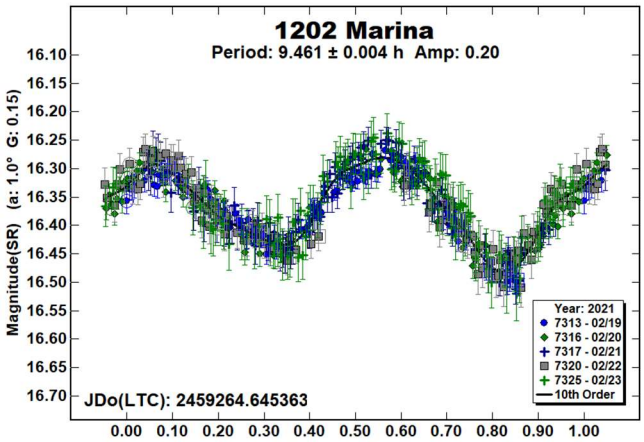

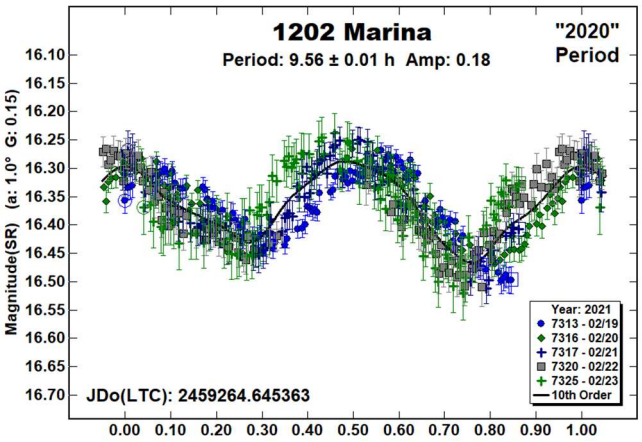

2067 Aksnes. The only previous result was from Dahlgren et al. (1998), who found a period of 17.75 h. Our more extensive data set helped refine the period to one about 0.07 h shorter. The unusual shape was confirmed by the split-halves plot, which showed two distinct parts of the lightcurve.

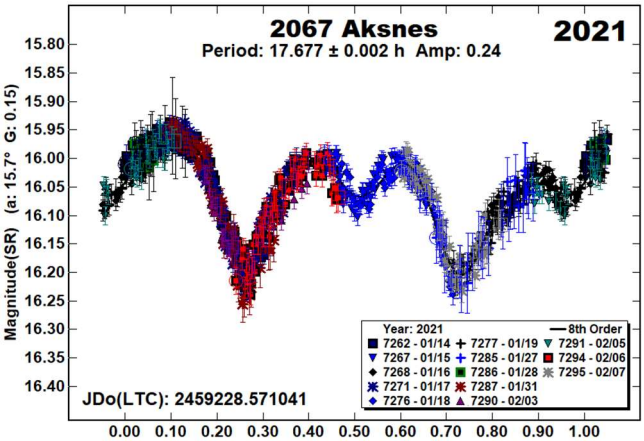

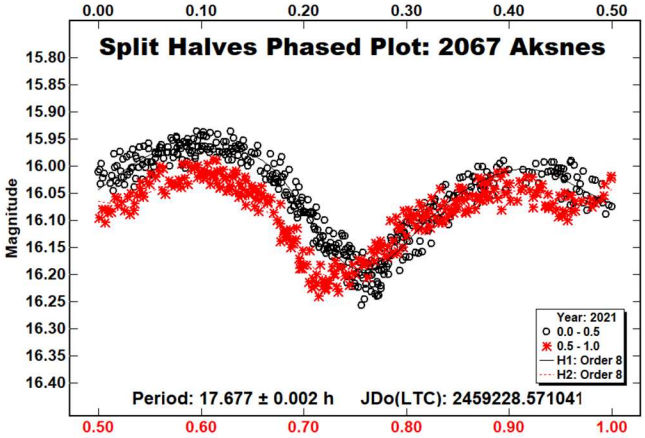

3990 Heimdal. Slyusarev et al. (2012), found only a minimum period of 20 h. Our 2021 observations spanned more than 60 days and had denser covered for most sessions. Finding a single-period solution proved difficult, as seen in the "NoSub" plot. A dual-period search wasn't run until after the session on March 3. It was only after the final observing run on March 31 that an acceptable, but far from perfect, solution could be found, mostly because *MPO Canopus* is not designed to handle the complex relationship of the periods of rotation and precession for tumbling asteroids.

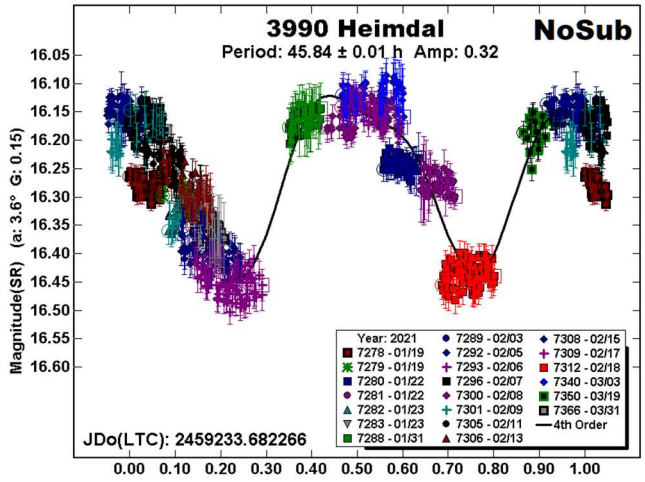

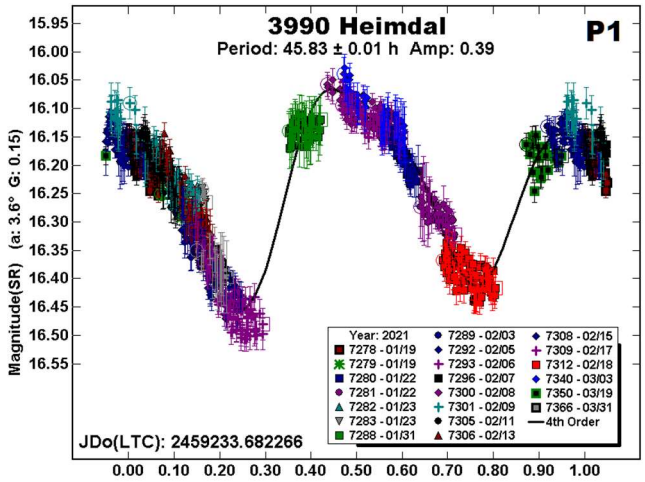

It is very apparent that subtracting P_2 = 47.86 h from the data set leads to a good fit for P_1 = 45.83 h. It's a concern that P_2 is so close to being commensurate with an Earth day and that the rules of thumb for the damping time of tumbler of Hemidal's size indicate that P_1 and/or P_2 are far less than what would be expected (Pravec et al., 2005; 2014). On the other hand, the two periods are consistent with one another if the asteroid is tumbling, i.e., a significantly shorter period for either one would be unlikely.

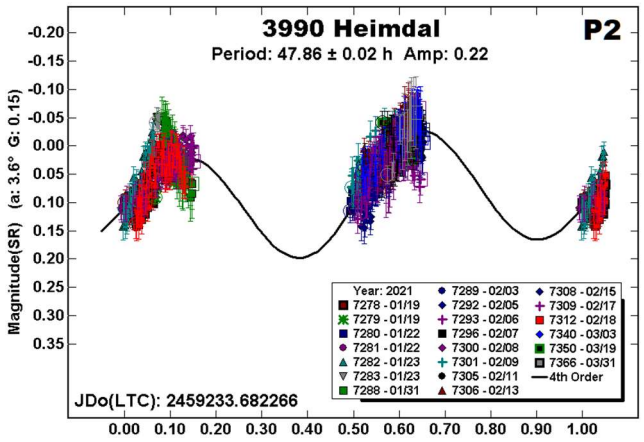

To get the mid-amplitude for each session for H-G phase curve modeling, we used the P_1 plot to find the date and time for a point in each session. Since that plot normalizes all the magnitudes to the first session, the reduced magnitude for a point in P_1 was not used directly. Instead, the offset from the average magnitude of the plot, given by the Fourier analysis, was recorded. For example, if the average of $P1$ = 16.270 and the selected data point in a session had a reduced magnitude of 16.350, a value of +0.08 was recorded.

We then plotted the raw data for each session one at a time. The data point corresponding to the saved date/time was found and its correction was applied to its reduced magnitude. This corrected value along with the date and timer were put into the H-G calculator of *MPO Canopus* with the final result being H_{SR} = 10.84 and G_{SR} = 0.26. Assuming V – SR = 0.22 (Warner and Stephens, 2021), this gives H = 11.06. The MPCORB file gives H = 10.88.

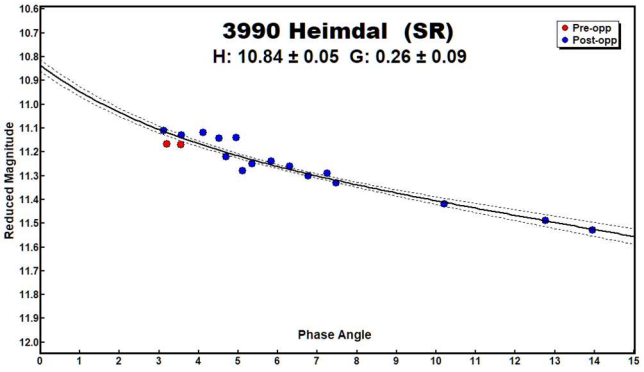

6237 Chikushi. Waszczak et al. (2015) used sparse data from the Palomar Transient Factory to find a period of 7.812 h. The result from our most recent dense data set (7.816 h), is very close to theirs as well as the sidereal period (7.81163 h) found by Durech et al. (2020). Our data set from 2017 (Warner and Stephens, 2018) led to 7.787 h. Since it spanned only three days, we consider it statistically the same with our recent result.

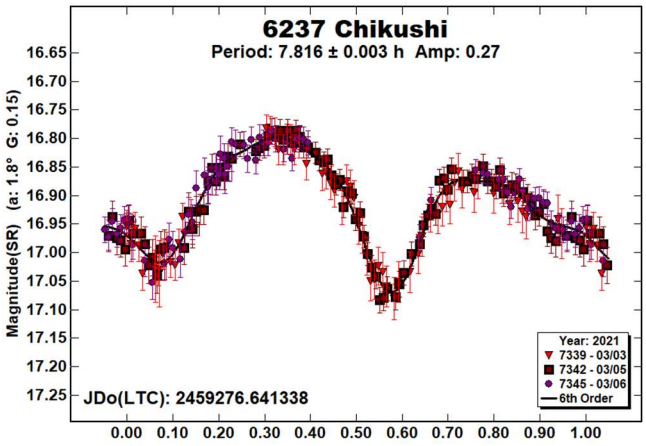

(7458) 1984 DE1. The estimated diameter of this Hilda is 25 km. Waszczak et al. (2015) found a period of 15.651 h and Durech and Hanus (2018) found a sidereal period of 15.7543 h for their model. Our result is in good keeping with the previously reported periods.

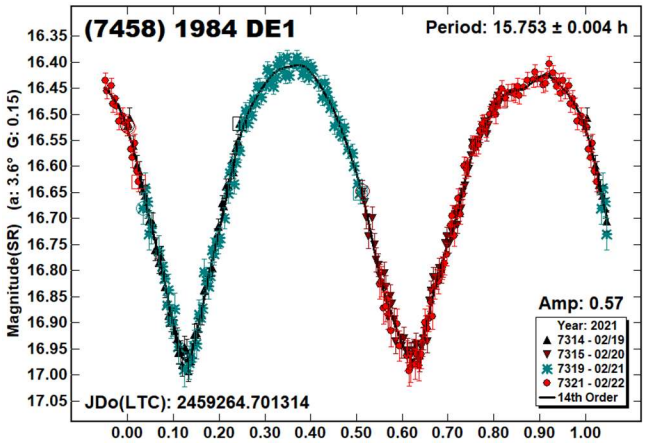

8743 Keneke. Two, very conflicting periods have been reported for this 27 km Hilda. Warner et al. (2017) found a period of 2.769 h while Pál et al. (2020) using data from TESS found 99.3076 h. Our 2021 observations spanned almost a month, Feb 19 - Mar 22, producing the 950 data points used in our analysis.

On the face of it, the period spectrum showed two possible periods and, in fact, *MPO Canopus* favored the longer one near 95 h. However, based on the plot at that period and one near 45 h, we worked on the premise that the shorter period was more likely correct.

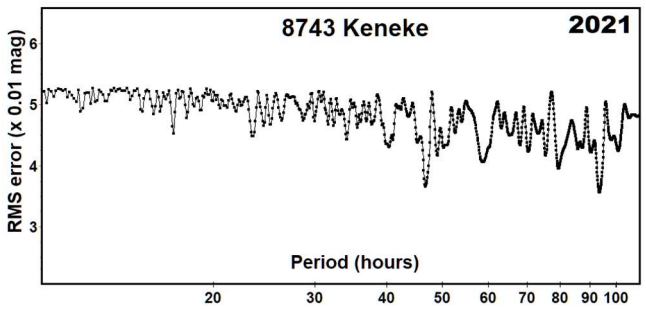

The "NoSub" plot shows the full data set phased to a period of 46.71 h. Despite the noisy data in a lightcurve with an amplitude of only about 0.20 mag, there were signs of a second period, e.g., session 19487 on March 5. The dual-period search method in *MPO Canopus* eventually found a second period of 34.21 h, which was one a small number of possible solutions but the most probable. Both of these periods are short of what would be expected for the asteroid to be tumbling (Pravec et al., 2005; 2014).

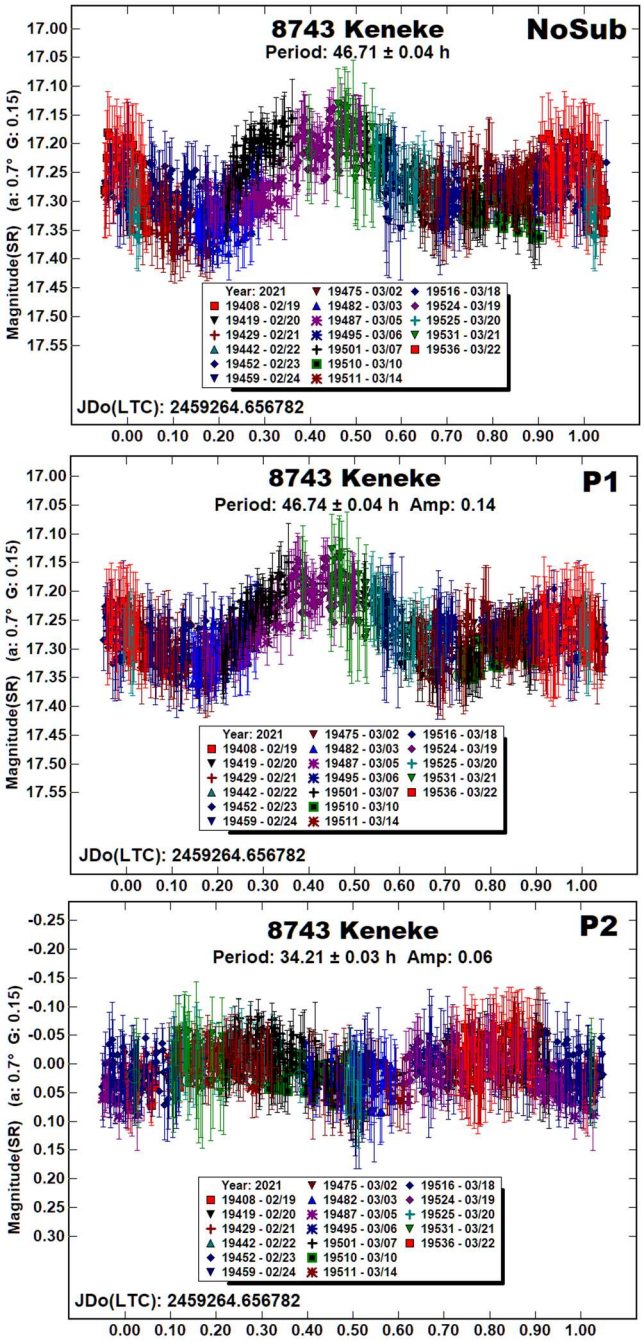

These results prompted another look at the 2016 results. The first step was to use SR magnitudes from the ATLAS catalog for the comparisons and remove any zero point of sets. Despite the very sparse data set obtained in 2016 ("2016 Raw"), there seemed to be a long period component to the data. This was not seen at the time since a catalog with uncertain accuracy was being used.

The period spectrum shows several poorly defined possibilities (broad minimums in the RMS values). The only solution that produced a realistic lightcurve was for 63.7 h which required going down to a second-order analysis in order avoid wild swings in the Fourier model curve. This revised result proved to be very intriguing since it is related in a to the results from 2021 that supports the possibility of the asteroid being in a tumbling state.

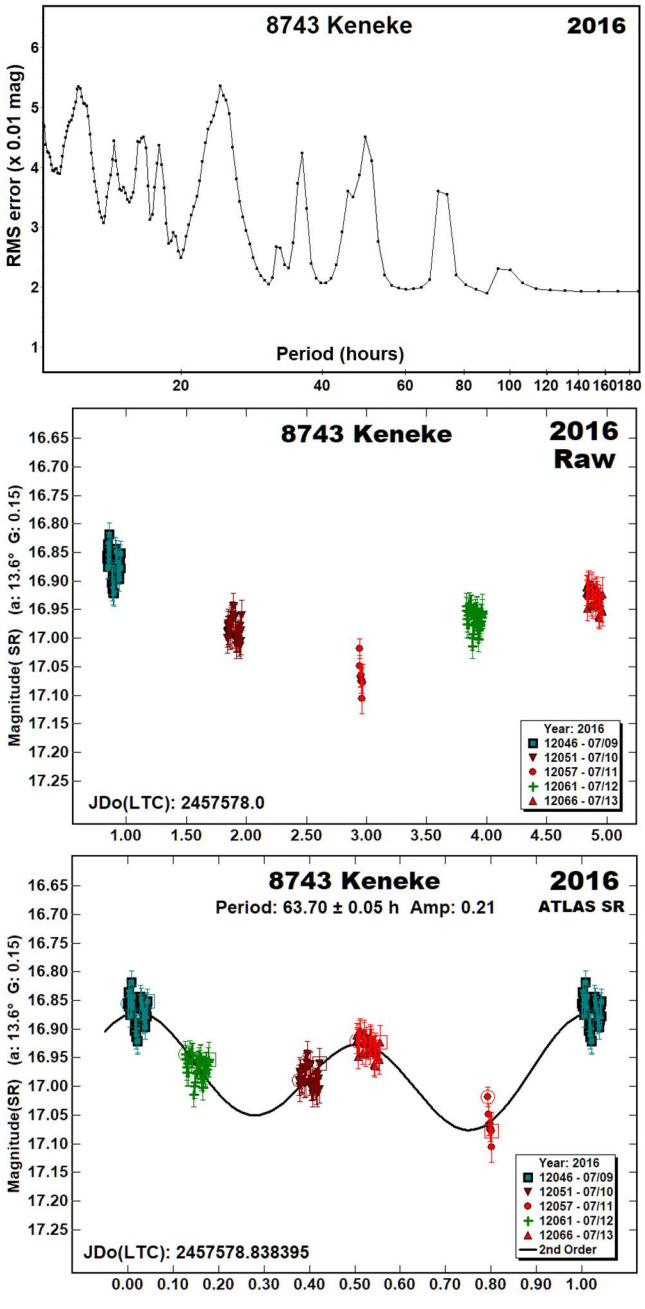

A tumbling asteroid lightcurve is defined in part by the sum of integral multiples of the frequencies, i.e.,

$$m/f1 + n/f2$$

The frequencies for each period are

$f1$ = (24/63.7) = 0.376766
$f2$ = (24/34.21) = 0.701549
$f3$ = (24/46.74) = 0.513479

Number	Name	21yy/mm/dd	Phase	L_{PAB}	B_{PAB}	Period(h)	P.E.	Amp	A.E.
153	Hilda	03/27-03/31	9.4,10.2	150	-8	6.076	0.0006	0.02	0.01
190	Ismene	01/18-02/12	16.6,16.7	50	-6	6.5198	0.0003	0.15	0.01
1202	Marina	02/19-02/23	1.0,1.6	149	4	9.461	0.004	0.20	0.02
2067	Aksnes	01/14-02/07	15.7,17.5	59	-3	17.677	0.002	0.24	0.02
3990	Heimdal	01/19-03/19	*3.6,12.8	125	-10	T45.83	0.01	0.39	0.03
						47.86	0.02	0.22	0.03
6237	Chikushi	03/03-03/06	1.8,2.4	159	5	7.816	0.003	0.27	0.02
7458	1984 DE1	02/19-02/21	3.6,2.9	161	-1	15.753	0.004	0.57	0.02
8743	Keneke	02/19-03/22				T46.74	0.04	0.14	0.02
						34.21	0.03	0.06	0.02
		16/07/09-07/13				63.7	0.9	0.21	0.02
23186	2000 PO8	03/10-03/18	8.9,7.2	194	15	5.012	0.001	0.29	0.02

Table II. Observing circumstances. T The dominant period of a tumbling asteroid. The phase angle (α) is given at the start and end of each date range. L_{PAB} and B_{PAB} are the average phase angle bisector longitude and latitude (see Harris *et al.*, 1984).

Number	Name	λ1	β1	Period	λ2	β2	Period (h)	a/b ratio	a/c ratio
153	Hilda	**335°**	**-1°**	**5.958538**	155°	-15°	5.958535	1.14	1.4839
23186	2000 PO8	**302°**	**+79°**	**5.011160**	30°	+40°	5.011169	1.2	2.3

Table III. Results of Pole/Shape modeling. Pole positions are J2000 ecliptic coordinates. The pole error is a circle with a 15° radius centered on the pole. The period error is 1-2 units of the last decimal place. The preferred solution is listed in bold text. The a/b and a/c ratios are from the preferred model.

These give

$f2 - f3 = 0.18807$
$f1 = 2 * (f2 - f3)$; $\Delta = 0.000626$

Therefore, it seems that the three periods are related even when no one period has a simple integral ratio with either of the other two. Even if assuming the asteroid is tumbling, because there are insufficient data, it is not possible to say with certainty that the periods of 45.83 h and 47.86 h are the true periods of precession and rotation.

(23186) 2000 PO8. We observed this asteroid twice before: Warner and Stephens (2018, 5.003 h; 2020b, 5.0165 h). The analysis of the 2021 data gave essentially the same results.

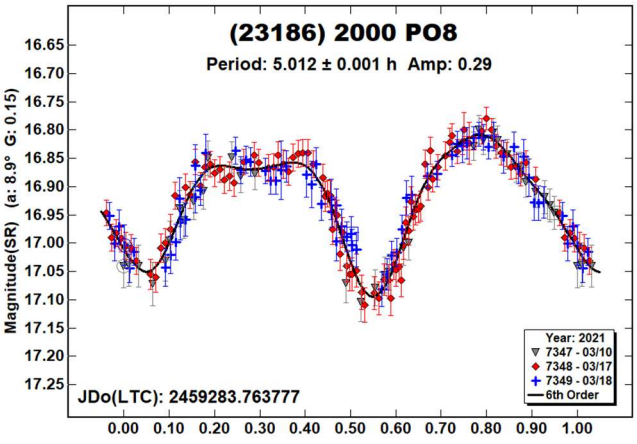

Acknowledgements

Funding for observations at CS3 and work on the asteroid lightcurve database (Warner et al., 2009) and ALCDEF database (*alcdef.org*) were supported by NASA grant 80NSSC18K0851.

This work includes data from the Asteroid Terrestrial-impact Last Alert System (ATLAS) project. ATLAS is primarily funded to search for near earth asteroids through NASA grants NN12AR55G, 80NSSC18K0284, and 80NSSC18K1575; byproducts of the NEO search include images and catalogs from the survey area. The ATLAS science products have been made possible through the contributions of the University of Hawaii Institute for Astronomy, the Queen's University Belfast, the Space Telescope Science Institute, and the South African Astronomical Observatory.

The authors gratefully acknowledge Shoemaker NEO Grants from the Planetary Society (2007, 2013). These were used to purchase some of the telescopes and CCD cameras used in this research.

References

Dahlgren, M.; Lahulla, J.F.; Lagerkvist, C.-I.; Lagerros, J.; Mottola, S.; Erikson, A.; Gonano-Beurer, M.; Di Martino, M. (1998). "A Study of Hilda Asteroids. V. Lightcurves of 47 Hilda Asteroids." *Icarus* **133**, 247-285.

Durech, J.; Hanus, J. (2018). "Reconstruction of asteroid spin states from Gaia DR2 photometry." *Astron. Astrophys*. **620**, A91.

Durech, J.; Tonry, J.; Erasmus, N.; Denneau, L.; Heinze, A.N.; Flewelling, H.; Vanco, R. (2020). "Asteroid models reconstructed from ATLAS photometry." *Astron. Astrophys*. **643**, A59.

Harris, A.W.; Young, J.W.; Scaltriti, F.; Zappala, V. (1984). "Lightcurves and phase relations of the asteroids 82 Alkmene and 444 Gyptis." *Icarus* **57**, 251-258.

Pál, A.; Szakáts, R.; Kiss, C.; Bódi, A.; Bognár, Z.; Kalup, C.; Kiss, L.L.; Marton, G.; Molnár, L.; Plachy, E.; Sárneczky, K.; Szabó, G.M.; Szabó, R. (2020). "Solar System Objects Observed with TESS – First Data Release: Bright Main-belt and Trojan Asteroids from the Souther Survey." *Ap. J. Suppl Ser*. **247**, id. 26.

Pilcher, F.; Benishek, V. (2019). "Lightcurves of 153 Hilda at Large Phase Angles." *Minor Planet Bull*. **46**, 318-319.

Pilcher, F. (2000). "Lightcurves and Rotation Periods of 83 Beatrix, 86 Semele, 118 Peitho 153 Hilda, 527 Euryanthe, and 549 Jessonda." *Minor Planet Bull*. **47**, 192-195.

Pravec, P.; Harris, A.W.; Scheirich, P.; Kušnirák, P.; Šarounová, L.; Hergenrother, C.W.; Mottola, S.; Hicks, M.D.; Masi, G.; Krugly, Yu.N.; Shevchenko, V.G.; Nolan, M.C.; Howell, E.S.; Kaasalainen, M.; Galád, A.; Brown, P.; Degraff, D.R.; Lambert, J.V.; Cooney, W.R.; Foglia, S. (2005). "Tumbling asteroids." *Icarus* **173**, 108-131.

Pravec, P.; Scheirich, P.; Durech, J.; Pollock, J.; Kusnirak, P.; Hornoch, K.; Galad, A.; Vokrouhlicky, D.; Harris, A.W.; Jehin, E.; Manfroid, J.; Opitom, C.; Gillon, M.; Colas, F.; Oey, J.; Vrastil, J.; Reichart, D.; Ivarsen, K.; Haislip, J.; LaCluyze, A. (2014). "The tumbling state of (99942) Apophis." *Icarus* **233**, 48-60.

Rubincam, D.P. (2000). "Relative Spin-up and Spin-down of Small Asteroids." *Icarus* **148**, 2-11.

Shevchenko, V.G.; Chiorny, V.G.; Gaftonyuk, N.M.; Krugly, Y.N.; Belskaya, I.N.; Tereschenko, I.A.; Velichko, F.P. (2008). "Asteroid observations at low phase angles. III. Brightness behavior of dark asteroids." *Icarus* **196**, 601-611.

Slyusarev, I.G.; Shevchenko, V.G.; Belskaya, I.N.; Krugly, Yu.N.; Chiorny, V.G. (2012). "CCD Photometry of Hilda Asteroids." ACM 2012, #6398.

Tonry, J.L.; Denneau, L.; Flewelling, H.; Heinze, A.N.; Onken, C.A.; Smartt, S.J.; Stalder, B.; Weiland, H.J.; Wolf, C. (2018). "The ATLAS All-Sky Stellar Reference Catalog." *Astrophys. J.* **867**, A105.

Warner, B.D.; Harris, A.W.; Pravec, P. (2009). "The Asteroid Lightcurve Database." *Icarus* **202**, 134-146. Updated 2020 Sep. *http://www.minorplanet.info/lightcurvedatabase.html*

Warner, B.D.; Stephens, R.D.; Coley, D.R. (2017). "Lightcurve Analysis of Hilda Asteroids at the Center for Solar System Studies: 2016 September-December." *Minor Planet Bull*. **44**, 36-41.

Warner, B.D.; Stephens, R.D. (2018). "Lightcurve Analysis of Hilda Asteroids at the Center for Solar System Studies: 2017 July Through September." *Minor Planet Bull.* **45**, 35-39.

Warner, B.D.; Stephens, R.D. (2020a). "Lightcurve Analysis of Hilda Asteroids at the Center for Solar System Studies: 2019 November." *Minor Planet Bull*. **47**, 123-124.

Warner, B.D.; Stephens, R.D. (2020b). "Lightcurve Analysis of Hilda Asteroids at the Center for Solar System Studies: 2019 December - 2020 April." *Minor Planet Bull.* **47**, 196-199.

Warner, B.D.; Stephens, R.D. (2021). "On Confirmed and Suspected Binary Asteroids at the Center for Solar System Studies." *Minor Planet Bull.* **47**, 187-193.

Waszczak, A.; Chang, C.-K.; Ofek, E.O.; Laher, R.; Masci, F.; Levitan, D.; Surace, J.; Cheng, Y.-C.; Ip, W.-H.; Kinoshita, D.; Helou, G.; Prince, T.A.; Kulkarni, S. (2015). "Asteroid Light Curves from the Palomar Transient Factory Survey: Rotation Periods and Phase Functions from Sparse Photometry." *Astron. J.* **150**, A75.

GENERAL REPORT OF POSITION OBSERVATIONS BY THE ALPO MINOR PLANETS SECTION FOR THE YEAR 2020

Frederick Pilcher
4438 Organ Mesa Loop
Las Cruces, NM 88011 USA
fpilcher35@gmail.com

Observations of positions of minor planets by members of the Minor Planets Section in calendar year 2020 are summarized.

During the year 2020 a total of 1486 observations of 419 different minor planets were reported by members of the Minor Planets Section. Of these, 1458 are approximate visual positions denoted V, and 28 are digital camera images denoted C not measured at the time of writing.

The summary lists minor planets in numerical order, the observer and telescope aperture (in cm), UT dates of the observations, and the total number of observations in that interval. When a significant departure from the predicted magnitude was noted, it is stated in the next line below the number of positions. The year is 2020 in each case.

Positional observations were contributed by the following observers:

Observer, Instrument	Location	Planets	Positions
Faure, Gerard	Col d'Arlezier,	29	72V
20 cm Celestron	Vaison la romaine, France		
35 cm Meade LX200	Col de L'Arzelier, France		
45 cm Dobson	Pas du Serpaton, France		
Harvey, G. Roger	Concord, North	347	1181V
81 cm Newtonian,	Carolina, USA		
Pryal, Jim	Ellensburg, WA USA	5	14V
20 cm f/10 SCT			
Rayon, Jean-Michel	Meylan, France	16	28C
15 cm Celestron 6			
25 cm Quattro			
45 cm Stargate			
APN Sony A6000 series cameras			
Werner, Robert	Pasadena, CA USA	39	191V
20 cm Celestron			

CCD observations are labeled C; all others are visual)

MINOR PLANET	OBSERVER & APERTURE (cm)	OBSERVING PERIOD (2019)	NO. OBS.
6 Hebe	Werner, 20	Apr 16-May 23	12
8 Flora	Werner, 20	Nov 15-Dec 16	8
16 Psyche	Werner, 20	Dec 5-16	2
20 Massalia	Werner, 20	Oct 13-21	7
23 Thalia	Pryal, 20	Apr 22	2
	Werner, 20	May 15-Jun 9	11
25 Phocaea	Werner, 20	Apr 16-23	3
27 Euterpe	Werner, 20	Apr 15-29	7
30 Urania	Werner, 20	Apr 15-22	3
32 Pomona	Werner, 20	Oct 13-15	2
40 Harmonia	Pryal, 20	Apr 22	2
	Werner, 20	May 15-Jun 17	12
42 Isis	Werner, 20	May 27-Jul 20	7
44 Nysa	Werner, 20	Oct 13-15	2
49 Pales	Werner, 20	Oct 13-17	4
56 Melete	Werner, 20	Jul 19-20	2
65 Cybele	Pryal, 20	Apr 22	2
	Werner, 20	Apr 16-May 28	12
67 Asia	Werner, 20	Nov 15-19	4
68 Leto	Werner, 20	Oct 17-21	3
71 Niobe	Werner, 20	Apr 16-28	5
74 Galatea	Werner, 20	Dec 5-16	3
82 Alkmene	Werner, 20	Nov 16-19	3
85 Io	Werner, 20	Jun 9-20	3
102 Miriam	Werner, 20	Oct 13-17	4
177 Irma	Werner, 20	Nov 16-17	2
185 Eunike	Werner, 20	Jul 19-29	2
194 Prokne	Werner, 20	Nov 15-Dec 5	5
200 Dynamene	Werner, 20	Nov 15-19	4
202 Chryseis	Werner, 20	Dec 6-7	2
250 Bettina	Werner, 20	Dec 5-6	2
252 Clementina	Harvey, 81	Nov 20	3
266 Aline	Faure, 20	Nov 19	2
	Werner, 20	Nov 16-17	2
270 Anahita	Werner, 20	May 20-Jun 9	4
349 Dembowska	Werner, 20	May 20-29	7
354 Eleonora	Pryal, 20	Apr 22	2
375 Ursula	Werner, 20	Oct 13-15	2
386 Siegena	Werner, 20	Dec 5-16	4
404 Arsinoe	Werner, 20	May 15-29	7
451 Patientia	Werner, 20	May 27-Jun 9	3
516 Amherstia	Werner, 20	Apr 15-29	5
737 Arequipa	Werner, 20	Oct 13-15	3
747 Winchester	Werner, 20	Nov 15-Dec 16	8
1012 Sarema	Faure, 35	Sep 16	2
1024 Hale	Faure, 20	Oct 17	4
1081 Reseda	Faure, 20	Nov 19	2
	Rayon, 45	Nov 18	2C
1092 Lilium	Faure, 35	Sep 21	2
1205 Ebella	Harvey, 81	Nov 8-16	12
1313 Berna	Rayon, 45	Nov 18	2C
1380 Volodia	Harvey, 81	Apr 17	6
1538 Detre	Harvey, 81	Oct 7	3
1564 Srbija	Faure, 20	Oct 17-18	2
1652 Herge	Faure, 20	Apr 14	3
1873 Agenor	Rayon, 25	May 26	1C
1877 Marsden	Faure, 45	Aug 22	2
	Harvey, 81	Aug 9	3
1900 Katyusha	Faure, 20	Oct 18	2
1966 Tristan	Harvey, 81	Apr 17	4
			0.4b@16.3
2074 Shoemaker	Faure, 20	Nov 18	4
	Rayon, 25, 45	Nov 14-18	3C
2171 Kiev	Faure, 35	May 26-27	2
2189 Zaragoza	Harvey, 81	Oct 14	3
2215 Sichuan	Faure, 20	Nov 19	2
	Rayon, 45	Nov 18	2C
2223 Sarpedon	Faure, 35	May 26-27	4
2317 Galya	Harvey, 81	Sep 11	3
2327 Gershberg	Harvey, 81	Oct 14	3
2363 Cebriones	Faure, 35	May 25	2
	Rayon, 25	May 26	1C
2456 Palamedes	Faure, 35	Sep 15	2
2518 Rutllant	Harvey, 81	Jun 14	6
2520 Novorossijsk	Harvey, 81	Sep 21	3
2614 Torrence	Harvey, 81	Oct 14	3
2674 Pandarus	Faure, 35	Jun 22	3
2821 Slavka	Harvey, 81	Oct 15	3
2823 van der Laan	Harvey, 81	Oct 18	3
2893 Peiroos	Faure, 35	May 25	2
	Rayon, 25	May 26	1C
2922 Dikan'ka	Harvey, 81	May 12	3
2935 Naerum	Harvey, 81	Jun 21	3
2960 Ohtaki	Harvey, 81	Jan 22	3
2993 Wendy	Faure, 35	Jul 21	2
2998 Berendeya	Harvey, 81	Aug 9-11	3
3002 Delasalle	Faure, 35	Sep 16	2

MINOR	PLANET	OBSERVER & APERTURE (cm)	OBSERVING PERIOD (2019)	NO. OBS.
3030	Vehrenberg	Faure, 45	Aug 20-21	3
		Harvey, 81	Aug 19	3
		Rayon, 45	Aug 27	2C
3088	Jinxiuzhonghua	Harvey, 81	Feb 15	3
			0.5f@16.1	
3096	Bezruc	Harvey, 81	Jul 14	3
3145	Walter Adams	Harvey, 81	Oct 19	3
3151	Talbot	Faure, 35	May 27	2
3187	Dalian	Harvey, 81	Jan 28	3
3321	Dasha	Harvey, 81	Nov 19	3
3323	Turgenev	Harvey, 81	Oct 15	3
			0.5f@16.2	
3349	Manas	Harvey, 81	Apr 17	3
3464	Owensby	Harvey, 81	Jan 28	3
3522	Becker	Harvey, 81	Aug 19	3
3558	Shishkin	Harvey, 81	Sep 14	3
			0.5f@16.2	
3572	Leogoldberg	Harvey, 81	Aug 9	3
3595	Gallagher	Harvey, 81	Nov 16	3
3596	Meriones	Harvey, 81	Oct 7	3
3608	Kataev	Harvey, 81	May 11	3
3612	Peale	Harvey, 81	Sep 14	3
3637	O'Meara	Faure, 35	Jun 23	2
3705	Hotellasilla	Harvey, 81	Oct 15	3
3714	Kenrussell	Harvey, 81	Oct 14	3
3781	Dufek	Harvey, 81	Oct 19	3
3814	Hoshi-no-mura	Harvey, 81	Apr 22	3
3823	Yorii	Harvey, 81	Feb 15	3
3828	Hoshino	Harvey, 81	Dec 11	3
3889	Menshikov	Harvey, 81	Aug 9	3
			0.4f@16.1	
4004	List'ev	Harvey, 81	Sep 22	3
4020	Dominique	Harvey, 81	Oct 15	3
4051	Hatanaka	Harvey, 81	Nov 19	3
4073	Ruianzhongxue	Harvey, 81	Aug 18	6
4103	Chahine	Faure, 20	Oct 18	2
4117	Wilke	Harvey, 81	Aug 11	3
4193	Salanave	Harvey, 81	Oct 8	3
4315	Pronik	Harvey, 81	Oct 18	3
4318	Bata	Harvey, 81	Jan 29	3
4322	Billjackson	Harvey, 81	Oct 19	3
4326	McNally	Harvey, 81	Jun 14	3
4380	Geyer	Harvey, 81	Oct 18	3
4582	Hank	Harvey, 81	Apr 22	3
4653	Tommaso	Harvey, 81	Apr 19	3
4771	Hayashi	Harvey, 81	Oct 14	3
4787	Shul'zhenko	Harvey, 81	Sep 21	3
4804	Pasteur	Rayon, 45	Nov 18	2C
4811	Semashko	Harvey, 81	Aug 19	3
4851	Vodop'yanova	Harvey, 81	Mar 1	3
4933	Tylerlinder	Harvey, 81	Apr 22	3
4942	Munroe	Harvey, 81	May 2	3
4978	Seitz	Harvey, 81	Oct 15	3
4997	Ksana	Harvey, 81	Sep 21	3
5088	Tancredi	Harvey, 81	Jan 28	3
5124	Muraoka	Harvey, 81	Apr 16	3
5152	Labs	Harvey, 81	Aug 19	3
5193	Tanakwataru	Harvey, 81	Jan 21	3
5220	Vika	Harvey, 81	Oct 7	3
5346	1981 QE3	Harvey, 81	Sep 14	3
5406	Jonjoseph	Harvey, 81	Feb 22	3
5464	Weller	Harvey, 81	Oct 14	3
5501	1982 FF2	Harvey, 81	Apr 14	3
5527	1991 UQ3	Harvey, 81	Apr 19	3
5542	Moffatt	Harvey, 81	Sep 21	3
			0.6f@15.8	
5558	Johnnapier	Harvey, 81	Feb 28	3
			0.3b@16.1	
5562	1991 VS	Harvey, 81	Jan 22	3
5577	Priestly	Harvey, 81	Jan 1	3
5600	1991 UY	Harvey, 81	Jan 23	3
5656	Oldfield	Harvey, 81	Jul 27	3
5672	Libby	Harvey, 81	Apr 21	3
5690	1992 EU	Harvey, 81	Feb 23	3
5742	1990 TN4	Harvey, 81	Feb 28	3
5753	Yoshidatadahiko	Harvey, 81	Aug 19	3
5765	Izett	Harvey, 81	Feb 15	3
5767	Moldun	Harvey, 81	Jul 27	3
5805	Glasgow	Harvey, 81	Feb 22	3
5862	Sakanoue	Harvey, 81	Feb 28	3
5893	Coltrane	Harvey, 81	Apr 4	3
5895	Zbirka	Harvey, 81	Oct 18	3
5912	Oyakoshiyuki	Harvey, 81	Jan 28	3
5921	1992 UL	Harvey, 81	Feb 28	3
5933	Kemurdzhian	Harvey, 81	Jun 1	3
5978	Kaminokuni	Harvey, 81	Jan 1	3
5996	Julioangel	Harvey, 81	Sep 7	3
6004	1988 XY1	Harvey, 81	Jan 1	3
6005	1989 BD	Harvey, 81	Jan 23	3
6049	Toda	Harvey, 81	Jul 28	3
6089	Izumi	Harvey, 81	Nov 16	3
6166	Univsima	Harvey, 81	Dec 11	3
6207	Bourvil	Harvey, 81	Jan 29	3
6222	1980 PB3	Harvey, 81	May 12	3
6231	Hundertwasser	Harvey, 81	Feb 28	3
6251	Setsuko	Harvey, 81	Apr 17	3
6259	Maillol	Harvey, 81	Apr 2	3
6282	Edwelda	Harvey, 81	Jan 1	3
6286	1983 EU	Harvey, 81	Mar 1	3
6397	1991 BJ	Harvey, 81	Feb 23	3
6403	Steverin	Harvey, 81	May 16	3
6434	Jewitt	Harvey, 81	Jul 28	3
6464	Kaburaki	Harvey, 81	Jan 23	3
6470	Aldrin	Harvey, 81	Nov 19	3
6496	Kazuko	Harvey, 81	May 16	3
6520	Sugawa	Harvey, 81	Jun 21	3
6536	Vysochinska	Harvey, 81	Aug 19	3
6542	Jacquescousteu	Harvey, 81	Mar 1	3
6561	Gruppetta	Harvey, 81	Sep 22	3
6569	Ondaatje	Harvey, 81	Jun 21	6
6586	Seydler	Harvey, 81	Jan 28	3
6594	Tasman	Harvey, 81	Sep 21	3
6603	Marycregg	Harvey, 81	Apr 22	3
6615	Plutarchos	Harvey, 81	May 12	3
6663	Tatebayashi	Harvey, 81	Jun 26	3
6709	Hiromiyuki	Harvey, 81	Nov 17	3
6759	1980 KD	Harvey, 81	Apr 17	3
6800	Saragamine	Harvey, 81	Oct 7	3
6846	Kansazan	Harvey, 81	Aug 18	3
6889	1971 RA	Harvey, 81	Sep 14	3
6919	Tomonaga	Harvey, 81	Feb 28	3
6925	Susumu	Harvey, 81	May 16	3
6977	Jaucourt	Harvey, 81	Jun 1	3
7014	Nietzsche	Harvey, 81	Jul 27	3
7024	1992 PA4	Harvey, 81	Oct 19	3
7094	Godaisan	Harvey, 81	Sep 21	3
7104	Manyousyu	Harvey, 81	Feb 15	3
7106	Kondakov	Harvey, 81	Aug 11	3
7118	Kuklov	Harvey, 81	Jan 20	3
7131	Longtom	Harvey, 81	Nov 19	3
7247	Robertstirling	Harvey, 81	Sep 22	6
7318	Dyukov	Harvey, 81	Sep 21	3
				0.6f@16.0
7329	Bettadotto	Harvey, 81	Apr 14	6
7333	Bec-Borsenberger	Harvey, 81	Sep 14	3
7368	Haldancohn	Harvey, 81	Feb 15	3
7451	Verbitskaya	Harvey, 81	Jul 14	3
7456	Doressoundiram	Harvey, 81	Jun 26	3
7540	1997 AK21	Harvey, 81	Jan 6	3
7605	Cindygraber	Harvey, 81	Jan 6	3
7609	1995 WX3	Harvey, 81	Apr 19	3
7632	Stanislav	Harvey, 81	Jan 29	3

MINOR PLANET	OBSERVER & APERTURE (cm)	OBSERVING PERIOD (2019)	NO. OBS.
7658 1993 BM12	Harvey, 81	Apr 21	3
7686 Wolfernst	Harvey, 81	Feb 22	3
7708 Fennimore	Harvey, 81	Apr 4	3
7753 1988 XB	Harvey, 81	Nov 29	6
7760 1990 RW3	Harvey, 81	Oct 14	3
7804 Boesgaard	Harvey, 81	Jul 27	3
7818 Muirhead	Harvey, 81	Jan 21	6
7910 Alexsola	Harvey, 81	May 11	3
8115 Sakabe	Harvey, 81	May 2	3
8143 Nezval	Harvey, 81	Dec 11	3
8165 Gandig	Harvey, 81	Apr 19	3
8246 Kotov	Harvey, 81	Sep 14	3
8256 Shenzhou	Harvey, 81	Sep 21	3
8285 1991 UK3	Harvey, 81	Feb 15	3
8294 Takayuki	Harvey, 81	Jan 28	3
8295 Toshifukushima	Harvey, 81	Nov 21	3
8321 Akim	Harvey, 81	Jan 29	3
8357 O'Connor	Harvey, 81	Oct 15	3
8514 1991 PK15	Harvey, 81	Aug 19	3
8655 1990 QJ1	Harvey, 81	Oct 6	3
8749 Beatles	Harvey, 81	Dec 11	3
8768 Barnowl	Harvey, 81	Jan 6	3
8852 Buxus	Harvey, 81	Nov 19	3
8995 Rachelstevenson	Harvey, 81	Aug 19	3
9011 Angelou	Harvey, 81	Sep 21	3
9013 Sansaturo	Harvey, 81	Jul 27	3
9034 Oleyuria	Harvey, 81	Aug 11	3
9037 1990 UJ2	Harvey, 81	Oct 8	3
9177 1990 YA	Harvey, 81	Jan 1	3
9246 Neimeyer	Harvey, 81	Aug 18	3
9308 Randyrose	Harvey, 81	Jul 27	3
9362 Miyajima	Harvey, 81	Sep 21	3
9545 Petrovedomosti	Harvey, 81	Jul 27	3
9574 Taku	Harvey, 81	Apr 17	3
9741 Solokhin	Harvey, 81	Feb 15	3
9893 1996 AA1	Harvey, 81	Apr 14	3
9896 1996 BL17	Harvey, 81	Apr 16	3
9933 Alekseev	Harvey, 81	Dec 11	3
10017 Jaosungi	Harvey, 81	Oct 18	3
			0.4b@15.8
10036 McGaha	Harvey, 81	Aug 9	3
10143 Kamogawa	Harvey, 81	Feb 15	3
10164 Akusekijima	Harvey, 81	Jan 20	3
10287 Smale	Harvey, 81	Oct 14	3
10608 Mameta	Harvey, 81	Nov 19	3
10668 Plansos	Harvey, 81	Apr 22	3
10793 Quito	Rayon, 45	Nov 18	1C
10805 Iwano	Harvey, 81	Jan 5	3
10909 1997 XB10	Harvey, 81	Jan 22	3
10944 1999 FJ26	Harvey, 81	Aug 11	3
11007 Granahan	Harvey, 81	Oct 6	3
11141 Jindrawalter	Harvey, 81	Jun 26	3
11192 1998 XX49	Harvey, 81	Jan 6	3
11279 1989 TC	Harvey, 81	Sep 21	3
11365 NASA	Harvey, 81	Jan 20	3
11401 Pierralba	Harvey, 81	Aug 9	3
			1.0f@16.1
11526 1991 UL3	Harvey, 81	Sep 4	3
11528 Mie	Harvey, 81	Aug 18	6
11575 1994 BN4	Harvey, 81	Sep 7	3
11684 1998 FY11	Harvey, 81	May 16	3
11789 Kempowski	Harvey, 81	Apr 22	3
11894 1991 GW	Harvey, 81	Apr 2	3
11958 Galiani	Harvey, 81	Nov 21	3
12014 Bobhawkes	Harvey, 81	Feb 22	3
12256 1989 CJ8	Harvey, 81	Feb 22	3
12283 1991 EC	Harvey, 81	Jan 5	3
12706 Tanezaki	Harvey, 81	Oct 15	3
12742 Delisle	Harvey, 81	Oct 15	3
12856 1998 HH93	Harvey, 81	Jan 20	3
12920 1998 VM15	Harvey, 81	Jun 14	3
12947 3099 T-1	Harvey, 81	Jan 6	3
13071 1991 RT5	Harvey, 81	Oct 14	3
13111 Papacosmas	Harvey, 81	Jul 12	6
13380 Yamamohammed	Harvey, 81	Apr 22	3
13390 Bouska	Harvey, 81	Jan 22	3
13398 1999 RF62	Harvey, 81	Jan 21	3
13491 1984 UJ1	Harvey, 81	Nov 19	3
13492 Vitalijzakharov	Harvey, 81	Nov 20	3
13538 1991 ST	Harvey, 81	Apr 22	3
13567 Urabe	Harvey, 81	Jan 1	3
13578 1993 MK	Harvey, 81	Jun 26	3
13581 1993 QX4	Harvey, 81	Feb 22	3
13920 Montecorvino	Harvey, 81	Sep 14	3
13923 Peterhof	Harvey, 81	Nov 21	3
13977 Frisch	Faure, 35	Jun 23	4
14006 Sakamotofumio	Harvey, 81	Oct 20	3
14198 1998 XZ73	Harvey, 81	Oct 20	3
14564 Heasley	Harvey, 81	Jul 14	3
14613 Sanchez	Harvey, 81	Oct 15	3
14989 Tutte	Harvey, 81	Oct 14	3
15129 Sparks	Harvey, 81	Oct 20	3
15430 1998 UR31	Harvey, 81	May 12	3
15436 1998 VU30	Harvey, 81	Oct 8	3
15689 1981 UP25	Harvey, 81	May 16	3
15791 Yoshiewatanabe	Harvey, 81	Jan 1	3
15799 1993 XN	Harvey, 81	Jan 22	3
15985 1998 WU20	Harvey, 81	May 11	3
16446 1989 MH	Harvey, 81	Apr 21	3
16447 Vauban	Harvey, 81	Sep 11	3
16466 Piyashiriyama	Harvey, 81	Jan 1	3
16528 Terakado	Harvey, 81	Aug 19	3
16559 1991 VA3	Harvey, 81	Aug 18	3
16681 1994 EV7	Harvey, 81	Feb 15	6
16704 1995 ED8	Harvey, 81	Feb 28	3
16908 Groeselenberg	Harvey, 81	Jan 20	3
16986 Archivestef	Harvey, 81	Feb 28	3
17012 1999 CY80	Harvey, 81	May 11	3
17485 1991 RP9	Harvey, 81	Dec 11	3
17509 Ikumadan	Harvey, 81	Feb 22	3
17711 1997 WA7	Harvey, 81	Apr 21	3
17814 1998 FH113	Harvey, 81	Jul 14	3
17953 1999 JB20	Harvey, 81	May 11	3
			0.5f@15.9
18029 1999 KA16	Harvey, 81	May 2	3
18129 2000 OH5	Harvey, 81	Feb 15	3
18285 Vladplatonov	Harvey, 81	Apr 19	3
18399 Tentoumushi	Harvey, 81	Nov 17	3
18418 Ujibe	Harvey, 81	Oct 18	3
18640 1998 EF9	Harvey, 81	Dec 15	3
19120 Doronina	Harvey, 81	Aug 9	6
19204 Joshuatree	Harvey, 81	Jun 26	3
			0.5f@15.9
19370 Yukyung	Harvey, 81	Jan 21	3
19402 1998 EG14	Harvey, 81	Oct 20	3
19511 1998 MC45	Harvey, 81	Oct 14	3
19551 Peterborden	Harvey, 81	Oct 8	3
19600 1999 NV41	Harvey, 81	Nov 20	3
19755 2000 EH34	Harvey, 81	Nov 16	3
19764 2000 NF5	Harvey, 81	Sep 11	6
20170 1996 VM30	Harvey, 81	Sep 21	3
20350 1998 HV125	Harvey, 81	Oct 15	3
21182 1994 EC2	Harvey, 81	Sep 14	3
21242 1995 WZ41	Faure, 20	Nov 19	3
	Harvey, 81	Nov 17	3
	Rayon, 45	Nov 18	2C
21561 Masterman	Harvey, 81	Nov 19	3
21757 1999 RQ194	Harvey, 81	Oct 18	3
22135 2000 UA100	Harvey, 81	Jun 21	3
22759 1998 XA4	Harvey, 81	Nov 16	3
23231 2000 WT59	Harvey, 81	Jun 1	3
23648 Kolar	Harvey, 81	Sep 14	3

MINOR PLANET	OBSERVER & APERTURE (cm)	OBSERVING PERIOD (2019)	NO. OBS.
23880 Tongil	Harvey, 81	Oct 19	3
23974 1999 CK12	Harvey, 81	Jan 21	3
23997 1999 RW27	Harvey, 81	Oct 15	3
		1.0f@15.5	
24280 Rohanderson	Harvey, 81	Sep 21	3
24298 1999 XC221	Harvey, 81	Oct 7	3
24433 2000 CF83	Harvey, 81	Jul 27	3
25068 1998 QV88	Harvey, 81	Aug 11	3
25505 1999 XQ95	Harvey, 81	Sep 11	3
25995 2001 FA83	Harvey, 81	Aug 11	3
26432 1999 XZ202	Harvey, 81	Nov 21	3
26818 1987 QM	Harvey, 81	Oct 6	3
26834 1990 RM9	Harvey, 81	Oct 19	3
28056 1998 MK5	Harvey, 81	Nov 21	3
28291 1999 CX52	Harvey, 81	Oct 19	3
		0.3f@16.3	
28565 2000 EO58	Harvey, 81	Jul 28	6
28887 2000 KQ58	Harvey, 81	Dec 11	3
30717 1937 UD	Harvey, 81	Sep 21	3
		0.5f@15.8	
30971 1995 DJ	Harvey, 81	Oct 18	3
33087 1997 XX	Harvey, 81	May 11	3
33881 2000 JK66	Harvey, 81	Jun 21	3
34373 2000 RT44	Harvey, 81	Aug 27	3
34882 2001 UK66	Harvey, 81	May 2	3
35371 Yokonozaki	Harvey, 81	Sep 22	3
35810 1999 JB44	Harvey, 81	Oct 7	3
36260 1999 XQ111	Harvey, 81	May 2	3
37152 2000 VV56	Harvey, 81	Apr 4	6
37187 2000 WP60	Harvey, 81	Jul 28	3
41331 1999 XB232	Harvey, 81	Nov 21	3
42570 1996 YA2	Harvey, 81	Feb 15	3
42685 1998 JY	Harvey, 81	Oct 15	3
46875 1998 QD104	Harvey, 81	Jan 20	3
48439 1989 WR2	Harvey, 81	Dec 11	4
48898 1998 MO5	Harvey, 81	Jul 14	6
49636 1999 HJ1	Harvey, 81	Jul 12	3
49737 1999 VS112	Harvey, 81	May 16	3
49978 1999 YT5	Harvey, 81	Oct 15	3
50713 2000 EZ135	Faure, 20	Oct 18	2
51442 2001 FZ25	Harvey, 81	Sep 21	3
51866 2001 PH3	Harvey, 81	Dec 15	3
51917 2001 QQ83	Rayon, 45	Apr 10	2C
52768 1998 OR2	Faure, 20	Apr 14	3
	Pryal, 20	Apr 26-28	6
	Rayon, 45, 15	Apr 10-14	4C
	Werner, 20	Apr 24-May 2	10
53308 1999 HJ8	Rayon, 45	Apr 10	1C
53435 1999 VM40	Rayon, 45	Nov 19	2C
56086 1999 AA21	Harvey, 81	Sep 14	3
65854 1997 EH46	Harvey, 81	Oct 6	3
68130 2001 AO17	Harvey, 81	Aug 18	3
76818 Brianenke	Harvey, 81	Jan 21	3
85184 1991 JG1	Harvey, 81	May 10	6
136108 Haumea	Faure, 35	May 26-27	2
	Rayon, 25	May 26	1C
137311 1999 TX9	Harvey, 81	Nov 16	6
137924 2000 BD19	Harvey, 81	Feb 2	6
153201 2000 WO107	Harvey, 81	Nov 29	6
163348 2002 NN4	Harvey, 81	Jun 13	6
163373 2002 PZ39	Harvey, 81	Jan 28	6
163902 2003 SW222	Harvey, 81	Dec 11	6
183230 2002 TC58	Harvey, 81	Jul 14	3
242450 2004 QY2	Harvey, 81	Jul 2	6
247484 2002 LC24	Harvey, 81	Jan 1	6
420302 2011 XZ1	Faure, 45	Aug 22	3
	Harvey, 81	Jun 26	6
437316 2013 OS3	Harvey, 81	Jan 20	6
438908 2009 XO	Harvey, 81	May 7-10	18
498066 2007 RM133	Harvey, 81	Jul 2	6
539940 2017 HW1	Harvey, 81	Apr 22	6
2000 KA	Harvey, 81	May 12	6
2006 NL	Harvey, 81	Jul 12	6
2013 UX14	Harvey, 81	Oct 18	6
2015 FC35	Harvey, 81	Apr	6
2016 PN	Harvey, 81	Jul 30	6
2019 WC5	Harvey, 81	Jan 9	6
2020 BT14	Harvey, 81	Feb 3	6
2020 RC	Harvey, 81	Sep 7	6
2020 ST1	Harvey, 81	Nov 16	6

ALL IN THE FAMILY: UPCOMING CHANGES IN THE LCDB

Brian D. Warner
Center for Solar System Studies / MoreData! Inc.
446 Sycamore Ave.
Eaton, CO 80615 USA
brian@MinorPlanetObserver.com

Alan W. Harris
MoreData! Inc.
La Cañada, CA 91011-3364 USA

Since 2005, the asteroid lightcurve database (LCDB; Warner et al., 2009) used osculating orbital elements to assign family/group membership. Including special subgroups, e.g., inner main-belt (MB-I) versus inner main-belt comets (MB-IC), there were fewer than 33 families/groups. The LCDB release expected in 2021 April or May, will incorporate families defined by Nesvorny et al. (2015; Nesvorny, 2015) and additional families defined on the AstDys web site. The change will include revised default albedo and phase slope parameter (G on H-G system) values for each family. In addition, the LCDB will include provisions for data on the H-G12 or H-G1G2 system (Muinonen et al., 2010), which has been formally adopted by the International Astronomical Union. The details of these changes are explained here.

Barring specific data otherwise, the asteroid lightcurve database (Warner et al., 2009) uses osculating orbital elements to define broad asteroid families/groups. This is done to help assign default taxonomic class, albedo, and derived diameter for an object when actual values were not available. This allows the LCDB to be used for its most common purpose: to compare rotation frequencies (periods) against diameter (Figure 1).

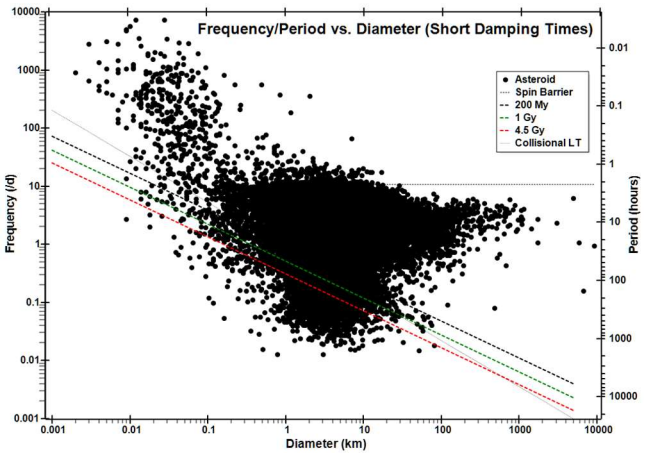

Figure 1. This frequency-diameter plot from the LCDB (2021 Apr 3) shows all objects with a statistically useful period, including those from dense and sparse wide-field surveys.

While these broad family/group assignments were generally sufficient, they didn't allow more refined statistical studies of the much larger number of true asteroid families, a number that is often under review and change.

In the 2021 April/May release of the LCDB, these broad groups will be replaced by adopting the dynamical families defined under Nesvorny (2015) and Nesvorny et al. (2015); *Nesvorny* refers to both references from here on) and AstDys (2021) web site (see the numerous references available there). The most important element of the revision is that family membership is based on proper elements, which are invariable over very long periods of time.

More so, *Nesvorny* used SDSS colors and WISE (Mainzer et al., 2019) albedos along with a parameter Cj to isolate objects that were more likely than not true family members (from the same parent) and those just occupying the orbital space of a family, what they called *dynamic interlopers*. For example, their list for the Hungaria family includes 2965 objects but 60 of those were flagged by the Cj parameter to by *dynamic interlopers*.

In the LCDB, any object not within one of the defined families is given an LCDB-defined family identification number (FIN; see *Nesvorny* for a discussion about the need and use of FINs) in the range 9000-9999.

Whether a true family member or a group member, a default albedo, taxonomic class, and *G* (on the H-G system) are assigned to an object when added to the LCDB, except in those cases when one or more of the actual values are known. These three values can have a complex relationship when the class and albedo are not directly obtained.

Nesvorny assigned default albedos and taxonomic class for most of the families in their list. As previously mentioned, the albedos are based on WISE observations, i.e., their *H* and the measured diameter were used to derive the albedo, while the taxonomic class was taken from the literature. When no actual values are available, the defaults are used. However, *Nesvorny* did not provide a default value for *G*. This value is assigned based on the adopted albedo as given in Table 1.

Taxonomic Classes	Albedo	G
C, G, B, F, P, T, D	0.057 ± 0.02	0.12 ± 0.08
M	0.16 ± 0.04	0.20 ± 0.07
S, Q	0.20 ± 0.07	0.24 ± 0.11
E, V, R	0.46 ± 0.06	0.43 ± 0.08

Table 1. Inter-relation of default taxonomic class, albedo, and *G* (H-G) from Warner et al. (2009)

Beyond this, Table 1 (originally in Warner et al., 2009) is used to assign default values when at least one of the three parameters is known. These defaults were based on objects with known values for all three parameters at the time.

It should be noted that if there is a measured *H* that is considered reliable, it will be used in lieu of value in the MPCORB file. Likewise, if there is a reliable diameter, e.g., from a spacecraft or occultation, it will be used in lieu of a default value or that measured by an IR survey. The associated values for *H* and albedo adjusted accordingly. In other words, whenever possible, a measured value takes precedence over its corresponding default value.

The *Nesvorny* family numbers were used for the initial assignments, including for those in AstDys families common to *Nesvorny*. However, there were 60 families in the AstDys list that were not in *Nesvorny*. These were assigned custom family numbers in the range 2000-2999.

Table 2 (after the References section) gives a full listing of the 202 family or orbital group assignments and default values used in the 2021 April/May release of the LCDB.

The *Number* column is the family number that appears in the LCDB text reports. Nesvorny numbers range from 001-999. Family numbers 2001-2060 are dynamical families that appear only in the list on the AstDys (2021) web site. Numbers > 9100 are "catch all" orbital groups for those objects that could not be tied to a dynamic family. The family name is appended with an asterisk.

The *Parent* is the MPC-assigned number of the parent (often largest) body of a family. The *Name* column gives the name of the parent body. The *Albedo* column value is usually that of the parent body as inferred by WISE (Mainzer et al., 2019) or, for a small number of families, the average of several albedos of family members, again using albedos inferred from WISE data.

If there is an asterisk after a class, it is assumed based on orbital location. Otherwise, it is the measured taxonomic class of the parent body. *Count* is the number of dynamic family members taken from the Nesvorny or AstDys lists.

Table 3 (after References section) gives the *osculating* orbital elements ranges for the broad groups with family numbers > 9000. For each core elements (*a*, *e*, *i*), the two columns represent the minimum and maximum values. *Q* is the aphelion distance and *q* is the perihelion distance.

Cave Usor – User Beware

We wish to make it clear as possible that an object being in the same orbital space defined for a family does not necessarily make it a member of that family but, instead, that it could be a *dynamic interloper*. The Hungaria family is just one example where there are numerous interlopers.

The true determination of family membership is possible only when its proper elements and taxonomic spectrum (not just broad taxonomic class) closely match those of a known family parent. The assignments in the LCDB are meant to be good starting points and may be useful in many cases but they are *not* the final word for critical studies.

The tabulation of absolute magnitude (*H*), phase slope parameter (*G*), and albedo (p_V or other band) are used to document how the value for diameter (*D*) was determined. These values are not intended to be fundamental or all that carefully edited. For the LCDB purposes, an error of even 50% in diameter is insignificant in a plot like Figure 1, which spans five orders of magnitude.

A Case in Point

For some time, 93 Minerva was considered the main (namesake) body for the Minerva family. Spectroscopic observations showed that it was actually an interloper among what is now called the Gefion family (after 1272 Gefion). What distinguishes the Gefion members is their higher than usual albedo for outer main-belt objects ($p_V \sim 0.25$) instead of the more typical $p_V \sim 0.06$.

The AstDys families list has only the Minerva group and contains only a relatively few members common to the *Nesvorny* Gefion family (516). The *Nesvorny* Gefion family is used in the LCDB. Members of the AstDys list not in the *Nesvorny* list were placed in the catch-all outer main-belt group (9106). However, they were not all set to use the defaults of class = C*, $G = 0.12 \pm 0.08$, and $p_V = 0.057$.

Instead, where available, WISE, AKARI, and/or SIMPS albedos were averaged and that value was assigned with the 'L' (details record) flag. Based on Table 1, objects with albedos < 0.12 were set to type "C*." Type "SC*" was assigned to objects within $0.12 \le p_V \le 0.18$ but the averaged albedo was used in lieu of the default of $p_V = 0.1$. Objects with $p_V > 0.18$ were assigned the "S*" class.

Another Case in Point

While there are some specific families within the common orbital space for the near-Earth asteroids, Hildas, Jupiter trojans, Centaurs, and TNO/KBO objects, in general these groups are treated without distinction between family and group members since there is no single parent body for each group.

For example, when searching the MPCORB file using the osculating elements limits for group 9107 (Hilda space in Table 3), a total of 4615 objects were found. However, looking deeper, 409 of those objects were in families or subfamilies defined by *Nesvorny* and/or AstDys other than the Hildas (e.g., Nesvorny 002, Schubart; AstDys 2022, Devine; and AstDys 2027, Mecklenburg).

The 2021 March 28 snapshot of the LCDB summary table found 1,484 objects, regardless of U rating, within the Hilda orbital space defined in Table 3. Of those, 258 were assigned to "outsider" families such as those in the previous paragraph.

These are just some of the many examples of the indefinite definitions of asteroid families and the possibility for numerous interlopers with "outlying" values in a presumed family. If trying to do critical studies based on true *family* membership, the LCDB should be considered a starting point but *not* the final destination.

"Cave Usor!"

The H-G, H-G12, and H-G1G2 Systems

To predict the magnitude of an asteroid and how it changes with phase angle versus a linear geometrical relationship, the H-G system (Bowell et al., 1989) was adopted by the IAU in 1985. A new system involving three parameters (Muinonen et al., 2010) was adopted by the IAU, although the H-G system still remains in wide use. Even so, the use of H-G12 system is becoming more common as large survey contribute large bulks of data. As a result, the LCDB tables have been altered to account for the new data format.

The H-G12 system uses only the first term of the two under the H-G1,G2 system and is most often used when there are limited data for finding a phase curve. The H-G1,G2 system uses two parameters that more effectively describe the asteroid's brightness at large and small phase angles. It has also been shown to be an effective tool for taxonomic classification (Shevchenko et al, 2016; Mahlke et al., 2021).

A strong discontinuity exists around G1 = 0.2 for the H-G12 and H-G1,G2 systems. See the Muinonen et al. (2010) paper for a discussion of this issue.

The large majority of *G* values given in the LCDB are under the H-G system. However, some surveys that produced large numbers of rotation periods also found G1 under H-G12 as part of their data reduction. To accommodate both systems, the Summary and Details of the LCDB tables include a "G" and "G2" field.

In both tables, if the *GSource* field has no value or one other than 'G', the *G* data field is on the H-G system. If the *GSource* field has 'G', then the value in the *G* field is G1 on the H-G12 or H-G1,G2 system. If the *G2* field has a value, then the *G* field is G1 on the H-G1,G2 system.

On-line Resource

The link below, to be updated prior to publication, allows you to retrieve information about a single object, including the new family/group membership.

minorplanet.info/PHP/OneAsteroidInfo.php

The search returns entries in the LCDB and dates of opposition, closest, and brightest through 2024 for the selected object, if found in the LCDB and/or opposition database, and a 30-day ephemeris (topocentric) based on unperturbed elements from a recent MPCORB file.

Acknowledgements

Development and maintenance of the current version LCDB, i.e., a relational database instead of single flat text file, has been carried out under five NASA and four NSF grants since 2005. We gratefully acknowledge the support of the two agencies over the past 16 years. The 2021 April/May release, carried out under 80NSSC18K0851, will be the last one under the auspices of either agency. We intend to carry on with LCDB maintenance in the foreseeable future but at a more "leisurely" pace. This includes providing a version of the 2021 April/May release for the NASA Planetary Data System (PDS) and, if possible, on the VizieR site (*http://vizier.u-strasbg.fr/*). The latter, however, usually requires the catalog be tied to a, preferably recent, published paper.

We also thank the many users of the LCDB for their feedback. Given the number of times we've seen a version of Figure 1 and papers based on LCDB data, we're gratified to know that the effort over the years has provided a useful and even important tool in asteroid research.

References

AstDys (2021). Asteroids - Dynamic site. *https://newton.spacedys.com/astdys/*

Bowell, E.; Hapke, B.; Domingue, D.; Lumme, K.; Peltoniemi, J.; Harris, A.W. (1989). "Application of photometric models to asteroids." in Asteroids II; Proceedings in the Conference, Tucson, AZ, Mar. 8-11, 1988. University of Arizona Press, pp. 524-556.

Mahlke, M.; Carry, B.; Denneau, L. (2021). "Asteroid phase curves from ATLAS dual-band photometry." *Icarus* **354**, id. 114094.

Mainzer, A.; Bauer, J.; Cutri, R.; Grav, T.; Kramer, E.; Masiero, J.; Sonnett, S.; Wright, E., Eds. (2019). "NEOWISE Diameters and Albedos V2.0." NASA Planetary Data System. urn:nasa:pds:neowise_diameters_albedos::2.0. *https://doi.org/10.26033/18S3-2Z54*

Muinonen, K.; Belskaya, I.N.; Cellino, A.; Delbo, M.; Levasseur-Regourd, A.-C.; Pentttila, A.; Tedesco, E.F. (2010). "A three-parameter magnitude phase function for asteroids." *Icarus* **209**, 542–555.

Nesvorny, D. (2015). "Nesvorny HCM Asteroids Families V3.0." NASA Planetary Data Systems, id. EAR-A-VARGBET-5-NESVORNYFAM-V3.0.

Nesvorny, D.; Broz, M.; Carruba, V. (2015). "Identification and Dynamical Properties of Asteroid Families." In *Asteroids IV* (P. Michel, F. DeMeo, W.F. Bottke, R. Binzel, Eds.). Univ. of Arizona Press, Tucson, also available on astro-ph.

Shevchenko, V.G.; Belsakya, I.N.; Muinonen, K.; Penttila, A.; Krugly, Y.N.; Velichko, F.P.; Chiorny, V.G.; Slyusarev, I.G.; Gaftonyuk, N.M.; Tereschenko, I.A. (2016). "Asteroid observations at low phase angles. IV. Average parameters for the new H, G1, G2 magnitude system." *Planet. Space Sci.* **123**, 101-116.

Warner, B.D.; Harris, A.W.; Pravec, P. (2009). "The Asteroid Lightcurve Database." *Icarus* **202**, 134-146. Updated 2021 Apr. *http://www.minorplanet.info/lightcurvedatabase.html*

SPIN-SHAPE MODEL FOR 374 BURGUNDIA

Lorenzo Franco
Balzaretto Observatory (A81), Rome, ITALY
lor_franco@libero.it

Alessandro Marchini, Riccardo Papini
Astronomical Observatory, DSFTA - University of Siena (K54)
Via Roma 56, 53100 - Siena, ITALY

Giorgio Baj
M57 Observatory (K38), Saltrio, ITALY

Giulio Scarfi
Iota Scorpii Observatory (K78), La Spezia, ITALY

Fabio Mortari
Hypatia Observatory (L62), Rimini, ITALY

Pietro Aceti
Seveso Observatory (C24), Seveso, ITALY

Richard E. Schmidt
Burleith Observatory (I13), Washington, DC 20007 USA

Robert A. Koff
Antelope Hills Observatory (H09), Bennett, CO 80102 USA

(Received: 2021 April 10. Revised: 2021 May 22)

We present a shape and spin axis model for main-belt asteroid 374 Burgundia. The model was achieved with the lightcurve inversion process, using combined dense photometric data acquired from four apparitions beetween 2000-2021 and sparse data from USNO Flagstaff. Analysis of the resulting data found a sidereal period P = 6.96397 ± 0.00002 hours and two mirrored pole solutions at (λ = 9°, β = 38°) and (λ = 178°, β = 28°) with an uncertainty of ± 10 degrees.

The Minor planet 374 Burgundia was recently observed by the Italian Amateur Astronomers Union (UAI; 2021) group in order to acquire data for lightcurve inversion work (Franco et al. 2019, 2021). Other dense photometric data were downloaded from ALCDEF (ALCDEF, 2021) and, to improve the coverage at various aspect angles, was used sparse data from USNO Flagstaff Station, downloaded from the Asteroids Dynamic Site (AstDyS-2, 2020), according Durech et al. (2009).

The observational details of the dense data used are reported in Table I with the mid-date, number of the lightcurves used for the inversion process, longitude and latitude of phase angle bisector (L_{PAB}, B_{PAB}).

Reference	Mid-date	# LC	L_{PAB}°	B_{PAB}°
Koff (2000)(*)	2000-11-15	3	41	-1
Schmidt (2017)(*)	2017-07-10	9	245	6
Franco et al. (2019)	2018-09-27	7	354	8
Franco et al. (2021)	2021-03-04	8	169	-9

Table I. Observational details for the data used in the lightcurve inversion process for 374 Burgundia.
(*) Published on 'alcdef.org' web site.

Lightcurve inversion was performed using *MPO LCInvert* v.11.8.2.0 (BDW Publishing, 2016). For a description of the modeling process see LCInvert Operating Instructions Manual, Durech et al. (2010); and references therein.

Figure 1 shows the PAB longitude/latitude distribution for the dense and sparse data used in the lightcurve inversion process. Figure 2 (top panel) shows the sparse photometric data distribution (intensities vs JD) and (bottom panel) the corresponding phase curve (reduced magnitudes vs phase angle).

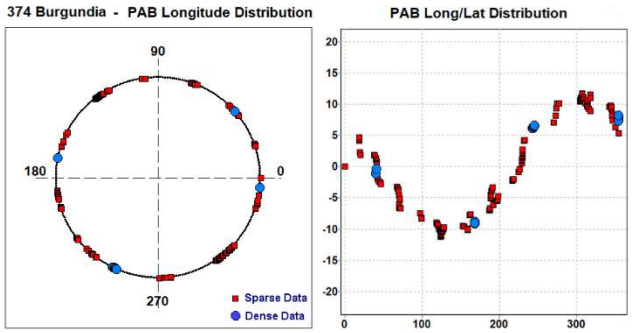

Figure 1: PAB longitude and latitude distribution of the data used for the lightcurve inversion model.

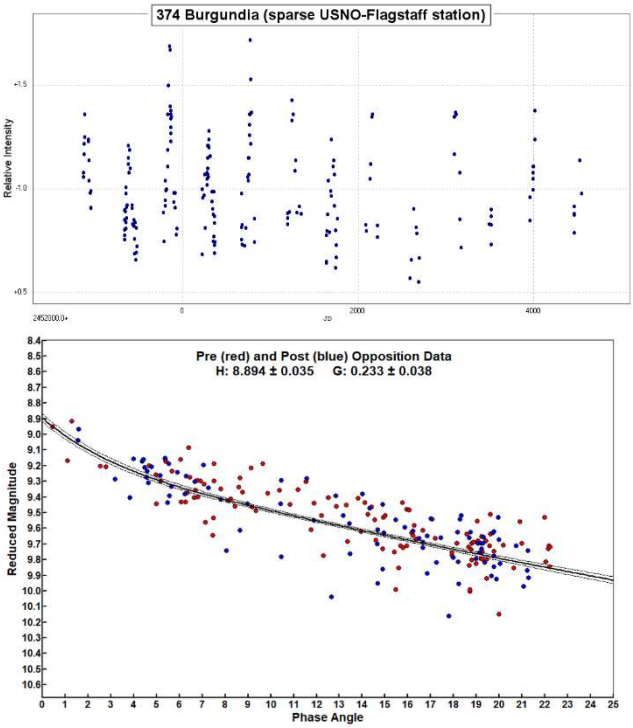

Figure. 2: Top: sparse photometric data point distribution from (689) USNO Flagstaff station (relative intensity of the asteroid's brightness vs Julian Day). Bottom: phase curve obtained from sparse data (reduced magnitude vs phase angle).

In the analysis the processing weighting factor was set to 1.0 for dense data and 0.3 for sparse data. The "dark facet" weighting factor was set to 0.7 to keep the dark facet area below 1% of total area and the number of iterations was set to 50.

In lightcurve inversion work the critical step is to find an accurate sidereal rotational period. For this purpose, we started the period scan around about the 3-sigma interval centered on the average of the synodic periods found in the asteroid lightcurve database (LCDB; Warner et al., 2009). We found one isolated sidereal period with a Chi-Sq value within 10% of the lowest Chi-Sq (Figure 3), according to the criterion for the "*unique solution*" defined by Durech et al. (2009).

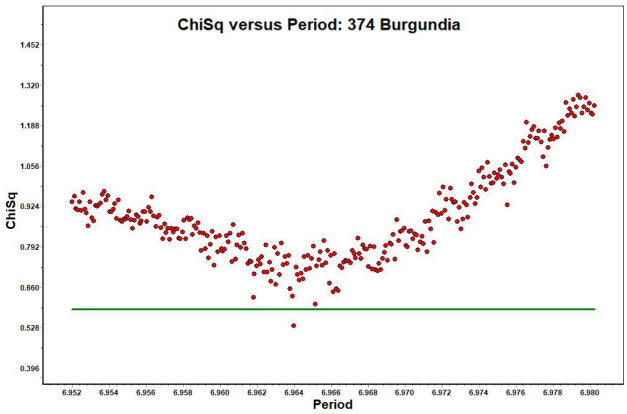

Figure 3: The period scan for 374 Burgundia shows one isolated sidereal period with Chi-Sq values within 10% of the lowest value.

The pole search was started using the "medium" search option (312 fixed pole position with 15° longitude-latitude steps) and the previously found sidereal period set to "float". From this step we found two roughly mirrored lower Chi-Sq solutions (Figure 4) separated by about 180° in longitude at ecliptic longitude-latitude pairs (15°, 45°) and (180°, 30°).

The subsequent "fine" search option (49 fixed pole steps with 10° longitude-latitude pairs set to "float") allowed us to refine the position of the pole (Figure 5). The analysis shows two set of clustered solutions within 10° of radius that had Chi-Sq values within 10% of the lowest value, centered at ecliptic longitude-latitude (9°, 39°) and (177°, 28°).

The two best solutions (lower Chi-Sq and RMS) are reported in Table II. The sidereal period was obtained by averaging the two solutions found in the pole search process. Typical errors in the pole solution are ± 10° and the uncertainty in sidereal period has been evaluated as a rotational error of 20° over the total time span of the dense data set. Figure 6 shows the shape model (first solution with lower Chi-Sq and RMS) while Figure 7 shows the fit between the model (black line) and some observed lightcurves (red points).

λ °	β °	Sidereal Period (hours)	Chi-Sq	RMS
9	38	6.96397 ± 0.00002	0.51225	0.0175
178	28		0.53161	0.0178

Table II. The two spin axis solutions for 374 Burgundia (ecliptic coordinates) with an uncertainty of ± 10 degrees. The sidereal period was the average of the two solutions found in the pole search process.

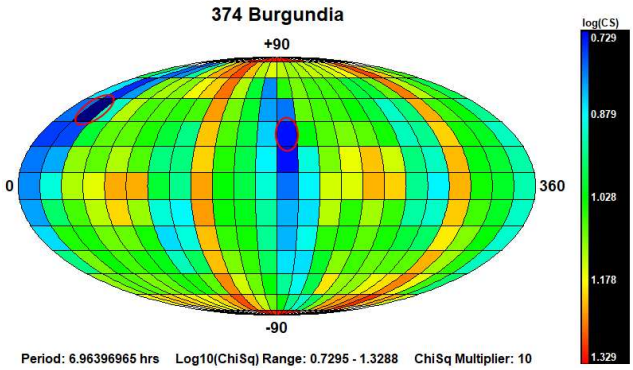

Figure 4: Pole search distribution. The dark blue region indicates the smallest Chi-Sq value while the dark red region indicates the largest.

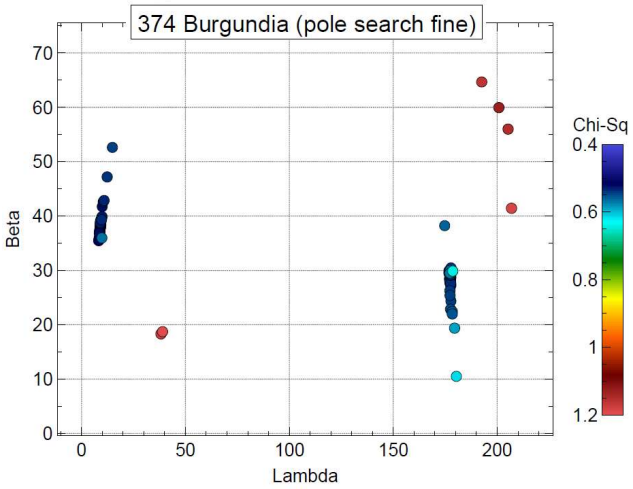

Figure 5: The "fine" pole search shows two clustered solutions centered at ecliptic longitude-latitude pairs (9°, 39°) and (177°, 28°) with radius approximately of 10° and Chi-Sq values within 10% of the lowest value.

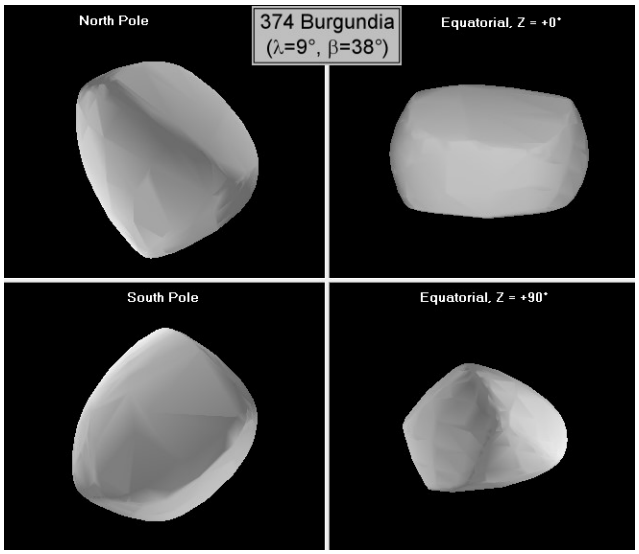

Figure 6: The shape model for 374 Burgundia (λ = 9°, β = 38°).

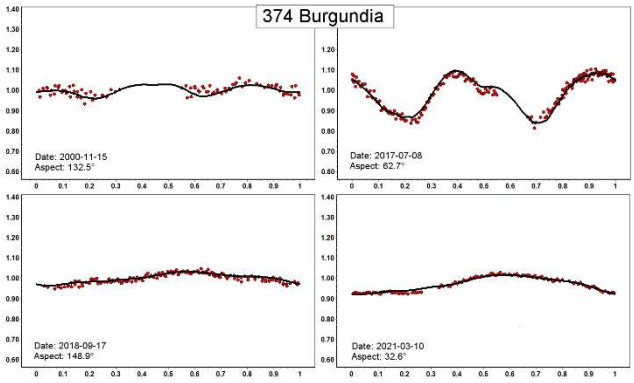

Figure 7: Model fit (black line) versus observed lightcurves (red points) for (λ = 9°, β = 38°) solution.

References

ALCDEF (2021). Asteroid Lightcurve Data Exchange Format web site. *http://www.alcdef.org/*

AstDyS-2 (2020). Asteroids - Dynamic Site. *https://newton.spacedys.com/astdys/*

BDW Publishing (2016). *http://www.minorplanetobserver.com/MPOSoftware/MPOLCInvert.htm*

Durech, J.; Kaasalainen, M.; Warner, B.D.; Fauerbach, M.; Marks, S.A.; Fauvaud, S.; Fauvaud, M.; Vugnon, J.-M.; Pilcher, F.; Bernasconi, L.; Behrend, R. (2009). "Asteroid models from combined sparse and dense photometric data." *A&A*, **493**, 291-297.

Durech, J.; Sidorin, V.; Kaasalainen, M. (2010). "DAMIT: a database of asteroid models." *A&A*, **513**, A46.

Franco, L.; Marchini, A.; Baj, G.; Scarfi, G.; Bacci, P.; Maestripieri, M.; Bacci, R.; Papini, R.; Salvaggio, F.; Banfi, M. (2019). "Lightcurves for 131 Vala, 374 Burgundia, 734 Brenda, and 929 Algunde." *Minor Planet Bulletin* **46**, 85-86.

Franco L.; Marchini, A.; Cavaglioni, L.; Papini, R.; Privitera, C.A.; Baj, G.; Galli, G.; Scarfi, G.; Aceti, P.; Banfi, M.; Bacci, P.; Maestripieri, M.; Mannucci, M.; Montigiani, N.; Tinelli, L.; Mortari, F. (2021). "Collaborative Asteroid Photometry from UAI: 2021 January-March." *Minor Planet Bulletin* **48**, 219-221.

UAI (2021). "Unione Astrofili Italiani" web site. *https://www.uai.it*

Warner, B.D.; Harris, A.W.; Pravec, P. (2009). "The asteroid lightcurve database." *Icarus* **202**, 134-146. Updated 2020 October. *http://www.minorplanet.info/lightcurvedatabase.html*

LIGHTCURVE PHOTOMETRY OPPORTUNITIES: 2021 JULY-SEPTEMBER

Brian D. Warner
Center for Solar System Studies / MoreData!
446 Sycamore Ave.
Eaton, CO 80615 USA
brian@MinorPlanetObserver.com

Alan W. Harris
MoreData!
La Cañada, CA 91011-3364 USA

Josef Ďurech
Astronomical Institute
Charles University
18000 Prague, CZECH REPUBLIC
durech@sirrah.troja.mff.cuni.cz

Lance A.M. Benner
Jet Propulsion Laboratory
Pasadena, CA 91109-8099 USA
lance.benner@jpl.nasa.gov

We present lists of asteroid photometry opportunities for objects reaching a favorable apparition and having no or poorly-defined lightcurve parameters. Additional data on these objects will help with shape and spin axis modeling using lightcurve inversion. We also include lists of objects that will be (or might be) radar targets. Lightcurves for these objects can help constrain pole solutions and/or remove rotation period ambiguities that might arise from using radar data alone.

We present several lists of asteroids that are prime targets for photometry during the period 2021 July-September.

In the first three sets of tables, "Dec" is the declination and "U" is the quality code of the lightcurve. See the latest asteroid lightcurve data base (LCDB from here on; Warner et al., 2009) documentation for an explanation of the U code:

http://www.minorplanet.info/lightcurvedatabase.html

The ephemeris generator on the CALL web site allows creating custom lists for objects reaching V ≤ 18.0 during any month in the current year and up to five years in the future, e.g., limiting the results by magnitude and declination, family, and more.

http://www.minorplanet.info/PHP/call_OppLCDBQuery.php

We refer you to past articles, e.g., Warner et al. (2021) for more detailed discussions about the individual lists and points of advice regarding observations for objects in each list.

Once you've obtained and analyzed your data, it's important to publish your results. Papers appearing in the *Minor Planet Bulletin* are indexed in the Astrophysical Data System (ADS) and so can be referenced by others in subsequent papers. It's also important to make the data available at least on a personal website or upon request. We urge you to consider submitting your raw data to the ALCDEF database. This can be accessed for uploading and downloading data at

http://www.alcdef.org

The database contains more than 3.9 million observations for 15,000+ objects, making it one of the more useful sources for raw asteroid *time-series* lightcurve data.

Lightcurve/Photometry Opportunities

Objects with U = 3– or 3 are excluded from this list since they will likely appear in the list for shape and spin axis modeling. Those asteroids rated U = 1 should be given higher priority over those rated U = 2 or 2+, but not necessarily over those with no period. On the other hand, *do not overlook asteroids with* U = 2/2+ *on the assumption that the period is sufficiently established.* Regardless, do not let the existing period influence your analysis since even highly-rated result have been proven wrong at times. Note that the lightcurve amplitude in the tables could be more or less than what's given. Use the listing only as a guide.

An entry in bold italics is a near-Earth asteroid (NEA).

		Brightest			LCDB Data		
Number	Name	Date	Mag	Dec	Period	Amp	U
3109	Machin	07 11.0	14.8	-35	20.3	0.46	2
9601	1991 UE3	07 11.5	14.9	-31	3.733	0.09	2+
3942	Churivannia	07 11.7	14.9	-32			
819	Barnardiana	07 17.5	13.4	-28	66.7	0.82	2+
2229	Mezzarco	07 17.7	15.0	-11			
1034	Mozartia	07 19.1	12.8	-22			
3485	Barucci	07 20.3	14.7	-22	14.65	0.19	1
2844	Hess	07 20.4	14.4	-19			
285571	***2000 PQ9***	***07 20.4***	***12.7***	***-22***			
1701	Okavango	07 22.5	14.4	-42	13.204	0.32-0.45	2
6975	Hiroaki	07 23.1	14.2	-24			
2898	Neuvo	07 25.8	14.9	-22	17.591	0.06-0.62	2-
1714	Sy	07 26.0	14.2	-19			
4396	Gressmann	07 27.3	14.9	-27			
4319	Jackierobinson	07 28.9	15.1	-26			
7198	Montelupo	07 30.7	14.9	-17			
2232	Altaj	07 31.0	14.8	-12			
6753	Fursenko	08 05.6	15.0	-16	4.99	0.19	1+
3702	Trubetskaya	08 07.0	14.1	-24			
1705	Tapio	08 07.5	14.7	-3	54.8	0.29-0.44	2
2412	Wil	08 07.8	14.4	-14			
2728	Yatskiv	08 11.0	14.7	-11			
2865	Laurel	08 12.3	14.3	-16	21.5	0.15	2
938	Chlosinde	08 12.7	14.5	-16	19.204	0.12-0.16	2
3112	Velimir	08 13.0	14.9	-22	3.653		2-
6916	Lewispearce	08 13.2	14.4	-11	23.497	0.25	2
7724	Moroso	08 13.8	15.0	-23			
3053	Dresden	08 15.0	14.8	-21	4.788	0.34	2
3116	Goodricke	08 18.2	13.9	-24	26.7	0.09- 0.3	2
2607	Yakutia	08 19.9	14.8	-15			
2098	Zyskin	08 20.1	14.5	-15	3.92	0.08	2
2431	Skovoroda	08 20.1	14.0	-13	3.13	0.21	2
	2016 AJ193	***08 20.3***	***13.5***	***-36***			
17081	Jaytee	08 20.8	15.2	-11			
4781	Sladkovic	08 23.0	14.9	-11			
5095	Escalante	08 28.7	14.8	-14	8.542	0.10-0.54	2
18863	1999 RC191	08 29.0	15.0	-8			
2824	Franke	08 29.9	14.7	-7	3.38	0.06	2
8416	Okada	09 02.7	14.8	-7			
1144	Oda	09 03.1	14.7	-9	648	0.41-0.55	2+
5786	***Talos***	***09 04.1***	***14.1***	***+7***	***23.6***	***0.23-0.30***	***2***
1285	Julietta	09 05.3	14.7	-3	20.3	0.07-0.23	1
9143	Burkhead	09 06.1	14.8	-5			
3165	Mikawa	09 06.9	14.3	-14	5.08	0.08-0.27	2
1519	Kajaani	09 13.0	14.5	-13			
10940	1999 CE52	09 13.4	14.9	-18			
3729	Yangzhou	09 19.7	14.2	-5	29.158	0.41	2
2646	Abetti	09 20.1	15.0	+0	38.889	0.25	2
994	Otthild	09 23.2	12.5	-1	5.95	0.09-0.15	2+
143649	***2003 QQ47***	***09 23.4***	***13.5***	***+20***	***3.679***	***0.19***	***2-***
22870	Rosing	09 23.9	15.0	+3			
3408	Shalamov	09 29.3	14.7	-2	10.495	0.28	1+
9200	1993 FK21	09 29.4	15.0	+3			
1357	Khama	09 30.1	14.9	-17	15.692	0.34	2
22449	Ottijeff	09 30.7	14.9	+7			

Low Phase Angle Opportunities

The Low Phase Angle list includes asteroids that reach very low phase angles ($\alpha < 1°$). The "α" column is the minimum solar phase angle for the asteroid. Getting accurate, calibrated measurements (usually V band) at or very near the day of opposition can provide important information for those studying the "opposition effect." Use the on-line query form for the LCDB to get more details about a specific asteroid.

http://www.minorplanet.info/PHP/call_OppLCDBQuery.php

You will have the best chance of success working objects with low amplitude and periods that allow covering at least half a cycle every night. Objects with large amplitudes and/or long periods are much more difficult for phase angle studies since, for proper analysis, the data must be reduced to the average magnitude of the asteroid for each night. This reduction requires that you determine the period and the amplitude of the lightcurve; for long period objects that can be difficult. Refer to Harris et al. (1989) for the details of the analysis procedure.

As an aside, some use the maximum light to find the phase slope parameter (*G*). Even though the results better resemble the behavior of a spherical object of the same albedo, it can produce significantly different values for both *H* and *G* versus when using average light, which is the method used for values listed by the Minor Planet Center.

The International Astronomical Union (IAU) has adopted a new system, H-G_{12}, introduced by Muinonen et al. (2010). It will be some years before H-G_{12} becomes widely used, but not until a discontinuity flaw in the G_{12} function has be resolved. This discontinuity results in false "clusters" or "holes" in the solution density and makes it impossible to draw accurate conclusions.

We strongly encourage obtaining data as close to 0° as possible, then every 1-2° out to 7°, below which the curve tends to be non-linear due to the opposition effect. From 7° out to about 30°, observations at 3-6° intervals should be sufficient. Coverage beyond about 50° is not generally helpful since the H-G system is best defined with data from 0-30°.

It's important to emphasize that all observations should (must) be made using high-quality catalogs to set the comparison star magnitudes. These include ATLAS, Pan-STARRS, SkyMapper, and GAIA2. Catalogs such as CMC-15, APASS, or the MPOSC from *MPO Canopus* should not be used due to significant systematic errors.

Also important is that that there are sufficient data from each observing run such that their location can be found on a combined, phased lightcurve derived from two or more nights obtained *near the same phase angle.* This is so that the lightcurve amplitude isn't significantly different. If necessary, the magnitudes for the given run should be adjusted so that they correspond to mid-light of the combined lightcurve. This goes back to the H-G system being based on average, not maximum or minimum light.

For this table, the asteroid magnitudes are brighter than in others. This is because higher precision is required for this work and the asteroid may be a full magnitude or fainter when it reaches phase angles out to 20-30°.

Num	Name	Date	α	V	Dec	Period	Amp	U
656	Beagle	04 14.3	0.16	13.8	-09	7.035	0.57-1.20	3
27	Euterpe	07 03.4	0.19	10.4	-23	10.4082	0.13-0.21	3
38	Leda	07 06.8	0.64	12.8	-25	12.838	0.05-0.16	3
24	Themis	07 12.2	0.31	11.9	-23	8.374	0.09-0.14	3
92	Undina	07 14.6	0.97	10.6	-24	15.941	0.16-0.20	3
1026	Ingrid	07 14.6	0.86	13.9	-23	5.	0.5	2
543	Charlotte	07 14.9	0.19	13.7	-22	10.718	0.23-0.28	3
462	Eriphyla	07 19.0	0.36	12.8	-22	8.659	0.11-0.39	3
1034	Mozartia	07 19.0	0.83	12.7	-22		0.10	
850	Altona	07 28.2	0.67	13.2	-21	11.1913	0.09-0.17	3
949	Hel	08 05.5	0.79	13.8	-19	8.215	0.13-0.14	2+
558	Carmen	08 06.2	0.75	13.1	-15	11.387	0.2 -0.31	3
781	Kartvelia	08 06.6	0.80	13.2	-15	19.04	0.16-0.28	3-
954	Li	08 09.1	0.34	13.3	-15	7.207	0.11-0.25	3
108	Hecuba	08 10.4	0.99	12.6	-19	14.256	0.09-0.12	3
2431	Skovoroda	08 20.2	0.16	14.0	-13	3.13	0.21	2
208	Lacrimosa	08 25.8	0.49	13.0	-12	14.085	0.15-0.33	3
1842	Hynek	08 27.3	0.21	14.0	-10	3.9410	0.07-0.17	3
53	Kalypso	09 01.0	0.77	12.5	-10	9.036	0.09-0.14	3
1247	Memoria	09 07.7	0.16	13.9	-06			
64	Angelina	09 14.3	0.47	11.8	-02	8.752	0.04-0.42	3
224	Oceana	09 15.2	0.10	11.8	-03	9.401	0.09-0.14	3
229	Adelinda	09 15.3	0.62	13.1	-05	6.60	0.04-0.30	3
117	Lomia	09 16.0	0.62	11.9	-01	9.127	0.10-0.35	3
214	Aschera	09 18.5	0.50	12.6	-01	6.835	0.20-0.23	3
571	Dulcinea	09 21.1	0.54	12.9	-02	126.3	0.50	3
468	Lina	09 22.0	0.11	12.6	-01	16.33	0.13-0.18	3
994	Otthild	09 23.3	0.50	12.5	-01	5.95	0.09-0.15	2+
615	Roswitha	09 29.7	0.23	13.6	+02	4.422	0.11	3
167	Urda	09 29.8	0.43	12.8	+01	13.07	0.24-0.39	3
359	Georgia	10 01.6	0.26	11.8	+04	5.537	0.16-0.54	3
312	Pierretta	10 04.6	0.46	12.4	+06	10.282	0.32	3
551	Ortrud	10 07.2	0.10	13.2	+06	17.416	0.14-0.19	3

Shape/Spin Modeling Opportunities

Those doing work for modeling should contact Josef Ďurech at the email address above. If looking to add lightcurves for objects with existing models, visit the Database of Asteroid Models from Inversion Techniques (DAMIT) web site

https://astro.troja.mff.cuni.cz/projects/damit/

Additional lightcurves could lead to the asteroid being added to or improving one in DAMIT, thus increasing the total number of asteroids with spin axis and shape models.

Included in the list below are objects that:

1. Are rated U = 3– or 3 in the LCDB.
2. Do not have reported pole in the LCDB Summary table.
3. Have at least three entries in the Details table of the LCDB where the lightcurve is rated U ≥ 2.

The caveat for condition #3 is that no check was made to see if the lightcurves are from the same apparition or if the phase angle bisector longitudes differ significantly from the upcoming apparition. The last check is often not possible because the LCDB does not list the approximate date of observations for all details records. Including that information is an on-going project.

Favorable apparitions are in bold text. NEAs are in italics.

Num	Name	Brightest Date	Mag	Dec	LCDB Data Period	Amp	U
2083	Smither	07 01.0	15.0	-9	2.672	0.08-0.11	3
696	Leonora	07 02.1	14.4	-30	26.896	0.04-0.31	3
78	Diana	07 03.7	12.8	-33	7.299	0.02-0.30	3
1589	Fanatica	07 08.5	14.8	-25	2.583	0.10-0.22	3
5985	**1942 RJ**	**07 09.0**	**14.5**	**-22**	**9.721**	**0.11-0.18**	**3**
1497	Tampere	07 09.6	14.9	-23	3.64	0.20-0.42	3-
14196	**1998 XH59**	**07 09.7**	**14.4**	**-20**	**3.244**	**0.20-0.25**	**3**
491	Carina	07 13.3	14.1	+2	14.836	0.08-0.13	3
1026	**Ingrid**	**07 14.7**	**13.9**	**-23**	**5.437**	**0.07- 0.5**	**3-**
1100	Arnica	07 15.5	14.4	-22	14.535	0.09-0.28	3
658	Asteria	07 18.4	14.4	-23	21.034	0.22-0.28	3
1625	**The NORC**	**07 21.4**	**13.9**	**-30**	**13.959**	**0.06-0.16**	**3-**
902	Probitas	07 24.6	14.8	-29	10.168	0.10-0.26	3
6708	**Bobbievaile**	**07 24.8**	**14.9**	**-22**	**12.341**	**0.26-0.41**	**3**
880	Herba	07 25.2	14.4	-4	12.266	0.11-0.21	3
790	Pretoria	07 27.5	12.5	+6	10.37	0.05-0.18	3
738	Alagasta	07 28.1	14.2	-18	17.89	0.11-0.20	3-
850	**Altona**	**07 28.1**	**13.2**	**-21**	**11.191**	**0.09-0.17**	**3**
2484	Parenago	07 28.3	14.4	-17	3.433	0.28-0.34	3
469	Argentina	08 02.2	13.5	-24	17.573	0.11-0.15	3
477	Italia	08 02.7	12.2	-27	19.413	0.15-0.32	3
1322	Coppernicus	08 06.5	15.0	+27	4.354	0.04-0.86	3
954	**Li**	**08 09.1**	**13.3**	**-15**	**7.207**	**0.11-0.25**	**3**
488	Kreusa	08 11.8	13.3	-27	32.645	0.08-0.20	3
466	Tisiphone	08 12.1	13.7	-2	8.834	0.03-0.18	3
58	Concordia	08 13.8	12.6	-12	9.895	0.01-0.15	3
3453	Dostoevsky	08 15.1	14.8	-11	3.163	0.05-0.14	3
1264	Letaba	08 16.4	13.8	+25	32.74	0.13-0.43	3
1274	Delportia	08 17.8	14.3	-14	5.56	0.05-0.29	3
1544	Vinterhansenia	08 18.5	14.7	-19	13.536	0.11-0.18	3-
388	**Charybdis**	**08 21.5**	**12.4**	**-16**	**9.516**	**0.14-0.25**	**3**
1116	Catriona	08 23.3	14.1	-23	8.832	0.09-0.28	3
57	Mnemosyne	08 26.3	11.5	+5	25.324	0.09-0.24	3-
1078	Mentha	08 26.4	14.9	-20	85	0.31-0.87	3
1842	**Hynek**	**08 27.2**	**14.0**	**-10**	**3.941**	**0.07-0.17**	**3**
653	Berenike	08 29.4	13.6	-15	12.489	0.03-0.11	3
654	Zelinda	08 29.4	12.7	+13	31.735	0.08- 0.3	3
1222	Tina	09 01.2	14.4	+26	13.395	0.17-0.30	3
5133	**Phillipadams**	**09 07.5**	**14.7**	**-26**	**6.665**	**0.40-0.46**	**3**
1304	Arosa	09 07.8	14.3	-29	7.748	0.13-0.38	3
295	Theresia	09 08.5	13.4	-2	10.702	0.11-0.22	3
464	**Megaira**	**09 10.0**	**12.5**	**-20**	**12.879**	**0.08-0.12**	**3**
921	Jovita	09 11.2	14.1	+9	15.57	0.05-0.13	3
1046	Edwin	09 11.4	14.7	-9	5.291	0.14-0.27	3
910	Anneliese	09 11.7	14.5	-15	11.286	0.13-0.55	3
777	Gutemberga	09 12.3	15.0	+11	12.838	0.11-0.28	3
224	**Oceana**	**09 15.1**	**11.8**	**-3**	**9.401**	**0.09-0.14**	**3**
1639	Bower	09 15.9	14.1	+3	22.181	0.15-0.38	3-
261	Prymno	09 17.9	12.7	-7	8.002	0.08-0.37	3
468	**Lina**	**09 22.0**	**12.7**	**-1**	**16.33**	**0.13-0.18**	**3**
392	**Wilhelmina**	**09 22.8**	**13.1**	**+11**	**13.058**	**0.06-0.70**	**3**
1031	Arctica	09 23.5	14.3	+15	24.904	0.16-0.22	3
1593	Fagnes	09 23.5	14.7	-15	25.25	0.27-0.47	3-
868	Lova	09 28.4	13.3	-7	41.118	0.28-0.40	3
191	**Kolga**	**09 29.4**	**12.5**	**-5**	**17.604**	**0.30-0.50**	**3**

Radar-Optical Opportunities

The loss of the Arecibo Observatory in late 2020 leaves a large gap in the study of NEAs and other solar system objects as well as atmospheric research. Since Arecibo is no longer available, we have modified our approach to this listing.

For one, the list of potential radar targets is much smaller since the Goldstone facility, while able to cover more of the sky, achieves a much lower SNR for an asteroid than would Arecibo. This means, broadly speaking, that potential targets must come closer to Earth and/or be significantly larger to achieve useable SNRs.

As before, we will present a list of targets that are within reach of radar, but considering only Goldstone. This allows continued coordination between the optical and radar communities. We will also provide of list that might be called “What Might Have Been”, i.e., objects that would have been considered if Arecibo were in service. Detailed discussions and ephemerides may not always be provided for these objects.

We hope that this second listing will encourage observations despite being out of Goldstone radar range *for this apparition*. The data can still be important for future Earth encounters that do come within reach of the facilities in operation at that time.

Goldstone targets:
http://echo.jpl.nasa.gov/asteroids/goldstone_asteroid_schedule.html

This list is based on *known* targets at the time they were prepared. It is very common for newly discovered objects to move into, out of, or up the list and become radar targets on short notice. We recommend that you keep up with the latest discoveries the Minor Planet Center observing tools.

In particular, monitor NEAs and be flexible with your observing program. In some cases, you may have only 1-3 days when the asteroid is within reach of your equipment. Be sure to keep in touch with the radar team (through Benner's email or their Facebook or Twitter accounts) if you get data. The team may not always be observing the target but your initial results may change their plans. In all cases, your efforts are greatly appreciated.

Use the ephemerides below as a guide to your better chances for observing, but remember that photometry may be possible before and/or after the dates in the ephemerides. Note that *geocentric* positions are given. Use these web sites to generate updated and *topocentric* positions:

MPC: *http://www.minorplanetcenter.net/iau/MPEph/MPEph.html*
JPL: *http://ssd.jpl.nasa.gov/?horizons*

In the ephemerides below, "ED" and "SD" are, respectively, the Earth and Sun distances (AU), "V" is the estimated Johnson V magnitude, and "α" is the phase angle. "SE" and "ME" are the great circle distances (in degrees) of the Sun and Moon from the asteroid. "MP" is the lunar phase and "GB" is the galactic latitude. "PHA" indicates that the object is a *potentially hazardous asteroid*, meaning that at some (long distant) time, its orbit might take it very close to Earth.

About YORP Acceleration

Many, if not all, of the targets in this section are near-Earth asteroids. These objects are particularly sensitive to YORP acceleration. YORP (Yarkovsky-O'Keefe-Radzievskii-Paddack) is the asymmetric thermal re-radiation of sunlight that can cause an asteroid's rotation period to increase or decrease. High precision lightcurves at multiple apparitions can be used to model the asteroid's *sidereal* rotation period and see if it's changing.

It usually takes four apparitions to have sufficient data to determine if the asteroid rotation rate is changing under the influence of YORP. This is why observing an asteroid that already has a well-known period remains a valuable use of telescope time. It is even more so when considering the BYORP (binary-YORP) effect among binary asteroids that has stabilized the spin so that acceleration of the primary body is not the same as if it would be if there were no satellite.

To help focus efforts in YORP detection, Table I gives a quick summary of this quarter's radar-optical targets. The family or group for the asteroid is given under the number/name line. Also, underneath the first list will be additional flags such as "PHA" for Potentially Hazardous Asteroid, "NPAR" for a tumbler, and/or "BIN" to indicate the asteroid is a binary (or multiple) system. "BIN?" means that the asteroid is a suspected but not confirmed binary. The period is in hours and, in the case of binary, for the primary. The "Amp" column gives the known range of lightcurve amplitudes. The "App" column gives the number of different apparitions at which a lightcurve period was reported while the "Last" column gives the year for the last reported period. The "R SNR" column indicates the estimated radar SNR using the tool at

http://www.naic.edu/~eriverav/scripts/index.php

The SNRs were calculated using the current MPCORB absolute magnitude (H), a period of 4 hours (2 hours if $D \leq 200$ m) if it's not known, and the approximate minimum Earth distance during the current quarter. These are estimates only and assume that the radar is fully functional.

If the row is in bold text, the object was found on the radar planning pages listed above. Otherwise, the planning tool at

http://www.minorplanet.info/PHP/call_OppLCDBQuery.php

was used to find known NEAs that were V < 18.0 during the quarter.

Asteroid	Period	Amp	App	Last	R SNR
(285571) 2000 PQ9 NEA	-	-	-	-	**A: 225 G: 55**
2012 BA35 NEA NHATS	-	-	-	-	**A: 485 G: 140**
2008 GO20 NEA	-	-	-	-	**A: 200 G: 55**
2016 AJ193 NEA PHA	-	-	-	-	**A: 6700 G: 1900**
(143649) 2003 QQ47 NEA PHA	**3.679**	**0.19**	**1**	**2014**	**A: 79 G: 22**

Table I. Summary of Goldstone-optical opportunities for the current quarter. Period and amplitude data are from the asteroid lightcurve database (LCDB; Warner et al., 2009). SNR values are estimates and are given for relative comparisons among the objects in the list.

Asteroid	Period	Amp	App	Last	R SNR
3103 Eger NEA Jul 26 14.7 0°	5.7059	0.49 1.18	8	2019	13
(523664) 2012 OD1 NEA Jul 29 16.6 57°	12.63	0.63	1	2018	28
(7822) 1991 CS NEA Aug 24 16.1 9°	2.389	0.26 0.39	3	2016	18

Table II. This list includes only those objects that would have been within reach of Arecibo but not Goldstone (assuming SNR > 10 for Arecibo). The columns are the same as for Table I. In the "R SNR" column, the estimated SNR is for Arecibo.

In Table II, the third line in the first column gives the approximate date when the asteroid is brightest along with the V magnitude and declination at the time.

It's rarely the case, especially for shape/spin axis modeling, that there are too many observations. Remember that the best set for modeling includes data not just from multiple apparitions but from a wide a range of phase angles during each apparition as well.

Unless otherwise said, the estimated diameters given below are based on an albedo of $p_V = 0.20$, the approximate average of the S taxonomic class that dominates the NEA region (Warner et al., 2009).

(285571) 2000 PQ9 (H = 18.1)
There are no rotation periods recorded in the LCDB. The estimated diameter is 700 m, so it's unlikely, but not impossible, that the rotation period will be less than 2 h. Note that the asteroid goes through a wide range of phase angles in July. This can present an excellent chance to get an H-G phase curve.

To get the best possible solution for the phase curve, you'll need to get a good idea of the rotation period and amplitude. If keeping strictly in the H-G system, data points should be based the on the mean amplitude of the lightcurve at the time of the observations. Try to take into account the fact that the lightcurve amplitude increases with increasing phase angle (Zappala et al., 1990).

DATE	RA	Dec	ED	SD	V	α	SE	ME	MP	GB
07/01	17 49.4	-64 59	0.13	1.12	15.5	38.1	137	87	-0.59	-18
07/11	18 52.9	-51 16	0.09	1.09	14.3	27.3	150	149	+0.01	-21
07/21	19 50.1	-17 47	0.07	1.08	12.8	3.6	176	40	+0.87	-21
07/31	20 31.2	+19 00	0.08	1.08	14.3	34.7	143	81	-0.55	-12
08/10	20 58.3	+36 32	0.12	1.09	15.5	47.3	128	124	+0.03	-6
08/20	21 16.9	+43 21	0.17	1.11	16.3	49.4	123	71	+0.92	-4
08/30	21 31.1	+45 35	0.21	1.14	16.8	47.4	124	81	-0.53	-4
09/09	21 43.3	+45 22	0.26	1.18	17.2	43.9	126	120	+0.05	-6
09/19	21 55.6	+43 42	0.31	1.22	17.6	40.0	128	60	+0.96	-9
09/29	22 08.8	+41 09	0.37	1.27	17.9	36.4	131	95	-0.51	-12

3103 Eger (*H* = 15.2)

The rotation period for this 2700 m NEA is close to 5.7 h (e.g., Warner and Stephens, 2019b). It's too distant for Goldstone observations and it's been modeled before (Ďurech et al. 2012), who reported evidence of YORP acceleration. Additional lightcurves this time around can help confirm and refine the amount of rotational increase (period decrease) that they found.

DATE	RA	Dec	ED	SD	V	α	SE	ME	MP	GB
07/01	22 48.3	+09 36	0.40	1.22	15.5	51.2	111	24	-0.59	-43
07/11	23 41.5	+07 41	0.32	1.16	15.0	55.5	110	120	+0.01	-51
07/21	00 55.3	+03 08	0.26	1.11	14.7	62.6	104	118	+0.87	-60
07/31	02 29.0	-04 01	0.24	1.06	14.7	73.1	94	15	-0.55	-57
08/10	04 04.0	-10 56	0.25	1.01	15.1	83.3	82	100	+0.03	-42
08/20	05 20.4	-15 04	0.30	0.97	15.7	89.0	74	126	+0.92	-27
08/30	06 16.8	-16 46	0.36	0.94	16.1	90.4	68	49	-0.53	-15
09/09	06 59.9	-17 06	0.43	0.92	16.3	89.1	66	88	+0.05	-6
09/19	07 35.2	-16 43	0.50	0.91	16.5	86.1	64	128	+0.96	+2
09/29	08 06.2	-15 57	0.56	0.91	16.6	82.3	64	49	-0.51	+9

(523664) 2012 OD1 (*H* = 18.6, PHA)

This 570-m PHA isn't on the Goldstone schedule until 2024 July. However, it's still worth observing this time around to confirm, if possible, the period of 12.63 h found by Warner and Stephens (2019a) and to provide updated astrometry. The low solar elongations will make this a challenging target.

DATE	RA	Dec	ED	SD	V	α	SE	ME	MP	GB
07/20	03 10.6	+20 40	0.13	0.97	18.1	106.7	66	169	+0.78	-32
07/23	02 26.0	+33 43	0.11	0.99	17.3	98.2	76	119	+0.98	-25
07/26	01 08.9	+47 55	0.10	1.02	16.8	87.1	87	76	-0.95	-15
07/29	23 09.1	+56 52	0.11	1.04	16.6	76.3	98	61	-0.74	-3
08/01	21 09.8	+57 05	0.13	1.06	16.7	68.5	105	75	-0.46	+6
08/04	19 53.9	+53 04	0.15	1.07	17.0	63.8	108	95	-0.19	+13
08/07	19 10.9	+48 39	0.18	1.09	17.3	61.0	110	106	-0.03	+17
08/10	18 45.3	+44 52	0.22	1.11	17.6	59.3	110	101	+0.03	+20
08/13	18 29.0	+41 47	0.25	1.12	17.9	58.2	110	85	+0.22	+22
08/16	18 18.2	+39 15	0.28	1.14	18.2	57.4	109	68	+0.55	+23

2012 BA35 (*H* = 23.8, NHATS)

Even though only 50 m in diameter, this object will be a strong radar target. The period is unknown, making observations all the more important. Given the size, it's very possible that the rotation period will be << 2 h.

DATE	RA	Dec	ED	SD	V	α	SE	ME	MP	GB
07/24	18 28.1	+43 40	0.05	1.03	19.5	65.5	112	72	+1.00	+22
07/25	18 24.3	+44 42	0.04	1.03	19.5	67.0	111	76	-0.99	+23
07/26	18 20.1	+45 48	0.04	1.03	19.4	68.5	109	81	-0.95	+24
07/27	18 15.3	+47 00	0.04	1.03	19.4	70.2	108	86	-0.90	+25
07/28	18 09.7	+48 18	0.04	1.03	19.3	72.0	106	91	-0.82	+27
07/29	18 03.2	+49 42	0.04	1.02	19.2	74.1	104	96	-0.74	+28
07/30	17 55.4	+51 15	0.03	1.02	19.2	76.3	102	100	-0.65	+29
07/31	17 46.1	+52 56	0.03	1.02	19.1	78.7	99	102	-0.55	+31
08/01	17 34.7	+54 47	0.03	1.02	19.1	81.5	97	103	-0.46	+33
08/02	17 20.5	+56 46	0.03	1.02	19.1	84.6	94	102	-0.36	+35
08/03	17 02.5	+58 54	0.03	1.02	19.1	88.0	90	99	-0.28	+37
08/04	16 39.0	+61 06	0.02	1.01	19.1	91.9	87	95	-0.19	+39
08/05	16 08.2	+63 16	0.02	1.01	19.1	96.4	82	88	-0.12	+42
08/06	15 27.5	+65 09	0.02	1.01	19.2	101.4	77	81	-0.07	+45
08/07	14 35.4	+66 20	0.02	1.01	19.4	107.1	72	72	-0.03	+48
08/08	13 33.8	+66 16	0.02	1.01	19.6	113.4	66	62	+0.00	+50

2008 GO20 (*H* = 22.3)

2008 GO20 will also be a solid target for Goldstone (SNR ~ 55). Here again, the period is not known for this 100-m NEA. Its size also makes it possible, maybe even likely, that the period is ≤ 2 h.

Normally, such faint objects are not included in this paper. However, given recent work by Peter Birtwhistle (2021), it may possible to get useable results, but that will depend in large part on the lightcurve amplitude being significantly larger than the individual errors and overall noise in the data set.

DATE	RA	Dec	ED	SD	V	α	SE	ME	MP	GB
08/01	03 14.2	+05 58	0.04	1.01	18.7	96.7	81	10	-0.46	-42
08/02	02 56.1	+04 26	0.04	1.01	18.7	90.8	87	17	-0.36	-46
08/03	02 40.8	+03 07	0.05	1.02	18.6	85.6	92	31	-0.28	-50
08/04	02 27.7	+01 58	0.05	1.02	18.6	81.0	96	46	-0.19	-53
08/05	02 16.6	+00 59	0.05	1.03	18.7	77.0	100	60	-0.12	-55
08/06	02 06.9	+00 08	0.06	1.03	18.7	73.3	104	75	-0.07	-57
08/07	01 58.4	-00 37	0.06	1.03	18.8	70.0	107	90	-0.03	-59
08/08	01 50.9	-01 16	0.07	1.04	18.8	66.9	110	104	+0.00	-60
08/09	01 44.3	-01 51	0.07	1.04	18.9	64.1	112	119	+0.00	-62
08/10	01 38.4	-02 22	0.07	1.05	18.9	61.5	115	133	+0.03	-63

2016 AJ193 (*H* = 18.5, PHA)

Barring a new discovery, this is going to be the best radar target this quarter. An extensive campaign is being planned using Goldstone and Canberra (Australia) with hopes for detailed delay-Doppler imaging. Having a rotation period before the planned radar observations would be extremely helpful.

Using the default albedo and MPCORB *H*, the estimated diameter is 590 m. However, Masiero et al. (2017) found a diameter of 1.37 km using *H* = 18.7; this leads to an unusually low albedo of 0.03. When correcting their values by using *H* = 18.5 (Harris and Harris, 1997), the albedo is closer to 0.04, which is still very dark. The revised values from Harris and Harris give *D* = 1.38 km.

All this is to say that the period is very likely to be > 2 h. Unfortunately, the phase angle range isn't sufficient to get a good H-G phase curve. Also unfortunate is that the sky motion when brightest in mid- to late August will be on the order of 80"/min. Getting good data will be a compromise of minimizing trailing but avoiding excessive scintillation noise when using short exposures.

DATE	RA	Dec	ED	SD	V	α	SE	ME	MP	GB
08/10	23 36.2	-37 57	0.18	1.16	16.4	32.1	142	153	+0.03	-71
08/11	23 40.0	-38 07	0.16	1.15	16.2	32.8	142	151	+0.07	-71
08/12	23 44.4	-38 17	0.15	1.13	16.0	33.6	142	144	+0.14	-72
08/13	23 49.8	-38 28	0.13	1.12	15.8	34.5	141	135	+0.22	-73
08/14	23 56.5	-38 41	0.12	1.11	15.5	35.7	140	125	+0.32	-74
08/15	00 05.1	-38 54	0.10	1.09	15.3	37.2	139	115	+0.43	-75
08/16	00 16.6	-39 07	0.09	1.08	15.0	39.2	138	104	+0.55	-76
08/17	00 32.5	-39 17	0.07	1.07	14.6	42.0	135	95	+0.66	-77
08/18	00 56.2	-39 17	0.06	1.05	14.2	46.2	131	87	+0.76	-78
08/19	01 33.7	-38 38	0.05	1.04	13.8	52.9	125	82	+0.85	-76
08/20	02 37.4	-35 44	0.03	1.03	13.5	64.9	113	85	+0.92	-66
08/21	04 21.2	-25 24	0.02	1.01	13.6	87.9	91	99	+0.97	-43

(7822) 1991 CS (*H* = 17.3)

The rotation period of 2.389 h has been determined several times (e.g., Pravec et al., 2019web). The reported amplitude has ranged from 0.26 to 1.02 mag. Large phase angles and low solar elongations conspire to make this a difficult target but it's worth a try in order to provide additional data for modeling. Mainzer et al. (2019) found a diameter of 1.21 km (*H* = 17.4) and derived an albedo of 0.133. This similar to what radar observations found (Benner et al., 1999).

DATE	RA	Dec	ED	SD	V	α	SE	ME	MP	GB
07/20	23 44.4	+52 30	0.44	1.12	18.1	65.2	92	122	+0.78	-9
07/27	00 14.9	+51 35	0.37	1.10	17.7	67.1	93	66	-0.90	-11
08/03	00 53.5	+49 09	0.30	1.08	17.3	69.3	95	50	-0.28	-14
08/10	01 43.1	+43 39	0.23	1.06	16.8	71.7	96	108	+0.03	-18
08/17	02 45.2	+31 45	0.18	1.04	16.3	74.9	95	152	+0.66	-25
08/24	03 56.3	+09 30	0.15	1.03	16.0	80.0	92	69	-0.97	-32
08/31	05 07.0	-16 53	0.16	1.01	16.3	85.6	85	40	-0.43	-30
09/07	06 08.1	-34 34	0.20	0.99	17.0	88.2	80	84	+0.00	-23
09/14	06 56.8	-43 46	0.26	0.98	17.5	88.2	77	109	+0.52	-17
09/21	07 35.0	-48 31	0.33	0.97	17.9	86.8	74	102	-1.00	-13

(143649) 2003 QQ47 (H = 17.4, PHA)

Carbognani (2014) reported a rotation period of 4.09 h while Warner (2014) found 3.679 h. Neither solution is considered definitive so additional observations this time around may help resolve the ambiguity. The best chance is for southern observations around mid-September but northern observations still have an opportunity from late September to early October.

DATE	RA	Dec	ED	SD	V	α	SE	ME	MP	GB
08/25	04 14.3	-25 42	0.52	1.18	18.5	58.8	95	61	-0.93	-45
09/04	04 02.6	-22 28	0.36	1.15	17.6	58.2	104	80	-0.10	-47
09/14	03 23.2	-13 44	0.20	1.12	16.0	50.2	121	131	+0.52	-52
09/24	00 17.0	+26 13	0.10	1.09	13.7	23.8	154	32	-0.91	-36
10/04	19 30.3	+41 46	0.20	1.06	16.4	67.0	102	109	-0.08	+11
10/14	18 24.7	+38 13	0.36	1.03	17.8	74.7	85	68	+0.60	+21

References

Benner, L.A.M.; Ostro, S.J.; Rosema, K.D.; Giorgini, J.D.; Choate, D.; Jurgens, R.F.; Rose, R.; Slade, M.A.; Thomas, M.L.; Winkler, R.; Yeomans, D.K. (1999). "Radar Observations of Asteroid 7822 (1991 CS)." *Icarus* **137**, 247-259.

Birtwhistle, P. (2021). "Lightcurve Analysis for Ten Near-Earth Asteroids." *Minor Planet Bull*. **48**, 180-186.

Carbognani, A. (2014). "Asteroid Lightcurves at OAVdA: 2013 December - 2014 June." *Minor Planet Bull*. **41**, 265-270.

Ďurech, J.; Vokrouhlický, D.; Baransky, A.R.; Breiter, S.; Burkhonov, O.A.; Cooney, W.; Fuller, V.; Gaftonyuk, N.M.; Gross, J.; Inasaridze, R.Y.; Kaasalainen, M.; Krugly, Yu.N.; Kvaratshelia, O.I.; Litvinenko, E.A.; Macomber, B.; Marchis, F.; Molotov, I.E.; Oey, J.; Polishook, D.; Pollock, J.; Pravec, P.; Sárneczky, K.; Shevchenko, V.G.; Slyusarev, I.; Stephens, R.; Szabó, Gy.; Terrell, D.; Vachier, F.; Vanderplate, Z.; Viikinkoski, M.; Warner, B.D. (2012). "Analysis of the rotation period of asteroids (1865) Cerberus, (2100) Ra-Shalom, and (3103) Eger - Search for the YORP effect." *Astron. Astrophys*. **547**, A10.

Harris, A.W.; Young, J.W.; Contreiras, L.; Dockweiler, T.; Belkora, L.; Salo, H.; Harris, W.D.; Bowell, E.; Poutanen, M.; Binzel, R.P.; Tholen, D.J.; Wang, S. (1989). "Phase relations of high albedo asteroids: The unusual opposition brightening of 44 Nysa and 64 Angelina." *Icarus* **81**, 365-374.

Harris, A.W.; Harris, A.W. (1997). "On the Revision of Radiometric Albedos and Diameters of Asteroids." *Icarus* **126**, 450-454.

Mainzer, A.; Bauer, J.; Cutri, R.; Grav, T.; Kramer, E.; Masiero, J.; Sonnett, S.; Wright, E., Eds. (2019). "NEOWISE Diameters and Albedos V2.0." NASA Planetary Data System. urn:nasa:pds:neowise_diameters_albedos::2.0. *https://doi.org/10.26033/18S3-2Z54*

Maisero, J.R.; Nugent, C.; Mainzer, A.K.; Wright, E.L.; Bauer, J.M.; Cutri, R.M.; Grant, T.; Kramer, E.; Sonnett, S. (2017). "NEOWISE Reactivation Mission Year Three: Asteroid Diameters and Albedos." *Astron. J.* **154**, id. 168.

Muinonen, K.; Belskaya, I.N.; Cellino, A.; Delbò, M.; Levasseur-Regourd, A.-C.; Penttilä, A.; Tedesco, E.F. (2010). "A three-parameter magnitude phase function for asteroids." *Icarus* **209**, 542-555.

Pravec, P.; Wolf, M.; Sarounova, L. (2019web). *http://www.asu.cas.cz/~ppravec/neo.htm*

Warner, B.D. (2014). "Near-Earth Asteroid Lightcurve Analysis at CS3-Palmer Divide Station: 2014 March-June." *Minor Planet Bull*. **41**, 213-224.

Warner, B.D.; Stephens, R.D. (2019a). "Near-Earth Asteroid Lightcurve Analysis at the Center for Solar System Studies: 2018 July-September." *Minor Planet Bull*. **46**, 27-40.

Warner, B.D.; Stephens, R.D. (2019b). "Near-Earth Asteroid Lightcurve Analysis at the Center for Solar System Studies: 2019 March-July." *Minor Planet Bull*. **46**, 423-438.

Warner, B.D.; Harris, A.W.; Pravec, P. (2009). "The asteroid lightcurve database." *Icarus* **202**, 134-146.

Warner, B.D.; Harris, A.W.; Ďurech, J.; Benner, L.A.M. (2021). "Lightcurve Photometry Opportunities: 2021 January-March." *Minor Planet Bull.* **48**, 89-97.

Zappala, V.; Cellini, A.; Barucci, A.M.; Fulchignoni, M.; Lupishko, D.E. (1990). "An anlaysis of the amplitude-phase relationship among asteroids." *Astron. Astrophys*. **231**, 548-560.

IN THIS ISSUE

This list gives those asteroids in this issue for which physical observations (excluding astrometric only) were made. This includes lightcurves, color index, and H-G determinations, etc. In some cases, no specific results are reported due to a lack of or poor-quality data. The page number is for the first page of the paper mentioning the asteroid. EP is the "go to page" value in the electronic version.

THE MINOR PLANET BULLETIN (ISSN 1052-8091) is the quarterly journal of the Minor Planets Section of the Association of Lunar and Planetary Observers (ALPO, http://www.alpo-astronomy.org). Current and most recent issues of the *MPB* are available on line, free of charge from:

http://www.minorplanet.info/MPB

The Minor Planets Section is directed by its Coordinator, Prof. Frederick Pilcher, 4438 Organ Mesa Loop, Las Cruces, NM 88011 USA (fpilcher35@gmail.com). Dr. Alan W. Harris (MoreData! Inc.; harrisaw@colorado.edu), and Dr. Petr Pravec (Ondrejov Observatory; ppravec@asu.cas.cz) serve as Scientific Advisors. The Asteroid Photometry Coordinator is Brian D. Warner (Center for Solar System Studies), Palmer Divide Observatory, 446 Sycamore Ave., Eaton, CO 80615 USA (brian@MinorPlanetObserver.com).

The Minor Planet Bulletin is edited by Professor Richard P. Binzel, MIT 54-410, 77 Massachusetts Ave, Cambridge, MA 02139 USA (rpb@mit.edu). Brian D. Warner (address above) is Associate Editor, and Dr. David Polishook, Department of Earth and Planetary Sciences, Weizmann Institute of Science (david.polishook@weizmann.ac.il) is Assistant Editor. The *MPB* is produced by Dr. Pedro A. Valdés Sada (psada2@ix.netcom.com). The MPB is distributed by Dr. Melissa Hayes-Gehrke. Direct all subscriptions, contributions, address changes, etc. to:

Dr. Melissa Hayes-Gehrke
UMD Astronomy Department
1113 PSC Bldg 415
College Park, MD 20742 USA
(mhayesge@umd.edu)

Effective with Volume 38, the *Minor Planet Bulletin* is a limited print journal, where print subscriptions are available only to libraries and major institutions for long-term archival purposes. In addition to the free electronic download of the *MPB* noted above, electronic retrieval of all *Minor Planet Bulletin* articles (back to Volume 1, Issue Number 1) is available through the Astrophysical Data System:

http://www.adsabs.harvard.edu/

Authors should submit their manuscripts by electronic mail (rpb@mit.edu). Author instructions and a Microsoft Word template document are available at the web page given above. All materials must arrive by the deadline for each issue. Visual photometry observations, positional observations, any type of observation not covered above, and general information requests should be sent to the Coordinator.

* * * * *

The deadline for the next issue (48-4) is July 15, 2021. The deadline for issue 49-1 is October 15, 2021.

THIS PAGE INTENTIONALLY LEFT BLANK